The geological record of ancient harbours

– using ancient harbour geoarchives of Corcyra (Greece) to reconstruct the palaeoenvironmental development and to identify extreme events by means of a multi-proxy based geoarchaeological approach

Dissertation
zur Erlangung des Grades
Doktor der Naturwissenschaften

im Promotionsfach Geographie
am Fachbereich Chemie, Pharmazie und Geowissenschaften
der Johannes Gutenberg-Universität in Mainz

Claudia Finkler
geb. in Lebach

.....

Mainz, November 2017

Berichterstatter
1. Gutachter: *[Name gelöscht]*
2: Gutachter: *[Name gelöscht]*

Tag der mündlichen Prüfung:
23. Januar 2018

Für Josef Gläser

Abstract

Ancient harbours represent valuable geoarchives where complex man-environment interactions are recorded. Both, anthropogenic and natural impacts and the human or natural responses to them might be archived, helping to reconstruct or comprehend the spatial and temporal development of ancient cities, their harbour basins and infrastructure as well as their occupation history. Thus, various ancient harbours were studied in the frame of geomorphological and geoarchaeological research in order to gain new insights into the (palaeo-)history of the Mediterranean region.

The ancient city of Corcyra, located on the island of Corfu in the northern Ionian Sea, has not been subject to geoarchaeological research so far, although Corcyra was one of the major commercial and political centres in the ancient Greek world. Located on the ancient sea routes between Italy, Sicily and Greece, Corcyra was a prevailing naval power since the Archaic period and kept its political status based on a considerable fleet and appropriated harbour infrastructure to host, load and repair it. At least two ancient harbours are known from historical records and traced by archaeological remains of related infrastructure, namely the military Alkinoos Harbour and the commercial Hyllaikos Harbour, located to the west and the north of the ancient city, respectively. However, information on the exact extent of these harbours as well as their temporal and spatial development are incomplete as much of the ancient infrastructure is concealed under modern urban structures nowadays.

The present study focusses the harbour geoarchives of Corcyra in order to decipher the complex and multifaceted palaeogeographical history of ancient Corcyra. In particular, the study aims to (i) trace the spatial extent of the ancient harbour basins, (ii) investigate the sedimentary record of these harbours in order to draw conclusions on their environmental conditions and protection levels, (iii) identify the main triggers for palaeoenvironmental changes in these harbours and their natural predecessors/successors and (iv) study the harbour's function as sediment traps for human interventions and natural extreme events. Six investigation sites were analysed by means of a comprehensive geoarchaeological multi-methodological approach including sedimentological, geomorphological, palaeontological, geochemical and geophysical investigations which were complemented by results from archaeological research. These study sites comprised three potential harbour sites, namely the Desylla, Kokotou and Pierri sites, which were identified based on historical accounts or archaeological remains, as well as three geomorphological key sites, essential for reconstructing the overall palaeoenvironmental evolution.

First rudimentary harbour installations in Corcyra trace back to the Archaic period, when a slightly-protected pre-harbour came to function by the construction of a nearby wall at the Desylla site in the northern ancient city. Out of this still shallow marine environment, the Classical Alkinoos Harbour developed before the 4th to 3rd cent. BC, extending to the east towards the Kokotou site, where the archaeological remains of monumental shipsheds bear witness of extensive harbour use. Probably, the harbour basin extended even further to the east as a contemporaneous harbour basin was reconstructed in the front of the Pierri quay wall. During Roman times, only the western part of the northern harbour zone was used and kept in function by extensive dredging

activities proved by stratigraphical gaps, chronological anomalies and geophysical evidence. In contrast, the Pierri site quay wall was buried under colluvial and anthropogenic deposits.

Apart from these man-made interventions that led to massive coastal change on the shores of the Analipsis Peninsula, where the ancient city was located, the coastal evolution of Corcyra was also strongly linked to natural extreme events. Evidence of multiple palaeotsunami landfalls was found in the investigated areas, documenting tsunami impact in the 6th mill. BC, the 4th mill. BC, between the 4th and 3rd cent. BC, between the 3rd and 6th cent. AD and between the 5th and 6th cent. AD. Most of these events seem to correlate with findings from Sicily, the Albanian coasts, the Greek mainland and other Ionian Islands and are therefore considered to be part of supra-regional impacts. Only the tsunami event that happened between the 4th and 3rd cent. BC was identified as local event triggered around Corfu, as associated strong co-seismic uplift was proved at the Pierri quay wall and by archaeoseismological traces on the Analipsis Peninsula. Due to decreased water depth caused by this crustal uplift and associated infill of tsunami event deposits, the Pierri was not navigable anymore and abandoned. Similarly, the decline of the Roman Alkinoos Harbour was initialised by event deposits which were most likely caused by the 365 AD Crete tsunami.

By conclusion, the ancient harbours of Corcyra turned out to be appropriate geoarchives to reconstruct the palaeoenvironmental history of Corcyra and to trace multiple interactions between men and the natural environment.

Zusammenfassung

Im gesamten Mittelmeer zeugen zahlreiche antike Häfen von den komplexen Wechselwirkungen zwischen dem Menschen und seiner physischen Umwelt. Diese Häfen fungieren als vielversprechende Geoarchive, in denen vom Menschen verursachte Umweltveränderungen oder natürliche Ereignisse wie Erdbeben oder Tsunamis aufgezeichnet und konserviert werden. Damit lässt sich die räumliche und zeitliche Entwicklung von antiken Städten und ihren Häfen nachvollziehen und rekonstruieren. Zahlreiche antike mediterrane Häfen wurden bislang mit dem Ziel untersucht, neue Erkenntnisse für die generelle (Paläo-) Geschichte des Mittelmeerraums zu gewinnen.

Im Gegensatz dazu wurden bislang keine geoarchäologischen Studien in Bezug auf das antike Corcyra durchgeführt. Die *Polis* von Corcyra liegt im zentralen Teil der Insel Korfu im nördlichen Ionischen Meer und war ein politisches und ökonomisches Zentrum im antiken Griechenland. Aufgrund seiner Lage entlang der antiken Seerouten zwischen Sizilien, Italien und dem griechischen Festland galt Corcyra seit Archaischer Zeit als eine der vorherrschenden Seemächte Griechenlands. Diesen Status konnte Corcyra nur mit Hilfe einer schlagkräftigen Flotte sowie umfassenden Hafenanlagen erlangen und bewahren. Mindestens zwei verschiedene Häfen sind dank historischen Überlieferungen und archäologischen Untersuchungen bekannt: Der Alkinoos Hafen, ein gut zu verteidigender Kriegshafen, sowie der Hyllaikos Hafen, der als Handelshafen fungierte. Diese Häfen lagen nördlich bzw. westlich der antiken Stadt. Detaillierte Informationen über die genaue Ausdehnung dieser Hafenanlagen sowie darüber, wie sie sich räumlich und zeitlich entwickelt haben, sind dagegen nicht bekannt – auch da ein Großteil der antiken Infrastruktur heute durch moderne Bebauung überdeckt ist.

Die vorliegende Studie befasst sich daher mit den Häfen der antiken Stadt Corcyra als Geoarchive, um die vielschichtige und komplexe Entwicklung der Stadt in einem paläogeographischen Kontext zu rekonstruieren. Im speziellen zielt die Studie darauf ab, (i) die räumliche Ausdehnung der antiken Hafenbecken nachzuzeichnen, (ii) die Paläoumweltbedingungen innerhalb dieser Häfen mithilfe sedimentologischer Untersuchungen nachzuvollziehen um Rückschlüsse auf ihre allgemeine Bauweise und Struktur ziehen zu können, (iii) Haupteinflussfaktoren für Küstenlinienveränderungen innerhalb dieser Häfen bzw. ihrer natürlichen Vorgänger und Nachfolger zu identifizieren, und (iv) die Eignung der antiken Hafenbecken als Sedimentfallen für natürliche Extremereignisse sowie menschgemachte Änderungen zu überprüfen. Sechs Untersuchungsgebiete wurden daher mittels eines umfassenden geoarchäologischen Ansatzes analysiert, der sedimentologische, geomorphologische, paläontologische, geochemische und geophysikalische Methoden enthielt und dessen Ergebnisse mit archäologischen Daten abgeglichen wurden. Die Untersuchungsgebiete erstrecken sich über drei potentielle Hafenstandorte (Desylla, Kokotou und Pierri Gelände), die anhand von archäologischen Überresten identifiziert wurden, hin zu drei geomorphologischen Schlüsselstellen, die für die generelle paläogeographische Entwicklungsgeschichte von Bedeutung sind.

Erste rudimentäre Hafenanlagen in Corcyra wurden bereits in Archaischer Zeit angelegt, als durch die Konstruktion einer massiven Mauer auf dem heutigen Desylla Gelände ein nur schwach abgeschirmter Proto-Hafen entstand. Aus diesem flachmarinen Milieu entwickelte sich der klassi-

sche Alkinoos Hafen vor dem 4. bis 3. Jh. v. Chr. Er erstreckte sich gen Osten bis zum Kokotou Gelände, wo die Reste monumentaler Schiffshäuser eine Hafennutzung belegen. Wahrscheinlich reichte das Hafenbecken auch noch weiter nach Osten bis zum Pierri Gelände, wo ähnlich alt datierte Hafensedimente vor einer Kaimauer aufgefunden wurden. Zu römischer Zeit wurde nur der westliche Teil des Alkinoos Hafens wiedergenutzt, der durch intensive Ausbaggerungsarbeiten schiffbar gehalten wurde. Letztere sind durch stratigraphische Lücken, Datierungsanomalien sowie geophysikalisch nachgewiesene Aushubspuren belegt. Dagegen wurde der Pierri Hafen nicht mehr genutzt und unter kolluvialen Sedimenten begraben.

Abgesehen von menschlichen Einflüssen, die maßgeblich auf die Küsten der Analipsis Halbinsel als Standort der antiken Stadt Corcyra eingewirkt haben, sind es vor allem natürliche Extremereignisse, die die Paläogeographie Corcyras nachhaltig geprägt haben. So konnten mehrere Paläotsunami-Ereignisse im Untersuchungsgebiet nachgewiesen werden, die Corcyra im 6. und 4. Jtsd. v. Chr., zwischen dem 4. und 3. Jh. v. Chr., zwischen dem 3. und 5. Jh. n. Chr. sowie zwischen dem 5. und 6. Jh. n. Chr. getroffen haben. Diese Ereignisse passen zeitlich zu Befunden von der Insel Sizilien, der albanischen Küste, dem griechischen Festland sowie anderen Ionischen Inseln, weswegen von großflächigen Ereignissen mit supra-regionaler Wirkung ausgegangen werden muss. Das Tsunami-Event, dass zwischen dem 4. und 3. Jh. v. Chr. stattfand, kann zudem als lokales Ereignis klassifiziert werden, welches nahe der Insel Korfu ausgelöst wurde. Das dazugehörige Erdbeben führte zu einer lokalen Hebung der Erdkruste, was auf dem Pierri Gelände sowie anhand archäoseismischer Spuren an antiken Gebäuden belegt werden kann. Aufgrund stark reduzierter Wassertiefen sowie der Verfüllung mit Tsunami-Sedimenten war der Pierri Hafen nicht mehr schiffbar und wurde aufgegeben. Ähnlich lässt sich die Aufgabe des römischen Alkinoos Hafen auf Tsunami-Sedimente zurückführen, die sehr wahrscheinlich auf das berühmte Erdbeben 365 n. Chr. auf Kreta zurückgehen.

Zusammenfassend lässt sich festhalten, dass sich die antiken Häfen Corcyras als außergewöhnliche Geoarchive erwiesen haben, um die paläogeographische Entwicklung Corcyras im Kontext vielfältiger Wechselwirkungen zwischen dem Menschen und seiner Umwelt rekonstruieren zu können.

Acknowledgment

The PhD-thesis at hand was realised in the frame of an interdisciplinary research project directed by the Institute of Geography at the Johannes Gutenberg-Universität Mainz, Germany, and the Ephorate of Antiquities of Corfu, Greece, associated with the Centre Camille Jullian UMR 7299, CNRS, Aix-Marseille Université, France.

Funding was granted by the German Research Foundation (DFG) in the context of the project *Extreme events in Holocene geoarchives on Corfu (Ionian Islands, Greece) and their impact on man and environment – XTREME EVENTS* (FI 1941/4-1 and VO 938/22-1). Work permits were kindly approved by the Institute of Geology and Mineral Exploration (IGME), Athens.

Numerous people were involved in realising and finishing this work. Without their assistance and perpetual encouragement this thesis would not have been possible!

[Namen und fortfolgende Abschnitte gelöscht]

Thank you.

Table of Contents

Table of Figures

Table of Tables

1 Introduction

1.1 Ancient Mediterranean harbours

On a global scale, the Mediterranean basin is the only region where three different continents meet forming a very distinctive and geologically highly dynamic physical environment where the interactions between man and environment are strong and complex (Woodward 2009). Not surprisingly, the Mediterranean Sea, its islands and bordering lands are considered to be one of the cradles of civilisation, inhabited by early humans already in early pre-history.

Here, first rudimentary sea-going abilities of hunter-gathers are suggested for at least the Middle Palaeolithic as indicated by the presence of stone tools on Crete, Sicily, Sardinia, Cephalonia, Zante or Cyprus (Abulafia 2011, Strasser et al. 2011) – islands, which were proven to have been already isolated from the mainland during that period of time (e.g. Ferentinos et al. 2012). These first seafaring activities were primarily introduced by environmental changes associated to the end of Pleistocene: Receding ice shields concomitant to a rapidly rising sea level led to the inundation of wide shelf areas (Fairbanks 1989), forcing coastal populations to move further inland, while rocky coasts were formed and islands were separated from the mainland. During the last stage of transgression, essentially around 4000 BC, when post-glacial sea level rise significantly decelerated (see for example Vött 2007b for northwestern Greece, Vacchi et al. 2016 for the western Mediterranean, Fontana et al. 2017 for Italy), waters gradually intruded lowlands, plains and valleys, forming plenty of coastal embayments. Simultaneous to stagnating sea level rise, increased sediment supply from the hinterland caused progradation of coastlines and the gradual re-shaping of formerly rough coasts towards deltaic and lagoonal systems – ideal nucleuses for intensive cultural development (Marriner et al. 2010, Anthony et al. 2014). It were these multifaceted environments along the present coasts, where human societies started to settle permanently due to easy access to the sea and the presence of fertile soils (van Andel 1989, Perissoratis & Conispoliatis 2003).

By the beginning of the Bronze Age around 2000 BC, inhabitants of the Mediterranean coasts came to value the vast opportunities of travel and trade by sea resulting in the beginning of significant sea trade activities all over the Mediterranean. While the incipiently small boats were certainly launched from land and stored at beaches, river mouth or estuaries, larger ships were needed for long-distance journeys (Franco 1996). The latter required appropriated harbours and docking facilities to be loaded and accommodated (Inman 1974, Oleson & Hohlfelder 2011).

Harbours were first constructed on river banks and deltas before they were established in the more difficult maritime context, where the techniques from fluvial infrastructure as well as the quasi-absence of tides in the Mediterranean Sea helped to build adequate sea-facing facilities (Marriner et al. 2008a). According to literary and archaeological sources, the construction of these sea-harbours propagated from the Levantine coast towards the west, most likely since the mid of the 2nd mill. BC (Raban & Galili 1985, Marriner et al. 2014a). However, dating the associated infrastructure unequivocally to the Bronze Age is very difficult, as the particular harbour facilities usually appear to be rock-cut such that sufficient stratigraphic information and adequate dating material are missing (Blackman 1982a). Thus, the first certainly dated harbour-related infrastruc-

ture constructed in a maritime context in the Mediterranean is associated to the Phoenicians. They built a pier at *Tabbat-el-Hammam* which was dated to 900 to 800 BC (Noureddine 2015, Knapp & Demesticha 2017). Nevertheless, certainly in 7th cent. BC, harbours were well-established at the Levantine coasts and not restricted to natural given features any more due to the new techniques in underwater constructions. During the same period of time and thus at least two centuries later than in the Levantine, harbour works also started in the Aegean Sea, where the broken, karstic landscapes offered various well-protected embayments that were used as natural harbours before (Blackman 1982a, Oleson & Hohlfelder 2011).

Due to the geopolitical situation in Geometrical and Archaic times, when no pan-Mediterranean Greek empire existed but hundreds of mostly independent entities and thalassocracies with no contiguous territory, supra-regional trade and military operations started to gain more and more importance, resulting in increased numbers of ships and considerable advancements in coastal engineering (Malkin 2011, Wilson 2011). One innovation of these times is the physical segregation of a military harbour on the one hand and a commercial one on the other hand reflecting not only emerging differences in the design of war- and merchant-ships but also the generally increasing sophistication of maritime technologies (Oleson & Hohlfelder 2011). Another new harbour feature was introduced by the western colonies of the Phoenicians, who established the so-called *cothon*, an artificially excavated harbour basin located onshore behind the coastline. The basin was connected to the sea by one or more channels and answered the problem of constructing ports on coasts that were exposed to waves or were lacking natural protection (Blackman 1982a, Franco 1996). This harbour design can be suggested as the predecessor of the Classical Greek *limen,* consisting of several natural bays that were protected by the construction of breakwaters built out from shore. The special type of a closable *limen kleistos* was even enclosed within the city's fortification and provided only small entrance channels, easy defendable (Lehmann-Hartleben 1923). Nevertheless and in spite of the general advantages in harbour engineering, beach harbours remained common (Oleson & Hohlfelder 2011).

In the Hellenistic Period, rising prosperity, intensified trade networks and the establishment of large kingdoms led to a further rapid increase of ships starting *c.* 200 BC, visible in a distinct peak in the number of found ship wrecks originating from this period of time (Wilson 2011). Consequently, more and especially larger harbours were built that feature new complex structures such as exterior and interior breakwaters, dry docks and dockyards, canals, causeways or even lighthouses, like in the example of the monumental harbour of Alexandria (McKenzie 2003, Oleson & Hohlfelder 2011). Such prominent infrastructure helped to reflect and save the maritime power of the Hellenistic kings (Blackman 2013a). The same is certainly true for Roman harbours. The Roman innovation of hydraulic concrete and the Romans' use of it led to the construction of large artificial harbour basins associated to structures that were built under water or on straight coastlines which otherwise would have remained unprotected due to missing natural protection (Blackman 1982b, Oleson & Hohlfelder 2011). These numerous and large harbour were used to host ships of increased size bearing witness of the distinctly intensified trade and military operations during the Roman period (Wilson 2011). Moreover, the Roman period is characterised by strong coastal artificialisation, during which waters were polluted by metals such as lead (e.g. Le Roux et al. 2003,

Elmaleh et al. 2012, Delile et al. 2014a, 2015b) and were older ports were severely re-modelled (e.g. Stanley & Bernasconi 2006, Marriner et al. 2014a, Hadler et al. 2015b).

In conclusion, ancient Mediterranean harbour basins provide a well-defined and time-related frame in maritime engineering and are thus expected to record useful chronostratigraphical information on the development of the harbours and their surrounding palaeoenvironment. Typical harbour characteristics range from semi- or hardly protected natural harbour bays at the very beginning in the Bronze Age to artificially constructed and well-protected basins that were built more or less independently from natural features during the time of the Roman Empire (Anthony 2014).

1.2 Ancient Harbours as key elements for geoarchaeological research

Independently from the period they were constructed in, ancient harbours represent unique geoarchives to detect and analyse environmental changes and complex interactions between humans and their environment (Inman 1974, Marriner et al. 2010). This is mainly due to the excellent preservation status of fine-grained harbour mud deposited under anoxic conditions (Marriner & Morhange 2007), numerous included cultural and biogenic remains helping to date the harbour sediments and associated infrastructure or even to reconstruct vegetation, climate or economy patterns in antiquity (Allevato et al. 2016), distinct geochemical patterns of harbour mud mirroring the magnitude of human influence (e.g. Lex Roux et al. 2003, 2005, Hadler et al. 2013, 2015, Vèron et al. 2006, Delile et al. 2014a) as well as several potential indicators for relative sea level changes (e.g. Auriemma & Solinas 2009).

However, harbours have been studied particularly by classical archaeology for a long time, focussing solely the analysis of the archaeological features and the reconstruction of ancient trade. Related paleoenvironmental settings were not considered as necessarily important and were reconstructed from literally sources mainly (Franco 1996, Marriner & Morhange 2007). Since the late 19th cent., however, geoscientific research was more and more involved into archaeological studies, as sedimentological information was found useful when written references were missing or ambiguous. The importance of this multi-disciplinary approach become apparent when considering the example of Troy, the famous Homeric city that has attracted travellers, historians and scientists for nearly two millennia (for location see Figure 1.1). In Antiquity, Homer (after Murray 1924) and Strabo (after Jones 1924) refer to Troy and its environs in several passages, providing hints for its exact location. Archaeological research, mainly encouraged by Schliemann (e.g. 1875), brought to light remains of the ancient city. Dating and topography of these remains together with findings from geomorphological research (e.g. Kraft et al. 1980, 2003) resulted in a comprehensive palaeogeographical reconstruction of Troy through space and time, ranging from the early Bronze Age, when Troy had a direct access to the sea, to the Roman period, when the coastline was located several kilometres further seaward because of deltaic progradation (see Vött & Brückner 2006 for a brief summary).

1.2.1 Geoarchaeology of Mediterranean harbours: State of the art

Until today, numerous harbour sites have been investigated in the Mediterranean in the frame of geoarchaeological studies since the 1990s (Figure 1.1) when pioneer projects were realized on the Levantine coast and France. At Caesarea Maritima in Israel, Reinhardt et al. (1994) investigated the development of the Roman harbour basin by use of micropalaeontological methods. At the same time, geoarchaeological research also started on the French coast at Marseille. Here, the evolution of the Greek-Roman harbour was reconstructed with regard to relative sea level fluctuations, human impact and natural variations in sedimentary processes by Hesnard (1994) and Morhange et al. (1996). During the following decades, the interdisciplinary research subject of harbour geoarchaeology established within the scientific community and multi-methodological studies were recognised as significant advancement when trying to understand complex sedimentological and archaeological systems (Marriner & Morhange 2007).

Facing the Levantine Sea, the harbours of Beirut, Sidon and Tyre (Figure 1.1) were the major centres of a widespread economic network since the Bronze Age. In recent years, the sedimentological record of these harbours was intensively investigated in order to obtain insights in the overall sea level and harbour history of the Levantine coasts (Le Roux et al. 2003, Marriner et al. 2005, 2006, 2008a, 2008b, 2014, Marriner & Morhange 2005, Elmaleh et al. 2012). The results show similar steps of harbour development at all three sites: Out of a transgressive lagoon, a proto-harbour developed during Bronze Age, which was transformed into an artificial basin by the beginning of the Iron Ages. During the Roman and Byzantine period, increased human impact is demonstrated by well-protected lagoon-type harbour mud showing high anthropogenic impacts at the land-sea interface before the harbours were abandoned and filled with debris (Marriner et al. 2014a). However, a completely different palaeoenvironmental development is considered for the harbours of Seleucia Pieria at the Levantine coast of Turkey (Pirazzoli et al. 1991, Erol & Pirazzoli 1992) and Caesarea Maritima in Israel (Reinhardt et al. 1994, 2006, Goodman-Tchernov et al. 2009, 2015), both strongly influenced by seismic impacts (see also chapter 1.2.2). Further to the south on the coast of Egypt, several studies tried to reconstruct the complex coastal geomorphology related to the monumental Hellenistic harbour basin of Alexandria by sedimentological (Stanley & Bernasconi 2006), geophysical (Chalari et al. 2009), palynological (Stanley & Bernhardt 2010) and palaeontological (Bernasconi et al. 2006) approaches.

Geoarchaeological research was also conducted in the Aegean Sea (Figure 1.1) in order to decipher the stratigraphy of the harbours of, amongst others, Ephesus (Stock et al. 2013, 2014, 2016, Delile et al. 2014b), Elaia (Seeliger et al. 2013, Pint et al. 2015), Rhodes (Stiros & Blackman 2014), Elaiussa Sebaste (Melis et al. 2015), Liman Tepe (Goodman et al. 2009) and Troy (e.g. Kraft et al. 2003). These sites turned out to be rich archives for reconstructing the history of man and environment in the eastern Mediterranean, covering a total time span of more than 3000 years from the Bronze Age (Troy, Liman Tepe) to the Roman-Byzantine Period (Ephesus, Elaiussa Sebaste).

Connecting the continents of Asia and Europe as well as the Mediterranean and the Black Sea, the importance of Istanbul in a geopolitical and historical context is self-evident. Istanbul's Byzantine harbour Theodosius was in function from the 4th to 11th cent. AD and built on top of archaeologi-

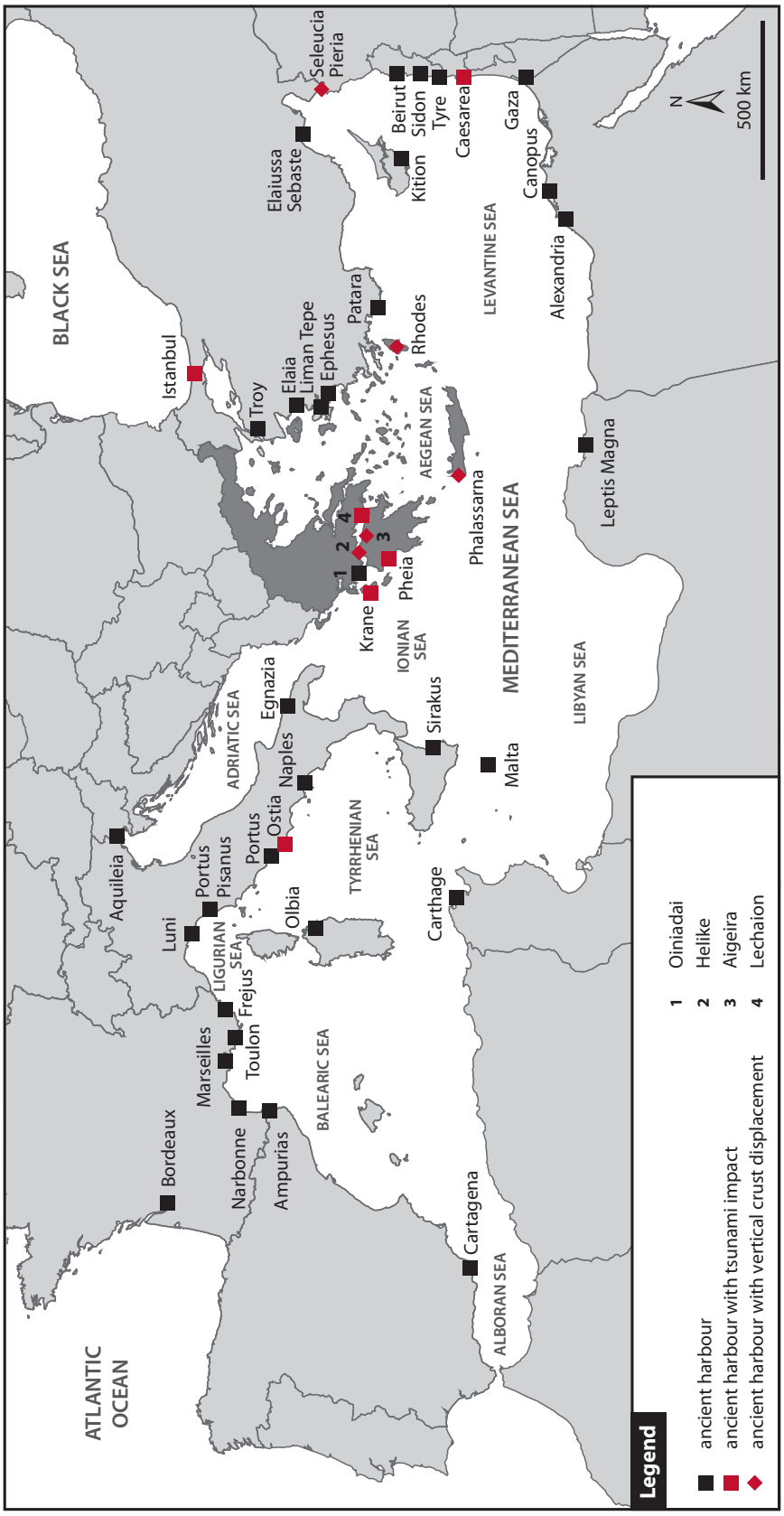

Figure 1.1: Map of selected ancient harbour sites in the Mediterranean that were studied in the frame of geoarchaeological research. Harbours are classified according to the seismic impacts trapped in their sedimentary and geomorphological record (map adapted and modified after Marriner & Morhange 2007 and De Graauw 2013 as well as studies cited in the text).

cal remains of a Neolithic settlement. Its sedimentary sequence provides numerous evidence for considerable sea level fluctuations, environmental changes and mirrors moreover the cultural history of the site (Algan et al. 2009, 2011, Bony et al. 2012).

In Italy, harbour geoarchaeology mainly concentrated on the ancient harbours of Rome, Portus and Ostia (Figure 1.1). Goiran et al. (2014) and Hadler et al. (2015) for example, worked in the Ostia harbour complex, stating the final abandonment of the harbour in the 1st cent. AD. The prominent harbour of Portus, only a few kilometres further to the north, was separated into two basins, those of Trajan and Claudius, which were both subject to comprehensive sedimentary, geochemical and microfaunal investigations (Goiran et al. 2010, Di Bella et al. 2011, Mazzini et al. 2011, Pepe et al. 2013, Sadori et al. 2010, Salomon et al. 2016). Further Italian harbours studied in the frame of multidisciplinary projects include, for example, those of Naples (Allevato et al 2016, Delile et al. 2016) and Luni (Bini et al. 2009).

Being one of the nucleuses for geoarchaeological research in the Mediterranean, the harbour site of Marseille turned out be an outstanding record for sea level changes in the younger Holocene. Based on marine fauna adhered to archaeological structures, Morhange et al. (2001, 2003) were able to construct a local sea level curve documenting that the Holocene sea level stand has never been higher than the present one. Le Roux et al. (2005) investigated the ancient harbour site with regard to lead pollution. They came to the conclusion, that it was especially Roman metallurgical activities causing vast lead contamination in the harbour, visible on increasing concentrations and shifts in isotopic ratios. In Frejus, located on the French Mediterranean coast as well, Bony et al. (2011) used sedimentological and biostratigraphical proxies to reconstruct pre-historic palaeogeographies and the development of the Roman harbour, which gradually transformed into a freshwater lake due to progradational processes.

Similarly, progradation was one of the key environmental triggers that affect the environs of the harbour site of Oiniadai (Figure 1.1), well-known because of its rock-cut Classical shipsheds (Gerding 2013). The harbour is located at the shores of the Acheloos River, where delta progradation started at 6000 BC resulting in the separation of a large lagoon that provided access to the shipsheds in Classical-Hellenistic times (Vött 2007a, Vött et al. 2007; see also Fouache et al. 2005).

For other parts of the Ionian Sea, the impact of tectonic events has been identified as main factor controlling the development, use and abandonment of ancient harbours (e.g. Pheia; Vött et al. 2011a). This is in particular true for harbours facing the Gulf of Corinth, seismically highly active. Here, comprehensive geoarchaeological studies were conducted in Aigeira (Papageorgiou et al. 1993), Helike (Soter & Katsonopoulou 2011) and Lechaion, the ancient harbour of Corinth (Morhange et al. 2012, Hadler et al. 2013; see also chapter 1.2.2 and discussion in Kolaiti et al. 2017) but also on Cefalonia Island in the ancient harbour of Krane (Hadler et al. 2013).

1.2.2 Mediterranean harbours as sediment traps for seismic events

The Mediterranean is one of the seismically most active regions on earth, influenced by various tectonic systems on a small scale (e.g. Sachpazi et al. 2000, Jolivet et al. 2009). The active nature of these systems is revealed by raised and submerged coastlines as well as earthquakes. The latter feature moment magnitudes of maximum 8.0 (Vannucci et al. 2004) and occur widespread in the Mediterranean, mostly associated to the main plate boundaries or clustered along microplates (Mather 2009). Together with landslides and volcanic eruptions these earthquakes function as triggers for tsunamis in the Mediterranean Sea, if their hypocentres are located in or close by the sea and in a shallow crust depths (Bryant 2008; Röbke & Vött 2017). Based on historical, geological and instrumental data, Papadopolous & Papageorgious (2014) classified distinct tsunamigenic zones along the Mediterranean coasts (Figure 1.2 A) depicting the general tsunami potential to be relatively high to very high in the Gulf of Corinth and along the Hellenic Arc, while an intermediate risk for tsunami triggering prevails on the coasts of the Ionian, Levantine and Tyrrhenian Seas. For Greece, tsunami potential was analysed by Papazachos & Dimitriu (1991, Figure 1.2 A), similarly identifying rifting in the Corinthian Gulf and subduction along the Hellenic Arc as main sources for tsunamis.

Seismic events related to this tectonically exposed location were already noticed, described and analysed in Antiquity. One of the earliest records is given by the Athenian historian and general Thucydides, who reported on an earthquake and associated tsunami that happened in the 5th cent. BC during the Peloponnesian War (Thucydides 3.89 after Crawley 1910). Based on these literary sources as well as on modern observations, earthquake and tsunami catalogues were assembled by e.g. Partsch (1887), Soloviev et al. (2000), Ambraseys & Synolakis (2010) and Stucchi et al. (2013). Even if unquestionable in use, these compilations comprise only a fractional amount of the total number of events as the historical record of seismic events is generally incomplete and furthermore highly depending on the time period and location (Hadler et al. 2012, Papadopoulos 2015). To complete these sparse datasets, sedimentological and geomorphological archives are urgently needed, preferably presenting sediment traps that provide relatively reliable sea level indicators and span long time series. Harbours turned out to completely fulfil these requirements. Moreover, their record can help to understand the human response to particular seismic events, as harbours were usually located in cultural centres (Mariner & Morhange 2007). Their distribution all over the Mediterranean Sea allows furthermore comparisons between distinct parts of the region.

Although harbour geoarchaeology has focussed the palaeoenvironmental reconstruction of harbours and their surrounding landscapes for a long time, concentrating on gradual coastal processes, recent studies also focussed abrupt palaeohazards as triggers for coastal changes in harbour settings (Figure 1.1, Morhange & Marriner 2011).

The harbour of Beirut, for example, has been repeatedly destroyed by catastrophic earthquakes. Ancient Beirut was located on a peninsula, facing the Levantine Sea. The area is considered to have an average return rate of 50 years for earthquakes >7 which is mainly related to three major fault lines, one of which directly intersects the harbour basin (Darawcheh et al. 2000, Marriner et al. 2008b). In the harbour archive itself, habitation layers originating to the Iron Age as well as the Ro-

man and Byzantine periods show distinct anomalies and fracture lines, linked to seismic impacts. The most prominent event, captured in the ancient harbour of Beirut, is the historical earthquake of July 9th 551 AD, that led to massive destruction of the harbour and the entire ancient city (Darawcheh et al. 2000). Most likely, the event also caused tsunami waves even if sedimentary traces were not observed in the ancient harbour basin itself. Nevertheless, after the event trade patterns in the Eastern Mediterranean changed and Beirut lost its status as economic and political centre shown by the fact that the harbour as well as many parts of the ancient cities were left in ruins and were abandoned (Marriner et al. 2008b).

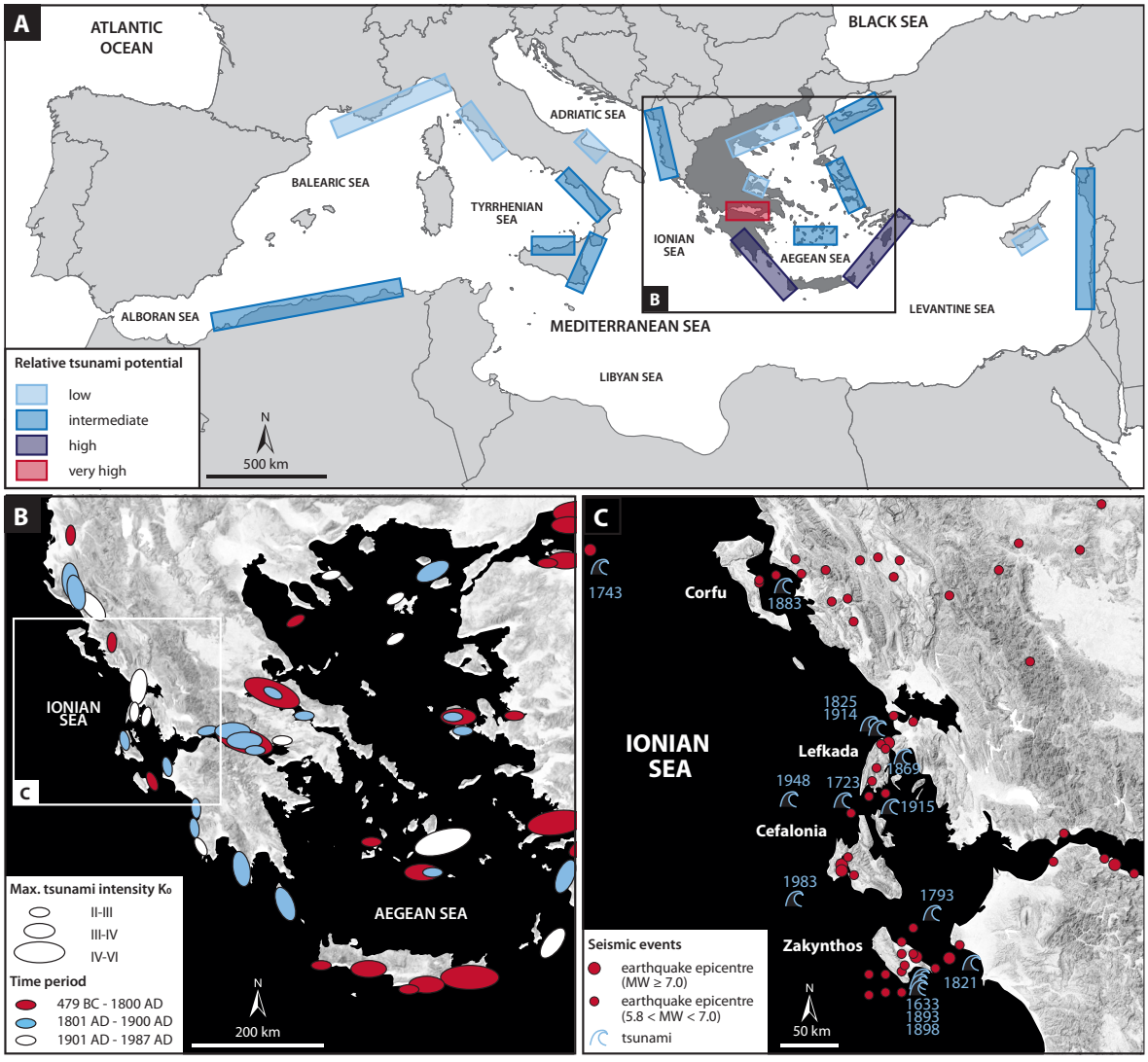

Figure 1.2: Tsunamigenic zones and tsunami events in the Mediterranean (A) Relative potential for tsunami events in the Mediterranean Sea according to documentary records showing highest tsunami risk in the Gulf of Corinth and along the Hellenic Arc (map modified after Papadopoulos & Papageorgiou 2014). (B) Known and Inferred tsunamigenic zones in the Ionian and Aegean Seas compiled by Papazachos & Dimitriu (1991). The elliptic form is orientated along the corresponding seismic fracture zone, while the size of the ellipses is proportional to the estimated maximum tsunami intensity. Colours refer to the time period, the tsunami event took place. Noticeable is the lack of pre-1800 events in the norther Ionian Sea. (C) Known tsunami events in the northern Ionian Sea as reported by modern tsunami catalogues supplemented by earthquake epicentres (red dots) from seismic events that occurred between 1000 and 1899 AD and featured moment magnitudes > 5.8. (map adapted and modified after Hadler et al. 2012, tsunami events after Partsch 1887, Soloviev et al. 2000, Ambraseys & Synolakis 2010; earthquake epicentres after Stucchi et al. 2013)

Apart from earthquake-induced damages, harbours may also face co-seismic movements, restraining their unrestricted navigability due to rapid coastal uplift or their protective location due to submerging of their protective infrastructures, e.g. moles, quays or breakwaters. The most prominent example for a harbour bearing witness of rapid coastal uplift is the one of Phalasarna, located in western Crete and facing the subduction zone of the Hellenic Arc towards the south. In Roman times, most probably in 365 AD, the harbour complex was uplifted by more than 6 m, (Pirazzoli et al. 1992, Dominey-Howes et al. 1998, Werner et al. 2017).

At Rhodes, seismic impacts generated by the Hellenic Arc were derived from ship ramps constructed in the Hellenistic period to pull ships out of the water. These ramps indicate two different seismic movements: subsidence of *c.* 1 m linked to a major earthquake that happened in Hellenistic times, requiring a re-pavement and reconstruction of the ramps, and co-seismic uplift of around 3 m causing the abandonment of the harbour in the 2nd cent. AD (Stiros & Blackman 2014).

Apart from the Hellenic Arc, the half-graben structure of the Gulf of Corinth represents one of the seismically most active area in the Mediterranean Sea (Figure 1.2 A, B). Its seismic activity is mainly related to continental rifting caused by the westward movement of the Anatolian Plate, resulting in a drift rate of 16 mm per year (e.g. Doutsos & Kokkalas 2001). On the southwestern coast of the Gulf, at the ancient site of Helike (Figure 1.1), numerous episodes of rapid co-seismic subsidence were observed by Soter & Katsonopoulou (2011). Opposite to gradually appearing regional uplift, rapid coastal submergence happened at least three times, for example in 373 BC, when the Classical city of Helike was submerged and drowned in a lagoon (Soter & Katsonopoulou 2011).

Tectonically induced fluctuations in local relative sea levels have also affected other parts of the Corinthian Gulf. Based on the geomorphological studies in the Roman harbour of Aigeira, Papageorgiou et al. (1993) found evidence of coastal uplift of 2 m since Hellenistic times. At Lechaion, the ancient harbour of Corinth, situated on the very eastern coast of the Corinthian Gulf, co-seismic uplift of *c.* 1 m occurred (Stiros et al. 1998). Hadler et al. (2013) provide arguments based on sedimentological features and microfaunal evidence supporting the idea that tsunamigenic impact was the main cause for siltation and abandonment of the ancient harbour at Lechaion. These findings are doubted by Kolaiti et al. (2017) in favour of gradual coastal processes that affected the area over centuries.

The word tsunami is derived from the Japanese language and means harbour wave, composed of the Japanese words *tsu* (wave) and *nami* (harbour). The term was established as tsunamis usually stay unnoticed on the open sea but cause strongest destruction at the coasts, especially in bays and harbours (Rajendran 2006, Sugawara et al. 2008). Thus, depending on the harbour's overall structure, its basin might function as sedimentological trap for tsunami imprints, independently whether the tsunami impact caused destruction at the harbour's infrastructure or not.

So far, several harbour sites throughout the Mediterranean have proved their function as sediment traps. For example, the Byzantine Theodosia harbour in Istanbul revealed a coarse-grained tsunami-related layer, probably associated to an earthquake in 557 AD. Harbour sediments helped to identify at least three tsunami wave trains differing in energy milieu and backwash flow (Bony et al. 2011). In Israel, numerous tsunami imprints from various time periods were found in

the Roman harbour of Caesarea Maritima, the oldest related to the Santorini eruption during the late Bronze Age and the youngest to an earthquake in 115 AD, leading to the rapid decline of the harbour site (Reinhardt et al. 2006, Goodman-Tchernov et al. 2009, Goodman-Tchernov & Austin 2015). At Ostia, the stratigraphical record revealed three tsunami landfalls, the latest associated to the burial of the lagoonal harbour and the establishment of a nearby river harbour, post-dated by a temple complex to the period before the 1st cent. AD (Hadler et al. 2015b).

For the Ionian Sea, no pre-Medieval tsunami event is known from historical records due to the incomplete nature of literary datasets (Figure 1.2 B, C; Hadler et al. 2012). However, older tsunami deposits were found in the sedimentological record of the ancient harbour sites of Krane (Hadler et al. 2011) and Pheia. The latter site, located on the western coast of the Peloponnese, hosted one of the harbours of ancient Olympia and was completely destroyed by rapid subsidence and related tsunami waves in the 6th cent. AD (Vött et al. 2011a).

1.2.3 Human interventions in harbours: Dredging

Harbour basins also comprise the magnitude and frequency of anthropogenically forced changes in coastal contexts (Marriner & Morhange 2007, Morhange & Marriner 2011). These anthropogenic interventions might be of morphological nature, e.g. in the form of harbour construction works and related infrastructure such as breakwaters or moles, or can be mirrored by palaeo-contaminations of lead, one of the first metals known and used by man (Le Roux et al. 2002, 2005, Vèron et al. 2006, Hadler et al. 2013, 2015, Delile et al. 2014a, Stock et al. 2016).

Harbours were built as protective and at least party enclosed basins, which is why natural sediment accumulation usually exceeded erosional processes. Following this, the main problem in ancient harbour maintenance was to keep the port navigable and to prevent it from silting up, a process that was even reinforced by local relative sea level fluctuations (e.g. co-seismic uplift and subsequent decrease of water depth; see chapter 1.2.2) and the input of waste and other debris (Marriner & Morhange 2007).

Thus, prevention of silting up was one of the main goals of many harbour-related infrastructures. Moles and breakwaters were built to shield the inner harbour from silt-loaded currents (e.g. van Rijn 1995). If constructions were not able to restrain sediment-bearing tides and currents from entering the harbour, the abrupt flushing of the basin by controlled currents through sluices, channels or underwater canals (see e.g. for the harbour of Sidon Poidebard & Lauffray 1951) was used as de-siltation method (Blackman 1982b). Already Strabo (14.1.24 after Jones 1924) reports on a mole at the harbour entrance of Ephesus (for location see Figure 1.1) that was built to protect the harbour from silting caused by sediments of the Caÿster River.

However, prevention policy did not succeed in every case and was – if successful – only effective for a relatively short period of time, such that repeated cleaning and dredging was the only way to ensure long-term sufficient harbour depths (Morhange & Marriner 2011, Wilson 2011, Morhange et al. 2016).

First rudimentary dredging activities are assumed for the Bronze Age (Fabre 2004), although archaeological or literary evidence is still missing to prove this speculation. In contrast, written evidence for dredging activities dates back to the Roman period and is given by Strabo (14.1.24 after Jones 1924) and Tacitus (16.23.1 after Church et al. 1942), both reporting on the opening of Ephesus in Roman times. This process required suitable devices and technical equipment like dredging vessels that allow to deepen the harbour's bottom on a large scale.

Archaeological evidence for such boats was found in Marseille where three ship wrecks (*Jules Verne* 3, 4 and 5) were found during archaeological excavations in the ancient harbour basin at *place Jules Verne*. These wrecks were dated to the 1st to 2nd cent. AD (Pomey 2011) and gained particular interest as they change the understanding of Roman harbour maintenance. All three ships were characterised by a very flat-bottomed form and feature a rectangle structure in their very centre, opening the hull to the sea (Figure 1.3). This extraordinary design accompanied with traces of extensive repair works indicate that the ships where constructed and needed for a special type of harbour work. As archaeological data documents dredging activities in the harbour basin for the same period of time, it is very likely that these vessels were used for dredging. Furthermore, a wooden gearwheel was found near one of the wrecks, which is why these ships were probably equipped by a dredging device, using a line of buckets and a gearwheel, similar to typical Roman hydraulic machines (Pomey 1995).

By using dredging vessel like those found in the record of the ancient Marseille harbour, the Romans were able to ensure a suitable depth of the harbour basin over a relatively long period of time. These dredging activities – especially when performed repeatedly – left sedimentological traces within ancient harbour records.

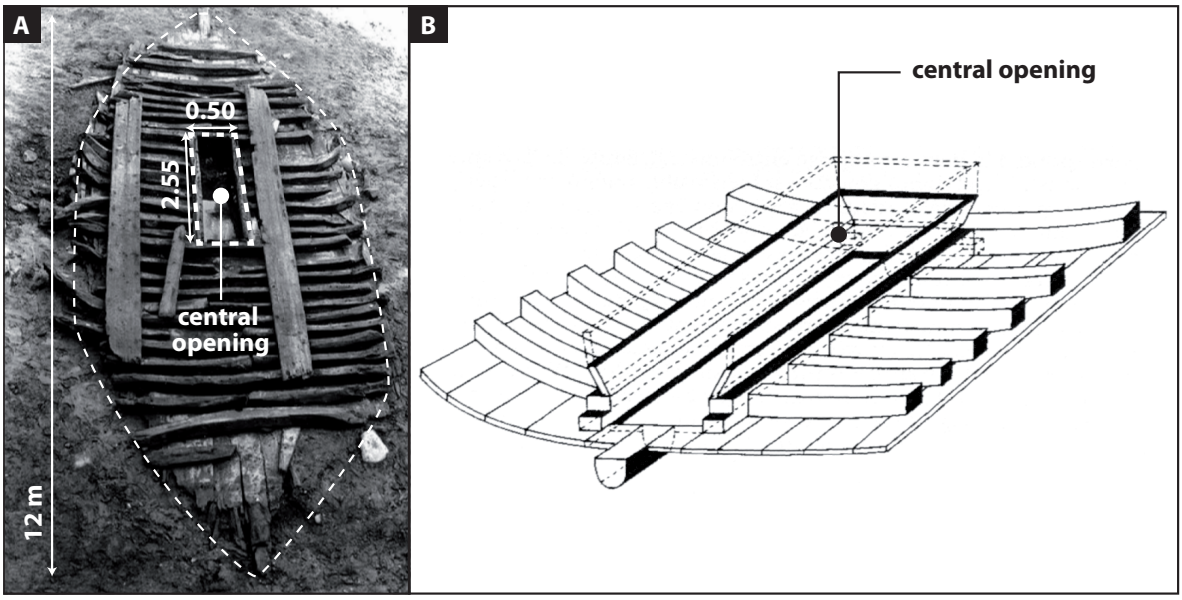

Figure 1.3: Roman dredging vessel. (A) Photograph of shipwreck *Jules Verne 3* excavated in the ancient harbour of Marseille. The wreck dates to the 1st to 2nd century AD and is characterised by a rectangle-formed structure in the centre, opening the hull towards the sea. (B) Reconstruction of a Roman dredging vessel based on shipwreck *Jules Verne 5*, including fragments of planks that originally formed an inner casing around the central opening of the hull (adapted and modified after Pomey 1995).

In very rare cases, dredging operations can be directly linked to translocated and dredged material, dumped by man in the close proximity of the dredging site. In the Netherlands in the Roman harbour of Velsen for example, van Rijn (1995) detected an uneven surface of the harbour bottom characterised by deep cuts into the underlying pre-Roman deposits while a homogenised layer of silty clay including typical harbour rubbish was found in the formerly deeper parts of the ancient basin. Apparently, the Romans repeatedly cleaned the Velsen harbour in its shallower parts and deposited the dredged material in greater depths.

Another example for an ancient harbour where dredged material is still preserved is Tyre, situated on the Levantine coast. Here a layer of fine-grained clay deposited south of the city attracted scientific attention. Based on granulometric investigations, Marriner et al. (2008a) hypothesises that these deposits represent Iron Age material which was removed from the northern harbour by Roman dredging and brought there to be used in the ceramics and construction industries.

A further case study is Lechaion, the ancient harbour of Corinth. It features large mounds along its s-shaped harbour basin which originated from dredging activities (e.g. Stiros et al. 1996, Morhange et al. 2012, Hadler et al. 2013). In contrast to typically fine-grained harbour sediments, the dredging mounds in Lechaion are made of sand and gravel and also include marine fauna and ceramics. For this reason, Hadler et al. (2013) state that these mounds refer to exceptional dredging operations after the input of coarse-grained marine sediments into the well-protected harbour basin by tsunami impact.

Dredging usually left erosional sedimentary features rather than accumulative ones. The former often show a poor conservation status and are consequently difficult to identify. This is not the case in the ancient harbour of Naples, where concave grooves caused by dredging practice were found well-preserved as they were carved into the solid volcanic substratum (e.g. Fregonese et al. 2016). These traces in Naples mirror dredging activities occurring already in the Hellenistic period between the end of the 4th cent. BC and the 2nd cent. BC (Carsana et al. 2009, Delile et al. 2016). They show that dredging was not restricted to Roman time but was also conducted by the ancient Greeks in order to prevent the harbour basins from silting.

Another type of erosional marks related to ancient dredging are erosional contacts between pre- or older harbour sediments and overlying harbour mud. In the harbour of Marseille, a typical erosional contact was found in the form of a fossilised scouring talus (Morhange & Marriner 2010). This talus represents a cut-and-fill structure which means that the formerly accumulated pre-Roman harbour record was cut down to a coarse-grained oyster-shell layer by dredging before the stratigraphical gap was filled by cohesive Roman harbour mud. Sedimentary remains of this process are today visible by a sharp and angular erosional contact in a trench that was excavated in the frame of geoarchaeological investigations in Marseille (Morhange & Marriner 2011).

Two further indicators of dredging are known from geoscientific studies, namely (i) chronological inversions and (ii) chronostratigraphical gaps (Morhange & Marriner 2007, 2010). Age inversions may occur when considerable amounts of sediment are disturbed or translocated during dredging operations (Salomon et al. 2016). At Lechaion, for example, Hadler et al. (2013) suggest that radiocarbon age inversions in the harbour record are due to dredging activities in the 1st cent. BC.

In the stratigraphical record of Tyre, age-inversions in radiocarbon dates concurrent with chronological anomalies were found as well, indicating cleaning and deepening of the harbour basin. This hypothesis is furthermore supported by linear regression of radiocarbon dates from the Graeco-Roman to Byzantine period, stating an average accumulation rate of 10 mm sediment per year, which would mean the complete filling of the harbour basin in 200 years without dredging (Marriner & Morhange 2006a).

Yet, the most common traces of dredging practice are stratigraphical gaps. At the harbour sites of Ostia and Portus, for instance, geoarchaeological reconstruction based on sedimentary data and radiocarbon dating revealed distinct chronostratigraphical gaps spanning several centuries (Goiran et al. 2014, Delile et al. 2014b, Salomon et al. 2016). Due to the strong sedimentary dynamics of the Tiber River resulting in generally high sedimentation rates, a hiatus of several centuries is not considered as natural and rather related to anthropogenic cleaning of the harbour site by dredging. However, for the cases of Portus and Ostia, further interpretations like erosion caused by the impact of extreme events should also be considered (Hadler et al. 2015b). At Naples, where erosional features attest dredging operations in the ancient harbour basin (see above), data published by Delile et al. (2016) strongly supports the idea of a second, later dredging phase due to an associated stratigraphical gap, namely between the 3rd and 5th cent. AD. Stratigraphical gaps due to dredging were also found in the harbour of Frejus (Bony et al. 2011).

Larger gaps in the stratigraphical records were detected in ancient harbours at the Levantine coasts. Here, repeated dredging activities caused the paradox of quasi archiveless Phoenician harbours (Marriner et al. 2008a, Morhange & Marriner 2010, 2011). At Sidon, the whole 1st mill. BC strata is missing in the harbour record (Marriner & Morhange 2005, 2006a, 2006b), while further to the south, at Tyre, sediments spanning the periods of the Bronze Age to Persian times (*c.* 4000 to 500 BC) are absent in the harbour archive (Marriner & Morhange 2006a, Marriner et al. 2008a, 2014), both indicating large-scaled harbour dredging during the Roman and Byzantine periods.

1.3 Tracing the harbours of ancient Corcyra

The compilation of multi-disciplinary geoarchaeological studies, presented in chapter 1.2 is not exhaustive at all but shows that ancient Mediterranean harbours are valuable geoarchives where complex man-environment interactions are preserved. The sedimentary record of these harbours might trap anthropogenic or seismic impacts and is thus of inevitable importance to comprehend the spatial evolution of cities and their occupation histories, as well as the human use and abuse of the Mediterranean physical environment or the impact of natural catastrophic impacts (Walsh 2004, Marriner & Morhange 2007).

However, comparable geoarchaeological studies focussing the harbour record of Corfu are missing so far, although ancient Corcyra was one of the prevailing naval powers in the Archaic period due to a considerable fleet of triremes and suitable harbour infrastructure to host it (Thucydides 1.36.3 after Dent 1910; Baika 2013a).

1.3.1 Study area

Corfu is the northernmost island of the Ionian archipelago situated in the northern part of the Ionian Sea, one of the seismically most active and rapidly deforming regions in Europe (Sachpazi et al. 2000, Figure 1.2 A, B). Here, geomorphological processes are strongly related to an extraordinary tectonic stress field which is influenced by the subduction zones of the Calabrian and Hellenic Arcs, continental collision of the Adriatic microplate and Apulia towards Eurasia, strike-slip motions of the Cefalonia Transform Fault as well as several smaller local fault systems like the Corfu Thrust as large thrust fault on the island itself (e.g. Hollenstein et al. 2006, Billi et al. 2007, Kokkalas et al. 2006; for a detailed description on the tectonic setting see chapters 2.2, 3.2.1 and 4.2.1).

Consequently, the area was repeatedly affected by large and numerous earthquakes of local to regional extent (Stucchi et al. 2013). Figure 1.2 C depicts epicentres of earthquakes that occur in the northern Ionian Sea between 1000 and 1899 AD and featured a moment magnitude of at least 5.8 attesting the generally high seismic vulnerability of the Ionian Sea. The most prominent earthquake with a moment magnitude of 7.2 happened in 1953 on Cefalonia, when considerable coastal areas on the island were severely destroyed. In the course of this massive event the island was uplifted for 0.3 to 0.7 m and tilted westward in its central part (Stiros et al. 1994). Co-seismic uplift was also overserved on Corfu, where the presence of emerged bio-erosive notches document at least two phases of crust uplift in the western and central parts (Pirazzoli et al. 1994, Evelpidou et al. 2014). Mastronuzzi et al. (2014) even suggest that these phases of crust movements where associated to tsunami landfall in adjacent regions, however, these authors do not present contemporaneous tsunamigenic layers on Corfu.

Nevertheless, several tsunami events are known in the Ionian Sea from historical records (Figure 1.2 C; cf. Partsch 1887, Soloviev et al. 2000, Ambraseys & Synolakis 2010, Stucchi et al. 2013). According to these catalogues, frequent tsunami inundation happed since the 17th cent. all over the Ionian Islands whereas no historical record is available for the time before. However, multiple post-medieval observations of tsunami landfall together with distinct sedimentary evidence of older tsunami traces on Cefalonia (Hadler et al. 2011, Vött et al. 2012, Willershäuser et al. 2013), Lefkada (Vött et al. 2006, 2009b, May et al. 2012a, 2012b), Akarnania (Vött et al. 2009a, 2011a) and southern Italy (Mastronuzzi et al. 2007, De Martini et al. 2012) rather indicate an incompleteness of the historical dataset than an absence of seismic events before the 17th cent. AD (Hadler et al. 2012).

One may therefore conclude that the island of Corfu is situated in a seismically active region, where earthquakes of destructive nature, multiple tsunami impact and local co-seismic crust movements happened frequently in history. Whereas these events have been investigated in the frame of numerous geoarchaeological studies focussing natural geoarchives and harbour basins on the Ionian islands of Cefalonia and Lefkada, only few studies deal with geoarchives on Corfu. These include geomorphological investigations on uplifted notches (Pirazzoli et al. 1994, Evelpidou et al. 2014, Mastronuzzi et al. 2014; see above) and geoarchaeological multi-proxy analyses of traces of extreme wave events recorded in coastal lagoons (Fischer et al. 2016a). However, ancient harbour geoarchives have not been used to reconstruct ancient landscapes as well as to identify seismic-induced events on Corfu.

Ancient Corcyra was founded in the late 8th cent. BC as Corinthian colony in the central part of the island, facing the shallow and quiescent Gulf of Corfu to the east (Kiechle 1979). The city evolved from the Analipsis Peninsula from where it extended to the coastal lowlands north and west of the ridge, up to 60 m high (Figure 1.4 A). Regarding the harbours of ancient Corcyra, historical records indicate at least three harbours (Thucydides 3.72.3 after Crawley 1910, Gehrke & Wirbelauer 2004, Baika 2013a) two of which are documented by archaeological traces.

The military Alkinoos Harbour was located north of the Analipsis Ridge and opened towards the Bay of Garitsa as documented by archaeological remains of trireme shipsheds (Figure 1.4 B, see also chapter 2). On the contrary, the Hyllaikos Harbour is assumed on the western shore of the Analipsis Peninsula, occupying the eastern coasts of the protected Chalikiopoulou Lagoon (Figure 1.4 A). Yet, the exact spatial extent and specific design of both harbour sites remains still conjectural. The eastern and western spatial limits of the Alkinoos Harbour, for example, have not yet been traced: Less than 200 m east of the shipsheds archaeological research brought to light the remains of a monumental quay wall, which might belong to the Alkinoos Harbour or represent a further, separated harbour basin (Figure 1.4 C). Similarly, it is still speculative, if the harbour basin extended to west, where archaeologists recently excavated a section of the ancient fortification wall close to an Archaic building (Figure 1.4 D; Andreadaki-Vlazaki 2012).

For the Hyllaikos Harbour, information on its distinct location are also sparse. On the southwestern coasts of the Analipsis Ridge remains of shipsheds indicate the broad location of the harbour basin (Blackman et al. 1998, Riginos et al. 2000, Kanta-Kitsou 2001, Baika 2013a) while the northern extent of the harbour cannot be defined by archaeological remains. Moreover, the adjacent area was severely reshaped and transformed by the construction of the nearby runway of the international airport in the 1950s. Nevertheless, remains of Classical-Hellenistic buildings in the very northern part of the assumed Hyllaikos harbour site indicate that this area was already land during the Classical period (Figure 1.4 E).

1.3.2 Aims of the study and outline of research

The present study aims to analyse different geoarchives on Corfu which are promising candidates in order to decipher the multi-faceted palaeoenvironmental history of the ancient city and its harbours. The main objectives of the study are

i. to search for ancient harbour sediments in order to reconstruct the exact location and extent of the harbours of Corcyra,

ii. to analyse harbour sediments with regard to their sedimentary, geochemical, and micropalaeontological characteristics to compare it to typical Ancient Harbour Parasequence (Marriner & Morhange 2007) and to other ancient harbour records,

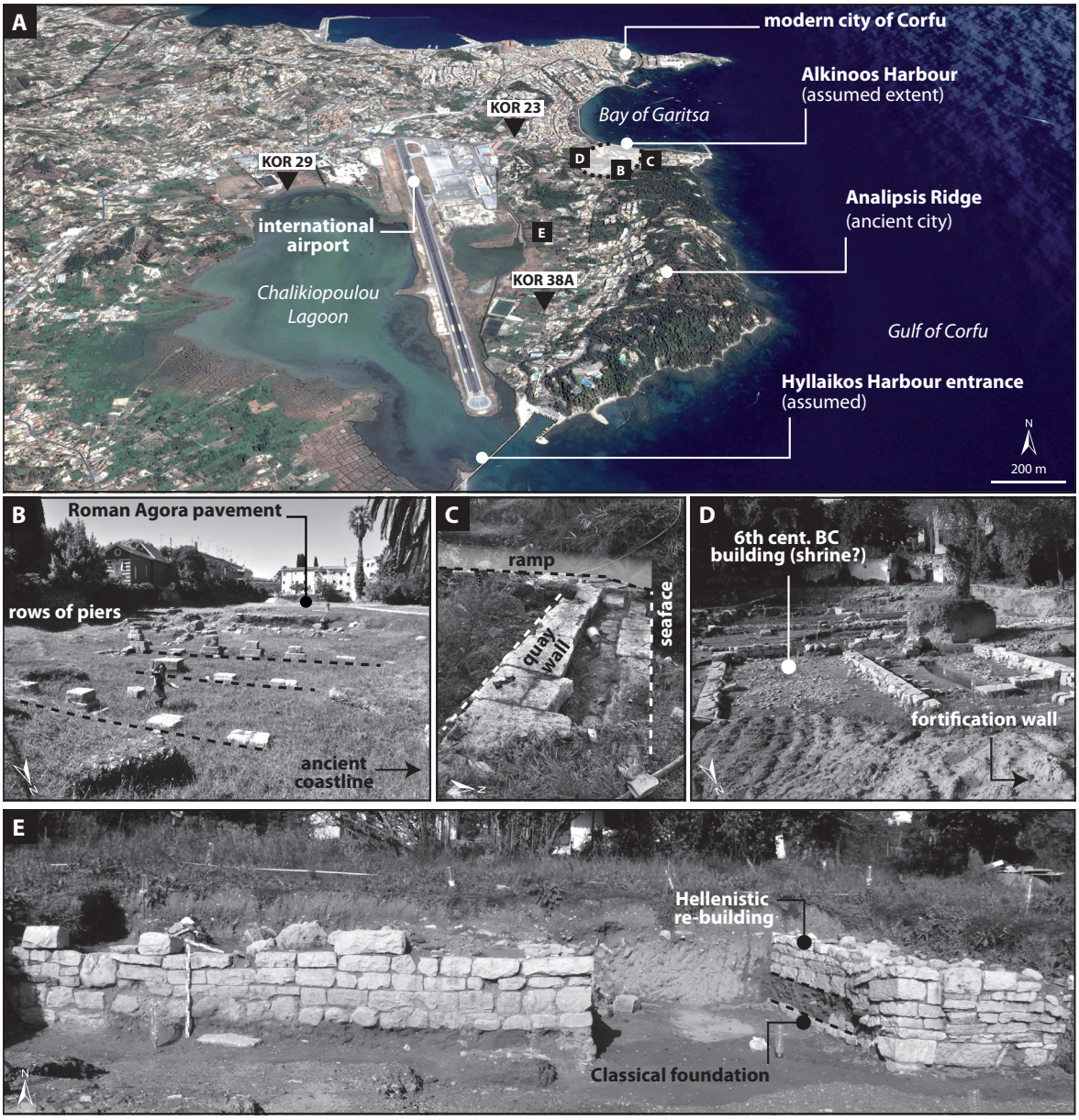

Figure 1.4: Bird's eye view on the study areas presented in this work (based on Google Earth image, taken in 2013). (A) Study areas are located along the shores of the Analipsis Peninsula where archaeological remains indicate the location of the ancient harbours of Corcyra (black rectangles, letters B to F) or at geomorphological key sites (black triangle; KOR 23, KOR 29). (B) Archaeological remains of shipsheds at the Kokotou site, dating to the Classical period. Today, the three rows of piers are situated c. 200 m away from the present coastline (photo by A. Vött 2012). (C) Segment of the Classical Pierri quay wall, which is interrupted by a ramp towards a western direction (photo by A. Vött 2013). (D) At the Desylla site, remains of an Archaic two-roomed building and a strong wall section that is interpreted as fortification wall were excavated in the frame of archaeological research. To the northeast of the site a further shipshed complex indicates the close proximity to an ancient harbour basin (modified after Andreaki-Vlazaki 2012). (E) Archaeological remains of Classical-Hellenistic buildings at the eastern shore of the Chalikiopoulou Lagoon (photo by A. Vött 2012).

iii. to establish a comprehensive geochronostratigraphical model by means of sedimentary data and dating approaches to decipher the palaeogeographical evolution of the study sites and the environs of Corcyra from the mid-Holocene to modern times,

iv. to detect and identify the main triggers for coastal changes on Corfu, both within ancient harbour settings and their natural predecessors/successors,

v. to check whether the harbours of Corfu might function as suitable archive for human interventions and extreme events in order to detect and analyse complex interactions between men and environment.

Study sites were chosen according to archaeological remains related to the northern harbour zone of ancient Corcyra (Figure 1.4 A).

First, on-site studies were conducted at the Kokotou site where archaeological remains of monumental Classical shipsheds indicate the location of a harbour basin (Figure 1.4 B, chapter 2), as well as at the Pierri quay (Figure 1.4 C, chapter 3). Further research was carried out on the very eastern part of the assumed Alkinoos Harbour basin, at the Desylla site (Figure 1.4 D, chapter 4), located in the surroundings of a further shipshed complex (Dontas shipsheds). Here, a two-roomed building dating to Archaic times and a wall section were found during archaeological excavations, the latter most likely related to the city's fortification. Finally, investigations within the frame of archaeological rescue excavations were realized on the western coasts of the Analipsis Ridge. Here, the remains of Classical to Hellenistic buildings indicate solid land already during the Classical period (Figure 1.4 E, chapter 4).

These on-site analyses were supplemented by off-site investigations at sedimentological key sites (Figure 1.5). In particular, studies were conducted at the northern fringe of the Chalikiopoulou Lagoon, in a very protected and shallow lagoonal environment in order to decipher the natural development of the lagoon and to identify triggers for environmental changes. Moreover, geoarchaeological investigations were also realised at the western coast of the Analipsis Peninsula to gain further insights in the palaeoenvironmental history of ancient Corcyra. A further archive containing comprehensive information on the environmental evolution of the Analipsis Peninsula through space and time was found on the narrow isthmus separating the Analipsis Ridge from the modern city (chapter 4).

A wide range of methods was used to analyse these key sites: Fieldwork comprised terrestrial vibracoring including sampling, geophysical prospection and direct push electrical conductivity (DP-EC) logging as well as differential GPS measurements to obtain high-resolution position data. Moreover, archaeological remains were surveyed and mapped regarding their age, position and features to link sedimentary data to the general archaeological context. In the laboratory, sediment samples retrieved from vibracoring were analysed regarding their geochemical characteristics by use of a portable XRF device and a magnetic susceptibility meter. Furthermore, grain size after the Köhn pipette method, loss on ignition and the content of palaeontological remains

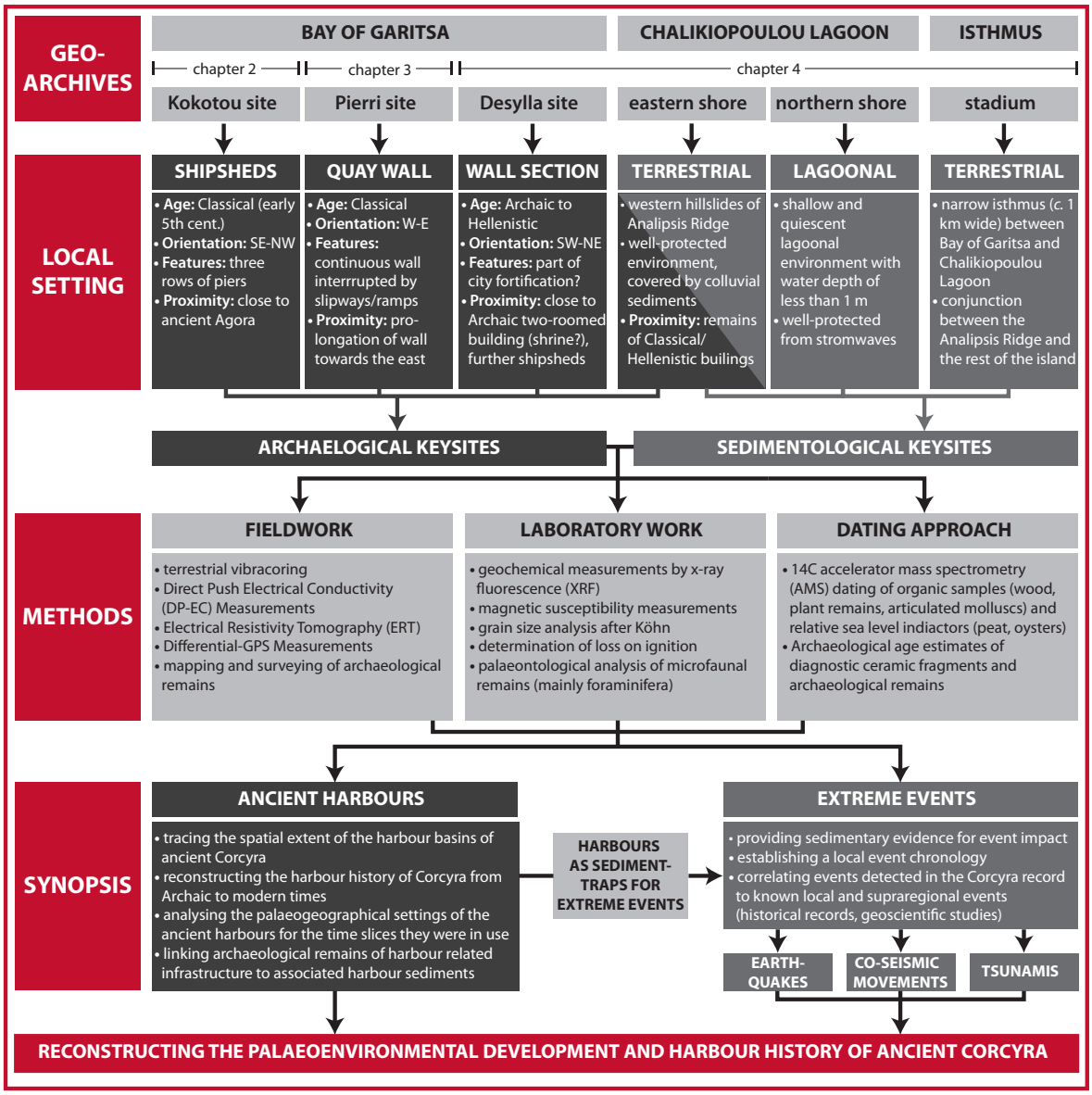

Figure 1.5: Conceptional framework and research design of the present study. Depicted are the main study areas with their local archaeological or geomorphological settings, the general methodological approach as well as the content-related key aspects.

(mainly foraminifera) were determined. Based on these analyses, different sedimentological facies were classified and geochronologically correlated by means of ^{14}C AMS dating of organic samples and archaeological age determination of diagnostic ceramic sherds. Detailed information on methodological approaches are given in the individual chapters (chapters 2 to 4)

Results based on this multi-methodological approach are presented and discussed with regard to the site-specific palaeoenvironmental development and their implications to the particular on-site harbour conditions (chapters 2 to 4).

Finally, findings from all study areas were linked and compared to each other in order to reconstruct the spatial extent, temporal development and palaeogeographical setting of the harbour basins of Corcyra from Archaic to modern times (chapters 4 and 5). Moreover, the present work

will examine the harbours' function as sediment-trap for seismic extreme events, including earthquakes, tsunami landfalls or co-seismic movements. These events detected in the Corcyra harbour record will be sedimentologically identified, classified and correlated to local regional and supra-regional events known from further geoscientific studies or historical records.

2 Tracing the Alkinoos Harbour of ancient Kerkyra and reconstructing its palaeotsunami history

ABSTRACT. In this study, the Alkinoos harbour of ancient Corfu was investigated by means of geomorphological and sedimentological methods in order to reconstruct the ancient harbour's construction, its period of use and spatial extent, and local palaeoenvironmental changes. We present first sedimentological evidence for the Alkinoos Harbor with distinct signs of dredging activities. Although the harbour must have been in use from the Archaic period onwards, a set of palaeoenvironmental proxies based on vibracoring, geophysical prospection, electrical conductivity logging, microfaunal studies and geochemical analyses revealed typical sediments of a closed, protected Roman harbour which was in use between the 1st and 6th cent. AD In addition, sedimentological and microfaunal evidence allow to differentiate between different parts of the Roman harbour. In contrast, the pre-Roman harbour and its shipsheds were built on a sandy seashore. Our data revealed two distinct stratigraphic disruptions related to tsunamigenic impact. These palaeotsunamis were dated between the 3rd and 6th cent. AD and between the 5th and 6th cent. AD, most probably correlating with the AD 365 (Crete) and 6th cent. AD (Peloponnese) supra-regional events, respectively. The Alkinoos Harbor turned out to be an outstanding geoarchive to reconstruct man-environment interactions during the late Holocene.

This chapter is based on Finkler et al. 2017a.

2.1 Introduction

The island of Corfu, located in the Ionian archipelago of northwestern Greece (Figure 2.1 A), has a multifaceted history. From the Archaic period onwards (8th to 6th cent. BC), the ancient harbour-city of Corcyra (modern Kerkyra = Corfu), emerged as a prevailing sea power in the Mediterranean and took part in the first naval battle ever recorded in Greek history (Thucydides 1.13.4 after Crawley 1910). In the beginning of the Classical period (early 5th cent. BC), it was one of the first Mediterranean city-states (*polis*) to acquire a considerable fleet of triremes and to build adequate harbour and naval installations to accommodate it (Baika 2003, 2013a).

Geoscientific analyses of palaeoenvironmental changes through space and time are relevant to better understand the naval status of Corfu, especially in relation to coastal dynamics and the manifold interactions between humans and the local environment. Coastal landscapes are prone to rapid change, and it is therefore important to detect and analyse palaeoenvironmental shifts and evaluate how cultures may respond to them. In particular, relative sea level changes, whether caused by abrupt phenomena like co-seismic movements and extreme wave events, or gradual shifts related to climatic oscillations and human impacts are all important triggers for palaeoenvironmental change in coastal settings like Corfu.

Unfortunately, geoarchives preserving sedimentary evidence suitable for disentangling the complex history of human-environmental interactions are rare. Ancient harbour deposits are of great interest for geoarchaeological research as they often display excellent preservation due to anoxic, quiescent conditions and are commonly located in cultural centres (Marriner & Morhange 2007, Morhange et al. 2014). Ancient harbours in the Mediterranean that have been investigated within a framework of interdisciplinary geoarchaeology include those along the coasts of Greece (Fouache et al. 2005, Vött 2007a, Vött et al. 2007, Mourtzas et al. 2014, Stiros & Blackman 2014, Hadler et al. 2015a), Italy (Bini et al. 2009, Di Bella et al. 2011, Mazzini et al. 2011, Goiran et al. 2014, Millet et

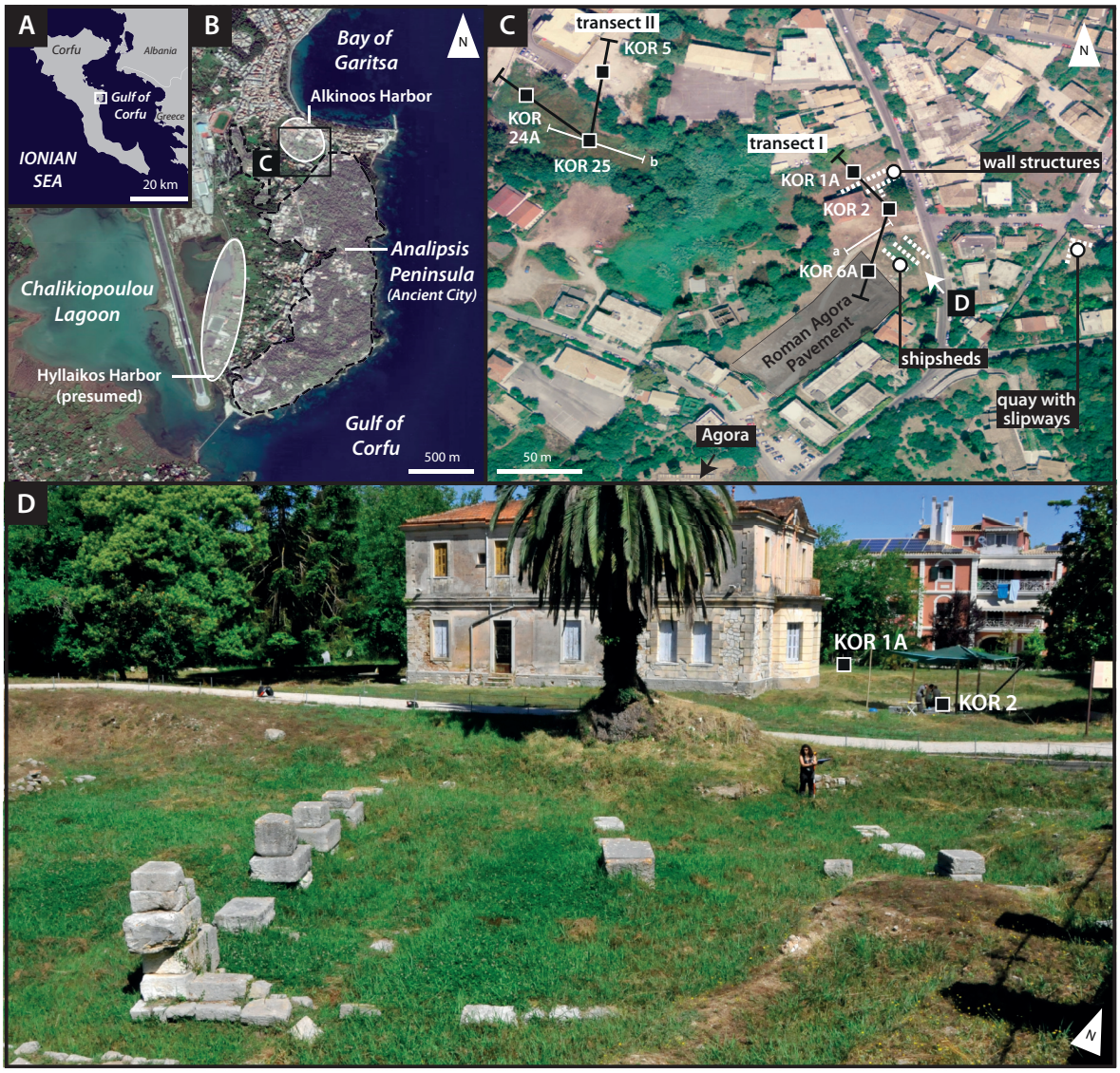

Figure 2.1: Geographical setting. The ancient city (Palaiopolis) is situated at the eastern shore of Corfu Island (A), adjoining the lake-like Gulf of Corfu in the east. The study site is located on the northern flank of the Analipsis or Kanoni Peninsula, separating the Chalikiopoulou Lagoon (location of the ancient Hyllaikos Harbour) in the west from the Bay of Garitsa (as part of the Gulf of Corfu) in the east (B). Geoarchaeological studies were conducted northwest of the remains of shipsheds (C, D) in the Alkinoos Harbour. Vibracoring sites are marked by black squares, Electrical Resistivity Tomography (ERT) transects by white lines (a-b). The black dashed line marks the boundary between bedrock outcrop (marl) and Holocene coastal and alluvial deposits according to IGME (1970) for the Analipsis Peninsula. Map is based on Bing Aerial Photograph, 2014, photo by A. Vött, 2012.

al. 2014), Turkey (Kraft et al. 2003, Algan et al. 2009, 2011, Goodman et al. 2009, Seeliger et al. 2013, 2014, Stock et al. 2013), France (Morhange et al. 2003, Bony et al., 2012) and Tunisia (Delile et al. 2015a).

Comparable geoarchaeological studies focusing on harbour sediments at Corfu are surprisingly lacking, even though the city was served by two or even three harbour basins, as reported in ancient sources. The Alkinoos Harbour was situated to the north whereas the Hyllaikos Harbour was located to the southwest along the west coast of the Analipsis Peninsula (Figure 2.1 B). These harbours and associated naval infrastructure were developed in order to establish and secure Corfu's supremacy as a naval power in the Mediterranean. Such efforts also reflect the status of the city due to its strategic key position between the Ionian and Adriatic Seas on the trade routes between Greece and Italy (Kiechle 1970, Blackman 1982b, Gehrke & Wirbelauer 2004). Both harbours are archaeologically well documented (Partsch 1887, Lehmann-Hartleben 1923, Dontas 1965, Kanta-Kitsou 2001, Baika 2003, 2013a), although their original topography remains conjectural. The harbours have undergone considerable environmental changes and anthropogenic interventions since antiquity such that their original shape is today partly concealed under modern urban development. Alkinoos Harbour, the focus of the present study, has been completely filled with sediments such that naval installations such as shipsheds of the Classical period lay several hundreds of meters inland today (Dontas 1966, Preka-Alexandri 1986, Baika 2003, 2013a).

From a tectonic point of view, the island of Corfu is seismically active, occupying a key position between the tectonically undisturbed shallow Adriatic Sea (Battaglia et al. 2004, Maramai et al. 2007) and the Ionian Sea. Located within a geologically complex system that includes the subduction zone of the Hellenic Arc, continent-continent collisions, and transform fault zones, the area belongs to one of the seismically most active regions in the Mediterranean (Pirazzoli et al. 1994, Sachpazi et al. 2000, van Hinsbergen et al. 2006). Traces of seismic and tsunamigenic events which were detected in southern Apulia (Italy), a tectonically stable region, by Mastronuzzi & Sansó (2004), Maramai et al. (2007) and Mastronuzzi et al. (2007) must therefore also have imprinted the sedimentary record of Corfu at the opposite side of the Strait of Otranto near the entrance to the Adriatic Sea.

Ancient harbours can be excellent sediment traps for tsunamis (e.g. Hadler et al. 2013). Furthermore, ancient harbours are usually located in storm-sheltered and quiescent natural positions to protect ships and nearby infrastructure from destructive storm waves. So far, several eastern Mediterranean harbours sites have been analysed as sediment trap for palaeotsunamis, including the Istanbul harbour complex by Bony et al. (2012), the Caesarea harbour by Reinhardt et al. (2006), the Lechaion harbour by Hadler et al. (2013), and the Pheia/Olympia harbour by Vött et al. (2011a).

By means of a multi-proxy approach, the present study aims to investigate the geoarchives of the ancient Alkinoos Harbour in order to

i. detect and analyse the sedimentary record of the ancient harbour thus far identified by archaeological evidence;

ii. reconstruct the development and use of the harbour in space and time;

iii. investigate the palaeoenvironmental record of the Alkinoos Harbour basin regarding possible high-energy events such as palaeotsunamis.

2.2 Physical and Cultural Setting

The Ionian archipelago in northwestern Greece is influenced by different tectonic systems. The eastern coasts of the Adriatic Sea are under the influence of continent-continent collision of the Adriatic Microplate towards the Eurasian Plate (Babbucci et al. 2004, Battaglia et al. 2004) and are associated with subsidence and uplift as well as slight deformations (Suric et al. 2014). On Corfu, compressional tectonics drive the Corfu Thrust accompanied by frequent shallow-focus earthquakes (Kokkalas et al. 2006). In contrast, the southern parts of the Adriatic Sea as well as the Ionian Sea are situated within a seismic stress field between the subduction zones of the Calabrian (southwest) and Hellenic Arc (southeast) (van Hinsbergen et al. 2006, Hollenstein et al. 2008). These subductions combined with the Kerkyra-Cefalonia depression, the Cefalonia Transform Fault and several adjoining fault systems strongly affect the geology and form of Corfu Island (Poulos et al. 1999). The Ionian Islands therefore show all types of tectonic plate boundaries within a radius of a few hundred kilometres (Sachpazi et al. 2000). Not surprisingly, Corfu is repeatedly listed in earthquake and tsunami catalogues (Partsch 1887, Soloviev et al. 2000, Albini 2004, Abraseys & Synolakis 2010, Hadler et al. 2012). These entries document several earthquakes with moment magnitude values around 6.0 (Stucchi et al. 2012) on and near the island of Corfu since Medieval times. However, no historical record is available for earlier events (Partsch1887).

This gap in historical data must not be interpreted as an absence of earthquakes but is rather related to the incompleteness of the data set (see also Hadler et al. 2012). In fact, on the coasts of Corfu and satellite islands, Evelpidou et al. (2014) detected geomorphological indicators of emergence as a result of ancient earthquakes in the form of erosional notches. As already stated by Pirazzoli et al. (1994), these notches document at least two co-seismic uplifts for the central and western parts of the island, the first one between the 8th and 4th cent. BC, the second one at a later date, so far undated. Similar findings of submerged notches are known from the Croatian coast (Faivre et al. 2011, Marriner et al. 2014b). Mastronuzzi et al. (2014) even provided geomorphological and sedimentological evidence for a series of tectonic events on Corfu which may be correlated

with tsunami impacts reported for comparable time periods from surrounding regions such as Adriatic Italy (Mastronuzzi & Sansó 2004, Maramai et al. 2007) and Sicily (Barbano et al. 2010, Smedile et al. 2011, De Martini et al. 2012). Concerning tsunamigenic sediments at Corfu itself, Fischer et al. (2016a) present geomorphological and microfaunal evidence of multiple palaeotsunamis, traces of which were investigated in coastal lagoons along the southwestern and eastern coasts of the island. Paleotsunami studies were also carried out on the Ionian Islands (Hadler et al. 2011, May et al. 2012, Willershäuser et al. 2013) and the northern Greek mainland (Vött et al. 2010, 2011b).

The ancient city of Corcyra and its harbours are located along the eastern shore of the island (Figure 2.1 A), separated from the Greek mainland and Albania by the Gulf of Corfu, a narrow strait with shallow water depths. Naturally sheltered from the predominating westerly winds by the curved shape of the island, the gulf features relatively low-energetic conditions with maximum water depths of 70 m. Within this sheltered lake-like situation (Partsch 1887), the ancient city was built on the northern part of the former Analipsis Peninsula (Figure 2.1 B), a ridge of Miocene marls (IGME 1970) extending up to 60 m above sea level. The ancient city extended northwards into the coastal lowlands of the Bay of Garitsa. The centre of the city was located both, on top of the Analipsis Peninsula and along its western hillslopes in the narrow strip between the two main harbours, the Alkinoos Harbour to the north, and the Hyllaikos Harbour to the southwest (Figure 2.1 C). It is assumed that the Hyllaikos Harbour was located at the eastern fringe of the modern Chalikiopoulou Lagoon, but the area was strongly transformed by the construction of the modern airport in the 1950s. The location of the Alkinoos Harbour is archaeologically attested by the remains of a series of harbour installations. The name of the harbour originally refers to the Homeric king of the Phaiacians and was adopted by archaeologists (Baika 2013a).

The most impressive harbour remains are those of monumental trireme shipsheds (Kokotou site), constructed in the early 5th cent. BC (Preka-Alexandri 1986, Spetsieri-Choremi 1996, Baika 2003, 2013a). The shipsheds consist of rows of piers out of local white limestone, running southeast-northwest towards the presumed ancient coastline (Figure 2.1 C, D; cf. Baika 2013a). This shipshed complex is located in close proximity to the ancient agora of the city and most probably belongs to the harbour installations as also referred to incidentally by ancient sources (Thucydides 3.72.3 after Crawley 1910, Baika 2013a, 2015). In the Roman period, the area was re-arranged and overbuilt. As a result, remains of the Roman agora pavement can now been seen to the southwest of the shipshed complex (Figure 2.1 C). Furthermore, a section of a quay wall, interrupted by slipways and showing a different, namely south-north orientation, was excavated to the east of the Kokotou shipsheds naval zone (Riginos et al. 2000, Baika 2013a; Figure 2.1 C). Although it is still uncertain whether all these harbour facilities belong to one and the same Alkinoos Harbour, the quay wall remains clearly demonstrate the existence of a harbour installation facing the Bay of Garitsa. Systematic geoarchaeological studies are needed concerning the structure and sediment fill of the Alkinoos Harbour and other harbour settings of the ancient city. A third harbour basin is mentioned in historical sources, but not yet located as archaeological and geological evidence is still missing (Partsch 1887, Lehmann-Hartleben 1923, Riginos et al. 2000, Baika 2003).

2.3 Methods

The study area within the ancient Alkinoos Harbour (Figure 2.1 C) was investigated using a multi-methodological approach. Vibracoring was conducted using engine-driven devices (Nordmeyer RS 0/2.3 drill rig and Atlas Copco Cobra mk 1) with core diameters of 50–80 mm to investigate the sedimentological record of the assumed harbour basin. Vibracores were cleaned, photographed and described in the field (AD HOC-ARBEITSGRUPPE BODEN 2005, SCHROTT 2015). Selected vibracores (suffix "*A*": KOR 1A, KOR 6A and KOR 24A; for location see Figure 2.1 C) were drilled using closed auger heads with enclosed plastic liners to enable in situ measurements in the laboratory.

On-site geoelectrical prospection allowed for identification of subsurface stratigraphy and archaeological structures due to variable electrical resistivity owing to differences in grain size, mineral composition, water content and pore structure (KEAREY et al. 2006). We conducted Electrical Resistivity Tomography (ERT) using a multi-electrode device type Syscal R1+ Switch 48 (Iris Instruments) and a Wenner-Schlumberger electrode array. Data were processed by means of the RES2DINV-Software and least-squares inversion (LOKE & DAHLIN 2002, LOKE et al. 2003). Elevation and position data of vibracoring sites and ERT locations were measured by means of a differential GPS (Topcon HiPer Pro).

In situ Direct Push electrical conductivity (DP EC) measurements turned out to be a valuable tool to trace grain size fluctuations with a high resolution, mirroring changes in the depositional environment (FISCHER et al. 2016b). DP EC logging was realized at selected vibracoring sites using a Geoprobe SC520 device. The probe consists of four electrodes in a linear arrangement. By using a Wenner electrode array the electrical conductivity as well as the rate of penetration were measured in a high resolution of 0.2 cm (see also SCHULMEISTER et al. 2003, HARRINGTON & HENDRY 2006).

In the laboratory, X-ray fluorescence (XRF) analyses were accomplished by means of a handheld Niton XL3t 900S GOLDD (calibration mode SOIL) to determine the concentrations of more than 30 elements which were used to trace geochemical fingerprints of different environmental settings. If possible, these measurements were conducted in situ at the sediment-filled liners with an average resolution of 2 cm or otherwise at selected samples. Additionally, we analysed grain size classes after the Köhn pipette method and measured loss on ignition (LOI) as an indicator for the concentration of organic material (BLUME et al. 2011).

The microfaunal contents of selected vibracores (KOR 1A, KOR 5) were analysed by means of a semi-quantitative screening. For this purpose, 15 ml of sediment were extracted from selected stratigraphic layers and sieved in fractions of > 400 µm, > 200 µm, > 125 µm and < 125 µm. Species were determined after LOEBLICH & TAPPAN (1988) and CIMERMAN & LANGER (1991) using a stereomicroscope. Additionally, photos of selected specimens were taken using a scanning electron microscope (SEM). Species were classified according their ecological habitat preferences after MURRAY (2006) and SEN GUPTA (1999). The determination of microfaunal remains helps to reconstruct environmental conditions and to detect allochthonous interferences (DOMINEY-HOWES et al. 2000, MAMO

et al. 2009, Hadler et al. 2013, Willershäuser et al. 2013) as progressive environmental changes will result in gradually shifting microfaunal assemblages, while abrupt changes will either severely stress or kill the pre-existing fauna, the latter visible in a sudden shift of species. We further calculated a simplified index considering the number of species (diversity) and the total amount of specimens (grouped abundance) to better visualize these shifts. We focused on foraminiferal fingerprints, as foraminifera occur commonly under various conditions and through geological times (Sen Gupta 1999, Murray 2006).

A local geochronostratigraphy was established by means of ^{14}C accelerator mass spectrometry (AMS) dating of nine selected organic samples (Table 2.1) performed by the Klaus-Tschira Laboratory of the Curt-Engelhorn-Centre Archaeometry gGmbH Mannheim (MAMS), Germany, and by the Keck Carbon Cycle AMS Facility (UCI), University of California at Irvine, USA.

2.4 Results: Deciphering the Geoarchive of the Ancient Harbour

Six vibracores were drilled along two transects where archaeological remains of harbour installations suggest the possible location of the ancient Alkinoos harbour basin (Figure 2.1 B, C; see also above). More specifically, the harbour basin is related to the trireme shipshed complex (Kokotou site) dating to the early 5th cent. BC, excavated at the northern fringe of the Analipsis Peninsula. In general, shipsheds were functional structures to accommodate and protect warships. They were built as roofed galleries perpendicular to the coastline and in inclination towards the sea, so that warships could be rapidly launched and hauled out of the water (Blackman 2013a). Therefore, in the Kokotou site, based on the shipsheds' orientation and its relationship to the presumed ancient coastline needed for the shipsheds to be operational, the harbour basin is assumed to be located directly in front of the recovered rows of piers towards the northwest. This hypothesis is further supported by the discovery of associated harbour facilities. These include the eastern entrance tower of the harbour located to the north of the study site, as well as another shipshed complex (Dontas 1966) located farther northwest of the Kokotou site (for further details see Baika 2013a, 2015).

Vibracoring sites KOR 1A and KOR 2 are located close to the excavated shipsheds (Figure 2.1 D), approximately 200 m from the present coastline. Vibracore KOR 1A was drilled some 50 m and vibracore KOR 2 some 20 m to the north of the shipshed remains. While vibracoring site KOR 2 is located near the wall remains of a Roman installation, another wall structure was encountered between both vibracoring sites. Vibracore KOR 6A is located some 10 m to the west of the shipshed remains. It was drilled on a higher level right next to the remains of the Roman agora pavement. In contrast, Transect II comprises vibracores KOR 5, KOR 25 and KOR 24A and covers the western part of the presumed ancient harbour zone lying about 150 m to the northwest of the Kokotou shipshed remains (see Figure 2.1 C).

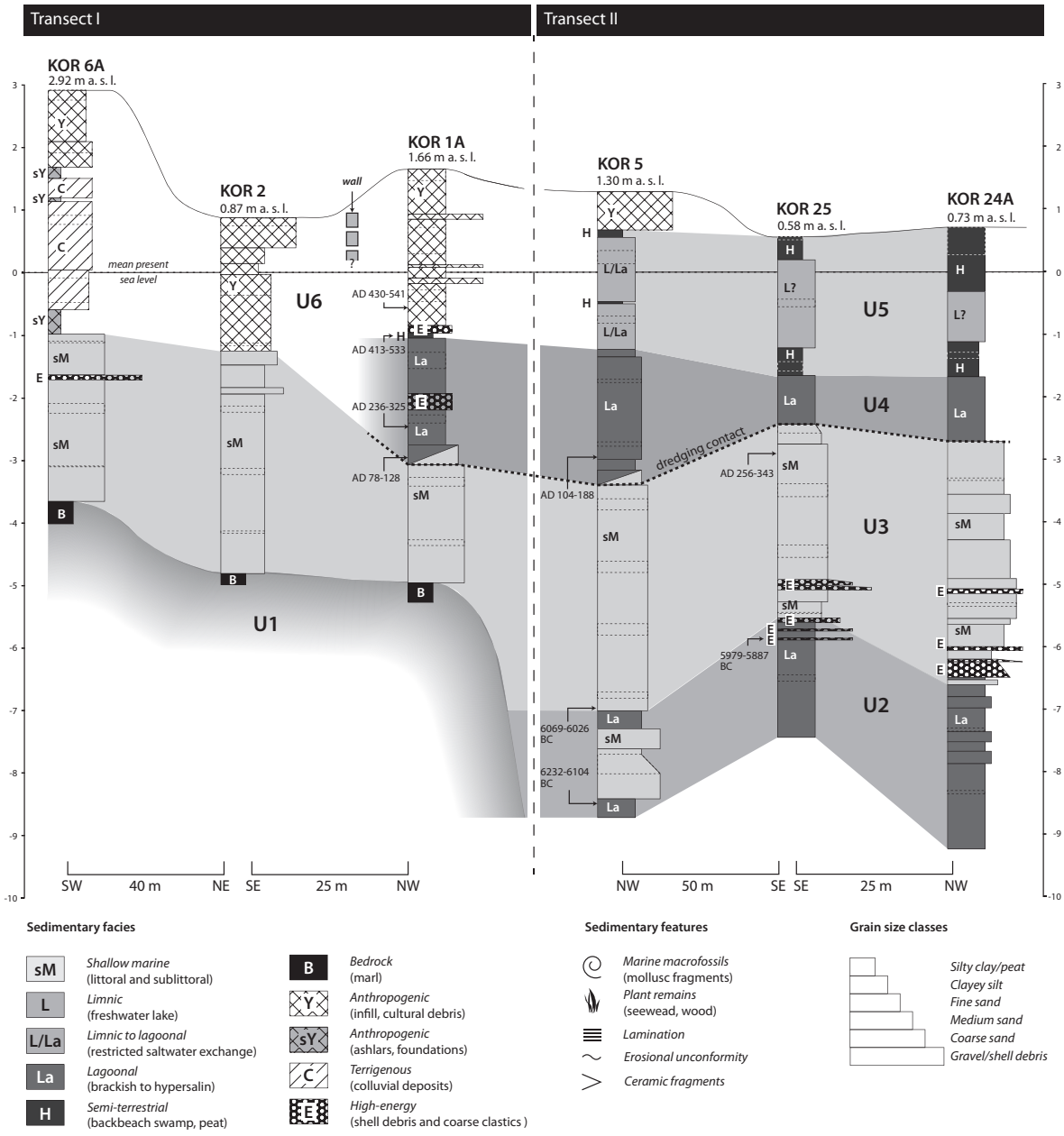

Figure 2.2: Simplified facies patterns found for vibracore Transect I (left) and II (right). For location of vibracoring sites see Figure 1. All radiocarbon ages are calibrated at 1σ (see Table 2.1).

Vibracore Transects I and II provide valuable insight into the local stratigraphic record (Figure 2.2): Bedrock was only found in the eastern part of Transect I and is composed of Miocene marl (Unit 1, IGME, 1970). The western part of Transect II revealed grey clayey to silty lagoonal deposits (Unit 2) dated to the mid-Holocene. Thereafter, a long period of stable shallow marine conditions (Unit 3) obviously lasted until ancient times. Towards the north, lagoonal sediments are alternating with shallow marine fine sand (KOR 5). In the most western part of the study area along Transect I, this marine sand unit directly covers the Miocene bedrock. Several coarse sand layers including marine shell debris within this unit were found at sites KOR 6A, KOR 25 and KOR 24A. Towards the east, Unit 3 is followed by dark grey to dark brown clayey silts representing the (re)establishment of lagoonal conditions (Unit 4). At site KOR 1A, this unit is again interrupted two times by coarse

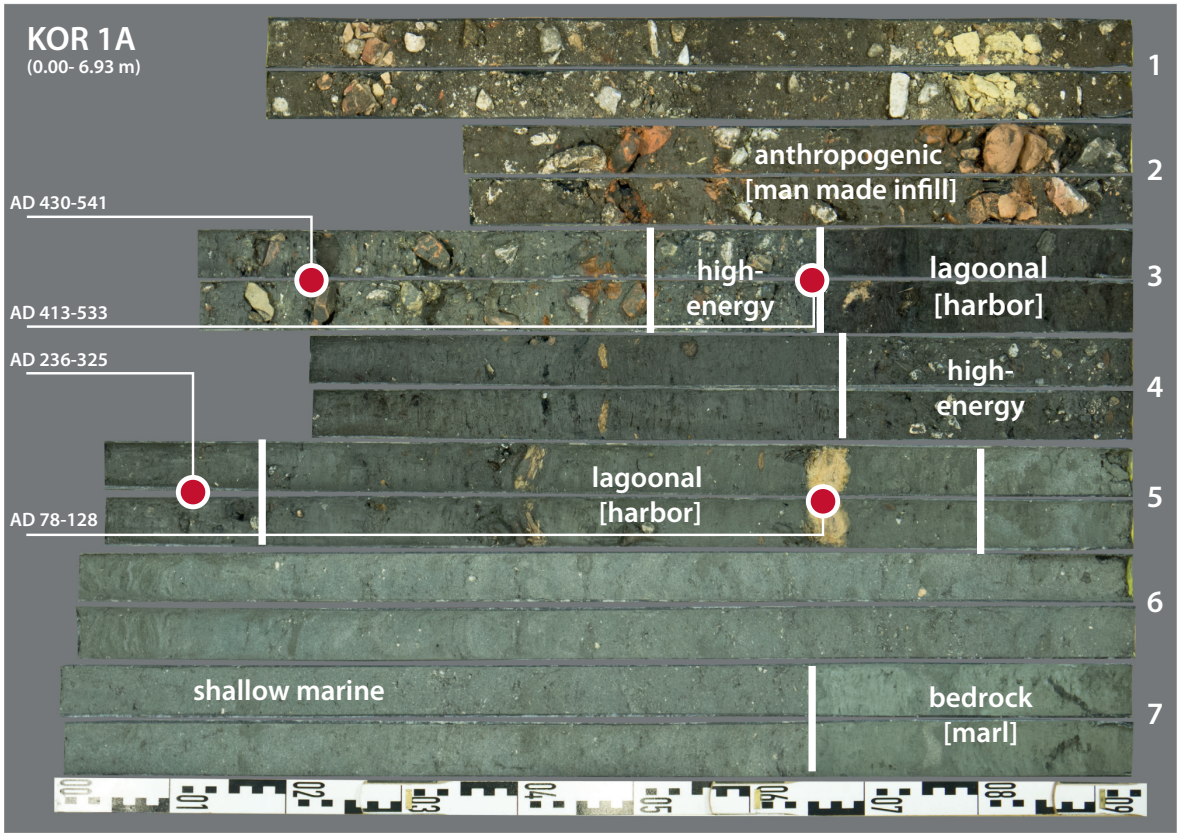

Figure 2.3: Photo of vibracore KOR 1A with the main stratigraphic units and radiocarbon ages (red circles; ages are 1σ values calibrated with Calib 7.0, see Table 2.1). For location of vibracoring site see Figure 2.1. Note the fine-grained, organic-rich lagoonal deposits, representing a harbour lagoon, which are interrupted and followed by coarse-grained high-energy layers.

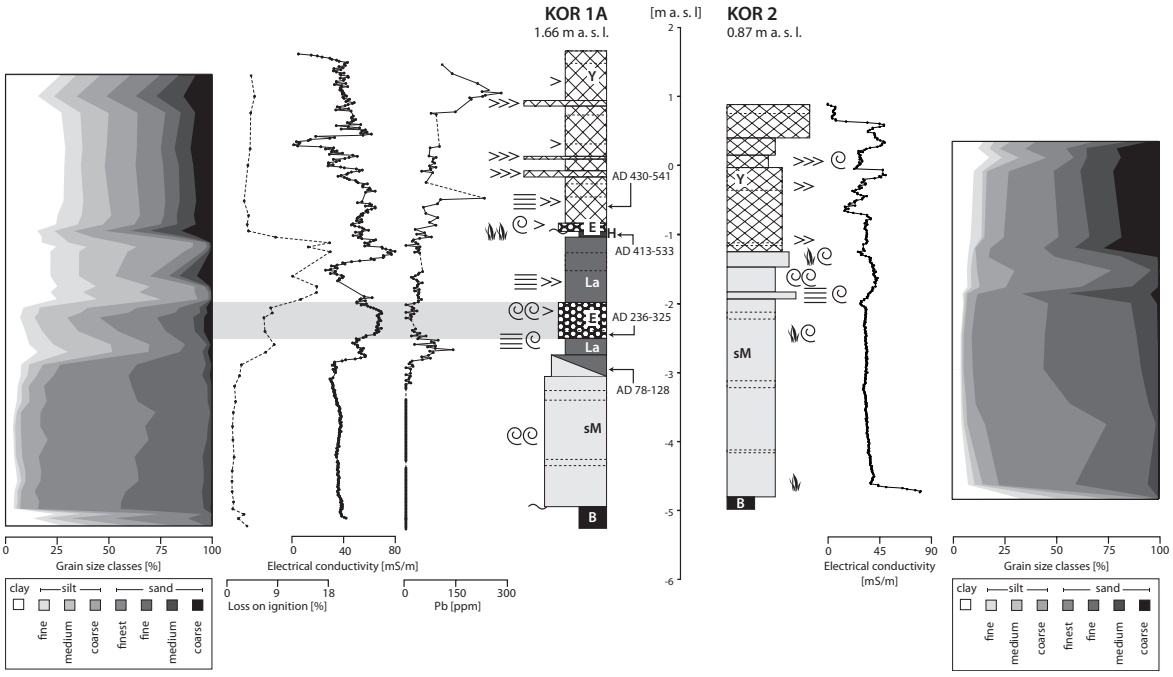

Figure 2.4: Results of multi-proxy analyses of vibracores retrieved from the Alkinoos Harbour showing facies classifications, sedimentary features, electrical conductivity, selected geochemical parameters and grain size data of vibracores KOR 1A (left) and KOR 2 (right). For location of vibracoring sites see Figure 2.1; legend according to Figure 2.2; see text for further explanation.

sand containing shell debris and ceramics. In contrast, Unit 4 is missing at sites KOR 2 and KOR 6A where the fine sand is covered by heterogeneous debris containing ceramics and bricks within a silt matrix (Unit 6). In the western part of Transect II, Unit 4 is followed by clayey silt of light grey colour (Unit 5) containing several intersecting dark grey to black peat-like organic layers which document semi-terrestrial conditions.

2.4.1 Stratigraphic Record at the Shipsheds Site (Transect I)

Figure 2.3 depicts depositional facies found at vibracoring site KOR 1A. Miocene marl is covered by shallow marine fine sand which in turn is overlain by darkgrey lagoonal mud. On top, we found anthropogenic fill containing bricks, ceramics and debris. Within and on top of the lagoonal deposits, two abrupt coarse-grained layers were encountered. These layers are also documented in Figure 2.4 where selected multi-proxy data for vibracores KOR 1A and KOR 2 are illustrated.

The grain size distribution of vibracore KOR 1A allows one to differentiate between distinct sedimentary units. Miocene bedrock is dominated by clay and silt, whereas overlying shallow marine deposits are characterized by high amounts of finest sand and fine sand. Lagoonal sediments, however, are dominated by clay and silt with low amounts of sand. Sand layers intersecting the

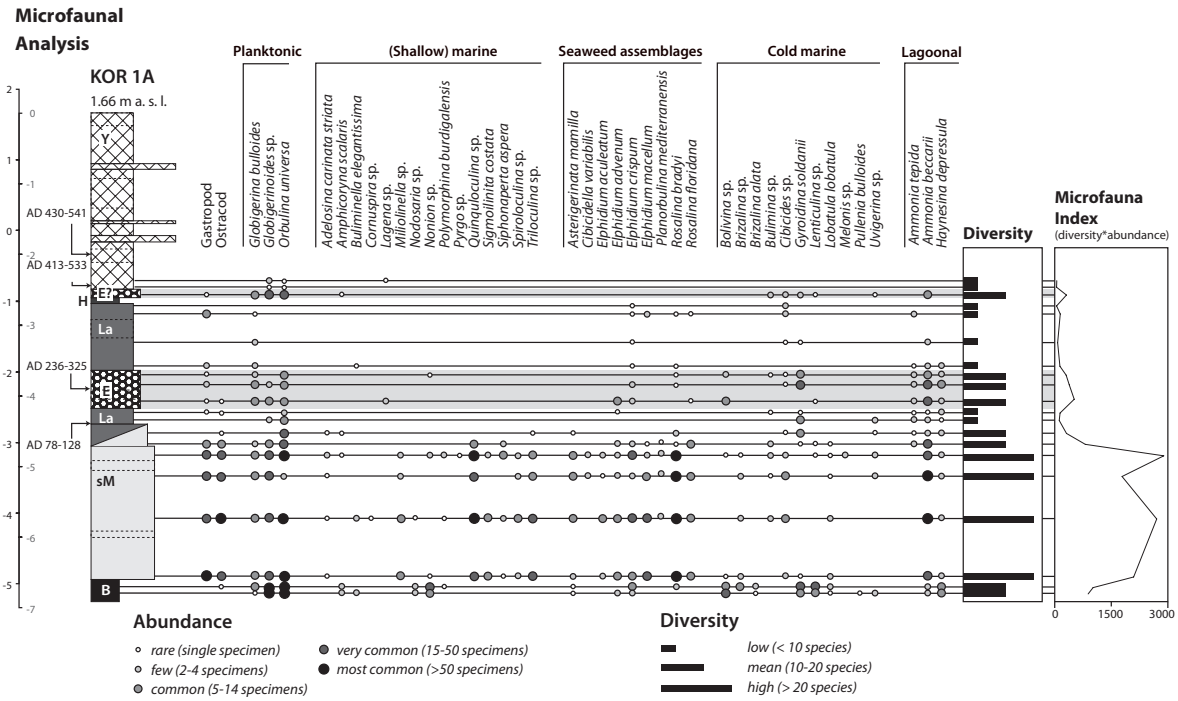

Figure 2.5: Results of microfaunal studies of selected samples from vibracore KOR 1A. For location of vibracoring site see Figure 2.1; for explanations see text and Figure 2.2. Foraminifera were determined after Loeblich & Tappan (1988) and Cimerman & Langer (1991) and are classified according to their ecological preferences after Murray (2006) and Sen Gupta (1999). Note the difference in abundance, diversity and species between the autochthonous lagoonal deposits and the intersecting high-energy layers.

lagoonal mud show abrupt changes in grain size distribution with multiple peaks within the sand fraction and high contents of skeletal components. LOI values are constantly high in lagoonal deposits reaching maximum values in the very upper part of this unit (Figure 2.4). EC values are consistently low (around 40 mS/m) for shallow marine sand deposits. In contrast, EC values clearly increase for the coarse-grained material intersecting lagoon-type deposits. Within anthropogenic units, EC values are strongly fluctuating. Differences in the EC log are due to differences in grain and pore size distributions and differences in the mineral composition (Schulmeister et al. 2003). Increasing lead (Pb) concentrations appear with the onset of lagoonal conditions while the lower half of the core is void of Pb. Maximum Pb concentrations were found within the anthropogenic fill on top.

In contrast to KOR 1A, the stratigraphic record of vibracore KOR 2 does not contain a lagoonal sedimentary unit. Sand-dominated shallow marine deposits on top of bedrock material are directly covered by cultural debris. Grain size distribution, however, reveals a distinct peak of coarse silt and fine sand in the shallow marine deposits towards the base of the anthropogenic fill. EC values are high within the bedrock but constantly low to medium in the shallow marine sand unit.

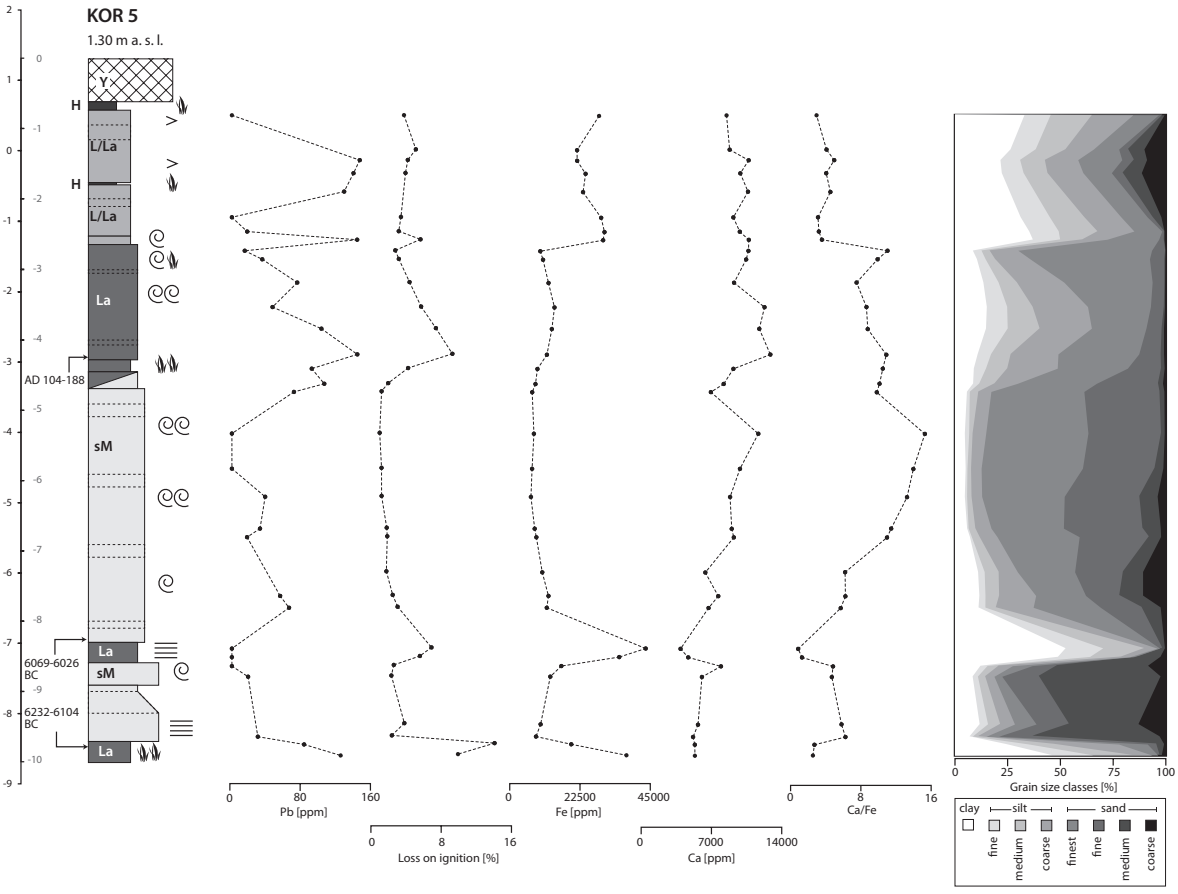

Figure 2.6: Sedimentary units and features, grain size data and selected geochemical parameters of vibracore KOR 5 from the western part of the Alkinoos Harbour basin. For location of vibracoring site see Figure 2.1, for explanations see text, legend according to Figure 2.2.

Microfaunal analyses (Figure 2.5) of selected samples of vibracore KOR 1A yielded distinct palaeo-environmental characteristics associated to the different sediment facies. Foraminifera found in the Miocene bedrock such as planktonic foraminifera, *Ammonia beccarii*, *Elphidium* sp. and *Uvigerina* sp. are also ubiquitous in other layers and are therefore considered as geogenic background signal. In addition, the marl contains some cold-marine species from the shelf to bathyal region like *Brizalina* sp. or *Lenticulina* sp. (Murray 2006). Shallow marine deposits, on the contrary, provide a distinct environmental signal and are characterized by high diversity and high abundance resulting in high microfauna index values. Many species, especially Milliolidae (e.g. *Quinqueloculia* sp., *Triloculia* sp., *Sigmoilinita costata*) appear solely in this environment. Additionally, typical inhabitants of seaweed meadows were found such as *Rosalina* sp. and *Elphidum macellum*. Within the lagoonal sediments, the microfaunal assemblage shifts abruptly towards very low abundance and diversity (Figure 2.5). Only few species such as *Ammonia tepida* and *Gyroidina* sp. are obviously able to inhabit this environment. In contrast, the sand layers intersecting the lagoonal unit again show higher abundance and diversity, visible in distinct peaks within the microfaunal index. Additionally to the species appearing in the lagoonal sediments, these sand layers also contain *Bolivina* sp., *Lenticulina* sp., A*mphicoryna scalaris* and *Lagena* sp.

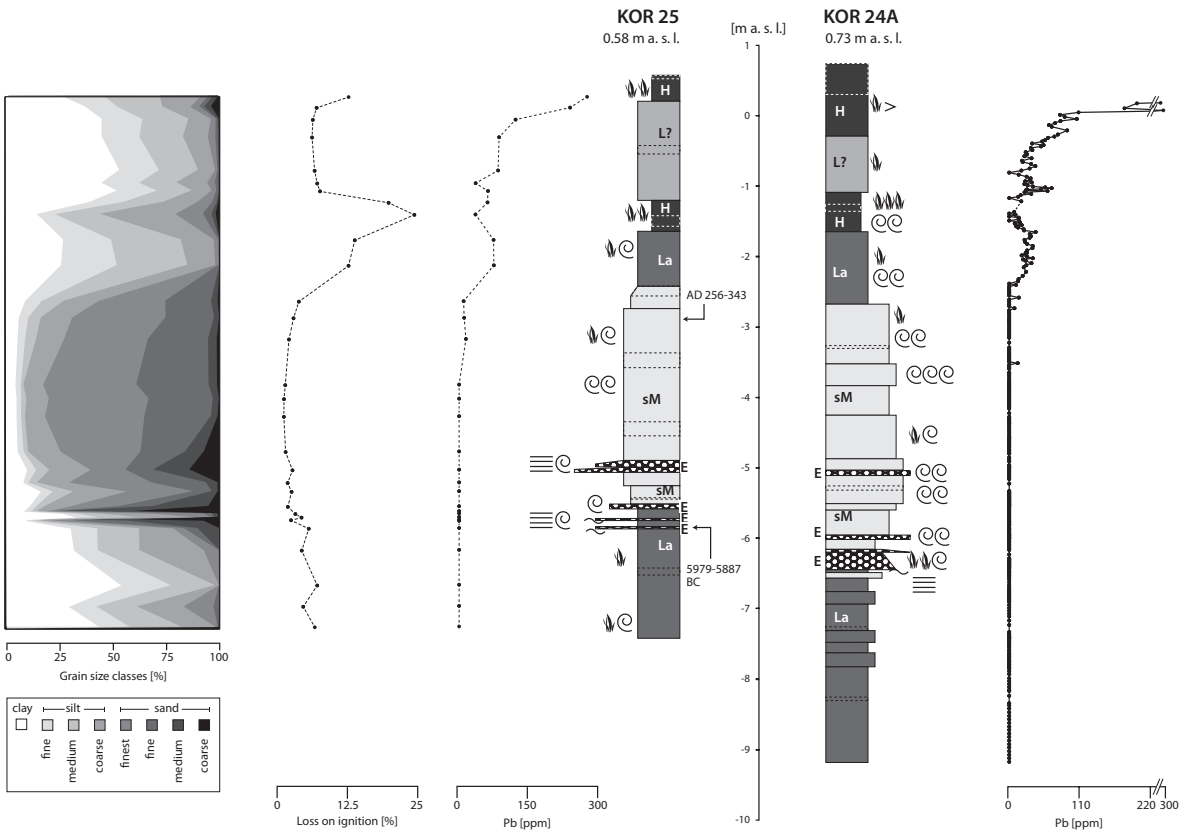

Figure 2.7: Facies classification, sedimentary features, selected geochemical parameters and grain size data of vibracores KOR 25 (left) and KOR 24A (right). For location of vibracoring sites see Figure 2.1; for explanations see text; legend according toFigure 2.2. Pb content of vibracore KOR 24A (right) was measured in situ with an average resolution of 2 cm while Pb content of vibracore KOR 25 (left) was measured with lower resolution at selected samples. In contrast to the lower lagoonal unit, the upper lagoonal mud shows distinct peaks in anthropogenic Pb content associated with high values in LOI.

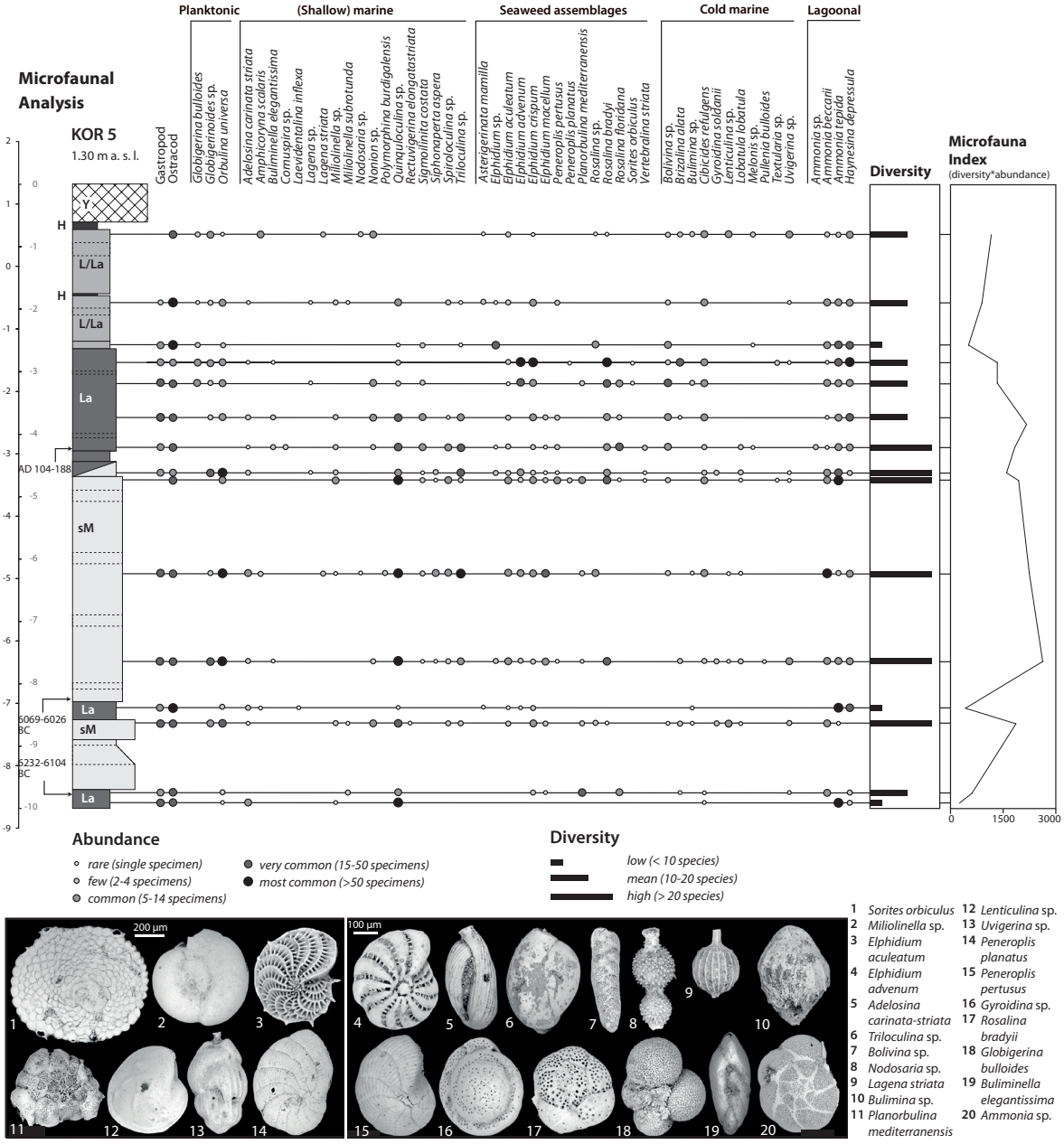

Figure 2.8: Results of microfaunal studies of selected samples from vibracore KOR 5. For location of vibracoring site seeFigure 2.1; for explanations see text; legend according to Figure 2.2. Photos of selected samples were taken using a scanning electron microscope (SEM). Foraminifera species were determined after Loeblich & Tappan (1988) and Cimerman & Langer (1991) and are classified according to their ecological preferences after Murray (2006) and Sen Gupta (1999). Note the different foraminiferal fingerprint of the upper lagoonal unit (high diversity, high abundance) compared to the lower lagoonal deposits which are characterized by a distinct lower abundance and diversity.

2.4.2 Sedimentary Record of the Western Harbour Area (Transect II)

Vibracore transect II was drilled in the western part of the study area (Figure 2.1). Figure 2.6 shows selected multi-proxy parameters of vibracore KOR 5. Clayey silt in the lower part of the core, representing lagoonal conditions, is covered by homogenous shallow marine sand mostly consisting of finest and fine sand. At 3.38 m below sea level (b.s.l.), the sand is overlain by clay- and silt-dominated lagoonal mud. This in turn is overlain by limnic to lagoonal clayey silt.

The concentration of Pb is subject to strong fluctuations within the core. While the values vary on a low level in the shallow marine sand unit, the Pb content reaches maximum values within lagoonal deposits. LOI values are uniformly low with only the lower and upper sections of the lagoonal deposits show values greater than 10 %. The lower lagoonal unit contains high iron (Fe) but relatively low calcium (Ca) concentrations, resulting in a low Ca/Fe-ratio, while the overlying marine sand shows increasing Ca values and constantly low Fe concentrations. Within the upper lagoonal unit, the Ca/Fe ratio is higher compared to the lower lagoonal unit, most probably associated with higher amounts of finest sand. Lagoonal sediments on top are characterized by a low Ca/Fe level.

Results of microfaunal analyses conducted for selected samples from core KOR 5 are depicted in Figure 2.8. Comparable to KOR 1A, some species are ubiquitous and seem to represent the geogenic background signal. Lagoonal mud from the base of the core, however, is characterized by low abundance of few species such as *Rosalina floridana*, *Planorbulina mediterranensis* and *Adelosina carinata-striata*. In contrast, the subsequent shallow marine sand shows a significantly high microfauna index due to large numbers of Milliolidae like *Triloculina* sp. or *Miliolinella subrotunda*, typical seaweed meadows inhabitants such as *Rosalina bradyi* or *Elphidium* sp. (Murray 2006) and species solely appearing in this (sub)littoral environment like *Gyroidina soldanii*. With the establishment of the following upper lagoonal unit, new species occur with decreasing abundance and diversity towards the top, namely Milliolidae, *Rosalina floridana*, *Elphidium advenum*, *Rosalinda bradyi* and *Globigerina bulloides*. A further shift in the foraminiferal remains documents a clear change with strongly restricted saltwater exchange in the lagoonal environment documented by only few saltwater species such as *Amphicoryna scalaris* and *Lenticulina* sp. but increasing numbers of ostracodes.

Vibracores KOR 25 and KOR 24A show minor differences regarding their sedimentary records compared to vibracore KOR 5. Grain size data reveal a clear dominance of clay and silt within the lower lagoonal unit of core KOR 25, intercalated by several sand layers including considerable amounts of medium and coarse sand (Figure 2.7). On the contrary, the subsequent thick unit of shallow marine sand is mostly made out of finest and fine sand. The overlying lagoonal unit is characterized by silt with only minor amounts of clay, especially when compared to the lower lagoonal unit and the limnic sediments in the upper part of the core. The latter consist of nearly equal amounts of clay and silt while sand is almost missing.

The concentration of Pb shows very similar patterns for vibracores KOR 24A and KOR 25. A distinct rise in Pb is observed with the onset of lagoonal sediments at approximately 2.40 m b.s.l. (Figure 2.7). Highest values are reached within semi-terrestrial peat-like deposits in the upper parts of the cores. LOI values increase in lagoonal mud and reach their maximum within the peat-like sediments.

2.4.3 Results from Electrical Resistivity Tomography

Electrical Resistivity Tomography (ERT) measurements were conducted along several transects at the Alkinoos Harbour site. Combining ERT and vibracoring stratigraphies, we obtained 2D and 3D information on the extent of specific layers. Figure 2.9 exemplarily shows the results of ERT transects KOR ERT 16 and 78.

Transect KOR ERT 16 (Figure 2.9 A) was conducted right in front of the excavated shipsheds between vibracoring sites KOR 1 and KOR 6A. The ERT depth section shows a sequence of low electrical resistivity values (< 20 Ωm; green/blue) at the base and high values towards the top. Whereas the lower unit appears to be very homogeneous, the upper surface-near unit includes clearly delimited structures with electrical resistivity values up to 80 Ωm. Four structures in the eastern part of the section were found for the same depth level at ~0.5 m above sea level, while other structures towards the west are located on a lower level at approximately present sea level. Also, an underlying section of lower resistivity dips in a step-like manner.

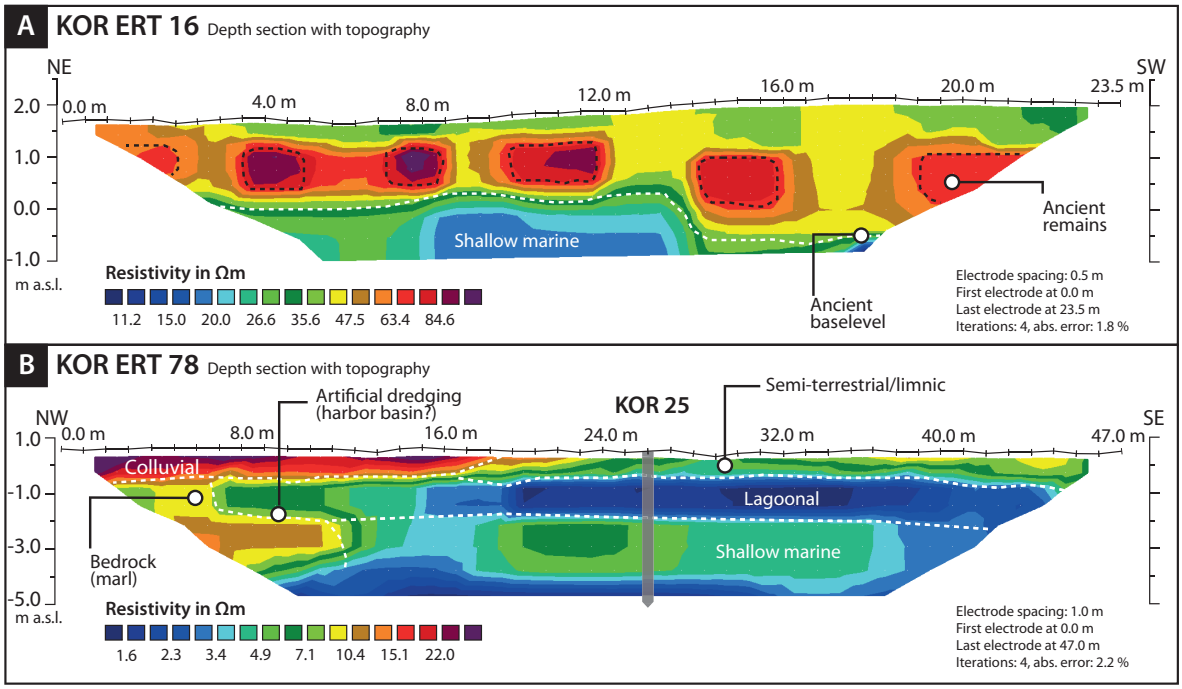

Figure 2.9: Results from Electrical Resistivity Tomography measured along transects KOR ERT 16 (A) and KOR ERT 78 (B). For location of ERT transects see Figure 2.1.

ERT results of transect KOR ERT 78 (Figure 2.9 B) reveal a more heterogeneous distribution of electrical resistivity. The south-eastern part of the transect shows uniform values < 7 Ωm, only material near the surface appears to be slightly more resistant. This distribution in electrical resistivity fits well with the stratigraphy of vibracore KOR 25 where shallow marine sands are followed by lagoonal deposits. Northwest of transect KOR ERT 78, the upper part of the depth section shows a high-resistivity layer reaching values up to 22 Ωm. A distinct shift in electrical resistivity is marked by a sharp contact to the unit below where electrical resistivity reaches approximately 10 Ωm. Note the step-like contour of this unit in Figure 2.9 (B).

2.5 Dating approach

Nine samples consisting of charcoal and plant remains were selected for ^{14}C AMS dating and calibrated with the IntCal13 curve using software Calib 7.0 (Stuiver & Reimer 1993, Reimer et al. 2013; Table 2.1). According to the relatively high $\delta^{13}C$ value of -14.1 ‰, sample KOR 5/14 PR suggests a marine origin (Walker 2005) and was calibrated using the Marine13 curve. A local marine reservoir curve for Corfu does not exist. Local variations of the reservoir effect for different types of organic material as well as different depositional environments are still unknown. Therefore, we used a mean global reservoir correction of 405 years within this study (Reimer et al. 2013). However, this correlates well with the reservoir ages estimated for the western Mediterranean, for Zante, and the eastern Adriatic Sea to be around 400 years, 439 years, and 421 years, respectively (Siani et al. 2000, Reimer & McCormac 2002).

Table 2.1: Radiocarbon dates from the Alkinoos Harbour area.

Sample ID	Depth [m b.s.]	Depth [m b.s.l.]	Sample material	Lab. No.	$\delta^{13}C$ [ppm]	^{14}C age [BP]	2σ age [cal BC/AD]	1σ age [cal BC/AD]
KOR 1A/6+ HK	2.22	0.56	charcoal	UCI 121508	[a]	1560 ± 25	424–554 AD	430–541 AD
KOR 1A/9+ HK	2.65	0.99	charcoal	UCI 121509	[a]	1600 ± 25	404–536 AD	413; 533 AD
KOR 1A/21+ PR	4.12	2.46	unidentified plant remain	UCI 121510	[a]	1770 ± 25	143; 342 AD	236; 325 AD
KOR 1A/24+ HR	4.65	2.99	wood fragment	UCI 121511	[a]	1895 ± 25	55; 211 AD	78–177 AD
KOR 5/14 PR	4.19	2.89	seaweed	MAMS 19768	-14.1 [b]	2200 ± 22	81–235 AD	104–188 AD
KOR 5/25+ HR2	8.27	6.97	wood fragment	MAMS 19769	-23.5	7199 ± 28	6198; 6003 BC	6069–6026 BC
KOR 5/32+ HR	9.81	8.51	unidentified plant remain	MAMS 19770	-27.4	7328 ± 28	6238–6089 BC	6232; 6104 BC
KOR 25/13 HR	3.47	2.89	wood fragment	MAMS 19778	-29.0	1729 ± 19	251; 381 AD	256; 343 AD
KOR 25/27+ PR	6.36	5.78	unidentified plant remain	MAMS 19779	-30.3	7022 ± 27	5984; 5846 BC	5979; 5887 BC

Note: b.s. – below ground surface; b.s.l. – below sea level; Lab. No. – laboratory number; Klaus-Tschira Laboratory of the Curt-Engelhorn-Centre Archaeometry gGmbH Mannheim, Germany (MAMS), and Keck Carbon Cycle AMS Facility, University of California at Irvine, U.S.A. (UCI); ";"– several possible age intervals due to multiple intersections with the calibration curve; 1σ/2σ age –calibrated ages, 1σ/2σ range; All dates are calibrated using the IntCal13/Marine13 curve by Calib 7.0 (Stuiver & Reimer, 1993; Reimer et al., 2013). [a] – ^{13}C correction is done automatically with a standard run; [b] – marine sample, calibrated by using the marine calibration dataset with an average reservoir age of 405 years.

Generally, ^{14}C results should be regarded as approximate timeframes rather than as fixed dates, because contamination or relocation of carbon, isotopic fractionation, local marine reservoir or hard water effects as well as long term variations with ^{14}C production may occur (Walker 2005). Moreover, dating high-energetic layers by means of radiocarbon dating is problematic due to reworking effects (Vött et al. 2009a). For this reason, where possible, we retrieved samples from the over- and underlying deposits. By this „sandwich" dating approach, a time window is framed by a *terminus post quem* (before the event) and a *terminus ante quem* (after the event) and provides time frames for the different stratigraphic layers for both vibracore transects (Figure 2.2). Ages presented in Table 2.1 and Figure 2.2 do not show age inversions and are therefore considered reliable.

2.6 Discussion

2.6.1 Ancient harbour sediments

Based on our multi-proxy geoarchaeological approach it was possible, for the first time, to obtain physical evidence for the development of Alkinoos Harbour that compliment archaeological evidence such as the excavated remains of shipsheds (Dontas 1966, Baika 2003, 2013a) as well as historical records (e.g. Thucydides 3.72.3 after Crawley 1910) indicating the broad approximate position of the harbour basin. Geophysical studies conducted close to the shipsheds (Figure 2.9) revealed several highly resistant structures, clearly delimited from the surrounded material. These structures are located in the direct alignment of the excavated shipsheds such that we are tempted to interpret them as a continuation of the shipsheds rows of piers, still uncovered, in a northwestern direction. However, this zone was re-arranged in Roman times, as documented by extensive Roman installations that were excavated directly on the presumed northwestern alignment of the shipsheds. Further archaeological excavation and stratigraphic surveys are, however, needed for validation. In any case, these wall remains, so far unknown, appear to be founded on a unit with low electrical resistivity which, according to vibracores KOR 6A and KOR 2, corresponds to fine sand deposited in a shallow marine environment. These conditions must have been established after *c.* 6000 BC and persisted until ancient times.

Vibracores KOR 1A, KOR 5, KOR 25 and KOR 24A show lagoonal mud overlying this shallow marine sand unit. The predominant grain size is clayey silt indicating quiescent environmental conditions, well protected from beach dynamics. Electrical conductivity is higher within lagoonal deposits compared to shallow marine sand. LOI values are greater in lagoonal deposits, which also fits well with the low-energy depositional character of the lagoon-type environment.

In contrast to the lower lagoonal unit, the upper lagoonal sediments reveal strongly higher Pb concentrations. Pb is one of the first metals to be processed and therefore represents an excellent tracer for ancient human activities (Véron et al. 2006, Bränvall et al. 2011). As early as the 1st mill-

ennium BC, Pb pollution appeared as a result of ore treatment and byproduct of silver smelting (Lessler 1988, Hong et al. 1996). During Roman times, Pb production reached extraordinarily high levels in places (Véron et al. 2006). Ancient Pb contamination has been documented in the Tiber River and Roman harbours of Portus, Marseille, and Sidon (Le Roux et al. 2003, 2005, Delile et al. 2014a). Significantly increased Pb concentrations were also observed in ancient harbour deposits of Lechaion, Greece (Hadler et al. 2013), Kyllini, Greece (Hadler et al. 2015a) and Tyre, Lebanon (Elmaleh et al. 2012). Thus, Pb and other trace metals are powerful proxies for detecting ancient harbours (Marriner & Morhange 2007). For the Alkinoos Harbour, natural sources of lead can be excluded, as the pre-lagoonal sediments are void of lead. Thus, we conclude that the upper lagoonal sediments encountered in cores KOR 1A, KOR 5, KOR 25 and KOR 24A are typical of ancient harbours (e.g. Hadler et al. 2013, Stock et al. 2013) and belong to the Alkinoos Harbour. Radiocarbon dates provide a *terminus post quem* of 78-128[1] cal AD and a *terminus ante quem* of 413-533 cal AD for these deposits (Table 2.1). Thus, the detected harbour sediments document a harbour in use from the 1st to 6thcent. AD. However, this age interval does not correspond to the age of the ancient shipsheds which had been originally constructed in the early 5thcent. BC (Baika 2013a).

Vibracore KOR 2 was drilled in the proximity of a Roman installation (Baika 2013a) and offers a promising candidate for pre-Roman harbour sediments. The pre-Roman stratigraphic record of vibracore KOR 2 does not show silt-dominated harbour deposits but is dominated by sand. However, there is a section of silty sand encountered in the upper part of the core (Figure 2.4) that may indicate slightly reduced littoral dynamics of the shallow marine system. As the shipsheds were also founded upon shallow marine sand, this sedimentary unit most likely represents pre-Roman deposits associated with harbour installations.

Farther to the northwest, no pre-Roman harbour deposits were found in the stratigraphy of vibracore KOR 1A and cores of Transect II (Figure 2.1), where the Classical/Hellenistic harbour basin would have extended. Instead, thick Roman harbour mud overlies homogeneous shallow marine deposits, reflecting a stable open marine inner-shelf environment which had been established already in 6000 BC. This stratigraphic gap and the presence of thick Roman harbour deposits are typical indicators for extensive Roman dredging (Marriner & Morhange 2006a). The Romans established a well-organized dredging technique, partly by using dredging ships, to prevent harbour basins closing from siltation and to preserve their navigability (Morhange & Marriner 2010).

Dredging in the Alkinoos Harbour is also corroborated by geophysical findings from the western part of the study area. In transect KOR ERT 78 (Figure 2.9), a clearly delimited step-like structure within a unit of low resistivity, probably representing Miocene bedrock, is visible. This artificial structure, correlating well with the base of the lagoonal harbour mud, is suggested to represent a dredging contact with the bedrock. The eastern border of the dredged basin is represented by the walls encountered between vibracoring sites KOR 1A and KOR 2 because beyond the wall structures, at site KOR 2, the pre-Roman harbour record is still preserved (Figure 2.4).

---

1 Even if there were several possible age intervals due to multiple intersections with the calibration curve radiocarbon ages are interpretated as single time frames to improve readability in the text. Please see Table 2.1, Table 3.3 and Table 4.2 for detailed information.

Concerning the Roman harbour basin, our results enable a sedimentological and microfaunal differentiation between different parts of the harbour. Multi-proxy data obtained for vibracore KOR 1A indicate a quiescent and sheltered basin. Only few, well-adapted microfaunal species were able to survive in this extreme and artificial environment. Due to subsequent siltation and desalinization, a low-energy quiescent environment evolved in this part of the harbour. In contrast, isochronous harbour sediments found at vibracoring site KOR 5 revealed a much higher energetic level as documented by the presence of coarser-grained sediments and a different microfaunal association. Abundance and diversity of foraminifera are much higher, almost comparable with the foraminiferal fingerprint of the underlying shallow marine sand unit. Therefore, palaeoenvironmental conditions within the harbour at vibracoring site KOR 5 must have been influenced by steady inflow of saltwater and stable salinity conditions. Hence, we suggest that vibracoring site KOR 1A is located within a sheltered, maybe isolated, inner part of the Roman Alkinoos harbour, whereas vibracoring site KOR 5 was situated near a water inlet or entrance channel.

2.6.2 The Alkinoos Harbour as Sediment Trap for Palaeotsunami Impact

The stratigraphic record of vibracore KOR 1A drilled in front of the shipshed remains yielded typical harbour sediments, dated to Roman times. Our stratigraphic data further revealed two distinctly delimited sand layers. One sand layer intersects lagoonal muds, the other one was found overlying quiescent harbour deposits. Similar sand layers were also detected at vibracoring sites KOR 6A, KOR 25 and KOR 24A in the Alkinoos Harbour area. Torrential runoff from higher parts of the Analipsis Ridge can be excluded as the source of the sands because we found significant differences in grain size and microfaunal content between the intersecting high-energy layers on the one hand, and the local marine bedrock, on the other hand (cf. Figure 2.4 and Figure 2.5). Based on distinct sedimentological, geochemical and micropalaeontological features, we interpret these layers as the results of high-energy impact to the Alkinoos Harbour site associated with tsunami landfall.

Grain size analyses revealed high amounts of medium to coarse sand and gravel indicating high-energy conditions (e.g. Goff & Chagué-Goff 1999, Yu et al. 2009, Veerasingam et al. 2014, Vött et. al. 2015b), especially when compared to silt-dominated deposits of the quiescent and sheltered Roman harbour. Modern tsunami research has shown, for example, that onshore sand sheets are typical deposits associated to tsunami landfall (e.g. Shi et al. 1995). Moreover, the sand layers encountered in the Alkinoos Harbour basin show distinct peaks of the Ca/Fe-ratio due to increasing input of calcium carbonate from the sea side in the form of shell debris and (micro-)faunal tests (e.g. Goff & Chagué-Goff 1999, Vött et al. 2011b, Sakuna et al. 2012, Mathes-Schmidt et al. 2013, Veerasingam et al. 2014, Vött et al. 2015b). The Alkinoos record also shows sedimentary features typical of high-energy impact such as erosional unconformities (KOR 1A, KOR 25, KOR 24A) or fining upward sequences (KOR 24A; e.g. Shi et al. 1995, Goff & Chagué-Goff 1999, Gelfenbaum & Jaffe 2003, Bahlburg & Weiss 2007, Morton et al. 2007).

Alkinoos Harbour sediments contained in vibracore KOR 1A are characterized by high Pb concentrations. In contrast, the high-energy sand layers show a strongly decreased Pb content which we interpret as the result of a dilution effect by the input of marine waters and sediments, void of Pb (Hadler et al. 2013). Furthermore, even though coarser in grain size, the intersecting sand layer in the harbour record of vibracore KOR 1A is characterized by higher electrical conductivity compared to fine-grained harbour sediments. This seems to be due to differences in the pore volume (influence of intruding salt water) as well as content and composition of organic material.

Finally, the microfauna record of vibracore KOR 1A revealed striking differences between Alkinoos Harbour deposits and sand layers associated to abrupt shifts in faunal assemblages. As many species are able to adapt to gradually changing conditions (Sen Gupta 1999, Murray 2006), such abrupt shifts within foraminiferal assemblages point to sudden changes of crucial ecological parameters. In case of the Alkinoos Harbour, abrupt changes were obviously associated to the temporary and high-energy input of marine water and sediments into the harbour basin so that the pre-existing harbour ecosystem was profoundly disturbed (e.g. Shennan et al. 1996, Goff et al. 2000, Hawkes et al. 2007). A further characteristic of high-energy events are strongly mixed foraminiferal assemblages (e.g. Dominey-Howes et al. 2006, Mamo et al. 2009, Briggs et al. 2014, Pilarczyk et al. 2014) as tsunami waters may erode, transport and rework allochthonous sediments from the different shelf and littoral zones (Goff et al. 2001). Within the sand layers of vibracore KOR 1A, we found species preferring littoral environments and species typical of harbour conditions. In addition, new, exotic species were found that are predominantly adapted to cold and deep water from areas farther away from the inner-shelf (Murray 2006). Such species were not found in the autochthonous shallow marine sands below. Mamo et al. (2009) consider this as a key diagnostic characteristic for tsunami-deposited sediments.

These multi-proxy features clearly document that the ecological harbour system was repeatedly interrupted by short-term high-energy impacts from the sea. In general and on a global scale, the differentiation between high-energy storm and tsunami influence based on diagnostic sedimentary data is highly problematic, because some high-energy characteristics may be caused by both storm and tsunami impact (e.g. Morton et al. 2007, Switzer & Jones 2008). For this reason, the natural wave climate of the wider study area has to be taken into consideration. The open Ionian Sea shows mean significant wave heights of 1.2–1.6 m (Cavaleri 2005) – its northern part and the neighbouring Adriatic Sea are known for the lowest significant wave heights in the whole Mediterranean (Lionello et al. 2012). Wave data recorded near the Ionian island of Zakynthos, lying some 200 km to the southeast of Corfu, show a mean significant wave height of less than 1 m (HCMR 2015) attesting a very low annual wave energy level (Karathanasi et al. 2015). However, heavy storms may occur frequently, often linked to Sirocco or tropical-type cyclones (Llasat 2009), which are a known phenomenon during winter and autumn. The track lines of such „medicanes" usually run farther south, but they may occur in the Ionian Sea as well (e.g. Davolio et al. 2009, Campins et al. 2011). Ghionis et al. (2015) found evidence of significant wave heights of more than 5 m offshore Lefkada Island, while maximum observed wave heights of 7 m are reported for the coasts of Sicily (Scicchitano et al. 2007). Nevertheless, as already stated, ancient Corfu is located at

the shore of the narrow Gulf of Corfu. This gulf is located between Corfu Island and the Greek-Albanian mainland. It is up to 70 m deep and at most 30 km wide. The northern entrance to the gulf is only 2 km wide, while its southern entrance measures 8 km in width. Due to its sheltered position, the influence of wind generated waves from the northwest is thus reduced to a minimum. Waves within the lake-like Gulf of Corfu reach less than 1 m in height (Lionello et al. 2012, Mazarakis et al. 2012). Thus, the Gulf of Corfu is one of the best protected natural harbours of the entire Mediterranean.

Based on local geography and wave climate data, storms can be excluded a priori as cause for the high-energy sediments detected in the Alkinoos Harbour geoarchive, as storm generated waves in the Gulf of Corfu are not able to deposit thick and wide-spread high-energy sand sheets as encountered in the Alkinoos Harbour area. Instead, tsunamis as high magnitude and low frequency events must be considered, especially when taking into account Corfu's location within this seismically active region in the Mediterranean. Several geoscientific studies revealed that the island of Corfu was subject to repeated local co-seismic movements (Pirazzoli et al. 1994, Evelpidou et al. 2014, Mastronuzzi et al. 2014). Such crust movements may have been associated with local tsunami phenomena. Apart from such local seismic origins, tsunamis may also hit Corfu in the form of teletsunamis originating along the Hellenic Trench as major seismic zone in the Mediterranean. The high tsunami hazard of Corfu is also reflected by the large number of entries found in earthquake and tsunami catalogues for the northern Ionian Sea around Corfu Island (Stiros et al. 1994, Hadler et al. 2012). Finally, Fischer et al. (2016a), for the first time, report on geomorphological and sedimentary traces of repeated tsunami impact in two lagoonal environments on Corfu.

Our findings document two discrete tsunami inundation phases for the Alkinoos Harbour (Figure 2.10). The harbour unit right underneath the first tsunami layer is radiocarbon dated to 78–128 cal AD (KOR 1A/24+ HR). This date is considered as *terminus ad or post quem* for the event. In addition, the sediments overlying the tsunami deposit yielded a *terminus ante quem* of 413–533 cal AD (KOR 1A/9+ HK). The first tsunami must therefore have occurred between the late 1st and the early 6thcent. AD. Another sample was taken from the tsunami layer itself and dated to 236–325 cal AD (KOR 1A/21+ PR). Due to possible reworking effects, this age has to be considered as maximum age for the event. We finally conclude that the first event took place between the late 3rd and the early 6thcent. AD. It is highly probable that it is related to the well-known earthquake and tsunami that hit the Mediterranean world on July, 21st 365 AD.

The 365 AD earthquake had its origin on Crete, but its effects were felt as far as the northern edge of the Ionian Sea (Shaw et al. 2008, Shaw 2012). Our geoarchaeological data from the Alkinoos Harbour strongly support the idea that the 365 AD event hit the Gulf of Corfu as teletsunami entering the bottleneck-type gulf from the south. This conclusion is also supported by numerical simulation results recently published by Fischer et al. (2016a) that define the hydrodynamic constellations and potential geomorphodynamic consequences associated with a hypothetical near-coast tsunami wave, 2.5 m high, approaching Corfu from different directions. In these scenarios, modelling results revealed strongest tsunami inundation of the inner Gulf of Corfu by tsunami

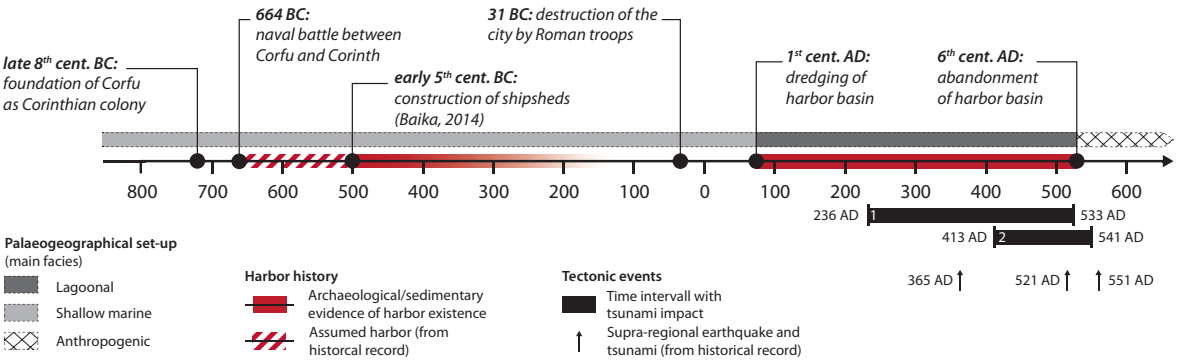

Figure 2.10: Schematic timeline with the main historical events concerning ancient Corfu and major geoarchaeological findings from this study. The pre-Roman Alkinoos Harbour naval installations were built on a sandy seashore. The Roman Alkinoos Harbour, a sheltered and quiescent basin, was used between the late 1st and early 6th cent. AD. It experienced two high-energy events related to tsunami landfall between the late 3rd and the early 6th cent. and between the beginning 5th and mid-6th cent. AD, most probably associated to the supra-regional 365 AD and 521/551 AD events, respectively.

waves approaching from the south (Fischer et al. 2016a). This hydrodynamic pattern has also to be assumed for the 365 AD tsunami event. Based on numerical models, Shaw et al. (2008) showed that teletsunami effects of the 365 AD tsunami impact generally hit Corfu from a southern direction. The height of the 365 AD tsunami waves at the southern entrance to the Gulf of Corfu is certainly controlled by shoaling effects bound to the shelf topography and to hydrodynamic local-scale effects bound to funnelling, refraction and diffraction of tsunami waters. Based on these general flow patterns (Shaw et al. 2008, Fischer et al. 2016a), we therefore hypothesize that the Gulf of Corfu was directly affected by the 365 AD tsunami event. This is also supported by sedimentary evidence that was found along the coasts of Sicily (Smedile et al. 2011, De Martini et al. 2012) and adjacent coasts of northwestern Greece (Vött et al. 2009a, May et al. 2012) proving that the 365 AD tsunami reached the northernmost parts of the Ionian Sea. The scenario of an 365 AD tsunami landfall on Corfu is thus more than likely.

Based on our results, a second tsunami event occurred between 413–533 cal AD (KOR 1A/9+ HK; *terminus ad* or *post quem*) and 430–541 cal AD (KOR 1A/6+ HK; *terminus ante quem*; Figure 2.3), namely between the beginning 5thand mid-6thcent. AD. Traces of this event were found in vibracore KOR 5 where the upper harbour sediments show increased input of fine sand. In a supra-regional context, radiocarbon dates for this event correlate well with historical records of a series of severe earthquakes and associated tsunamis that occurred in 521 AD and 551 AD as registered by modern seismological catalogues for the Gulf of Corinth (Soloviev et al. 2000, Ambrasys & Synolakis 2010, Hadler et al. 2012). This relation, however, remains speculative as the spatial extent of these historic events beyond the Gulf of Corinth is in question and not proven by historical accounts. However, traces of tsunami impact in the 6thcent. AD are also known from across the eastern Mediterranean, for instance from the Levantine coast (Goodman-Tchernov et al. 2009) and the western Peloponnese (Vött et al. 2011a). Beyond this question, the second historical event detected in the Alkinoos Harbour geoarchive provides a terminus post quem for the abandonment of the harbour, as these event deposits, lying on top of harbour sediments, are buried underneath anthropogenic infill.

2.7 Conclusions

The focus of our geoarchaeological study was to detect and investigate the geoarchive of the ancient Alkinoos Harbour thus far ascertained by archaeological excavation of harbour facilities, mainly shipshed remains. Our main objectives were to reconstruct coastline shifts and palaeoenvironmental changes and infer related human-environmental interactions. Methodologically, we carried out detailed sedimentological, geophysical, microfaunal and geochemical investigations using a multi-proxy approach. The main conclusions can be summarized as follows:

i. For the first time, sedimentary evidence of a harbour situation was found and analysed. Harbour deposits were identified by their characteristic silt-dominant grain size, by their richness in organic material and, finally, by distinctly high amounts of Pb as tracer for human activity. Sediments encountered suggest a closed and protected, low-energy harbour environment, at least for the Roman period.

ii. Based on geochronological data, the harbour was in use between the late 1st and early 6thcent. AD. The pre-Roman harbour basin, associated with the shipshed complex of the early 5thcent. BC, was not clearly traced in the sedimentary record. As a result, we assume that at least a considerable part of the Classical/Hellenistic harbour sediments was removed by extensive Roman dredging in the 1st cent. AD. The dredged Roman harbour basin was traced over a distance of 160+ m in an east-west direction (KOR 1A, KOR 5, KOR 24A). Its eastern border seems to be represented by a wall structure situated between vibracores KOR 1A and KOR 2.

iii. Grain size data and microfaunal assemblages reveal a significant difference between the eastern and western parts of the Roman harbour. Whereas the eastern part (KOR 1A, Figure 2.4 and Figure 2.5) is characterized by fine-grained sediments deposited in a quiescent low-energy zone, the western part (KOR 5, Figure 2.8 and Figure 2.7) seem to be partly exposed to higher dynamics and sea water influence. We suppose that there was a harbour entrance or channel close to site KOR 5.

iv. Pre-Roman harbour deposits were found in vibracore KOR 2 (Figure 2.4) drilled in proximity of a Roman installation. These older harbour deposits are dominated by silty sand of a beach facies. This fits well with geophysical and stratigraphic data as well as archaeological stratigraphy, documenting that the Alkinoos shipsheds were founded on fine sand.

v. We found two distinct high-energy sand layers intersecting Roman Alkinoos Harbour mud which we interpret as evidence of periodic tsunami landfall on Corfu Island (Figure 2.10). Tsunami deposits are characterized by erosional contacts, fining upward of grain size and a distinctly allochthonous microfaunal fingerprint. Based on radiocarbon dating, the first event occurred between the late 3rd and the early 6thcent. AD and most probably corresponds to the 365 AD earthquake (Crete) and tsunami event. The second event took place between the beginning 5th and mid-6th cent. AD. By interpretation of our geomorphological and geochronological evidence, both tsunami layers are thus considered to be the results of teletsunami impact and not generated by local fault movements. The Alkinoos Harbour revealed to be an excellent sediment trap for palaeotsunami signatures.

3 Geoarchaeological investigations of a prominent quay wall in ancient Corcyra – implications for harbour development, palaeoenvironmental changes and tectonic geomorphology of Corfu Island (Ionian Islands, Greece)

ABSTRACT. In antiquity, the harbour-city of Corcyra (modern: Corfu) was a prevailing naval power in the Mediterranean and had several harbours to host a considerable fleet. Today, these harbours are totally or partly silted and concealed under modern urban infrastructure. Comprehensive geoarchaeological studies were conducted on the northeastern fringe of the Analipsis Peninsula where excavations have revealed the archaeological remains of a massive quay wall (Pierri and Arion sites). These remains are located east of known ancient harbour structures that belong to the Alkinoos Harbour. Our study aimed to reconstruct the palaeoenvironmental setting of the harbour facilities at the Pierri site, including the analysis of the local sedimentary record in order to detect and differentiate natural and man-made triggers that caused environmental shifts. At the Pierri site, we found geoarchaeological evidence for an ancient harbour basin related to the prominent quay wall. Associated harbour sediments indicate a protected harbour which was developed from an open shallow marine environment, most probably by the construction of breakwaters. Harbour deposits were dated using radiocarbon analyses and diagnostic ceramic fragments to the 4th to 3rd cent. BC. This is in good agreement with the age of the harbour installations as such archaeologically assigned to the Classical and Hellenistic period. The Pierri site was possibly in function as a harbour facility even before the 4th cent. BC. In any case, it was strongly hit by an earthquake and associated tsunami event during Classical to Hellenistic times. By this event, the harbour was uplifted and covered by event deposits so that it was not usable any more. It was subsequently buried by anthropogenic and colluvial sediments. Overall, the Pierri coastal archive allowed to identify three distinct tsunami landfall events, namely before 2483-2400 cal BC (event I), after 2483-2400 cal BC and before 370-214 cal BC (event II), and during Classical to Hellenistic times, most probably between the 4th and 3rd cent. BC (event III). Another tsunami event (event IV) potentially hit the site when it was dry land. Ages of tsunami events I-II and candidate tsunami IV are consistent with tsunamis known from the coasts of western Greece and southern Italy and where thus classified as supra-regional tele-events. Event III was identified as associated to a local earthquake and tsunami by which Corfu Island was uplifted and, at the same time, tilted with a vertical offset of 1.74 m from W to E.

This chapter is based on
Finkler et al. 2017b

3.1 Introduction

In the Mediterranean, early seafaring took probably place as early as in the Middle Palaeolithic (Ferentinos et al. 2012). However, in antiquity harbours played a major role for colonization, trade and military expansion and were the hubs of local, regional and supra-regional traffic systems. Originally installed as basic utilitarian facilities enabling the transportation of goods, harbours evolved as fundamental structures of coastal cities and ensured extensive trade activities and economic welfare. Even those ancient cities that were located further inland spared no effort to obtain access to the sea and harbour infrastructure. Thus, harbours existed in large numbers and were the direct expression of power.

Early travellers and savants of early modern times were the first to describe ancient harbours after they had been buried in oblivion for hundreds of years. During the past two centuries, however, historians and archaeologists became more and more intrigued by ancient harbours, giving rise to profound scientific harbour research (Lehmann-Hartleben 1923, Blackman 1982b). Modern harbour geoarchaeology has evolved during the past three decades. It is a young, rapidly emerging and growing discipline that experiences increasing attention (e.g. Marriner & Morhange 2007).

Harbour basins represent rich geoarchaeological archives that can be used to detect manifold past environmental changes. In ancient harbours, particularly suitable indicators for palaeoenvironmental reconstructions such as pollen, microfauna, charcoal or plant remains are preserved (Marriner & Morhange 2006a, Morhange et al. 2014). Apart from sedimentological aspects, harbour-related facilities such as quays, breakwaters, fortification walls or towers, slipways and shipsheds (e.g. Blackman 2013b, Baika 2003, 2013a) might also bear relevant information concerning palaeoenvironmental conditions and the overall set-up of the harbour complex (Baika 2013b, 2015, Stiros & Blackman 2014).

Today, ancient harbours are either submerged and partly eroded or landlocked, now often lying distant from the present coastline. Both is due to extensive coastal changes that took place since the time they were in use (Blackman 1982b, Vött & Brückner 2006, Vött 2007b, Brückner et al. 2010). Among the natural factors, why harbour basins lost their functionality and were finally abandoned, gradual relative sea level changes and strong siltation but also extreme events like co-seismic uplift or destruction by earthquakes and tsunamis are the most prominent.

Regarding these extreme events, the island of Corfu is located in a key position between the seismically relatively stable Adriatic Sea (D'Agostino et al. 2008, Di Bucci & Angeloni 2013) and the Ionian Sea, one of the most seismically active regions in the Mediterranean (Sachpazi et al. 2000, Figure 3.1 A). Uplifted and submerged notches document that coastal changes on Corfu can be linked to earthquakes (Pirazzoli et al. 1994, Evelpidou et al. 2014, Mastronuzzi et al. 2014). On Corfu, there is also geoscientific evidence of repeated tsunami landfall as shown by recent investigations in near-coast lagoonal environments (Fischer et al. 2016a) and documented by traces of historical tsunami events recorded in the Roman Alkinoos harbour (Finkler et al. 2017a). Ever since, ancient

harbours are well-known as excellent sediment traps for extreme wave events such as tsunami inundation (e.g. Vött et al. 2011a, Bony et al. 2012, Hadler et al. 2013, 2015a, 2015b).

However, ancient harbours of Corfu were subject to only few geoarchaeological studies so far (Finkler et al. 2017a). This is surprising as ancient Corcyra, located on the east coast of Corfu Island, was part of an extensive trade network in the Adriatic and Ionian Seas since the Archaic period. Moreover, it was one of the first city states throughout the Mediterranean to construct a large fleet of warships requiring harbour facilities to store and repair them. According to ancient sources, Corcyra had at least two harbours with associated infrastructure, namely the Alkinoos Harbour in the north and the Hyllaikos Harbour in the southwest of the Analipsis Peninsula (Figure 3.2 A; Lehmann-Hartleben 1923, Kielche 1979, Baika 2013a). A third harbour, mentioned by Skylax (Per. 29) and probably referred to by Thucydides (3.75.5, after Crawley 1910), may be located at the northeastern fringe of the city (Riginos et al. 2000, Baika 2003). The Alkinoos Harbour in the north is well documented in an archaeological context and provides an excellent archive for geoarchaeological research (Finkler et al. 2017a). Yet, the overall harbour topography along the entire northern part of the peninsula is complex and difficult to understand. In any case, a number of specific archaeological remains of harbour-related infrastructure (Baika 2013a) are reliable indicators to reconstruct the ancient harbour setting along the northern fringe of the Analipsis Peninsula.

The present study focusses on the Pierri site at the northern fringe of the Analipsis Peninsula where distinct elements of ancient harbour facilities were found within the framework of archaeological excavations, such as a section of a quay wall, probably associated with a presumed ramp structure. Together with the associated sedimentary record, the harbour site represents a promising setting where complex interactions between man-made infrastructure and palaeoenvironmental changes have been recorded.

We conducted detailed investigations of the sedimentary record in this part of the harbour in order

i. to reconstruct the palaeoenvironmental setting for the time when the harbour facilities were used,

ii. to identify coastal changes and relative sea level fluctuations in the late Holocene and their major triggering factors, and

iii. to check whether the harbour can be used to reconstruct seismo-tectonic events, such as tsunami impacts, co-seismic crust movements and tectonic influences.

3.2 Regional Setting

3.2.1 Natural Setting

Corfu is located in the northern Ionian Sea, close to the Street of Otranto which is the entrance to the Adriatic Sea. Corfu is the northernmost island of the Ionian archipelago where all types of plate boundaries can be observed within a distance of only 100 km (Figure 3.1 A; Sachpazi et al. 2000). In the north, the eastern coasts of the Adriatic Sea are under the influence of both subsidence and uplift due to the continent-continent collision caused by the movement of the Adriatic Microplate towards the Eurasian Plate (Babbucci et al. 2004, Suric et al. 2014). The Ionian Sea itself is situated between the subduction zones of the Calabrian Arc in the southwest and the Hellenic Arc in the southeast (van Hinsbergen et al. 2006, Hollenstein et al. 2008). Both systems, the subduction zones in the south and the collision belt in the north, are separated by the Cefalonia Transform Fault (CTF), a large dextral strike-slip fault zone right south of Corfu (Kokkalas et al. 2006), and the Kerkyra-Cefalonia submarine valley system with associated faults as northern branch of the Ionian subduction zone (Poulos et al. 1999).

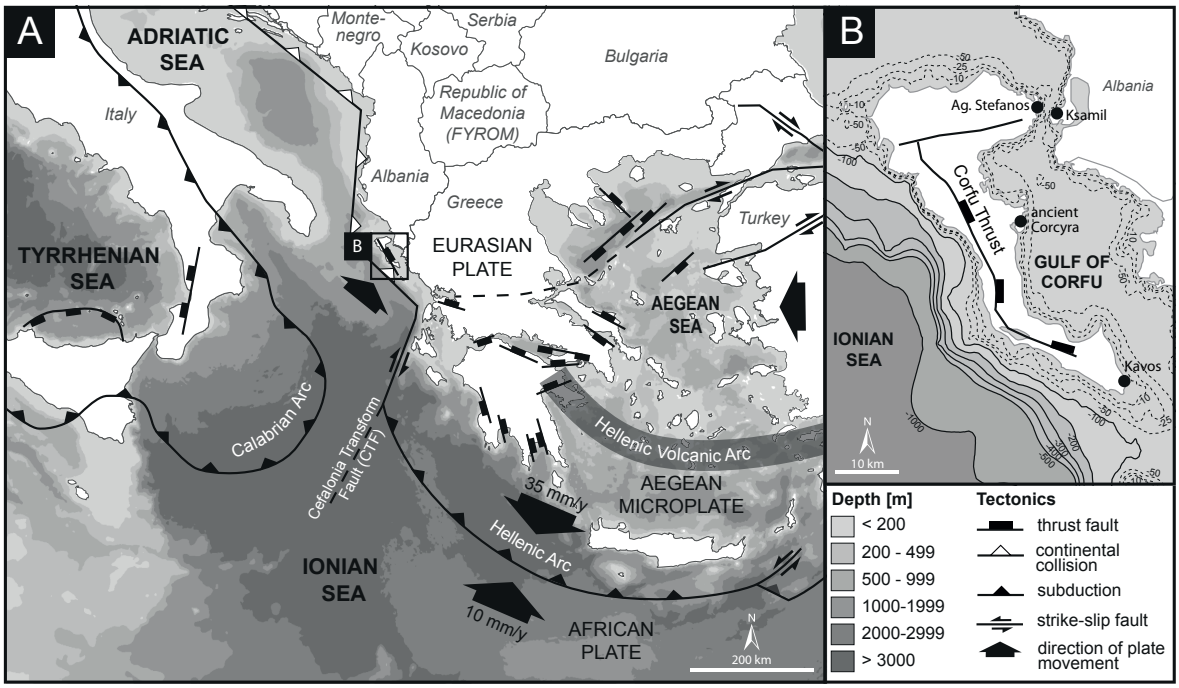

Figure 3.1: Tectonic structures and bathymetric conditions in the eastern Mediterranean. (A) Simplified tectonic map of the Ionian, Adriatic and Aegean Seas. Corfu Island (black box) is exposed to the Adriatic continental collision belt in the north, the subduction zones of the Hellenic and Calabrian Arc in the South and the Cefalonia Transform fault (CTF) right southwest of the island. Owing to compressional tectonics, the Corfu thrust as thrust fault runs across the island. (B) Simplified bathymetry map of Corfu Island. While the lake-like Gulf of Corfu (Partsch1887) between the island and the Greek/Albanian mainland features water depths of less than 70 m, the steep continental slop west of Corfu reaches more than 1000 m water depth. Main tectonic structures after Billi et al. (2007), Doutsos & Kokkalas (2001); bathymetry after GEBCO (2014).

Corfu Island is therefore located within an exceptional tectonic stress field resulting in the Corfu thrust, a NNW-SSE running compressional structure on the island, accompanied by frequent shallow focus earthquakes (van Hinsbergen et al. 2006, Kokkalas et al. 2006). They reach moment magnitude values around 6 (Stucchi et al. 2013) and are documented by several entries in earthquake and tsunami catalogues since medieval times (Partsch 1887, Soloviev et al. 2000, Ambraseys & Synolakis 2010, Hadler et al. 2012).

Pirazzoli et al. (1994) and Evelpidou et al. (2014) detected emerged coastal notches on Corfu and satellite islands indicating co-seismic uplift. The notches on Corfu document at least two periods of crust uplift for the central and western part of the island. The first is dated to the 8th–4th cent. BC, while the second event has remained undated so far. Mastronuzzi et al. (2014) suggests a tectonic up- and down movement of the island. They also describe further earthquakes and assume associated tsunami inundations, for example at around 1000 cal BC, contemporaneous with a tsunami landfall reported from northwestern Greece (Vött et al. 2006, 2011b).

On Corfu, Fischer et al. (2016a) detected geomorphological and microfaunal traces of multiple tsunami inundation in near-coast lagoons, proving Corfu's sensitivity towards tsunami events, and Finkler et al. (2017a) present geoscientific evidence of historical tsunami impact to the Roman Alkinoos Harbour. Palaeotsunami signatures in coastal geoarchives are also reported from the other Ionian Islands (Hadler et al. 2011, May et al. 2012, Willershäuser et al. 2013), the northern Greek mainland (Vött et al. 2009a, 2010, 2011b), and the Italian coasts of the Ionian and Adriatic Seas (Gianfreda et al. 2001, Mastronuzzi et al. 2007, Smedile et al. 2011, De Martini et al. 2012). Local seismic events might also cause submarine debris flows, mainly bound to the slopes of the Kerkyra-Cefalonia valley system and the steep continental slope to the west of Corfu (Figure 3.1 B; Poulos et al. 1999).

The wind and wave climate of the northern Ionian Sea is dominated by mainly westerly winds and low significant wave heights with average values of less than 1 m (Cavaleri 2005, Lionello et al. 2012). During winter season, storms occur frequently, often linked to Sirocco or tropical-type cyclones, so-called medicanes (Llasat 2009). Even though the track lines of such medicanes usually run further south, they are a known phenomenon in the northern Ionian Sea (cf. Davolio et al. 2009). Due to the prevailing westerly winds, it is mainly the western coast of Corfu, facing the open Ionian Sea, which is affected by such conditions. In contrast, the eastern shores of the island with the ancient city of Corfu (Corcyra) and its harbours adjoin the Gulf of Corfu. The Gulf of Corfu has water depths of less than 70 m and is described as almost lake-like (Partsch 1887; Figure 3.1 B) with a very weak wave climate (Mazarakis et al. 2012, Zacharioudaki et al. 2015). Topographically, ancient Corcyra is located on the Analipsis Peninsula (Figure 3.2 A) which separates the Chalikiopoulou Lagoon in the west from the Bay of Garitsa in the east. The peninsula is built of Miocene marls (IGME 1970) forming a ridge up to 60 m high.

3.2.2 Archaeological and historical background

Ancient Corcyra was founded as a Corinthian colony in the late 8th cent. BC due to its strategic position between the Adriatic and Ionian Seas along the sea routes between Greece and Italy (Kiechle 1979). Soon, the former colony emerged as a prevailing naval power in the Mediterranean, documented by its participation in the first naval battle ever recorded in Greek history in 664 BC against its metropolis Corinth (Thucydides 1.13.4 after Crawley 1910). Corcyra was one of the first Mediterranean city states that invested in a considerable fleet of triremes and appropriate harbour infrastructure (Baika 2013a). According to Thucydides (1.25.4, after Crawley 1910), Corfu is supposed to have owned at least 120 ships before the Peloponnesian War.

The Archaic polis of Corcyra evolved on the naturally fortified Analipsis Peninsula, where the remains of several sanctuaries, such as the Heraion, one of the earliest major temples in Greece (Sapirstein 2012), are still preserved (Figure 3.2 A and Figure 3.11). From here, the city extended towards the western and northern hill slopes into the coastal lowlands where the harbours of the city were situated according to ancient sources (Schmidt 1890, Lehmann-Hartleben 1923, Baika 2003). While two of the ports, the military Alkinoos Harbour in the Bay of Garitsa and the Hyllaikos Harbour on the eastern shore of the Chalikiopoulou Lagoon (Figure 3.2 A), are well documented in an archaeological context (Partsch 1887, Dontas 1965, Kanta-Kitsou 2001, Baika 2013a), a third harbour suggested along the northern fringe of the peninsula remains conjectural (Riginos et al. 2000, Gehrke & Wirbelauer 2004, Baika 2013a).

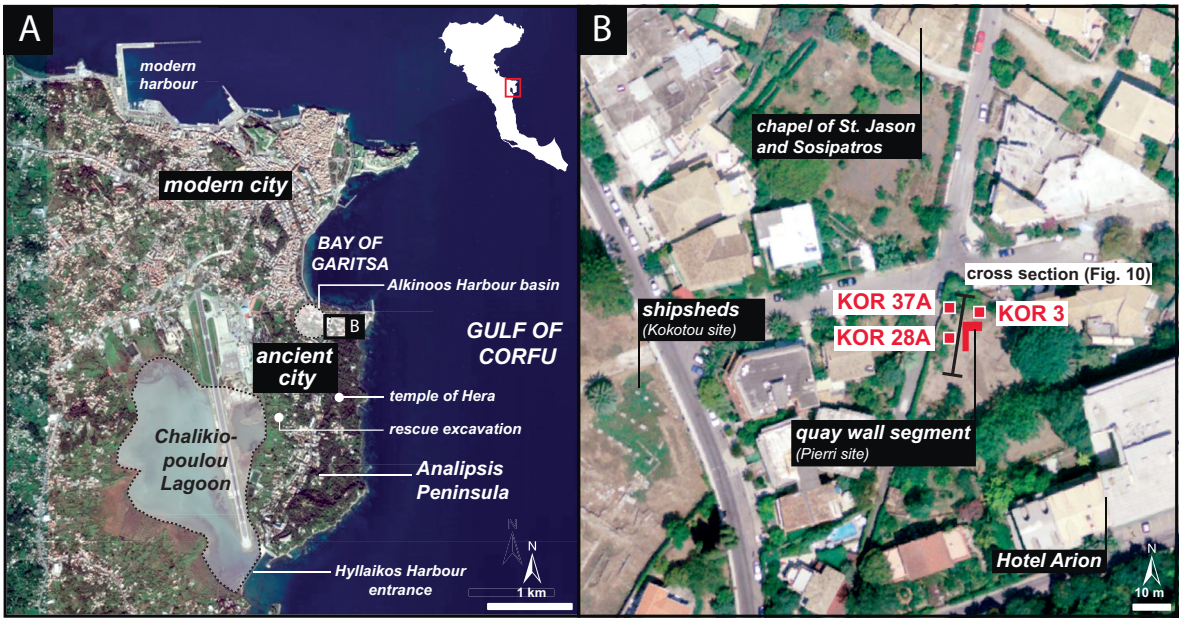

Figure 3.2: Topographic overview and detailed map of the study area. (A) Corfu city is situated at the eastern shore of the island and separated from the Greek and Albanian mainland by the Gulf of Corfu. Ancient Corcyra was built on the Analipsis Peninsula between the Chalikiopoulou Lagoon in the southwest and the Bay of Garitsa in the north. (B) The area associated with the ancient Alkinoos Harbour, traced by archaeological remains of shipsheds (Kokotou site), lies *c.* 200 m distant to the present coastline. At the Pierri site, remains of a quay wall document the use as a harbour (Baika 2013a). Vibracoring sites are marked by red rectangles. Map modified after Bing Aerial (2016) and NCMA S.A. (2014).

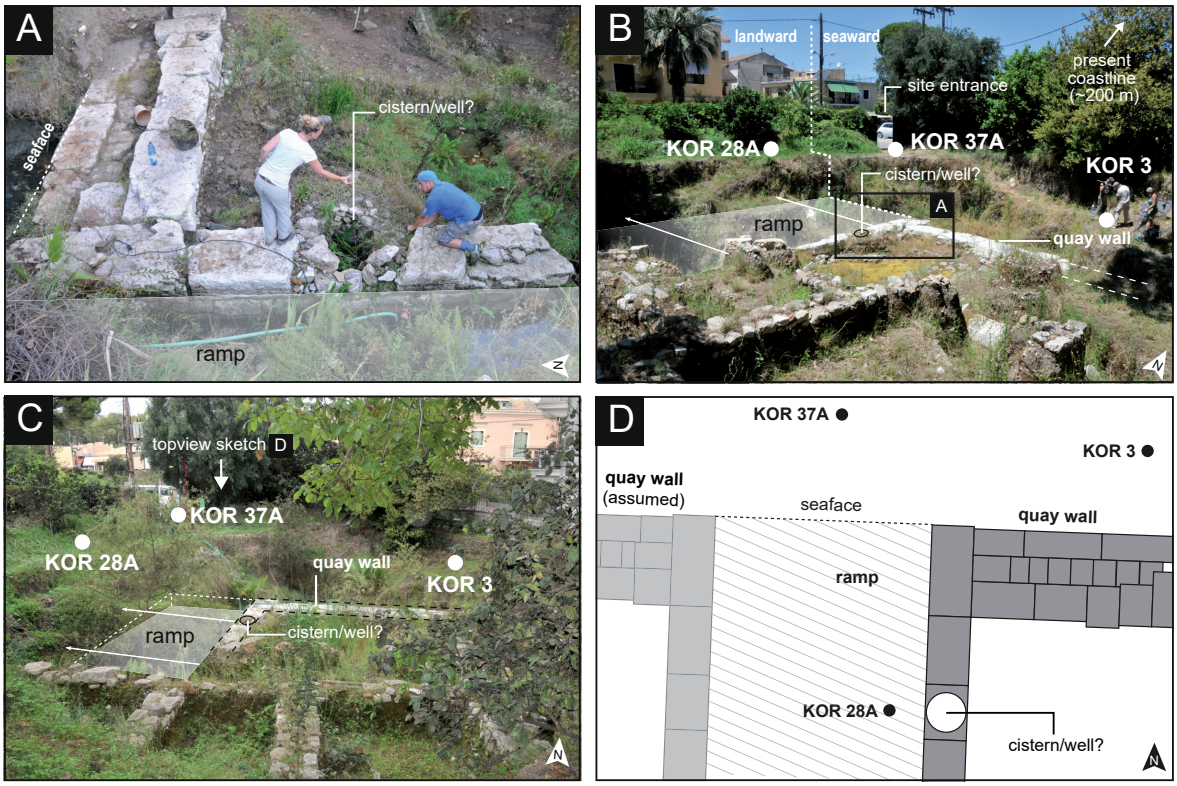

Figure 3.3: Photographic overview of the Pierri site. (A) Detailed view of the quay wall segment and vertical wall section, excavated at the Pierri site. View to the east. (B), (C) Location of vibracoring sites in relation to the Pierri quay wall and the associated ramp. View to the northwest and north, respectively. Vibracore KOR 28A was drilled on the landward site of the quay, covering the area of the assumed ramp, while vibracore KOR 3 is situated seaward right in front of the quay wall. Vibracoring site KOR 37A was drilled right in front of the assumed ramp. (D) Simplified sketch (top view, not true to scale) of the Pierri Site quay wall segment with associated ramp. (Photos by A. Vött 2012, 2013, 2014).

The present study focuses on remains of harbour facilities at the so called Pierri site on the northeastern coast of the peninsula. West of it, at the Kokotou site, the basin of the Alkinoos Harbour, though silted, can be traced by harbour infrastructure which developed on its shore, namely a section of a monumental complex of trireme shipsheds (Figure 3.2 B) dating to the early 5th cent. BC (Preka-Alexandri 1986, Spetsieri-Choremi 1997, Baika 2003, 2013a). This shipshed complex was excavated in the 1980s and 1990s and has been subject to geoarchaeological research (Finkler et al. 2017a), still ongoing. At the Pierri site, located approximately 80 m to the east of the shipsheds, recent rescue excavations brought to light remains of a continuous W-E running quay wall (Figure 3.3). This quay is interrupted by slipways or ramps that slope towards the sea at regular intervals (Riginos et al. 2000; Figure 3.3). The prolongation of the quay wall and ramp system towards the east of the Pierri site is nowadays covered by modern buildings, for example by the Hotel Arion complex. Here, the most significant section of the quay wall was excavated before the construction of the hotel (Arion site, Figure 3.2 B).

Structurally, the quay wall section at the Pierri site is made out of white limestone ashlars and characterized by a corner with a vertically disposed branch, orientated north-south. This wall section seems to be the lateral delimitation of a ramp, today covered by younger deposits. The western

part of the presumed ramp is assumed under a modern road construction (Figure 3.2 B). The archaeological remains found at the Pierri site are yet unpublished. Geoarchaeological and geomorphological investigations presented in this paper considerably enhance the understanding of the evolution of the harbour environment.

The northern harbour zone was heavily used and modified since the destruction of the city by the Roman troops of Agrippa in 31 BC, right before the battle near Actium. In Roman times, the harbour basins were partly covered with debris from different remodelling phases of the city. Moreover, some sections of the harbour area were used as a cemetery, reshaping the pre-Roman structures and deposits. Remains of Roman residential quarters and warehouses have been sporadically unearthed lying on top of Classical and Hellenistic structures (Riginos et al. 2000, Baika 2013a).

In general, the seaward shift of the coastline since antiquity and modern urban building activities have concealed the harbour topography. At the Pierri site, the quay structure is located more than 200 m distant from the present coastline (Figure 3.2), bearing witness of significant palaeogeographical changes. Due to the extensive urban development of the modern city, the archaeological reconstruction of the northern harbour topography is still conjectural. It is still unclear if all known remains of harbour facilities, such as the Kokotou shipsheds and the Pierri and Arion quay wall sections, belonged to one and the same harbour, namely the Alkinoos Harbour. Even in case they did, we are uncertain on the overall form, extent and topographical configuration of this harbour. However, all these harbour facilities may be of the same age or may have been used simultaneously for a certain period of time, in particular during the Classical and Hellenistic periods (5th to 1st cent. BC). Archaeological research needs to be intensified to clarify their precise ages.

3.3 Methods

This study used a multi-methodological approach including sedimentological, geochemical and microfaunal methods in order to reconstruct palaeoenvironmental conditions of the harbour environment at the Pierri site.

Vibracoring was conducted to retrieve the stratigraphical sequence in the context of archaeological structures. Three vibracores covered all relevant parts of the Pierri site, namely the landward area of the assumed ramp, its seaward continuation and the area right in front of the excavated quay wall section (Figure 3.2 B, Figure 3.3). We used an automotive drill rig (Nordmeyer RS 0/2.3) and a handheld vibracorer (Atlas Copco Cobra mk 1) with core diameters of 50 to 80 mm. Vibracores were cleaned, photographed, described and sampled with regard to stratigraphical units. Selected vibracores (suffix "*A*") were drilled using plastic liners to enable high-resolution in-situ measurements in the laboratory.

At vibracoring site KOR 37A, in-situ Direct Push Electrical Conductivity (DP EC) logging was conducted. The used DP EC probe (Geoprobe SC520) had four electrodes in a linear Wenner arrangement to measure electrical conductivity and the rate of penetration every 2 cm (Schulmeister et al. 2003, Harrington & Hendry 2006, Fischer et al. 2016b).

Position and elevation of vibracoring and DP EC sites were determined by means of a differential GPS (Topcon HiPer Pro FC-250).

In the laboratory, grain size distribution of samples from selected sediment layers was analysed using the Köhn method (Köhn 1929, DIN ISO 11277: 2002, Blume et al. 2011). After separating skeletal components > 2 mm, each subsample of 15 g was first pretreated by H_2O_2 and dispersants. The amounts of clay and silt were determined by pipetting, while sand was analysed by dry-sieving. Magnetic susceptibility was measured using a Bartington Instruments MS3 with a MS2K surface sensor. Laboratory work also comprised X-ray fluorescence (XRF) analyses by means of a portable Niton XL3t 900S GOLDD (calibration mode SOIL) instrument, yielding concentrations of Ca, Fe, Pb and more than 25 other elements. Measurements were conducted in-situ on the undisturbed sediment cores with an average resolution of 2 cm. Data obtained by handheld XRF devices, analogues to data obtained by XRF core scanners, are considered to be of semi-quantitative nature because of matrix effects. Such matrix effects may be due to possible variations in particle size, uniformity, surface geometry and moisture (EPA 2007, Chagué-Goff et al. 2017). Compared to alternative analysing methods, absolute elemental concentrations might be slightly differing and/or shifted to higher or lower levels depending on such matrix effects (Argyraki et al. 1997, Shefsky 1997). To ensure comparison, we therefore preferred elemental ratios and focussed on distinct shifts in general distribution patterns and overall trends of elemental concentrations that indicate major changes in palaeoenvironmental conditions. Geochemical analyses based on pXRF are an approved and accepted tool in palaeoenvironmental research (Judd et al. 2017).

Selected sediment samples from vibracores KOR 28A and KOR 37A were examined regarding their microfaunal content. We mainly concentrated on foraminifera as they occur under marine to rarely brackish conditions and thus represent excellent indicators for the reconstruction of different palaeoenvironmental settings due to their different ecological requirements (Murray 1991, 2006). Thus, foraminiferal assemblages help to differentiate between abrupt and gradual changes as well as to detect allochthonous interferences (Dominey-Howes et al. 2000, Mamo et al. 2009, Pilarczyk et al. 2014). In the frame of the presented study, 15 ml of sediment from each sample were pretreated with H_2O_2 and sieved into fractions of > 400 µm, > 200 µm and > 125 µm. We used up to 5 ml of sample material for a semi-quantitative microfaunal analysis. Foraminifera were counted and determined after Loeblich & Tappan (1988) and Cimerman & Langer (1991) using a stereo microscope. Species were classified according to their habitat preferences after Murray (1991, 2006) and Sen Gupta (1999). Additionally, photos of selected specimens were taken using a scanning electron microscope (SEM).

Altogether ten organic samples were dated by means of ^{14}C-AMS analysis, which was accomplished at the Klaus-Tschira Laboratory of the Curt-Engelhorn-Centre Archaeometry gGmbH Mannheim, Germany (MAMS), and the Keck Carbon Cycle AMS Facility, University of California at Irvine, USA (UCI; Table 3.3). Five samples of charcoal, wood and seaweed were extracted from vibracores KOR 28A and KOR 37A in order to establish a local geochronostratigraphy of the harbour development at Pierri. This geochronostratigraphy was complemented by a local age-depth-model based on relative sea level indicators (peat, oysters) or on samples that were collected right above peat-like layers; thus, the latter samples were also in close relation to the local sea level at the time of their deposition. Concretely, this model is based on two samples from vibracores that were drilled in the surroundings of the ancient city (Finkler et al. 2017a) consisting of charcoal and peat, respectively. Additionally, three oyster samples were collected from a band of oysters that was found adhered to a section of the Pierri quay wall which was recently unearthed. Calibration of all samples was realised based on the software Calib 7.1 (Stuiver & Reimer 1993, Reimer et al. 2013). Archaeological age estimates of diagnostic ceramic fragments (Table 3.4) were used to cross-check radiometric ages.

3.4 Results: Stratigraphical record at the Pierri site

Three vibracores were drilled at the Pierri site (Figure 3.2 and Figure 3.3), including the landward area of the presumed ramp structure (vibracore KOR 28A; Figure 3.4, Figure 3.5 and Figure 3.6), its seaward continuation (vibracore KOR 37A; Figure 3.7, Figure 3.8 and Figure 3.9) and the harbour basin to the north of the quay (vibracore KOR 3; Figure 3.5). Moreover, we obtained high-resolution stratigraphical data at vibracoring site KOR 37A by DP EC logging.

Vibracoring sites KOR 3, KOR 28A and KOR 37A (Table 3.1) are located in a short distance to one another, their position being closely related to the archaeological quay structure. Vibracore KOR 3 was drilled to the immediate north of the Pierri quay wall. It shows a layer of compact silty clay at its base, covered by a thick sequence of grey fine to finest sand. At 2.77 m b.s., sediment texture changes towards silt and silty sand of dark grey colour. Towards the top, at 2.35-1.61 m b.s., a layer of gravel embedded in a sandy matrix was found followed by brownish clayey silt including cultural debris.

At the base of vibracore KOR 28A, drilled on a presumed ramp structure several meters 'inland' of the quay wall, a thick basal section of greyish fine to finest sand is intersected two times by layers of coarse sand and sandy gravel, respectively. At 4.40 m b.s. a layer of homogeneous light-grey fine sand appears, which is covered by solid stones. Finally, we found a section of greyish-brownish coarse sand followed by a thick unit of clayey silt with embedded ceramics and debris that marks the upper part of the core.

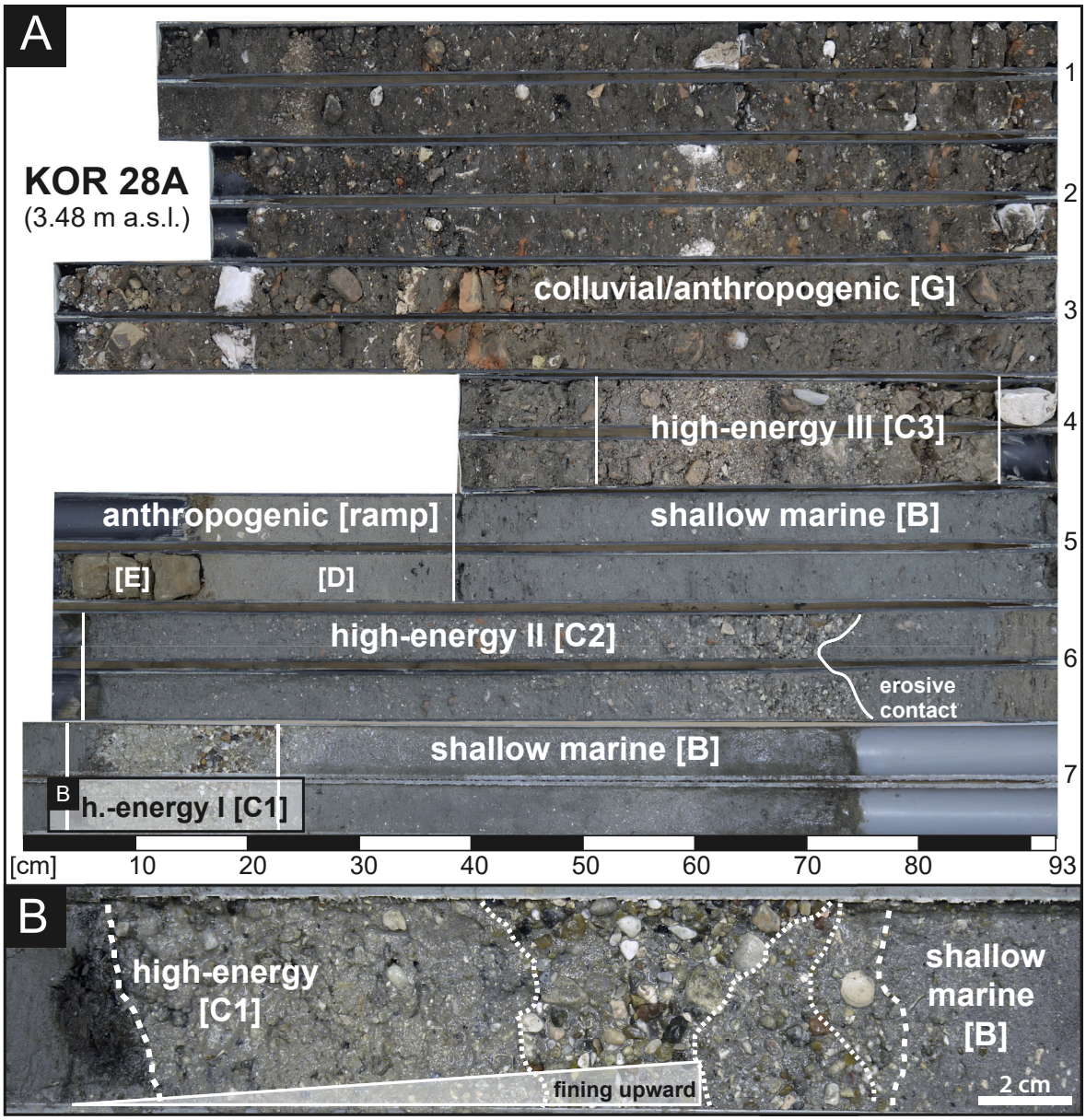

Figure 3.4: Stratigraphical record of vibracore KOR 28A. (A) On top of a thick unit of shallow marine sand, intersected by two high-energy layers (I and II), a solid ashlar out of calcareous sandstone and underlying homogeneous fine sand mark the base of the ramp at the Pierri site. It is covered by sediments of a high-energy facies (event III) and subsequent sediments of colluvial to anthropogenic origin. Capital letters B-G represent associated stratigraphical units; see text for explanation. (B) Detailed photo of high-energy deposits (event I, 6.61-6.06 m b.s) intersecting shallow marine sands. Mark the fining upward tendency in grain size and the peat-like sediments on top.

The stratigraphy of vibracore KOR 37A, drilled in front of the presumed ramp and the quay wall abreast to site KOR 3, is characterised by fine to finest sand at the base. This sand layer is intersected by two layers of coarse-grained deposits, namely coarse sand and gravel. After a sharp contact at 4.63-4.17 m b.s., a sequence of very heterogeneous silty sand and silt was found, containing large amounts of organic remains and debris. Following a section of multi-coloured sandy gravels at 3.87-3.53 m b.s. a sequence of brownish clayey silt, more than 3 m thick, characterises the upper part of the core. This layer was found intersected by a comparatively thin layer of light and slightly coarser deposits.

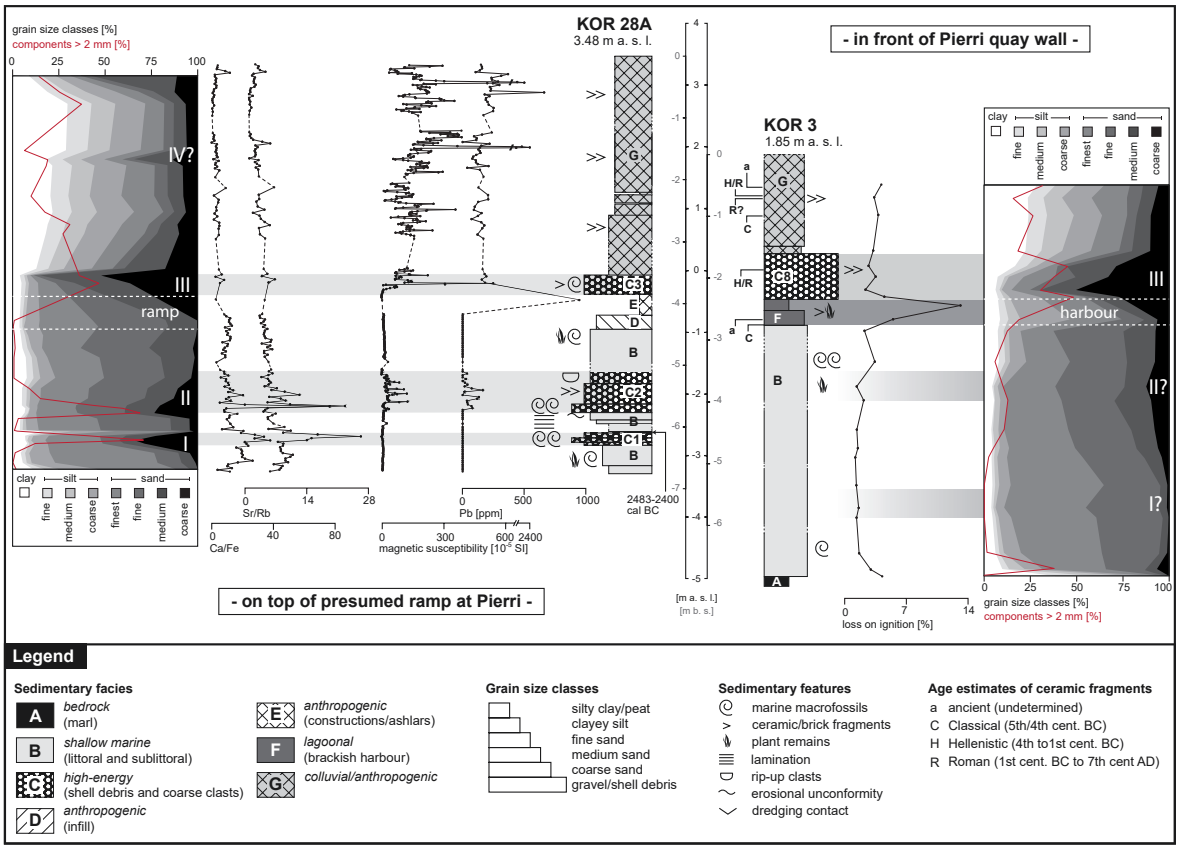

Figure 3.5: Results from grain size analysis, magnetic susceptibility measurements and selected geochemical proxies of vibracores KOR 28A (left) and KOR 3 (right). Lagoon-type harbour deposits (highlighted by dark grey colour) in vibracore KOR 3 were found in a stratigraphical position consistent with anthropogenic deposits marking most likely the base of a ramp. High-energy layers (highlighted by light grey colour) are characterised by increased amounts of medium to coarse sand but show different geochemical fingerprints.

Based on distinct similarities in grain size, colour, geochemical parameters and microfaunal content, the local sedimentary records of vibracores KOR 3, KOR 28A and KOR 37A was classified into the following stratigraphical units A to G. Due to the high variability of unit C sediments, we differentiate between eight subunits C1 to C8.

Unit A (8.85–7.00 m b.s. in KOR 3, Figure 3.5) is restricted to vibracore KOR 3. It is characterised by compact silty clay of grey colour, rich in $CaCO_3$, showing medium LOI values of *c.* 5 %.

In contrast, ***Unit B*** was found in all vibracores (6.85–2.77 m b.s. in KOR 3; 6.93–6.23, 6.06–5.75, 5.08–4.40 m b.s. in KOR 28A; 8.53–6.75, 6.36–5.65, 5.42–4.63 m b.s. in KOR 37A). It consists of greyish fine sand with minor amounts of medium and coarse sand and components > 2 mm. Geochemically, the unit is characterised by a low to medium Ca/Fe ratio and a medium Sr/Rb ratio. The deposits are void of Pb and show a very low magnetic susceptibility. High-resolution DP EC logging at vibracoring site KOR 37A (Figure 3.8) revealed strongly increased EC values to the base of the unit. The sand within unit B contain medium to high abundances of well-preserved marine foraminifera from different ecological habitats. However, the distribution of species shows a depth-related shift in vibracore KOR 28A: In the lower part, Miliolidae (especially *Quinqueloculina*

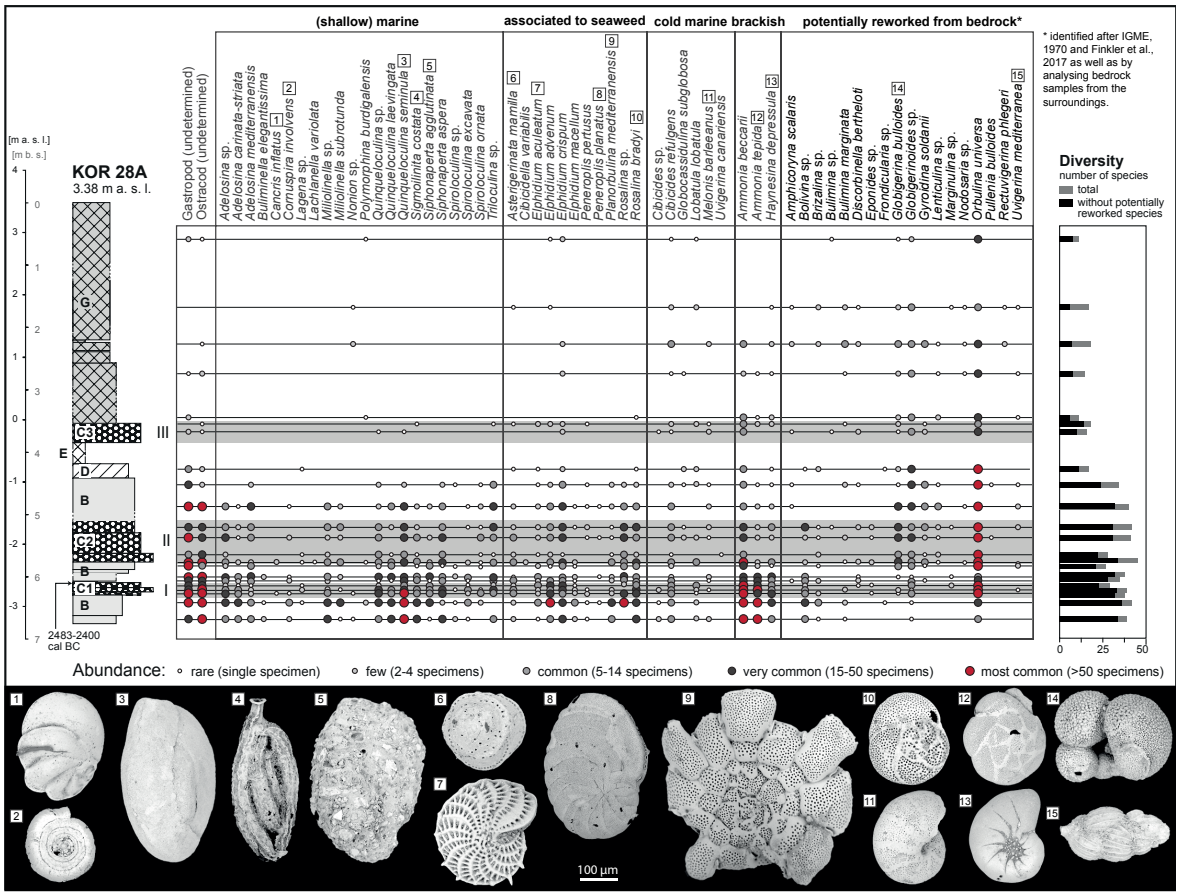

Figure 3.6: Results of microfaunal analyses for samples from vibracore KOR 28A based on a semi-quantitative approach. Species are classified according to their ecological preferences after Murray (2006) and Sen Gupta (1999). Potentially reworked species from the Neogene bedrock were identified after IGME (1970), Finkler et al. (2017a) and by analysing bedrock samples from the surroundings. Shallow marine sands show decreasing diversity and abundance of foraminifera towards the top. The two high-energy event layers found in the lower part of the core are similar to shallow marine sediments regarding their microfaunal content. In contrast, high-energy deposits found on top of the ramp are characterised by lower abundance and diversity.

seminula), habitants of seaweed meadows and species, tolerating also brackish water (*Ammonia tepida, A. beccarii, Haynesina depressula*) occur in high numbers. In contrast, their abundances decrease in the upper part of unit B. Instead, planktonic foraminifera and species preferring deeper and colder waters appear with increasing numbers.

Unit C is characterised by badly sorted sand with distinctly increased amounts of medium to coarse sand and skeletal components > 2 mm. As sediments from this unit appear highly variable, we differentiate between the following subunits (Table 3.2).

Subunit C1 (6.23–6.06 m b.s. in KOR 28A, Figure 3.4 B) is characterised by greyish medium and coarse sand including high numbers of multi-coloured gravels and abundant marine macrofauna. To the top of the unit, grain size distribution reveals a general fining-upward tendency with a clayey mud layer, rich in organic material, on the very top. Similar to unit B, Pb and magnetic susceptibility show low values, whereas Ca/Fe and Sr/Rb ratios reveal distinct peaks, the latter even reaching the highest values within the whole profile. Palaeontologically, the coarse sand

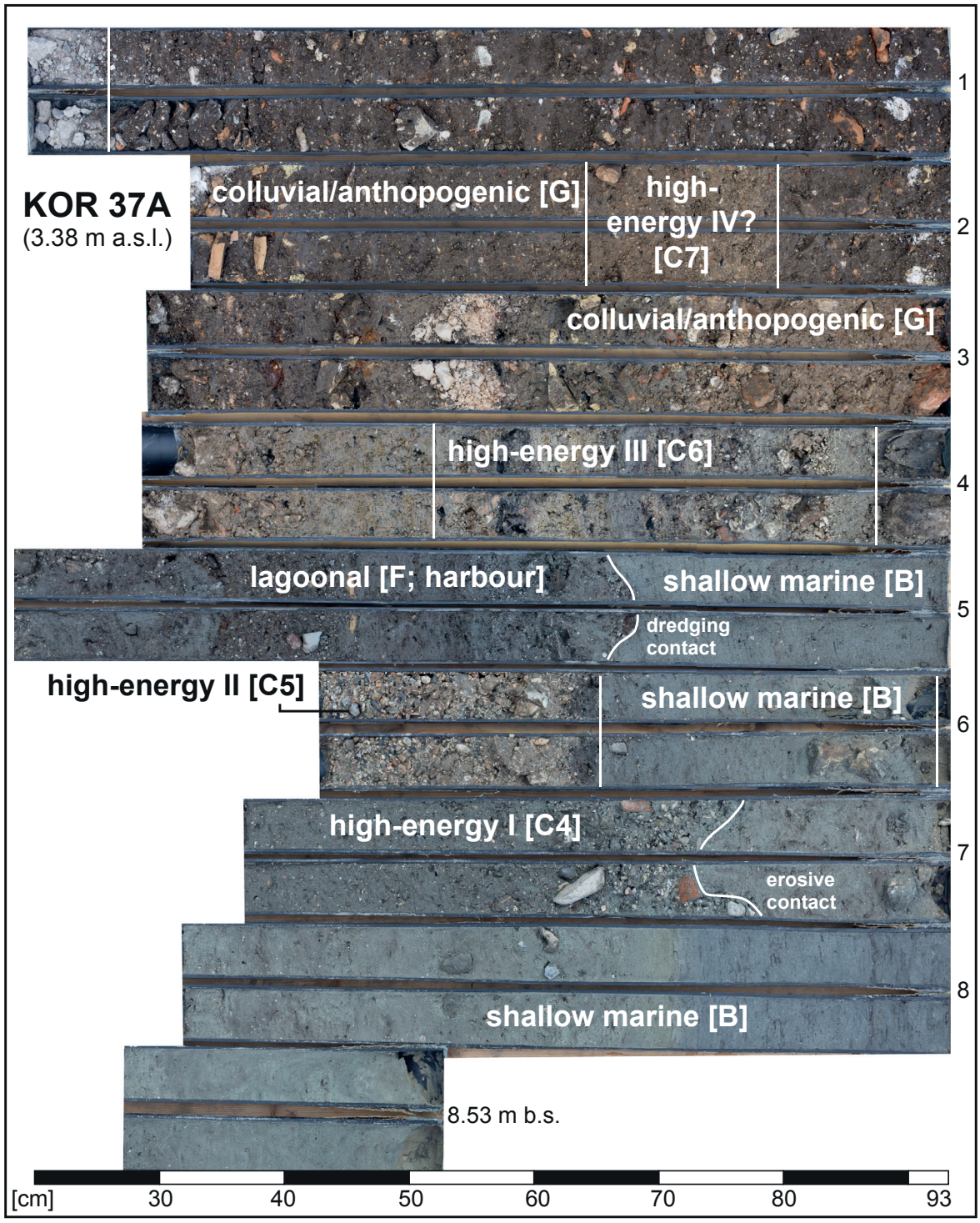

Figure 3.7: Stratigraphical record of vibracore KOR 37A. Shallow marine sands show intersected high-energy layers and are followed by thick colluvial to anthropogenic deposits. Harbour deposits (4.63-4.17 m b.s.) are characterised by an abrupt increase of silt content and contain stones, ceramic fragments and organic material. Capital letters B-G represent associated stratigraphical units described in the results chapter.

of subunit C1 is dominated by marine and seaweed assemblages with decreased numbers of Miliolidae but a slightly increased abundance of cold-marine and planktonic species like *Orbulina universa,* and *Lobatula lobatula* (Murray 2006). Moreover, *Globigerina bulloides* and *Globigerinoides* sp. appear initially.

Subunit C2 (5.75–5.08 m b.s. in KOR 28A) was found on top of an erosive contact and is characterised by gravel embedded in a matrix of medium to coarse sand. The unit further reveals a fining upward sequence in grain size and contains plenty ceramic fragments and clasts, consisting of clayey silt. Ca/Fe and Sr/Rb values were found on a medium level with distinct peaks. In contrast to the geochemical characteristics of unit B, peaks in Pb concentration and magnetic susceptibility are visible. Microfaunal analyses indicate a similar foraminiferal fingerprint as found for unit B and subunit C1 with increased abundance of *Lenticulina* sp. and *Gyroidina soldanii*, both preferring cold-marine conditions (Murray 2006) and missing in the sediments below.

Subunit C3 (3.87–3.52 m b.s. in KOR 28A) features greyish to brownish coarse sand with considerable amounts of medium sand and gravel. The sand contains various marine macrofauna, ceramics and charcoal. While Ca/Fe and Sr/Rb ratios are very similar to those of the underlying units, Pb contents reach medium to high values. Moreover, magnetic susceptibility increases distinctly. The microfaunal fingerprint strongly resembles unit D: seaweed–related and especially (shallow) marine species occur only in small numbers. Instead, cold-marine and brackish species are dominant.

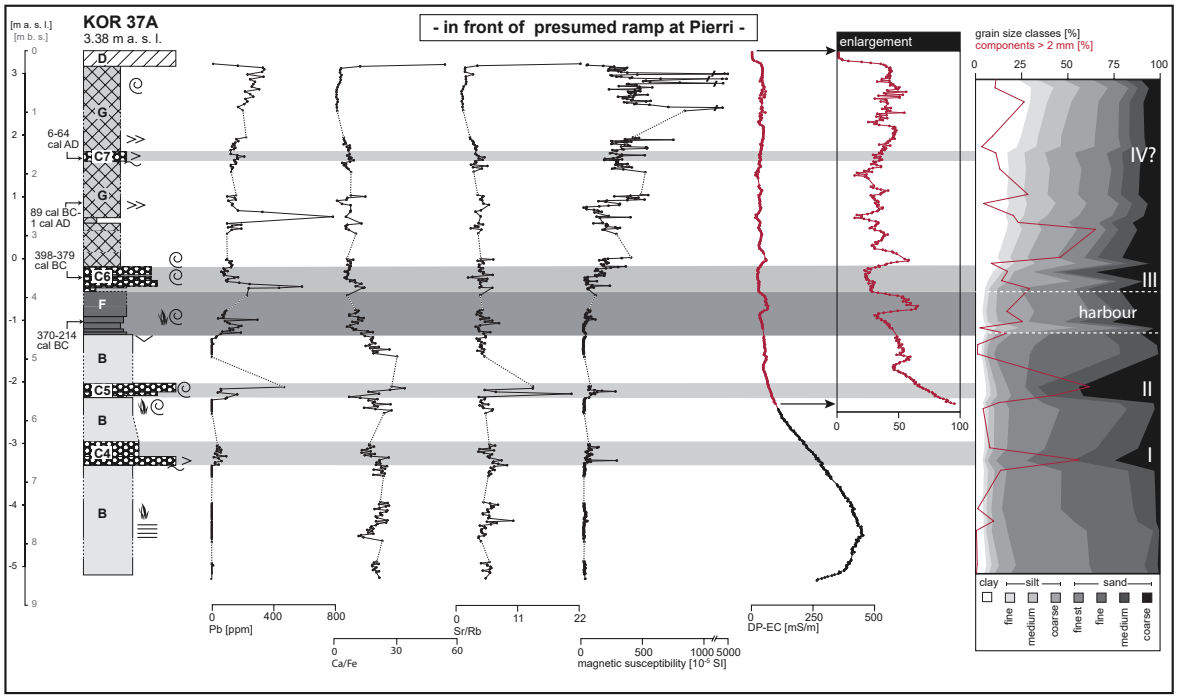

Figure 3.8: Results of grain size analysis, magnetic susceptibility measurements, Direct Push EC logging and selected geochemical proxies for vibracore KOR 37A. High-energy layers are highlighted by light grey colour and are characterised by coarser grain size and distinct peaks of Pb concentration, magnetic susceptibility values and marine ratios. In contrast, silty harbour deposits on top of the shallow marine sands (dark grey) show strongly reduced marine influence (lower Ca/Fe values, finer grain size). Legend according to Figure 3.5.

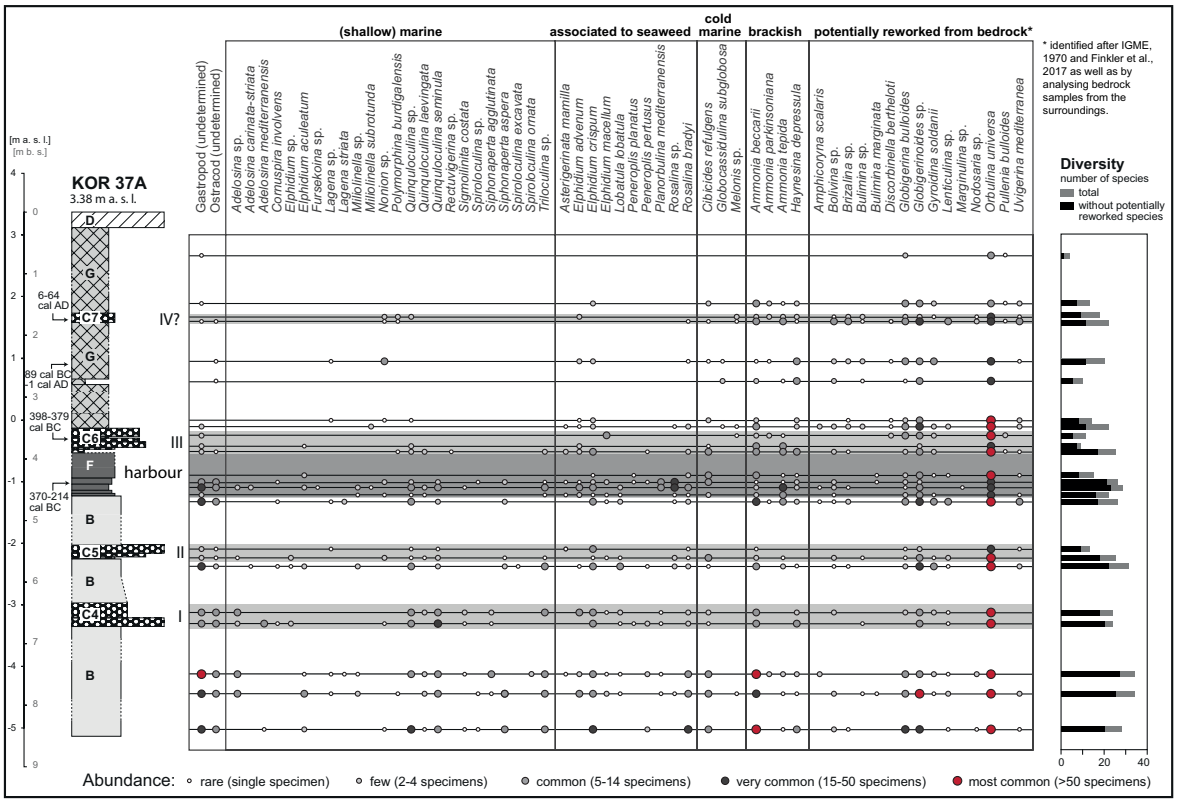

Figure 3.9: Results of microfaunal analysis for selected samples from vibracore KOR 37A. Species are classified according to their ecological preferences after Murray (2006) and Sen Gupta (1999). Potentially reworked species from the Neogene bedrock were identified after IGME (1970), Finkler et al. (2017a), and by analysing bedrock samples from the surroundings. The two lower high-energy layers (I, II) show a similar foraminiferal assemblage as the basal shallow marine sands, characterised by high diversity and high abundance. In contrast, diversity decreases in the upper part of the harbour sediments. Here, foraminifera tolerant to brackish conditions and species of shallow seaweed assemblages are dominating. This foraminiferal fingerprint mirrors a protected environment, probably shielded by a breakwater or similar constructions. High-energy layer III strongly resembles these harbour deposits while a potential high-energy IV differs from the over- and underlying colluvial sediments due to the input of marine and brackish fauna.

Subunit C4 (6.75–6.36 m b.s. in KOR 37A) overlies unit B on top of an erosional contact and is formed of grey fine to coarse sand, containing considerable amounts of components > 2 mm, such as gravels and ceramics. The amount of skeletal material decreases upward, concurrently grain size (< 2 mm) fines upward as well. The sediments show the same geochemical and microfaunal signals as unit B except for magnetic susceptibility and Pb, where distinct peaks are visible.

Subunit C5 (5.65–5.42 m b.s. in KOR 37A) is characterised by gravel within a matrix of medium and coarse sand. Ca/Fe and Sr/Rb ratios were found on a medium level, while magnetic susceptibility as well as Pb values are distinctly increased. Regarding their microfaunal content, the sediments do not significantly differ from those of unit B.

Subunit C6 (3.87–3.53 m b.s. in KOR 37A) represents a poorly sorted sequence of gravel towards coarse sand and silt with embedded macrofossils and ceramics. While Sr/Rb values are similar to those of unit B, the Ca/Fe ratio is strongly decreased, similar to the one of unit F. In addition, Pb concentration and magnetic susceptibility show distinct peaks. The foraminiferal content shows low diversity and abundance of mainly *Ammonia* spp., *Gyroidina soldanii and Globigerinoides* sp.

Table 3.1: Simplified local stratigraphic records of vibracores KOR 3, KOR 28A and KOR 37A.

Vibracore	Depth [m b.s.]	Grain size	Colour	Characteristics	Unit
KOR 3	0.00-1.61	clayey silt	brownish	contains cultural debris	G
	1.61-2.35	gravel in sand matrix	brownish	contains ceramics	C8
	2.35-2.77	silt to silty sand	dark grey	contains organic material, peat to the top	F
	2.77-6.93	fine to finest sand	greyish	well sorted	B
	7.00-8.85	silty clay	grey	compact	A
KOR 28A	0.00-3.52	clayey silt	brownish	contains cultural debris	G
	3.52-3.87	coarse sand	greyish/brownish	contains ceramics	C3
	3.87-4.17	solid stone	white/yellowish	calcareous	E
	4.17-4.40	fine sand	light-grey	very homogeneous	D
	4.40-5.08	fine to finest sand	grey	well sorted, plant remains at the top	B
	5.08-5.75	gravel in sand matrix	multi-coloured	sharp basal contact, contains ceramics	C2
	6.75-6.06	fine to finest sand	grey	well sorted	B
	6.06-6.23	medium to coarse sand	grey	fining upward tendency	C1
	6.23-6.93	fine to finest sand	grey	well sorted	B
KOR 37A	0.00-1.64	clayey silt	brownish	contains cultural debris	G
	1.64-1.79	clayey silt	light brown	sharp basal contact	C7
	1.79-3.53	clayey silt	brownish	contains cultural debris	G
	3.87-3.53	gravel and sand	multi-coloured	contains ceramics	C6
	4.17-4.63	silt to silty sand	dark grey	sharp basal contact, poorly sorted	F
	4.63-5.42	fine to finest sand	grey	well sorted	B
	5.42-5.65	gravel in sand matrix	brownish/multi-coloured	heterogeneous	C5
	5.65-5.93	fine to finest sand	grey	well sorted	B
	6.36-6.75	fine to coarse sand	grey	sharp basal contact, contains ceramics	C4
	6.75-8.53-	fine to finest sand	grey	well sorted	B

These species are also abundant in ***subunit C7*** (1.79–1.64 m b.s. in KOR 37A), which is intersecting a thick sequence of unit G in vibracore KOR 37A. Apart from different microfaunal content and a slightly increased amount of medium and coarse sand the unit does not differ strongly from unit G.

Subunit C8 (2.35–1.61 m b.s. in KOR 3) is formed by gravel embedded in a matrix of medium to coarse sand with only low amounts of clay and silt. The unit features a basal erosional contact and contains high amounts of ceramic sherds and marine macrofauna.

Unit D was only found in vibracore KOR 28 (4.40–4.17 m b.s. in KOR 28A). It is characterised by homogeneous light-grey fine sand with minor amounts of clay, silt and coarser sands. Geochemically, this unit strongly resembles unit B, whereas its microfaunal fingerprint differs significantly. Apart from planktonic species and *Ammonia beccarii* only few other species appear in very low abundance.

Table 3.2: Sedimentary, geochemical and palaeontological features of high-energy layers (subunits C1-C8) detected in the Pierri site sedimentary record (vibracores KOR 3, KOR 28A, KOR 37A). Foraminiferal fingerprints were classified according to Figure 3.6 and Figure 3.9.

	vibracore	KOR 28A				KOR 37A			KOR 3
	subunit	C1	C2	C3	C4	C5	C6	C7	C8
Sedimentary features	multimodal grain size distribution	+	+	+	+	+	+	+	+
	erosional basal contact	**-**	**+**	**-**	**+**	**+**	o	**+**	**+**
	fining upward tendency	+	+	-	+	+	+	-	-
	bad sorting	+	+	+	+	+	+	+	+
	mup cap	+	-	-	-	-	-	-	-
	rip-up clasts	-	+	-	-	-	-	-	-
	embedded gravel	+	+	+	+	+	+	-	+
	embedded ceramic sherds	-	+	+	+	-	+	+	+
geochemical signals	increased marine ratios	+	+	-	-	+	-	-	o
	increased Pb values	**-**	**+**	**+**	**+**	**+**	**+**	**-**	o
	increased magnetic susceptibility	-	+	+	+	+	+	-	o
	decreased LOI values	o	o	o	o	o	o	o	**+**
palaeontological features	marine macrofauna	+	+	+	-	+	+	-	-
	shell debris	+	+	-	-	-	-	-	-
	Foraminifera fingerprint	B	B	F	B	B	F	m	o
evennt chronology		I	II	III	I	II	II	IV?	III

Explanations: **+** = feature existent; **-** = feature absent; o = no data available; B = shallow marine; F = lagoonal; m = mixed

Unit E (4.17–3.87 m b.s. in KOR 28A) is characterised by solid calcareous sandstone of yellowish colour, overlain by white limestone.

Unit F, located at the same elevation level as units D and E, appears in vibracores KOR 3 and KOR 37A (2.77–2.35 m b. and 4.63–4.17 m b.s., respectively). In vibracore KOR 37A, the unit overlies the underlying unit B on top of a sharp contact. The unit itself is dominated by poorly sorted silt to silty sand. It further contains considerable amounts of medium sand, ceramics, marine macrofossils and plenty of seaweed. LOI values are strongly, Pb values slightly increased. Microfaunal analyses revealed high diversity especially in the lower section. Foraminifera tolerant to brackish conditions (Murray 2006), such as *Ammonia beccarii, A. tepida* and *Haynesina depressula,* as well as species of seaweed assemblages, such as *Rosalina sp., Planorbulina mediterranea* or *Peneroplis* sp. were found.

Finally, ***unit G*** (1.61–0.00 m b.s. in KOR 3; 3.52–0.00 m b.s. in KOR 28A; 3.53–1.79, 1.64–0.00 m b.s. in KOR 37A) consists of brownish clayey silt including high amounts of cultural debris and charcoal and characterises the upper part of the cores. Pb concentrations and magnetic susceptibility are distinctly increased but strongly fluctuating. Apart from *Orbulina universa*, *Globigerina bulloides* and *Globigerinoides* sp., only few strongly-weathered species were found within this unit.

3.5 Interpretation and Discussion

3.5.1 Facies interpretation

Based on their geochemical, microfaunal and grain-size related characteristics, the different units retrieved from the Pierri site sedimentary record can be associated to the following sedimentary facies:

Unit A is identified as Neogene marl that forms the ***bedrock*** at a depth of approximately 5 m b.s.l. at the Pierri site. These Neogene marls crop out in the south of the Analipsis Peninsula, forming a ridge up to 60 m high (Figure 3.2 A; IGME 1970). However, the presence of Neogene marls is problematic with regard to its microfaunal signature as reworked older fossils might contaminate younger, Holocene deposits. In order to separate potentially reworked Neogene bedrock species from Holocene fauna, we analysed several bedrock samples regarding their microfaunal content (e.g. Finkler et al. 2017a). Apart from planktonic species, already known from literature (cf. IGME 1970), we found several cold-marine species such as *Lenticulina*_sp. and *Uvigerina mediterranea* within the local bedrock (please see species classification in Figure 3.6 and Figure 3.9). These species must be regarded as potentially reworked and are thus considered as geogenic background signal.

Grain size and geochemical characteristics of unit B sediments indicate a mid-energy littoral environment. ***Shallow marine*** conditions are reflected by foraminiferal assemblages containing high numbers of calcareous marine and seaweed-related species, typical of shallow (some 10 m) inner-shelf bays with normal marine salinity and stable temperate to high water temperatures (Murray 1991, 2006, Sen Gupta 1999). The lower part of the shallow marine fine sands shows a changed pore water geochemistry due to salt water influence, represented by steadily increasing DP-EC values in vibracore KOR 37A.

Unit C and associated sublayers are characterised by distinct coarser grain sizes depicted by input of medium and coarse sand as well as gravel, suggesting ***high-energy*** conditions, especially when compared to the basal shallow marine sands. Based on the sedimentary signatures of unit C deposits, the material originates from shallow marine and/or marine environments partly also including reworked lagoonal material. Unit C thus indicates event-related high-energy inundation from the sea side.

Units D and E were retrieved from vibracore KOR 28A and occurred in a stratigraphical position consistent with the harbour deposits encountered at site KOR 37A. Due to the position of coring site KOR 28A, approximately in the midst of the Pierri site ramp, we interpret the stone layer (E) and the underlying homogeneous fine sands (D) as ***anthropogenic***, brought in by man and being probably the artificial base of a ramp.

In contrast to unit B, unit F is characterised by ***lagoonal*** conditions, represented by the entry of silt associated with slightly decreased marine indicators. Moreover, the foraminifers *Planorbulina mediterranea* and *Peneroplis* sp. were found, both related to *Posidonia*, that indicate quiet and shallow water conditions (Murray 2006). Salinity most likely changed towards brackish conditions to the top of the unit. This is mirrored by decreased diversity of species and the dominance of *Ammonia* which is one of a few genera tolerant towards brackish waters. Unit F deposits were found right in front of and associated with archaeological remains of the Pierri quay wall so that we interpret them as ***harbour deposits***. Our data further show that this harbour environment was subject to Pb pollution indicating intense use of Pb as ballast for ships and working material. Pb is one of the first metals used by man (Lessler 1988) with a very low natural background signal. Therefore, extensive occurrence of Pb is strongly linked to mining and metallurgy (Hong et al. 1994, Bränvall et al. 2001) and acts as an excellent tracer for human activities (Marriner & Morhange 2007). Pb pollution reaches its highest level during Roman times causing considerable Pb accumulations in ancient harbour basins (e.g. Le Roux et al. 2003, 2005, Véron et al. 2006, Elmaleh et al. 2012, Delile et al. 2014a, Hadler et al. 2013, 2015a, Stock et al. 2016).

Unit G, forming the uppermost part of all cores, contains a high amount of cultural debris and ceramic sherds, embedded in a silty matrix. Its brown colour documents weathering processes and pedogenesis. Findings of reworked planktonic and cold-marine species indicate erosion from the adjoining hillslopes of the Analipsis Ridge. Unit G thus represents post-harbour ***colluvial to anthropogenic*** sediments.

3.5.2 High-energy impacts on the harbour site

In the following, we will discuss potential causes for the deposition of the specific high-energy deposits that were found in vibracores at the Pierri site.

First, slope erosion associated with torrential run-off from the adjoining Analipsis Ridge can be easily excluded as potential trigger. The Pierri event layers (unit C) are not dominated by those foraminifera species that are typical of the local Neogene bedrock. They rather show a huge variation in species diversity (Figure 3.6 and Figure 3.9; Table 3.2) documenting the input of foraminifera from different Holocene marine environments. Thus, it is obvious that these layers are the result of extreme wave impact from the sea side that hit the Gulf of Corfu and the ancient harbour zone to the north of the Analipsis Peninsula. By these events, water masses intruded with high flow velocities and eroded, transported and strongly reworked autochthonous littoral and shallow marine sediments from the direct environs of the harbour bay and the adjacent gulf. These sediments with a mixed palaeoenvironmental signature were then deposited at the Pierri site. Based on the sedimentary record at Pierri, high-energy marine inundations are to be characterized as high magnitude-low frequency events.

Extreme wave impact from the seaside is potentially caused by both, storms and tsunamis, and, in outer-Mediterranean regions, both phenomena show similar sedimentological effects (cf. Morton et al. 2007, Switzer & Jones 2008, Lario et al. 2010); however, the forcing agents are completely different.

The northern Ionian Sea is characterised by a weak to medium wind and wave climate with mean significant wave heights of 1.2-1.6 m and very low annual wave energy flux (Cavaleri 2005, Karathanasi et al. 2015). However, heavy storms may occasionally occur associated to cyclones of the west wind zone, sometimes related to so-called medicanes (Cavicchia et al. 2014). Such medicanes appear with a low frequency but are reported from the Ionian Sea by several authors (e.g. Daviolo et al. 2009, Miglietta et al. 2015). They may generate extreme wave heights in the open sea such as offshore the Ionian Islands where Ghionis et al. (2015) measured significant wave heights of more than 5 m during a storm in 2007 only a few kilometres west of Corfu Island. The maximum observed storm wave height in the open Ionian Sea does, however, not exceed 6-7 m (Scicchitano et al. 2007). Nevertheless, such high waves are bound to open sea conditions and are strongly reduced when propagating towards the coasts by wave shoaling.

Moreover, local geographical and topographical conditions have to be taken into account. The Gulf of Corfu is a shallow marine indentation with a maximum width of 25 km and water depths not deeper than 70 m. It is connected to the open sea by narrow straits, namely the strait between Aghios Stefanos and Ksamil in the north and the strait between Syvota and Kavos in the south, 2 km and 8 km wide, respectively (Figure 3.1 B). The widely-travelled geographer Partsch (1887) described it as a lake-like embayment. It is extremely well protected from the rough waves of the open Ionian Sea and represents one of the best sheltered natural harbour settings of the eastern Mediterranean. In contrast, the open Ionian Sea west off Corfu shows a narrow shelf zone and water depths reaching 1000 m only few kilometers distant from the western coast of the island. Storm wave models reveal wave heights of more than 10 m for the open Ionian Sea whereas the Gulf of Corfu shows small wave heights of less than 1.5 m (Mazarakis et al. 2012, Zacharioudaki et al. 2015).

From these points of view, storms can be excluded as agents for repeated extreme wave impacts in the Gulf of Corfu as recorded at Pierri. Instead, earthquakes and tsunamis, which are both known to have repeatedly affected Corfu Island during history (Section 3.2.1), must be considered. Recent investigations on extreme event deposits found on the east coast of Corfu prove that both, teletsunamis and local tsunamis, for example triggered by submarine mass movements off the west coast of the island, may produce considerable tsunami waves in the Gulf of Corfu due to wave refraction and diffraction (Fischer et al. 2016a, Finkler et al. 2017a). Furthermore, repeated tsunami landfall on Corfu is well documented in earthquake and tsunami catalogues (Partsch 1887, Soloviev et al. 2000, Albini 2004, Ambraseys & Synolakis 2010).

Distinct sedimentological and geochemical features known from modern tsunami and palaeotsunami research were detected in high-energy subunits C1-C8.

Amongst others, such features are

i. a sharp erosional contact towards the underlying autochthonous deposits due to high flow velocities (Fujiwara et al. 2000, Hawkes et al. 2007, Sakuna et al. 2012),

ii. silt-dominated rip up clasts due to reworking of finer grained underlying material (Goff et al. 2001, Gelfenbaum & Jaffe 2003),

iii. fining upward sequences caused by varying and overall decreasing energy in the course of tsunami inundation (Shi et al. 1995, Hawkes et al. 2007, Sakuna et al. 2012),

iv. the input of marine calcium carbonate in the form of shells and faunal tests (Goff et al. 2001, Fujiwara et al. 2000, Vött et al. 2011a, 2011b), entailing the increase in concentrations and distinct peaks of Ca, Sr, Ca/Fe and Sr/Rb, the latter including terrestrial elements like Fe or Rb (Mathes-Schmidt et al. 2013, Chagué-Goff et al. 2015, Vött et al. 2011a, 2011b, 2015b), and

v. breaks in the geochemical pattern indicate short-term abrupt, mostly temporary changes in the palaeoenvironmental conditions through the input of allochthonous sediments. For example, nearly all event layers encountered in the Pierri geoarchive show strongly increased Pb concentrations, whereas under- and overlying autochthonous sands are almost void of Pb. Increased Pb concentrations in event layers can be explained by the strong affection of Pb-polluted areas, such as harbours, by the inundation event and the consequent entrainment of polluted material further inland. Ancient harbours are known to be related with high Pb concentrations (e.g. Hadler et al. 2013) due to the overall use of Pb for stabilizing ships and to join quay ashlars by Pb clamps. Abrupt changes of geochemical proxies are typically related to temporary high-energy impact. As, for the Pierri site, the influence of both severe storms and torrential runoff is excluded, we interpret high-energy event layers found at Pierri as the results of tsunami landfall.

On a small scale, high-energy sediments trapped in the Pierri record show different characteristics (Table 3.2) and can be grouped into four tsunami event layers (I to IV). Subunits C1 and C4 are located in consistent stratigraphical positions and are thus classified as ***high-energy layer I***; both show distinctly increased multimodal grain size, a general fining upward tendency and bad sorting. Their microfaunal signature mostly mirrors the shallow marine signal of local near-coast environments. We conclude that by tsunami flooding autochthonous near-coast littoral deposits were eroded, reworked and transported over a short distance (cf. Goff et al. 2001, Bahlburg & Weiss 2007, Hawkes et al. 2007). Yet, subunit C1 seems to have been subject to already slightly reduced flow velocities and wave energy, resulting in a missing erosional contact, smaller grain size when

compared to subunit C4 as well as the presence of a mud cap on top (Figure 3.4 B). Increased Pb values in the event layer in KOR 37A might be caused by early Bronze Age human influence the presence of whom is shown by embedded ceramic sherds.

High-energy layer II (subunits C2 and C5) is also made out of near-coast littoral material. Both subunits show nearly identical features (Table 3.2), even if grain size in subunit C5 (KOR 37A) is characterised by coarser clasts and embedded ceramic sherds similar to subunit C4.

Both high-energy layers I and II could not be identified macroscopically within the sedimentary record of vibracore KOR 3. However, grain size distribution reveals two minor peaks in the amounts of medium and coarse sand (Figure 3.5), which might be related to the impact of tsunami events I and II.

In contrast to high-energy layers I and II, subunits C3/C6 and C8 are not embedded in shallow marine sands but are located on top of harbour sediments or a ramp structure, respectively. The foraminiferal fingerprint of this ***high-energy layer III*** reflects reworking of lagoon-type harbour sediments which were obviously primarily eroded and reworked in the course of the event. Apart from that, the sedimentary subunits show similar features (Table 3.2).

Finally, a ***potential event layer IV*** (C7) was found in the record of vibracore KOR 37A. As the layer lies on top of thick colluvial/anthropogenic deposits, the Pierri site was already solid ground when these sediments were deposited. However, the geochemical and microfaunal fingerprint of this potential high-energy layer differs slightly from the under- and overlying colluvial/anthropogenic deposits. Still, potential extreme wave impact is mirrored by slightly increased grain size and few marine to brackish species which occur next to potentially reworked species of colluvial origin.

We conclude that high-energy layers encountered in vibracores at the Pierri site were deposited within the course of multiple tsunami landfalls. Three events occurred when the Pierri site was still dominated by shallow marine (events I and II) or lagoon-type harbour conditions (event III). Another impact (event IV), the traces of which are weaker than those recognized for events I to III, may potentially be related to tsunami landfall when the Pierri harbour zone was already dry land.

3.5.3 Dating approach, marine reservoir effect and relative sea level indicators

We established a geochronostratigraphical frame for the Pierri site based on five ^{14}C AMS samples out of organic material extracted from vibracores KOR 28A and KOR 37A (Table 3.3). These dates are supplemented by radiocarbon ages of three oyster samples collected from the Pierri quay

Table 3.3: Radiocarbon dates

Sample ID	Depth [m b.s.]	Depth [m a.s.l.]	Sample material	Lab. No.	$\delta^{13}C$ [ppm]	^{14}C age [BP]	2σ age [cal BC/AD]	1σ age [cal BC/AD]
KOR 28A/PR 3	6.07	-2.59	seaweed	MAMS 24902	-18.3 [a]	4276 ± 23	2539–2347 BC	2483–2400 BC
KOR 37A/HK 2	1.75	1.63	charcoal	MAMS 24912	-34.4	1968 ± 25	38; 78 AD	6–64 AD
KOR 37A/HK 3	2.47	0.91	charcoal	MAMS 24913	-35.0	2040 ± 24	156 BC; 23 AD	89 BC; 1 AD
KOR 37A/HK 10	3.69	-0.31	charcoal	MAMS 24911	-28.8	2301 ± 22	404; 262 BC	398–379 BC
KOR 37A/HR 0	4.39	-1.01	wood	MAMS 24914	-29.6	2236 ± 23	370; 214 BC	383; 207 BC
KOR Pierri Tx16 L1	--	-0.21	oyster	MAMS 29601	2.4 [a]	2511 ± 23	336–154 BC	293–183 BC
KOR Pierri Tx16 M2	--	-0.17	oyster	MAMS 29602	1.3 [a]	2550 ± 24	354–191 BC	335–235 BC
KOR Pierri Tx16 U3	--	-0.03	oyster	MAMS 29603	2.0 [a]	2517 ± 23	339–161 BC	298–191 BC
KOR 1A/HK 9+ [c]	2.65	-0.99	charcoal	UCI 121509	[b]	1600 ± 25	404–536 AD	413;536 AD
KOR 5/32+ HR [c]	9.81	-8.51	peat	MAMS 19770	-27.4	7328 ± 28	6238–6089 BC	6232; 6140 BC

Note: b.s. – below ground surface. a.s.l. – above sea level. MAMS – Klaus-Tschira Laboratory of the Curt-Engelhorn-Centre Archaeometry gGmbH Mannheim, Germany. UCI – Keck Carbon Cycle AMS Facility, University of California at Irvine, USA. 1σ/2σ age – calibrated ages, 1σ/2σ range. ";"– several possible age intervals due to multiple intersections with the calibration curve. [a] – marine sample, calibrated by using the marine13 calibration dataset with an average reservoir age of 405 years. [b] – ^{13}C correction is done automatically with a standard run. [c] – published in Finkler et al. (2017a). All dates are calibrated using Calib 7.1 (Stuiver & Reimer 1993, Reimer et al. 2013).

wall segment (Figure 3.10) and additional two radiocarbon dates from the close proximity (Finkler et al. 2017a), providing information on relative sea level changes (Table 3.3). Archaeological age estimates of seven ceramic fragments were used to cross-check radiometric ages (Table 3.4).

Calibration of radiocarbon ages was performed by means of the software Calib 7.1 (Stuiver & Reimer 1993, Reimer et al. 2013). However, even when calibrated, radiocarbon dates only yield approximate time frames and no exact dates, as inaccuracies caused by long term variations within the production of atmospheric ^{14}C, isotopic fractionation, contamination or relocation of sample material may occur (Geyh 2005, Walker 2005). The latter is especially true for samples retrieved from high-energy layers, as high-energy events usually erode and rework older deposits (Goff et al. 2001). This erosion can also produce considerable hiatuses. For this reasons, the sandwich-dating technique using both, a *terminus ante quem* (before) and a *terminus post quem* (after) for the event is the best appropriate manner to date high-energy layers. Unfortunately, sandwich-dating was not possible in this study, as there was no datable material available below and above the encountered high-energy deposits. Therefore, three samples were extracted from high-energy layers themselves. The resulting ages must be considered as *termini ad* or *post quos*, thus mere maximum ages.

Radiocarbon data of the Pierri site (Table 3.3) result in a consistent age model reaching from the 3rd millennium BC to the 1st cent. AD and correlate well with archaeological ages estimates of diagnostic ceramic fragments (Table 3.4). Only sample KOR 37A/HK 1 produces an age-inversion of some decades when compared to sample KOR 37A/HR 0. As this sample was extracted from a high-every layer, the slight inversion is most likely caused by reworking effects.

Table 3.4: Archaeological age estimates for diagnostic ceramic fragments found in vibracores drilled at the Pierri site

Sample ID	Depth [m b.s.]	Depth [m a.s.l.]	Sample description	Age estimation
KOR 3/1+ K1	0.56	1.29	undetermined	ancient
KOR 3/2 K	0.65	1.20	fragment of *skyphos*	late 6th-5th cent. BC
KOR 3/2 K2	0.69	1.16	undetermined	Hellenistic or Roman
KOR 3/3 K	0.99	0.86	fragment of brick	Roman?
KOR 3/5+ K	1.85	0.00	fragment of cookware	Hellenistic or Roman
KOR 3/10 K	2.67	-0.82	undetermined	ancient
KOR 3/10+ K	2.74	-0.89	fragment of ceramics	Classical
KOR 37A/K1	2.68	0.7	undetermined	undetermined

Radiocarbon dating of samples out of marine material is problematic as oceans function as large carbon reservoirs, resulting in significantly older ages compared to contemporaneous terrestrial material. Marine calibration requires the correction of the local reservoir age of the environment where the particular samples were taken from (e.g. Reimer & McCormac 2002). This marine reservoir effect (MRE) is, however, subject to variations in space (different MRE for different environmental settings), time (MRE variations through the Holocene) and species (different MRE for different species), even on a local to regional scale (Walker 2005). As for most of the coastal regions worldwide, these regional to local variations of the MRE are unknown for Corfu, so that we used the global marine13 dataset with an average reservoir correction of 405 years (Reimer et al. 2013) to guarantee comparability.

Sample KOR 28A/PR3 was identified as marine sample due to a $\delta^{13}C$-value of -18.3 ppm (Table 3.3; Walker 2005). Its calibrated age must therefore be treated with caution, as the real MRE is not known.

Additionally, a band of marine bioconstruction including abundant oyster shells was found adhered to ashlars that belong to the foundation level of the Pierri quay wall (see sections 3.5.4 and 3.5.5 as well as Figure 3.10 and Figure 3.12). This bioconstruction band mirrors the approximate relative sea level in the Pierri harbour basin for the time when it was in use. In order to obtain a reliable age determination of this important geoarchaeological sea level indicator, oyster samples were taken from the upper and lower edges of the bioconstruction band as well as from in between, namely samples KOR Pierri Tx16 L1, KOR Pierri Tx16 U3 and KOR Pierri Tx16 M2, respectively. The three samples yielded radiocarbon ages that are identical within the range of errors, in particular 293-183 cal BC, 298-191 cal BC and 335-235 cal BC, respectively (1σ intervals, see Table 3.3). Thus, the entire time period spanned by the three oyster samples is 335-183 cal BC. These results are in perfect accordance with the archaeological age of the Pierri harbour dated to the Classical-Hellenistic Period (Riginos et al. 2000). Moreover, they fit well with the age of the terres-

trial wooden radiocarbon sample KOR 37A/HR 0, dated to 370-214 cal BC (see Table 3.3) and the archaeological age of the diagnostic ceramic fragment KOR 3/10+ K, dated to Classical times (see Table 3.4 and sections 3.5.4 and 3.5.5).

From a methodological point of view, the calibrated age of the bioconstruction band corroborates that the local MRE is, indeed, very well approximated with the average reservoir age of 405 years (Reimer et al. 2013) suggested within this study. If based on the non-marine calibration curve intcal13, oyster samples KOR Pierri Tx16 L1, KOR Pierri Tx16 U3 and KOR Pierri Tx16 M2 would yield 771-561 cal BC, 775-566 cal BC and 796-672 cal BC, respectively (1σ intervals, see Table 3.3), resulting in a total time span of 796-561 cal BC. Compared with the in situ sample KOR 37A/HR 0 that reflects the time when the harbour was in use and was dated to 370-214 cal BC (see Table 3.3), the age of the oyster band with MRE unconsidered would be 426-347 years too young. However, this MRE estimation is only valid for the Pierri oysters of this particular time frame and environmental setting.

Also, sample KOR 5/32+ HR represents a reliable indicator of local relative sea level during the mid-Holocene as it was extracted from a paralic peat layer. Sample KOR 1A/HK 9+ (terrestrial) roughly indicates the approximate relative sea level during early medieval times; it was taken from a section a few centimetres above a peat layer that was associated to the sea level at that time (Finkler et al. 2017a).

3.5.4 Palaeogeographical evolution of the northern harbour zone in the environs of the Pierri site

Using a multi-proxy based approach, we were able to decipher the palaeoenvironmental evolution of the harbour environment associated with the Pierri site harbour facilities (Figure 3.10 A).

All vibracores drilled in the study area show shallow marine conditions at the base or right above the Neogene bedrock. These shallow marine sands are associated to an open marine inner shelf-environment with normal marine salinity and temperate to high water temperature (Murray 2006; Figure 3.6 and Figure 3.9). Radiocarbon sample KOR 28A/PR 3 (Table 3.3), recovered from in situ shallow marine sands, implies that this system was already established before 2483-2400 cal BC. Besides, basal homogeneous sands were interrupted by two high-energy event layers (see chapter 3.5.5). By the establishment of the Pierri harbour and evidenced by local harbour sediments, a clear change from pre-harbour sand-dominated mid-energy open shallow marine conditions to a protected mid- to low-energy quiescent water body took place, the latter represented by silty grain size. Sample KOR 37A/HR 0 from the lower part of the harbour sediments yielded a radiocarbon age of 370-214 cal BC (Table 3.3). As a result, the harbour basin in front of the quay wall seems to have been in use during Classical to Hellenistic times. This is in accordance with the approximate age of the Pierri quay wall itself which was dated by the excavators to the Classical-Hellenistic period (Riginos et al. 2000).

The KOR 3 harbour sequence can be directly dated based on a diagnostic ceramic fragment dating to the Classical period. Here, increased amounts of silt and high amounts of organic material also document reduced wave dynamics. In contrast, the contemporaneous harbour sequence retrieved from vibracore KOR 37A is more heterogeneous and comprises fine and medium sand and even coarser clasts, maybe due to material input from the nearby Pierri quay wall.

The Pierri vibracore records neatly show that the harbour was developed out of an open shallow marine environment, most probably by the construction of breakwaters and associated harbour infrastructure that triggered a change from mid- to low-energy conditions at the site. However, the harbour architecture needed to create a protected harbour basin has to be clarified by detailed archaeological research. The KOR 37A harbour deposits sit right on top of a sharp contact in shallow marine fine sands which we interpret as evidence of a man-made excavation of the harbour basin or later dredging activities. Within the upper part of the harbour sediments, microfaunal analyses revealed an alteration of salinity towards more brackish conditions caused

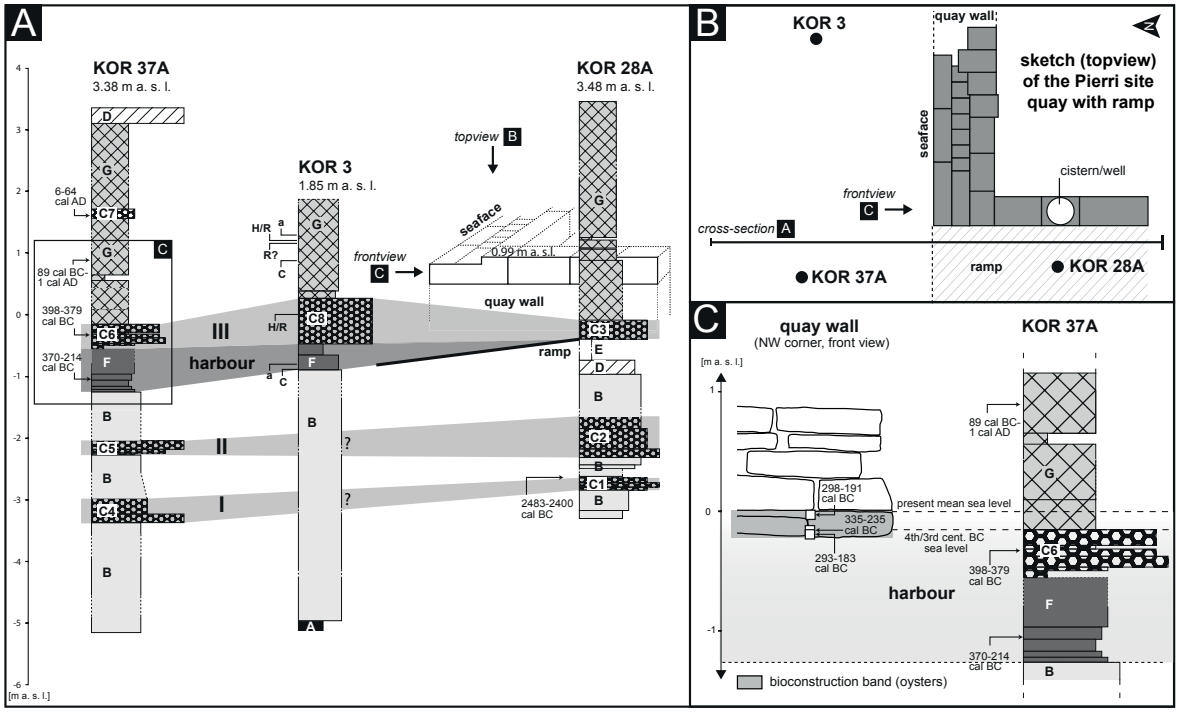

Figure 3.10: (A) Cross-section of all vibracores retrieved at the Pierri site with simplified facies pattern and ^{14}C ages. Note the location of the Pierri quay wall (only true to scale in vertical direction) with associated harbour sediments and ramp. (B) Simplified sketch (top view) of the Pierri site quay and locations of the vibracores depicted in A. (C) Sketch of the northwestern corner of the quay wall segment (front view) compared to the associated stratigraphy of vibracore KOR 37A (please see A for detailed section). Oyster bioconstruction band adhesive to the lower Pierri quay wall ashlar is depicted by grey colour, oyster samples that were radiocarbon dated are marked by white rectangles. The overall time span when oysters were alive was found to be 335-183 cal BC which is in accordance with the archaeological age of the harbour, dated to Classical-Hellenistic times (Riginos et al. 2000). Legend according to Figure 3.5.

by the abrupt man-made protection of the environment, possibly in the form of breakwaters or other protective harbour facilities (Figure 3.6 and Figure 3.9). Additionally, vibracore 37A revealed decreasing Ca/Fe values due to an increase in terrestrial input of Fe.

During the time of its use, the harbour was hit by high-energy event III as documented by the coarse-grained subunits C3, C6 and C8 encountered in consistent depths in vibracores KOR 3, KOR 28A and KOR 37A. A piece of reworked charcoal retrieved from event layer III yielded a radiocarbon age of 398-379 cal BC. Another age is provided by a diagnostic ceramic fragment found in a consistent stratigraphical position in vibracore KOR 3 dating to Hellenistic to Roman times. Vibracores KOR 28A and KOR 37A show that the Pierri site was strongly hit by this event and subsequently lost its function as a harbour.

Finally, the harbour site was covered by colluvial to anthropogenic deposits during the 1st cent. BC and the 1st cent. AD as documented by radiocarbon samples from vibracore KOR 37A (Figure 3.10 A). This time window encloses the destruction of Corcyra by Roman troops in 31 BC so that the colluvial deposits encountered in up-core position of cores KOR 28A and KOR 37A possibly represent the associated destruction layer. The potential high-energy layer IV insects these colluvial to anthropogenic deposits in vibracore KOR 37A, suggesting that the area was possibly hit by another high-energy impact when the Pierri harbour was already silted up.

Although the harbour sequence recorded in vibracore KOR 37A starts in the 4th cent. BC only, it cannot be excluded that the Pierri site was already used as a harbour from the beginning of the Corcyrean seafaring activities from the Archaic period (8th cent. BC) onwards. The sharp dredging contact in vibracore KOR 37A may indicate a hiatus in the early harbour record concealing the harbour's history between Archaic and Classical times.

3.5.5 Archaeoseismological and tectonic implications of the Pierri record

Results from the Pierri site allow to draw conclusions with respect to the general palaeoseismological and tectonic history of Corfu Island, including

i. the establishment of a tsunami event chronology as well as

ii. the reconstruction of local co-seismic movements in space and of relative sea level fluctuations.

At least three tsunami events hit the eastern coast of Corfu, when shallow marine or lagoon-type harbour conditions prevailed at the Pierri site. Tsunami event I occurred before 2483-2400 cal BC as sample KOR 28A/PR 3 provides a minimum age for this event. The associated high-energy layer was found in consistent stratigraphical positions in cores KOR 30A, KOR 37A and KOR 28A (Figure 3.10 A).

Traces of tsunami event II were found in vibracores KOR 28A and KOR 37A in stratigraphically consistent positions. Its geochemical fingerprint comprises considerable concentrations of Pb. This indicates that early harbour installations of the Helladic period, where Pb was ubiquitously used, were affected by this impact. Instead, Pb was not found in deposits of natural marine environments. Dating of event II is difficult because radiometric ages are not available. Yet, it must have taken place after 2483-2400 cal BC and before 370-214 cal BC taking ages of older and younger units in vibracore stratigraphies KOR 28A and KOR 37A, respectively, into consideration.

Tsunami event III can be dated as younger than 398-379 cal BC (reworked) and even younger than 370-214 cal BC based on the geochronostratigraphy available for vibracore KOR 37A (Figure 3.10 A). Event III deposits are lying right on top of the presumed Pierri ramp, the approximate age of which is dated to the Classical-Hellenistic period. Also, a diagnostic sherd dating to Hellenistic to Roman times was found in between event III deposits at site KOR 3. Finally, vibracore KOR 37A yielded a *terminus ante quem* of 89 cal BC to 1 cal AD for event III.

Traces of a possible event IV were detected in vibracore KOR 37A intersecting colluvial deposits. As this is a singular finding and there are no layers in consistent stratigraphical positions at neighbouring coring sites, tsunami origin of this layer is questionable. Its maximum age is dating to the 1st cent. AD.

Overall, these results correlate well with geomorphological and archaeoseismological studies conducted in western Greece along the shores of the eastern Ionian Sea and on Corfu Island itself. Event I can be correlated with an event of supra-regional dimensions described from various sites in western Greece dating to the early 3rd millennium BC (Vött et al. 2011b, 2015b). Event II may possibly be related to a strong event around 1000 cal BC which has produced considerable local crust uplift on Corfu Island (Mastronuzzi et al. 2014) and for which tsunami traces were reported from different geological archives of Lefkada Island and the adjacent Greek mainland (Vött et al. 2006, 2009). If of tsunami origin, event candidate IV can be related to tsunami deposits found in the Roman phase of the Alkinoos Harbour dating to the 4th cent. AD (Finkler et al. 2017a), most likely associated with teletsunami effects of the 365 AD tsunami. Traces of the 365 AD event, which was caused by a strong earthquake along a fault system offshore western Crete, are reported from southern Italy (e.g. De Martini et al. 2003, Mastronuzzi & Sansò 2012), but also from the Sound of Lefkada and adjacent mainland Greece (Vött et al. 2009a, May et al. 2012). Remains of

Roman buildings from the 2nd to 3rd cent. AD in proximity to the Pierri quay wall (Morgan 2010) document that the Pierri harbour site was solid ground already in the early 1st millennium AD. We conclude that events I, II and IV were triggered by supra-regional tsunamis that affected the Gulf of Corfu in the form of teletsunamis (see Finkler et al. 2017a, Fischer et al. 2016a).

Most interesting conclusions can be drawn for event III. Pirazzoli et al. (1994) and Mastronuzzi et al. (2014) found evidence of a period of strong co-seismic uplift for the same time period, namely after 790-400 cal BC and after the 5th-4th cent. BC, respectively. We dated event III at Pierri to the time between the 4th and 1st cent. BC so that it may be hypothesised that it was caused by the earthquake that also triggered co-seismic uplift on the island as reported by Pirazzoli et al. (1994) and Mastronuzzi et al. (2014). This hypothesis is supported by archaeoseismological findings and sedimentological traces of tectonically induced crust movements:

Firstly, there is evidence from the side of archaeology, in particular from the monumental Hera temple on top of the Analipsis Peninsula (Figure 3.2 A), one of the earliest major temples in Greece built in *c.* 610 BC. Most of its architectural features date to late Classical or early Hellenistic times (Sapirstein 2012). Earthquake-induced destruction of the temple and, above all, of its northern retaining wall can be seen since detailed excavations have started in 2012. Amongst others, the retaining wall shows abundant and clear archaeoseismological traces that document final destruction of the building by an earthquake, such as toppled ashlars and triangle-shaped corner break-outs (Figure 3.11).

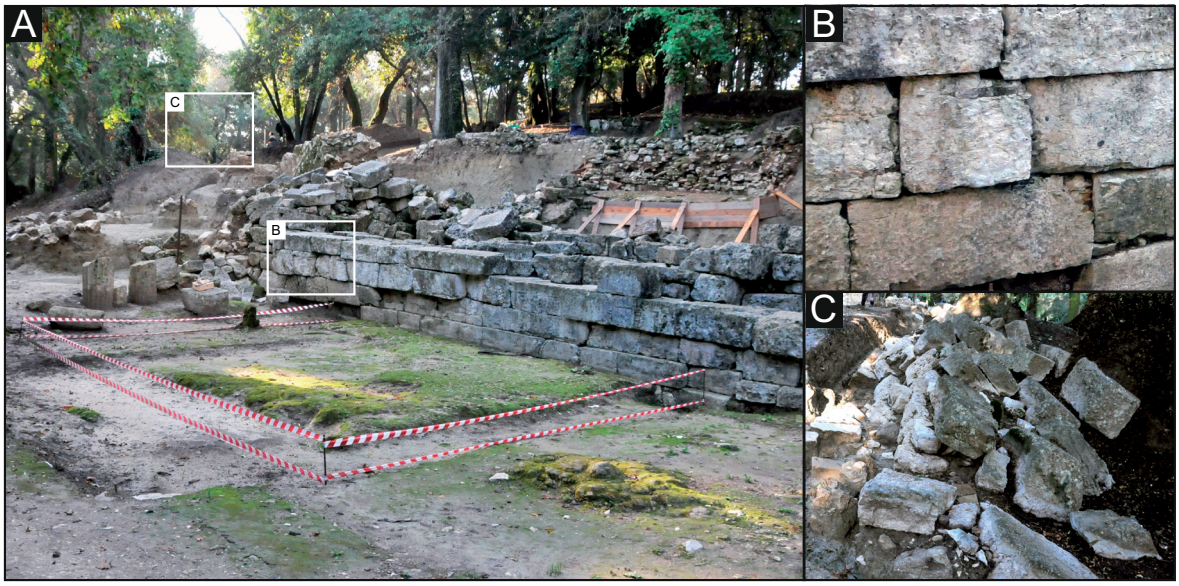

Figure 3.11: Northern retaining wall of the temple of Hera showing typical archaeoseismological features, which indicate damage by an earthquake: (A) Parts of the wall have been shifted forward, (B) single ashlars show triangle-shaped corner breakouts and (C) large wall sections imply earthquake-related dislocation in a slopeward direction. (Photos by A. Vött, 2012).

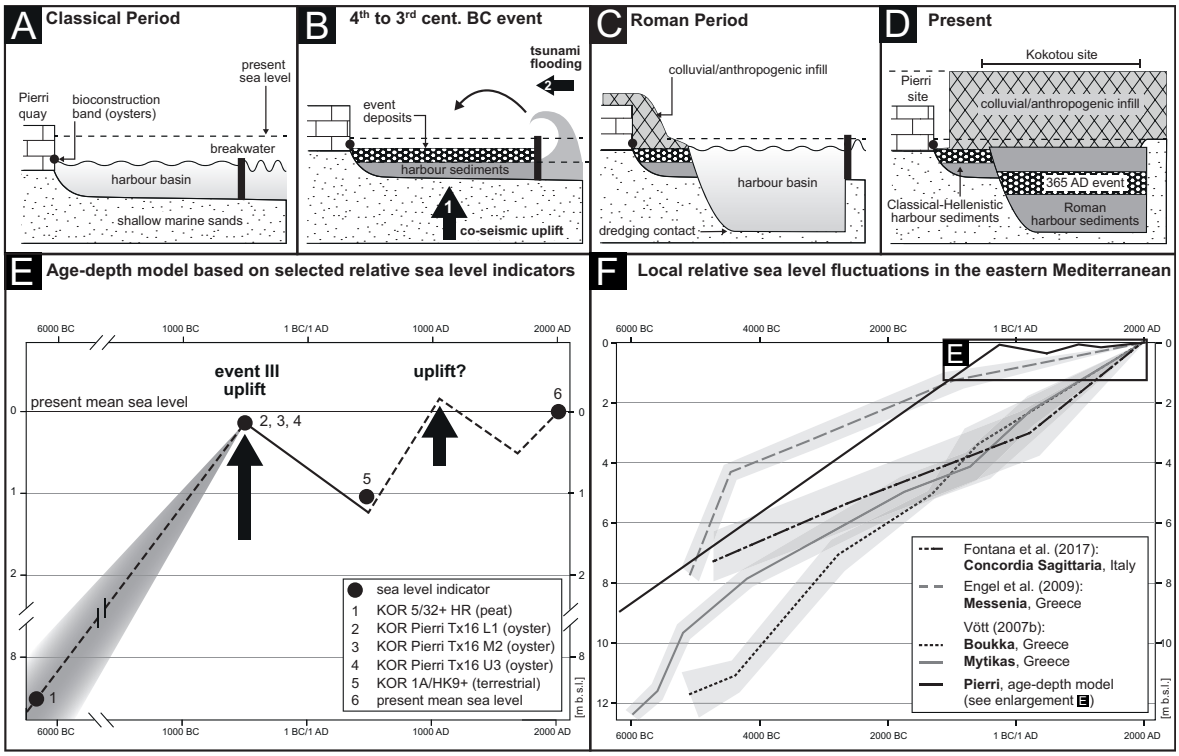

Figure 3.12: Schematic palaeoenvironmental development of the Pierri harbour site. (A) The harbour of the Classical period developed from shallow marine conditions by protective harbour infrastructure, possibly breakwaters. Oyster colonisation marked the approximate relative sea level at that time, resulting in a water depth of *c.* 1.2 m. (B) Between the 4th and 3rd cent. BC, the site experienced (i) co-seismic uplift causing decreasing water depths in the harbour, and, shortly afterwards, (ii) associated tsunami inundation. Due to co-seismic uplift and input of event deposits, the Classical-Hellenistic harbour was not navigable anymore. (C) During the Roman period, considerable parts of the buried Classical basin were deeply excavated, dredged and re-used, forming a more than 2 m deep harbour basin to the west of the Pierri site (Finkler et al. 2017a). Comparing depths of the Classical and Roman harbour basins clearly reveals co-seismic uplift. (D) Today, harbour sediments of the Pierri site are covered by colluvial and anthropogenic material. Classical harbour infrastructure in form of a quay wall was found during archaeological excavations. (E) Age-depth model of selected relative sea level indicators from the Pierri site. Marine oysters dating to 335-183 cal BC were found on higher elevations than younger terrestrial material which causes a clear shift within the age-depth model. This break documents the co-seismic uplift of the Pierri site related to tsunami inundation of event III that occurred during Classical to Hellenistic times. It may be speculated that the time of dieback of oysters that took place between 335-183 cal BC represents the best-fit age estimate for this event. (F) Local relative sea level curves from different study sites in the eastern Mediterranean compared to relative sea level indicators encountered at the Pierri site.

Secondly, archaeoseismological traces of seismically induced destruction between Classical and Hellenistic times were detected in the frame of a rescue excavation on the eastern shore of the Chalikiopoulou Lagoon in 2012 (Figure 3.2 A). Here, the Classical foundation of a building is covered by a thick layer of reworked lagoonal mud, containing sand, embedded allochthonous marine fauna, bones, ceramics and debris. On top of this destruction layer, the building was rebuilt in the Hellenistic period. Furthermore, parts of the excavated walls are strongly tilted, bearing witness of a strong and abrupt seismic impulse. The destruction layer described is consistent in age and stratigraphic position with event layer III found at Pierri and shows that tsunami landfall occurred all around the Analipsis Peninsula.

Thirdly, sedimentary evidence of co-seismic uplift is provided by the Pierri harbour deposits themselves. Harbour deposits of the Classical Pierri harbour complex were found at an elevation level of 1.25 m b.s.l. and higher. In contrast, the base of the younger Roman harbour mud, detected at the Kokotou site only 100 m to the west, was found at a distinctly lower elevation level of 3.40 m b.s.l. (Finkler et al. 2017a). Obviously, the Classical harbour at Pierri was not navigable anymore in Roman times: it was uplifted what caused strongly decreased water depths within the remaining harbour. Associated to co-seismic uplift, caused by a local earthquake, tsunami waves hit the Pierri harbour leading to the deposition of corresponding event deposits (Figure 3.12 B). Traces of extensive dredging activities at the Kokotou site (Finkler et al. 2017a) reflect the efforts to re-use at least the western part of the Classical harbour by dredging and deepening considerable parts of the former basin during Roman times (Figure 3.12 C). Regarding the exact timing of event III, the point in time when the oysters from the bioconstruction band found adhered to the Pierri quay wall died back between or right after 335-183 cal BC represents the best-fit age estimate for this event. The time span when oysters were alive was found to be maximum 335-183 cal BC which is in accordance with the archaeological age of the harbour, dated to Classical-Hellenistic times (Table 3.3; see Riginos et al. 2000).

Finally, we present an age-depth model of selected radiocarbon samples yielding information on relative sea level changes (Figure 3.12 E). During the mid-Holocene, the area was obviously dominated by tectonic subsidence as evidenced by sample KOR 5/32+ HR found at 8.51 m b.s.l. (Figure 3.12 E). The local age-depth relation given for this time period is consistent with age-depth relations recognized by Vött (2007b) for the strongly subsiding coastal plains of Mytikas, Astakos and Boukka (Akarnania, northwestern mainland Greece; Figure 3.12 F). Our results are also in good accordance with the results of Marinos & Sakellariou-Mane (1964) who stated that subsidence on Corfu Island happened for the last time during the Neolithic era.

Figure 3.12 further documents at least one abrupt change of the relative sea level (Figure 3.12 E): Marine oysters, spanning the time period 335-183 cal BC (see section 3.5.3), were taken from an in situ bioconstruction band at the Pierri quay wall reflecting the relative sea level at the time when the harbour was in use. They are located on a distinctly higher elevation level compared to sample KOR 1A/HK 9+ dating to the 4th to 5th cent. AD. This sample was taken only 1 cm above a layer out of paralic peat that can be regarded at relative sea level indicator. Therefore, considerable co-seismic uplift must have occurred after Classical times, when the harbour had a stable water level and oysters colonised the quay wall, and before the 4th cent. AD. A second co-seismic movement, so far undated, as described by Pirazzoli et al. (1994) or even a yoyo-type fluctuation of the relative sea level as assumed by Mastronuzzi et al. (2014) are not reflected by the provided age-depth-model (Figure 3.12 E), most possibly due to the lack of appropriate dating material.

The earthquake-related destructions that were observed both at the Hera temple and associated to buildings at the eastern shore of the Chalikiopoulou Lagoon seem to have been caused by one and the same event. They can be dated, at both sites, to Classical-Hellenistic times. This date is consistent with the age of event layer III found at the Pierri site and with the dating of co-seismic

uplift as recorded by the uplifted band of oysters, also at Pierri. We therefore suggest that the entire island was subject to strong earthquake influence at that time. This earthquake must have been caused by a local fault system, induced co-seismic uplift and triggered seismic sea waves that hit the east coast of Corfu. Considering radiocarbon dates and diagnostic ceramic fragments from the Pierri site as well as the dating of archaeoseismological traces described above, event III can be concisely dated to Classical to Hellenistic times, most probably to the 4th to 3rd cent. BC.

Beyond this aspect, important conclusions can be drawn with respect to the tectonic geomorphological development of the island. For the same time period, Pirazzoli et al. (1994) found co-seismically uplifted bio-erosional notches at the west coast of Corfu at an elevation of 1.6 m a.s.l. Even if the absolute amount of local co-seismic crust uplift at Pierri is not clear so far, we conclude that, here, the total uplift was clearly weaker compared to the west coast. In the east, the dated band of contemporaneous oysters at Pierri is located at 0.14 b.s.l. in average. Based on the vertical offset of *c.* 1.74 m, Corfu Island was not uplifted uniformly but rather asymmetrically; it was strongly tilted towards the east within the course of this local seismic event that occurred at a specific point in time during Classical to Hellenistic times.

3.6 Conclusions

Our study aimed to reconstruct the palaeoenvironmental setting in the environs of the prominent quay wall and presumed ramp structure at the Pierri site that are related to the northern harbour zone of ancient Corcyra. We drilled three vibracores in the direct surrounding of the Pierri quay wall and ramp. Vibracores were investigated by means of a multi-proxy geoarchaeological approach comprising sedimentological, geochemical, micropalaeontological and geophysical methods. Our main conclusions can be summarized as follows:

i. Based on vibracore stratigraphies, geoarchaeological studies and the archaeological context, we found that the quay wall segment and the ramp structure at Pierri belonged to a protected harbour basin. This harbour basin was developed from open littoral conditions of a shallow marine embayment most probably by the construction of breakwaters and/or other harbour facilities. Harbour deposits were dated by radiocarbon dating and archaeological age estimation of diagnostic ceramic fragments to the 4th to 3rd cent. BC which is in very good agreement with the quay wall structure which was dated to the Classical-Hellenistic period.

ii. The harbour basin associated with the harbour infrastructure at the Pierri site was possibly in function even before the 4th cent. BC; older harbour sediments may have been removed by dredging, traces of which were detected right in front of the presumed ramp structure.

iii. The geological archives in the study area revealed three distinct periods of time when the Pierri site, still part of a shallow marine embayment or used as a harbour, was hit by tsunami landfall, namely before 2483-2400 cal BC (event I), after 2483-2400 cal BC and before 370-214 cal BC (event II), and during Classical to Hellenistic times, most probably during the 4th to 3rd cent. BC (event III). Another tsunami event (event IV) potentially hit the site when it was already dry land. Ages of tsunami events I-II and candidate tsunami IV are consistent with supra-regional tsunamis known from the coasts of western Greece and southern Italy. Corresponding deposits at the Pierri site are thus triggered by tele-tsunamis.

iv. Tsunami event III, dated to Classical to Hellenistic times, most probably to the 4th to 3rd cent. BC, must be regarded as associated to a local earthquake. Archaeoseismological features and sedimentary evidence of associated co-seismic uplift were found. By this event, the Pierri harbour site was uplifted and buried by event deposits so that it was not usable as a harbour any more. The site was then covered by anthropogenic debris and colluvial deposits, eroded from the hills of the Analipsis Peninsula.

v. Finally, our results document that vertical crust uplift of the west coast of Corfu during event III exceeded crust uplift of the east coast by *c.* 1.74 m. This means that Corfu Island was strongly tilted from west to east within the course of the local earthquake and tsunami event III.

4 The sedimentary record of the Alkinoos Harbour of ancient Corcyra (Corfu Island, Greece) – geoarchaeological evidence for rapid coastal changes induced by co-seismic uplift, tsunami inundation and human interventions

ABSTRACT. Ancient Corcyra (modern Kerkyra or Corfu) was an important harbour city and commercial centre since the Archaic period, also due to its geostrategic position on the trade routes between Greece and Italy or Sicily. Corcyra kept its status as one of the prevailing naval powers in the Mediterranean by means of a large naval fleet, needing appropriated harbour basins to be stored and repaired. At least two harbours are documented by historical records and associated archaeological remains, namely the Alkinoos and the Hyllaikos Harbours, both located on either side of a narrow isthmus to the north of the Analipsis Peninsula, where the ancient polis developed. Today, the ancient harbour basins are silted and overbuilt by modern urban infrastructure, concealing their overall extent and topography. The present study aims to reconstruct the complex palaeogeographies of the ancient Alkinoos harbour of Corcyra based on a multi-methodological palaeoenvironmental and geoarchaeological approach. The methods used include sedimentary, geochemical, microfaunal and geophysical investigations that were complemented by archaeological data and results from previous geoarchaeological research. Spatially, the study focusses on the area of the so-called Desylla site west of known Alkinoos Harbour sediments in the midst of the modern city of Corfu. These results were complemented by findings from two geomorphological key sites as well as archaeoseismological traces from the western part of the Analipsis Peninsula. At the Desylla site, we found sedimentary evidence of an Archaic preharbour, partly open to the Gulf of Corfu, which was the predecessor of a protected Classical harbour basin. This basin, in use between at least the 4th to 3rd cent. BC and the 1st cent. AD, was delimited to the west by a wall. It represents the central part of the Classical Alkinoos Harbour which was sedimentologically traced, for the first time, from the Desylla site in the west to the Kokotou site in the east, where monumental shipsheds were unearthed during earlier archaeological excavations. Probably, the harbour zone extended even further to the east, where contemporaneous harbour deposits were found associated with the prominent quay wall at the Pierri and Arion sites. Our results show, that, apart from man-made interventions, Corcyra's palaeogeographical evolution is strongly linked to multiple impacts of extreme wave events in the form of tsunami inundation. At least four events (I-IV) are recorded in the natural geoarchives of the Analipsis Peninsula and its surroundings as well as the northern harbour zone of ancient Corcyra. In particular, these events happened between 5600 and 5200 cal BC (event I), after 3900 cal BC (event II), between the 4th and 3rd cent. BC (event III) and between the 3rd and 6th cent. AD, most likely at 365 AD (event IV). Ages of all events correlate well with ages of tsunami traces found on Sicily, the Greek mainland and other Ionian Islands. Tsunami events I and II led to massive environmental changes around the Analipsis Peninsula, while event III was associated to strong co-seismic uplift, leading to the abandon-

ment of the harbour site at Pierri. Decreasing water depths by siltation of the Kokotou and Desylla sites, however, were redressed by dredging, giving rise to an extensive Roman re-use of the western part of the Alkinoos Harbour zone. Yet, both harbour sites were hit again by event IV filling the harbour basins by a thick sequence of event deposits.

This chapter is based on
Finkler et al. 2018

4.1 Introduction

Ancient Corcyra (modern Corfu or Kerkyra) is located on the island of Corfu, the northernmost island of the Ionian archipelago, and was an important city-state and commercial centre since the Archaic period. Corfu's harbours and related infrastructure played a major role for the island's colonisation, the establishment of a *polis* and the rise of a powerful and autonomous thalassocracy.

In the 8th cent. BC, Corcyra was founded as a Corinthian colony due to its geostrategic position between the Greek mainland and Italy, allowing to control naval operations and near-coast trade routes in the northern Ionian Sea and Adriatic Italy (Kiechle 1979, Warnecke 2002, Gehrke & Wirbelauer 2004). The colony Corcyra rapidly evolved as considerable naval power in the Mediterranean and soon tried to gain independence from its *metropolis* Corinth. These efforts finally climaxed in the first naval battle in Greek history, fought between Corcyra and Corinth probably in 664 BC, marking the beginning of a more or less autonomous Corcyrean policy (Thucydides 1.13.4 after Crawley 1910). Henceforth, a severe rivalry and a continuous power struggle characterised the relationship between both city states, most probably reinforced by Corcyrean efforts to establish own colonies at the opposite mainland, the Corcyrean *peraia*, partly lying on the Albanian coast nowadays (Dierichs 2004, Baika 2013a).

Ancient Corfu flourished as one of the most powerful Mediterranean city states with regard to economic and military influence in the beginning of the Classical period (Fauber 2002). At the beginning of the Peloponnesian War, for instance, the Corcyrean navy is supposed to have owned the second largest fleet in entire Greece, only surpassed by the Athenians (Thucydides 1.33.1 after Crawley 1910, Gehrke & Wirbelauer 2004, Baika 2013a). Thus, appropriate harbour basins and related infrastructure were needed to repair and store high numbers of warships. According to Thucydides (3.72.3 after Crawley 1910) the city possessed at least two harbours, the fortified Alkinoos Harbour and the Hyllaikos Harbour, located in the coastal lowlands north and west of the *Acropolis* (Figure 4.2 A, Lehmann-Hartleben 1923), respectively. Both harbours are well documented regarding their archaeological context (e.g. Dontas 1965, Kanta-Kitsou 2001, Baika 2003, 2013a). The eastern part of the Alkinoos Harbour was subject of recent extensive geoarchaeological investigations (Finkler et al. 2017a, 2017b), while studies focussing the sedimentological record of the Hyllaikos Harbour are missing so far.

During the Classical period, Corcyra's harbours functioned as important naval bases, for example for Corcyra's ally Athens, and were repeatedly claimed by different political entities from all over the Mediterranean (Schmidt 1890, Baika 2013a). Internal conflicts and a subsequent civil war introduced the progressive political decline of Corcyra. In the Hellenistic period, the city not able to compete with emerging kingdoms that successively attacked and conquered the island. In 229 BC Corcyra was captured by the Romans, who sieged and destroyed it in 31 BC, on the eve of the naval battle of Actium. Under Roman supremacy, the ancient city underwent considerable alteration: Buildings were destroyed or overbuilt by Roman urban facilities, while other infrastructure was re-arranged or re-used.

The latter is particularly true for the harbour basins, which were certainly of huge importance for the Roman naval and commerical fleets. Not surprisingly, dredging activities and subsequent Roman re-use is geoarchaeologically proved for a part of the Alkinoos Harbour (Finkler et al. 2017a). Apart from changes due to anthropogenic interventions, also vast environmental changes took place. For the Alkinoos Harbour, multiple tsunami impacts between the Classical and Roman periods as well as abrupt co-seismic uplift between Classical and Hellenistic times were documented (Finkler et al. 2017a, 2017b). Moreover, post-Roman siltation strongly affected the harbour sites. The Alkinoos Harbour, for example, was progressively transformed into a lake lake in the Medieval period and finally into solid ground. Today, the former harbour basins is situated approximately 200 m distant from the present coastline (Figure 4.2 A). Likewise, the Chalikiopoulou Lagoon, where the Hyllaikos Harbour is assumed, was subject to siltation, resulting in a decrease of water depths to around 0.5 m measured today. The area was furthermore strongly re-arranged and overbuilt by the construction of the modern airport in the midst of the 20th cent. and by modern urban spread.

The present study uses a multi-methodological approach to reconstruct the complex constellation of Corfu's ancient Alkinoos harbour and its spatial configuration. Based on extensive archaeological research (Dontas 1965, 1966, Preka-Alexandri 1986, Spetsieri-Choremi 1997, Riginos 2000, Baika 2003, 2013a) and previous geoarchaeological studies (Finkler et al. 2017a, 2017b) the harbour's palaeoenvironmental development will be traced in space and time. In particular, we aim

i. to reconstruct the western delimitation of the Alkinoos Harbour in the area of the former Desylla factory,

ii. to study the narrow isthmus between the Analipsis Peninsula and the area of the modern city of Corfu representing a key site for reconstructing the overall palaeogeographical evolution of the ancient city, and finally

iii. to compare the results of the present study with known sedimentological and archaeological information in order to establish a chronological and spatial model of the northern harbour zone of Corfu.

4.2 Regional setting

The island of Corfu is situated in the northern Ionian Sea, close to the Strait of Otranto and the Adriatic Sea (Figure 4.1). To the east, the narrow Gulf of Corfu separates the island from the Greek and Albanian mainland, providing a storm-protected environment with water depths of less than 70 m (Partsch 1887, GEBCO 2014). In contrast, the western coasts of Corfu face the open Ionian Sea, rapidly reaching water depths of more than 1000 m. The narrow continental shelf drops rapidly and the adjacent steep continental slope causes a high risk of mass movements and turbidity currents (Poulos et al. 1999),), potential triggers for anomalous waves (Mastronuzzi 2010). Geologically, Corfu belongs to the Ionian Zone and is built up of Mesozoic sedimentary rocks and marine sediments, dating to the Plio- and Miocene (IGME 1970, Higgins & Higgins 1996).

4.2.1 Geotectonic setting

Corfu is located in one of the most rapidly deforming regions in Europe, where all types of plate boundaries encounter within a distance of only 100 km (Sachpazi et al. 2000, Broadley et al. 2006; Figure 4.1). Essentially, the seismic activity is related to the collision of the African plate towards Europe represented by the Hellenic Arc in the southeast, where oceanic lithosphere is subducted beneath the Aegean microplate (Hollenstein et al. 2006, Shaw & Jackson 2010), and the Calabrian Arc in the western Ionian Sea (Monaco & Tortorici 2000, Billi et al. 2007). To the North, the Adriatic microplate and Apulia collide towards the Eurasian plate resulting in a complex continental collision belt. The latter is separated from the subduction area in the south by a dextral strike-slip system primarily formed by the Cefalonia Transform Fault (CTF) right south of Corfu (Kokkalas et al. 2006; Figure 4.1). Moreover, collisional tectonics are associated with first NE-SW and later NW-SE compression and the uplift of the Ionian Islands, while southwestern Greece is under the influence of extensional tectonics (Doutsos & Kokkalas 2001, van Hinsbergen et al. 2006).

West of Corfu, these tectonics are demonstrated by the Kerkyra-Kefalonia submarine valley system that mirrors the continental convergence by its NNW-SSE orientated northern part while its southern part follows the ENE-WSW-direction of the Cefalonia Transform Fault (Poulos et al. 1999). On Corfu itself, active faulting is mainly dominated by thrust faults originating from the Pliocene and trending in a NW-SE direction, partly giving rise to upwelling salt diapers (Jacobshagen 1986). The most prominent of these faults, the Corfu thrust, carries evaporates towards the west and is mirrored by a cluster of shallow-focus earthquakes (Kokkalas et al. 2006, van Hinsbergen et al. 2006). Consequently, Corfu is listed repeatedly in earthquake catalogues, where earthquakes with moment magnitudes around 6.5 are reported since Medieval times (Partsch 1887, Stucchi et al. 2013). However, no record is available for earlier events, which is most probably related to the incompleteness of historical data sets (Hadler et al. 2012, Papadopoulos 2015)

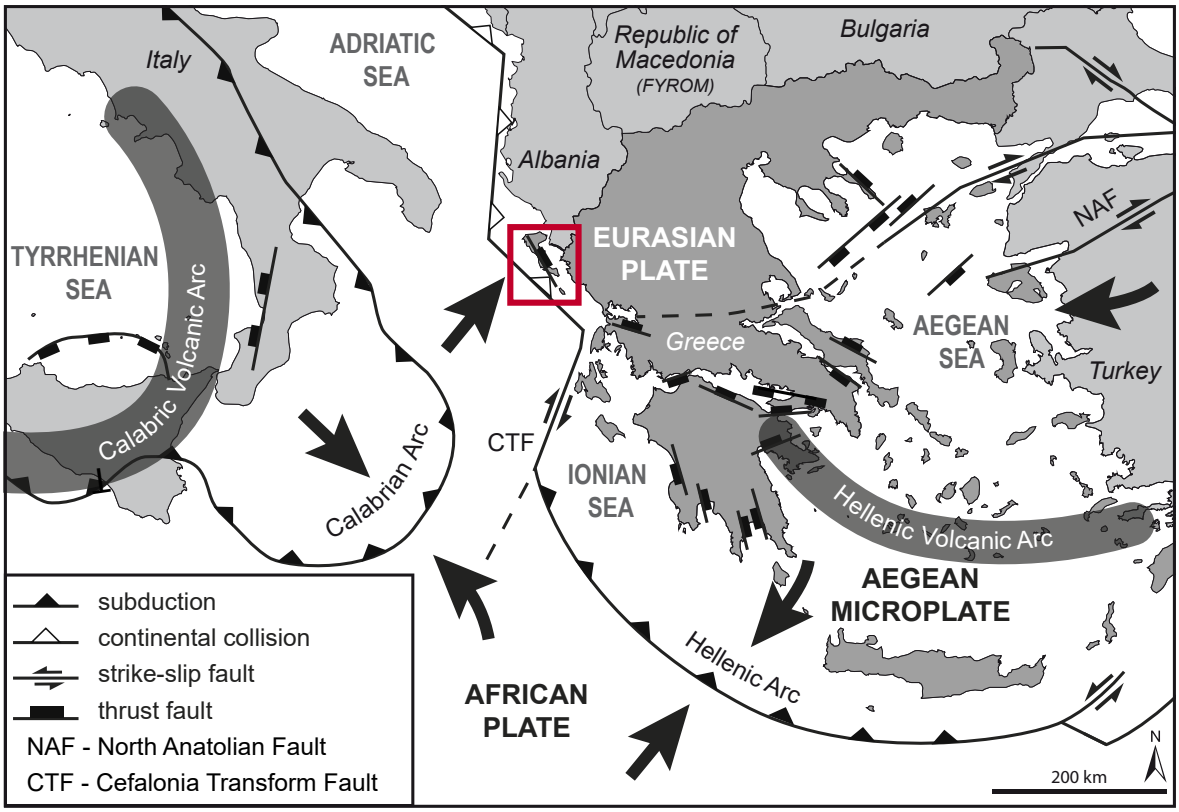

Figure 4.1: Simplified geotectonic setting of the eastern Mediterranean, including the Ionian, Adriatic and Aegean Seas. Corfu Island (red box) is located within a seismic stress field between the subduction zones of the Hellenic and Calabrian Arcs, the Adriatic collision belt and the Cefalonia Transform Fault. On Corfu, the Corfu thrust mirrors strong compressional tectonics. Main tectonic structures were simplified after Doutsos & Kokkalas (2001) and Billi et al. (2007).

In fact, geomorphological studies by Pirazzoli et al. (1994), Evelpidou et al. (2014) and Mastronuzzi et al. (2014) proved repeated pre-Medieval crust movements on Corfu, triggered by local seismic events. Today, these co-seismic movements are documented by emerged erosional notches on the coasts of Corfu, proving at least two periods of co-seismic crust uplift for the western and central parts of Corfu, in particular between the 8th and 4th cent. BC and to a younger date, so far unknown. Recent geoarchaeological studies on the harbour sediments of ancient Corcyra (Finkler et al. 2017a, 2017b) helped to frame this older event the Classical to Hellenistic period, most probably between the 4rd to 3rd cent. BC. Roman harbour mud (Finkler et al. 2017a) is located on a level distinctly lower than older Classical harbour deposits, reflecting co-seismic uplift and subsequent dredging activities that were realised by the Romans in order to re-use parts of the harbour basin. In addition, this prominent seismic event produced tsunami waves hitting the ancient harbour facilities and leaving corresponding event signals in the sedimentary record of the Classical harbour (Finkler et al. 2017b).

Several other tsunami events that hit Corfu are known geomorphological studies (Fischer et al. 2016a) as well as from from historical records (Soloviev et al. 2000, Ambraseys & Synolakis 2010, Hadler et al. 2012), the latter proving exclusively post-medieval events. Mastronuzzi et al. (2014)) proved a sequence of local co-seismic uplift and subsidence movements on Corfu, temporally correlating with known tsunami inundations in the Ionian Sea. Tsunami traces were found in numerous

coastal geoarchives in the vicinity of Corfu, for example on the Ionian islands of Cefalonia (Hadler et al. 2011, Willershäuser et al. 2013) and the environs of Lefkada (Vött et al. 2009a, 2009b, 2011a, May et al. 2012a, 2012b), as well as in southern Italy (e.g. Mastronuzzi et al. 2007, De Martini et al. 2012, Gerardi et al. 2012). Fischer et al. (2016a) and Finkler et al. (2017a, 2017b) present sedimentary and microfaunal evidence for multiple tsunami inundation of near-coast lagoons and the ancient harbours of Corcyra. We therefore conclude that seismic and especially tsunami impacts play a major role in shaping the coasts of Corfu.

4.2.2 Archaeological background

First traces of pre-historic human activities on Corfu were revealed in the form of lithic tools on the west coast near the Korission Lagoon, in the Grava rock shelter and near the village of Sidari dating to the Lower Palaeolithic, the Middle to Upper Palaeolithic and the Mesolithic, respectively (Kourtessi-Philippakis 1999, Runnels 1995, Sordinas 2003, Metallinou 2007, Ferentinos et al. 2012). Already in the Neolithic and Bronze age inhabitants of Corfu were in contact with Adriatic Italy (Berger et al. 2014), most likely due to Corfu's strategical position. The latter also allowed Corfu to control the ancient sea routes between Greece and Italy. Corfu soon prospered as considerable trading base and finally came under the rule of the Corinthians, who founded the colony "Corcyra" on the east coast of the island in the late 8th cent. BC (Kiechle 1979, Gehrke & Wirbelauer 2004). The urban centre with its public buildings and sanctuaries developed on the central Analipsis Peninsula, built up of Miocene marls, and soon extended to the hill slopes and coastal lowlands to the north (Figure 4.2 A). Corcyra evolved as prominent naval power in the Mediterranean, owing one of the first large fleets of triremes and fought against its mother state Corinth in the first sea battle in Greek history (Thucydides 1.13.4 after Crawley 1910). Consequently, adequate harbour basins with associated infrastructure (quays, shipsheds, storehouses) were needed to guarantee and sustain Corcyra's naval status. Historical sources indicate at least three harbours (Thucydides 3.72.3 after Crawley 1910, Gehrke & Wirbelauer 2004); two of them are archaeologically well documented by topographical considerations and corresponding infrastructure.

The naval Alkinoos Harbour was located north of the Analipsis Peninsula and – according to written records and archaeological research – close to the ancient agora (Figure 4.2 A; Thucydides 3.72.3 after Crawley 1910; see Baika 2013a, 2013b). At the Kokotou site (Figure 4.2 A), a section of a trireme shipshed complex was excavated in the 1980s and 1990s. The rows of piers were dated to the beginning of the Classical period and indicated the presence of an associated harbour basin to the northwest (Preka-Alexandri 1986, Spetsieri-Choremi 1997, Baika 2003, 2013a). Today, this basin lies several hundreds of meters distant from the present coastline; it is completely silted up and partly covered by modern urban infrastructure. Geoarchaeological research revealed that considerable parts of this harbour were dredged and re-used by the Romans, removing the older Classical harbour deposits and concealing the original extent of the Classical harbour (see Roman harbour basin in Figure 4.2 B; Finkler et al. 2017a). Yet, remains of an entrance tower preserved un-

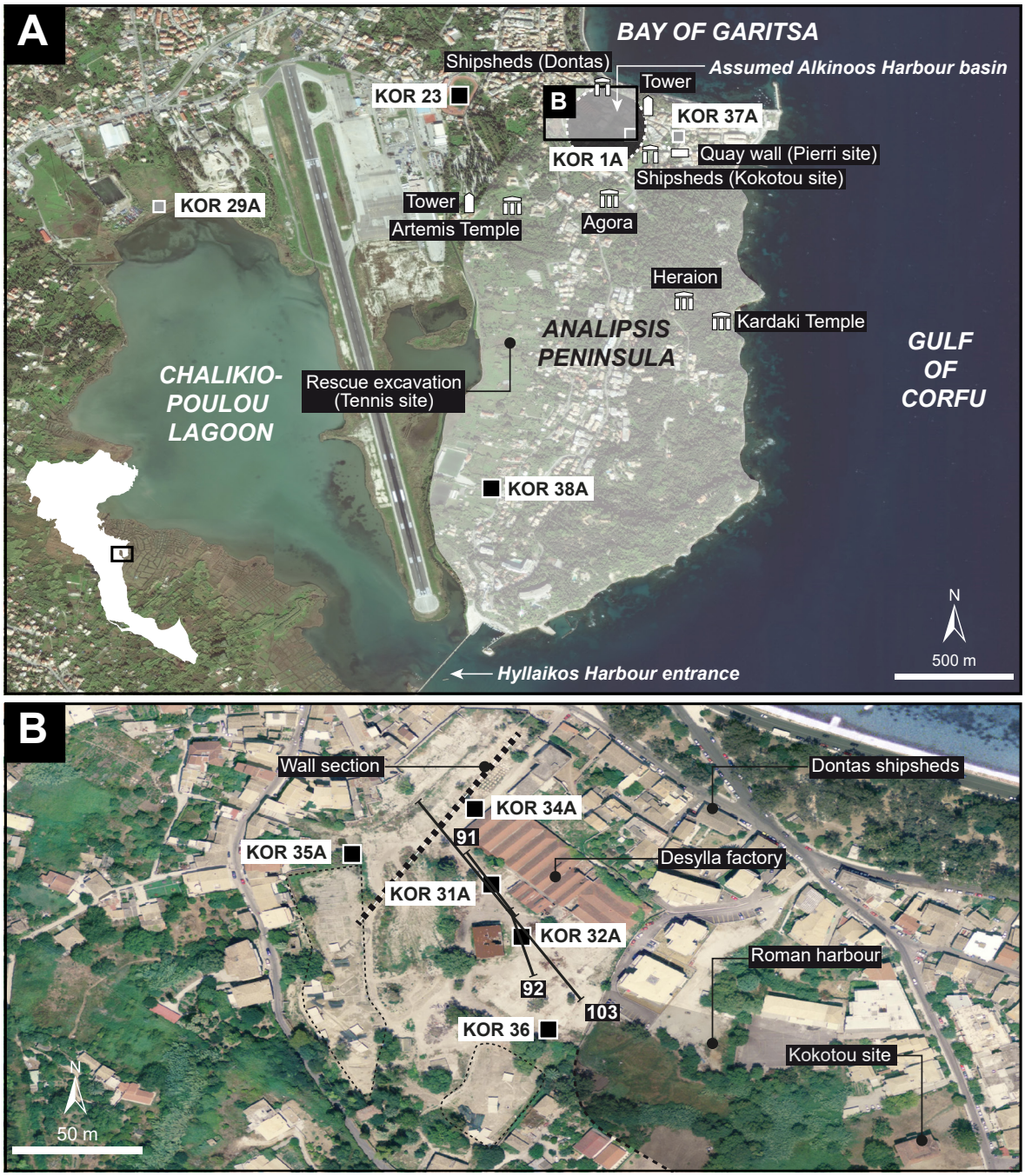

Figure 4.2: Geographical overview of the study sites on Corfu. (A) Physical setting of ancient Corcyra with main archaeological remains after Baika (2013a, 2015). The localisation of the Alkinoos Harbour is based on historical sources and archaeological findings. (B) Overview of the Desylla site. Vibracores of the present study are marked by black boxes, supplementary vibracores from studies by Fischer et al. (2016a) and Finkler et al. (2017a, 2017b) by grey boxes. Black bold lines in inlay map B refer to Electrical Resistivity Tomography (ERT) transects depicted in Figure 4.6. Maps modified after Bing aerial image of the year 2006 and NCMA S. A. (2014).

der the chapel of Ag. Athanasios and dating to the late 5th or early 4th cent. BC suggest a fortified harbour entrance to the northwest of the Kokotou site (Figure 4.2 A, Daux 1966, Baika 2013a). Its presence demonstrates that the Alkinoos Harbour was enclosed within the city's fortifications, representing thus a *kleistos limen*, a closed harbour (Pseudo-Scyllax, *Periplus* 29; see Baika 2013b 2013c, 2015). East of the Kokotou shipshed complex, at the Pierri site, harbour sediments dating

to the 4th to 3rd cent. BC were found in front of a monumental quay wall (Riginos et al. 2000, Finkler et al. 2017b).

It is still uncertain if all revealed harbour sediments were associated to one and the same Alkinoos Harbour basin such that more geoarchaeological fieldwork is needed to clarify this major research question.

Regarding the western part of the Alkinoos Harbour, excavations by Dontas (1966) to the north of the former Desylla factory (Figure 4.2 A, B) revealed scarce but probable traces of a further sequence of shipsheds, namely a row of five possible piers, most likely marking the western delimitation of the harbour basin (Dontas 1966). This suggestion correlates well with archaeological remains of a massive wall section, probably belonging to the urban fortification, excavated less than 50 m away to the southwest of the Desylla site and dating to the Archaic to Hellenistic periods (Morgan 2012). Next to this wall, a two-roomed building, most likely a shrine, dating to the 6th cent. BC was unearthed (Andreadaki-Vlazaki 2012, Figure 4.2 B). Both, this wall section and the orientation of the Dontas shipshed remains, indicate a harbour basin to the east, today entirely silted up and deliminated to the east by the the Kokotou shipshed complex. Therefore, the Desylla sedimentary record is a promising candidate to reveal well-preserved Classical harbour deposits and to trace the western part of the Alkinoos Harbour.

4.3 Methods

We applied a multi-methodological approach, combining different sedimentological, geophysical, geochemical and micropalaeontological methods.

Vibracoring was realised using an automotive drill drig (Nordmeyer RS 0/2.3) and a handheld Atlas Copco Cobra mk 1 to obtain stratigraphical information. Altogether, seven vibracores were drilled to a maximum depth of 15 m using half-open auger heads and core diameters of 50 cm, 60 cm and 80 cm. Five vibracoring sites were chosen from within the area of the former Desylla rope factory. There are abundant known archaeological structures in the vicinity of this location (see chapter 4.2.2). Another vibracore was drilled on the narrow isthmus between the Chalikiopoulou Lagoon to the west and the Bay of Garitsa to the east, in the midst of the modern football arena of Corfu (KOR 23, *Athlitikos Omilos Kerkyra, Super League*), representing a geomorphological key site for the reconstruction of the palaeogeographical development of the Analipsis Peninsula. Its results were complemented by the record of a further vibracore (KOR 38A) located on the eastern shore of the Chalikiopoulou Lagoon some hundred meters to the south of known archaeological structures (see Figure 4.2 A).

Sediment cores were photographically documented and significant facies were described according to their sedimentary characteristics (e.g. grain size, colour, carbonate content, macrofossils, sorting) and sampled in detail. Selected vibracores marked by the suffix "A" (e.g. KOR 32A) were

drilled as parallel cores using plastic liners to enable high-resolution in-situ measurements in the laboratory.

Moreover, in-situ Direct Push electrical conductivity (DP EC) logging by means of a Geoprobe SC520 device was conducted at two vibracoring sites within the former Desylla factory area. The DP EC probe has four electrodes in a row measuring electrical resistivity (2 cm vertical resolution) using a Wenner electrode array as well as the rate of penetration (ROP). DP EC logging yields high-resolution data on local stratigraphies and groundwater conditions (Harrington & Hendry 2006, Fischer et al. 2016b).

Electrical Resistivity Tomography (ERT) measurements were used to screen near-surface stratigraphies and to detect archaeological remains. At the former Desylla factory area, three ERT transects using a multi-electrode Syscal R1+ Switch 48 unit (Iris Instruments) and Wenner-Schlumberger arrays with electrode spacings of 1 m and 3 m were realised. Depth sections were calculated by means of the RES2DINV software (e.g. Loke et al. 2003). For better comparing DP EC data with ERT data, DP EC data were converted in resistivity values (Ωm).

Position and elevation data were measured by a Topcon HiPer Pro FC-250 Differential GPS device with a vertical and horizontal accuracy of higher than 2 cm.

In the laboratory, sediment samples from selected key cores were oven dried and separated into skeletal (> 2 mm) and fine-grained (< 2 mm) components by dry-sieving. Subsamples of 15 g were pre-treated by H_2O_2 and dispersants to determine grain size classes after the Köhn pipette method, where amounts of clay and silt were ascertained by pipetting while sand fraction was analysed by dry-sieving (Köhn 1929, DIN ISO 11277: 2002). Additionally, the dried samples were used to measure loss on ignition (LOI) that is used to indicate the amount of organic material in a sediment sample (Blume et al. 2011).

Sediment samples and sediment-filled liners were analysed using a multi-proxy approach. Methods applied include magnetic susceptibility measurements using a Bartington Instruments MS3 device with a MS2K surface sensor. Moreover, X-ray fluorescence (XRF) by means of a portable Niton XL3t 900S GOLDD (SOIL mode) allowed for determining elemental concentrations, namely Ca, Fe, Pb and almost 30 other elements. Data obtained by portable XRF devices are regarded as semi-quantitative and may show minor shifts when compared to other methods. Normalized XRF data are commonly used in palaeoenvironmental studies, mostly in the form of element-to-element ratios independent from grain size; they provide high-resolution information on the chemical composition of sediments and changing environmental conditions (EPA 2007, Chagué-Goff et al. 2017, Judd et al. 2017).

Geochemical analyses were complemented by a semi-quantitative micropalaeontological analysis of representative samples retrieved from vibracores KOR 23, KOR 32A and KOR 35A. For this purpose, 15 ml of sediment were pre-treated by H_2O_2 and separated into fractions of > 400 µm,

> 200 µm and > 125 µm by means of wet-sieving. Subsequently, *c.* 5 ml of each sample was examined under a binocular microscope in order to determine and count foraminiferal genera and species after Loeblich & Tappan (1988) and Cimerman & Langer (1991).

Microfossil assemblages reflect prevailing ecological conditions. Depending on their ecological tolerances and preferences foraminifera species are typical of specific brackish to marine conditions (Murray 2006). Their determination helps to reconstruct former environmental conditions (e.g. water depth, salinity or association with particular plants) and to detect shifts due to both gradual or abrupt coastal changes, the latter, for instance, in relation with extreme wave events (cf. Mamo et al. 2009, Pilarczyk et al. 2014). Species were classified according to their habitat preferences after Murray (2006) and Sen Gupta (1999). Moreover, we analysed samples from local bedrock units to identify potentially reworked Neogene species (Finkler et al. 2017a). Selected specimens retrieved from vibracore KOR 23 were documented using a scanning electron microscope (SEM).

Finally, 22 samples of organic material or biogenic carbonate were dated using the ^{14}C accelerator mass spectrometry (AMS) technique accomplished at the Klaus-Tschira Laboratory of the Curt-Engelhorn-Centre Archaeometry gGmbH Mannheim, Germany (MAMS) to establish a local chronological framework. Seven radiocarbon samples from vibracore KOR 29, drilled at the northern shore of the Chalikiopoulou Lagoon, were additionally dated (Fischer et al. 2016a). Organic samples comprised peat, wood and plant remains, biogenic carbonate samples comprised articulated specimens of bivalves (see Table 4.2 and section 4.5.3). Calibration of conventional radiocarbon ages was realised using the Calib 7.1 software (Stuiver & Reimer 1993; Reimer et al. 2013). Calibrated radiocarbon ages and archaeological age estimates of diagnostic ceramic fragments (Table 4.3) were used to construct a comprehensive geochronology for ancient Corcyra and its harbours.

4.4 Results

4.4.1 Sedimentary and geophysical results from the Desylla site

Five vibracores were drilled along a transect within the area of the former Desylla factory (Figure 4.2 B, Figure 4.13), approximately 150 m to the southwest of the present coastline. Vibracoring sites KOR 31A, 32A and 34A are located in the area of the presumed Alkinoos Harbour basin, the location of which is assumed based on nearby shipshed remains to the northwest and southeast, respectively (Dontas 1966, Baika 2013a; see chapter 4.2.2). Vibracore KOR 35A was drilled where archaeological remains of the 6th cent. BC were discovered. Amongst these remains is a large SW-NE orientated wall section (Figure 4.2 B), possibly being part of the ancient city fortification system (Andreadaki-Vlazaki 2012). Vibracoring site KOR 36A is situated at the very south-eastern part of the Desylla factory area, where geophysical investigations helped to detect wall structures in the shallow subsurface. Vibracores KOR 32A and KOR 35A are considered as master cores for this study site and are therefore described as follows.

At the base of vibracore KOR 32A (Figure 4.2 B, Figure 4.3, Figure 4.4 and Figure 4.5; Table 4.1), we found well-sorted greyish fine sand. On top of a calcareous stone fragment at 3.56 to 3.62 m b.s. (= m below surface), sediment texture changes towards clayey silt. This unit is covered by a layer of greyish sandy silt with a sharp contact at its base. Following another basal erosion unconformity, we encountered reddish to yellowish fine sand, almost 1 m thick (1.52–2.47 m b.s.). The uppermost parts of the profile were made out of brownish clayey silt and sandy silt, the latter containing large amounts of cultural debris.

Vibracore KOR 35A (Figure 4.2 B, Figure 4.3, Figure 4.4 and Figure 4.5; Table 4.1) shows grey fine sands with considerable amounts of silt in the lower part of the core, containing sediment-filled

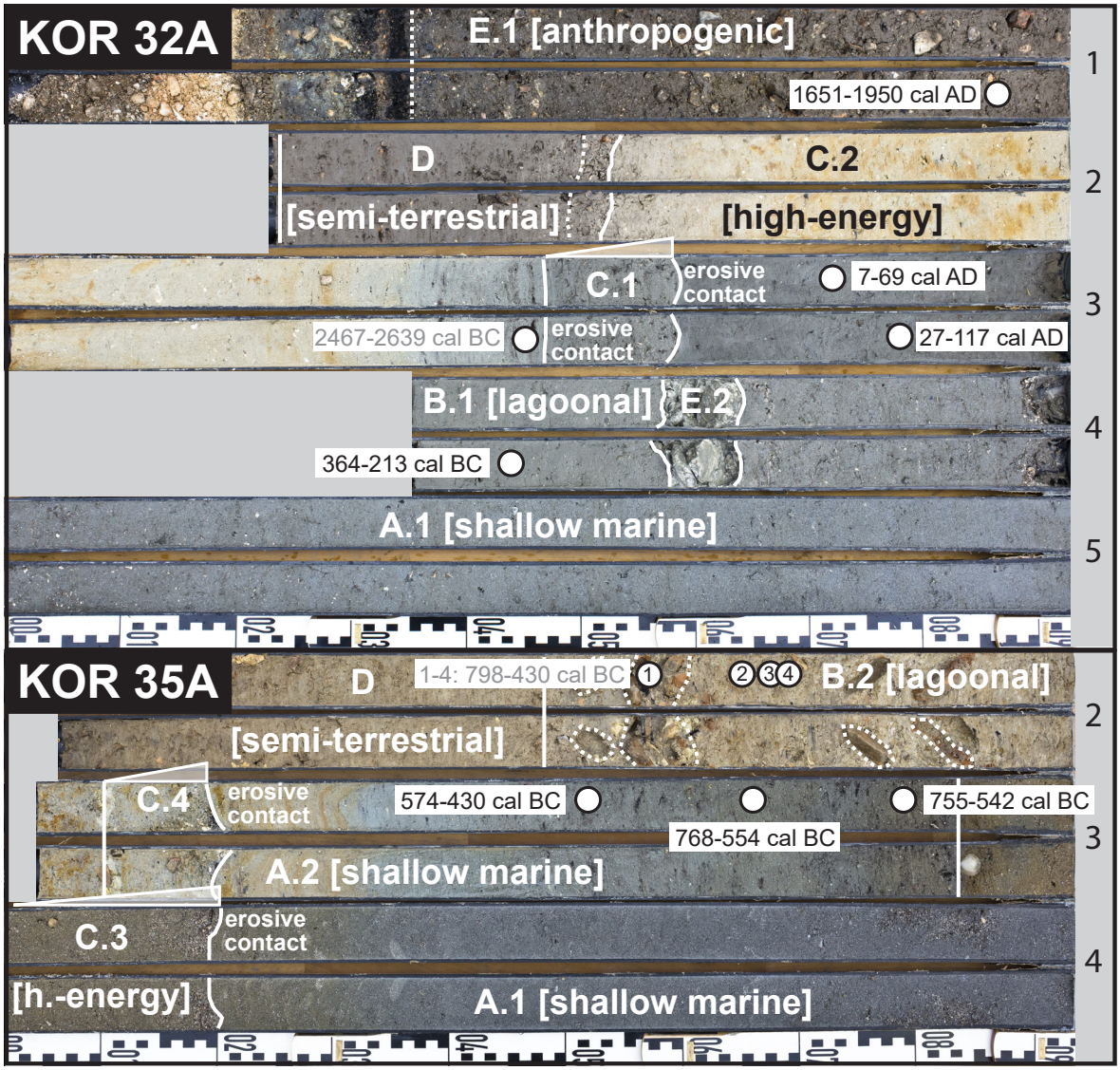

Figure 4.3: Sedimentary records and main stratigraphic units of vibracores KOR 32A and KOR 35A, drilled in the area of the former Desylla rope factory. Radiocarbon samples and associated ages (1σ confidential interval) are marked by white dots. Unreliable dates (see section 4.5.3 for further explanations) are depicted in grey. Both vibracores are characterised by first shallow marine and later lagoonal deposits and include several high-energy layers related to extreme wave events. In the upper part of both profiles silting processes are represented by semi-terrestrial deposits, which are buried under anthropogenic infill in vibracore KOR 32A.

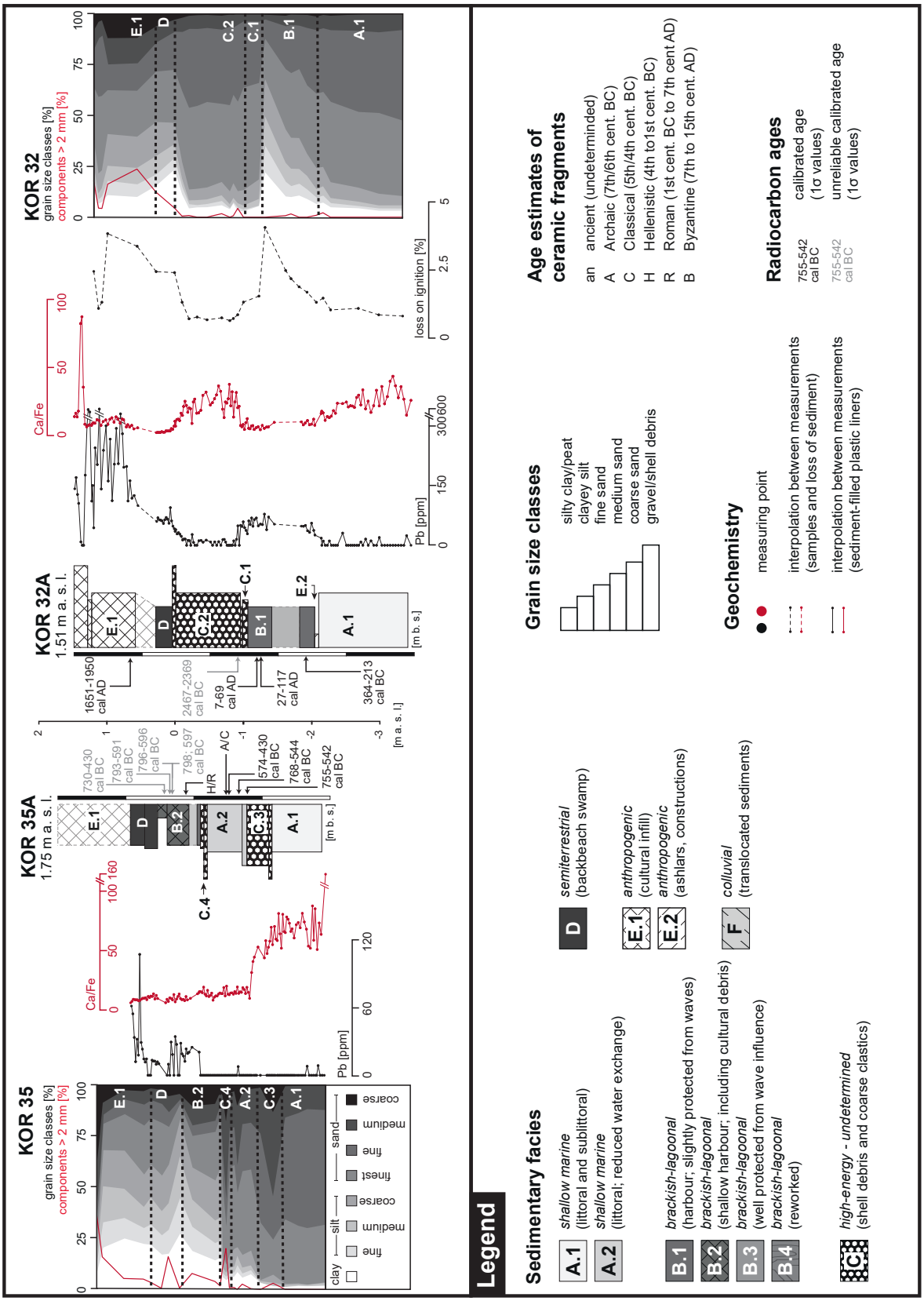

Figure 4.4: Results from multiproxy analyses of vibracores KOR 35A (left) and KOR 32A (right), including grain size data, magnetic susceptibility measurements, loss on ignition, selected geochemical proxies and radiocarbon ages. 14C-ages not considered for interpretation are depicted in grey (see section 4.5.3 for further explanations) Lagoonal sediments retrieved in the sedimentary record of KOR 32A features harbour-related Pb contamination and high LOI values due to a wave-protected environment. In contrast, Pb-polluted harbour deposits in KOR 35A are located on a distinct higher elevation level and are of younger age.

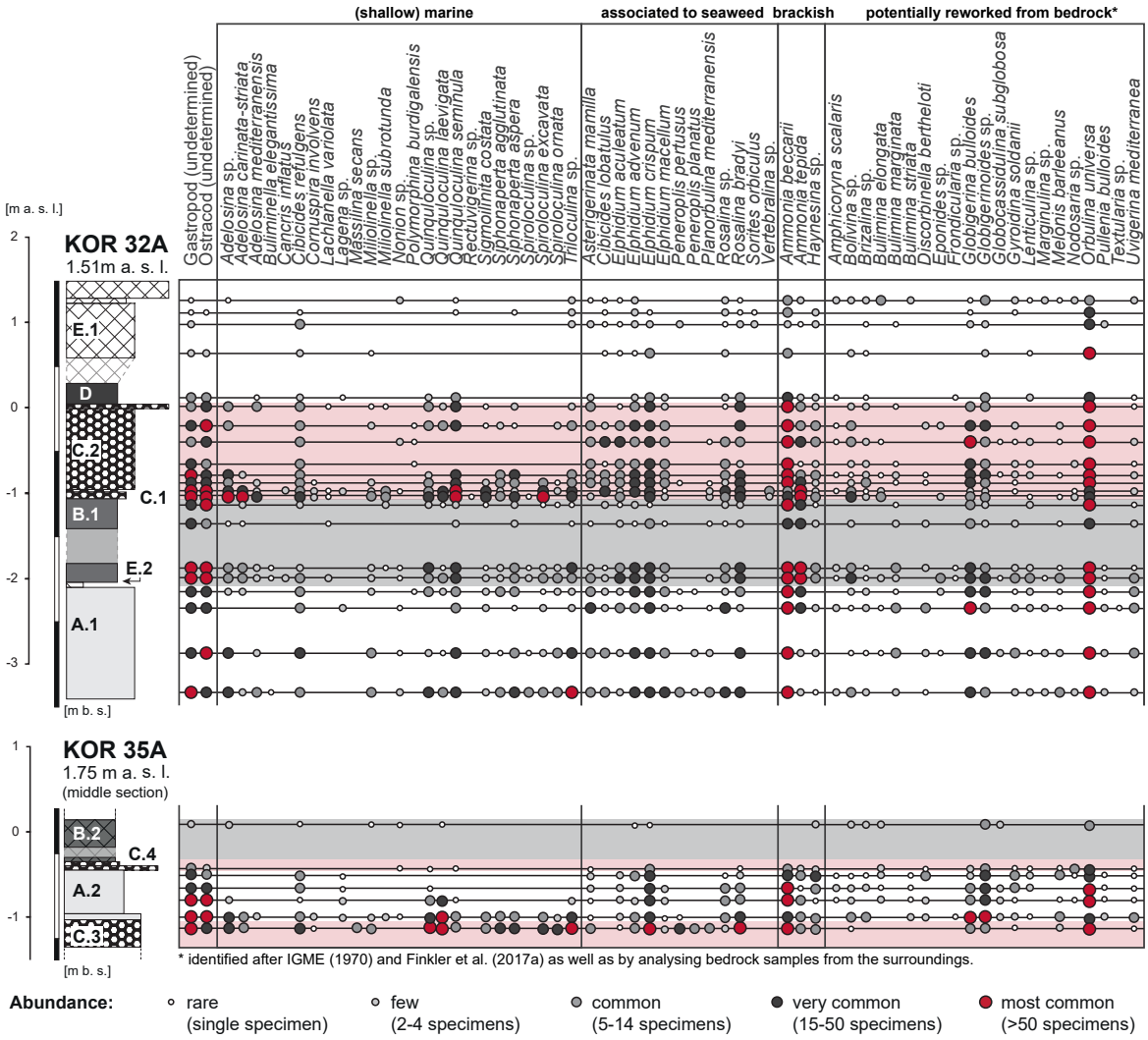

Figure 4.5: Results from microfaunal studies of selected samples collected from vibracores KOR 32A (top) and KOR 35A (bottom). Species were determined after Loeblich & Tappan (1988) and Cimerman & Langer (1991) and classified according to their ecological preferences after Sen Gupta (1999) and Murray (2006). Potentially reworked species of the local Neogene bedrock identified after IGME (1970) and Finkler et al. (2016) were depicted separately. Microfaunal analysis of core KOR 32A indicates an open-marine sublittoral to littoral system with marine salinity that slightly changed into a brackish milieu in the upper part of the harbour sediments. High-energy layers C.1 and C.2 mirror the entry of first reworked harbour mud and then sublittoral sands. Moreover, microfaunal studies on KOR 35A show a clear difference between marine high-energy layer C.3 and the overlying A.2 sands, indicating the establishment of protected and brackish conditions due to protective constructions by man.

burrows. At 3.20 m b.s. an erosive contact marks an abrupt change towards medium sand of brownish colour, covered by grey to reddish finest sand with lots of plant remains in their lower part. Following another sharp erosional contact, medium to coarse sand was found at 2.10–2.19 m b.s. showing a general fining-upward tendency. Subsequently, we encountered clayey silt of greyish brown colour comprising many ceramic sherds and charcoal fragments. Towards the top, the profile is characterised by homogeneous brown clayey silt.

Additionally to vibracoring, ERT measurements were conducted along three transects at the Desylla site, all running in a NNW-SSE direction (Figure 4.2 B). They were complemented by two DP-EC logs at vibracoring sites KOR 31A and KOR 32A. ERT transect KOR ERT 103 (Figure 4.6 A)

covers the drilling sites KOR 31A and KOR 32A as well as DP-EC logging sites KOR DP 31 and KOR DP 32. Both, DP EC logs and ERT, show uniformly low resistivity values < 10 Ωm at the base of the depth section. In contrast, the upper part of the ERT transect shows a heterogeneous pattern with resistivity values generally higher than those found for the lower part of the depth section. At DP EC site KOR DP 32, medium to high values up to 50 Ωm (orange/brown in colour) were measured down to *c.* 6 m b.s.l. (= m below present sea level), thinning out towards the centre of the ERT transect. In log KOR DP 31 such high values were only found higher than *c.* 2 m b.s.l. Separated by a low resistivity structure, another medium to high resistivity layer was found towards the north

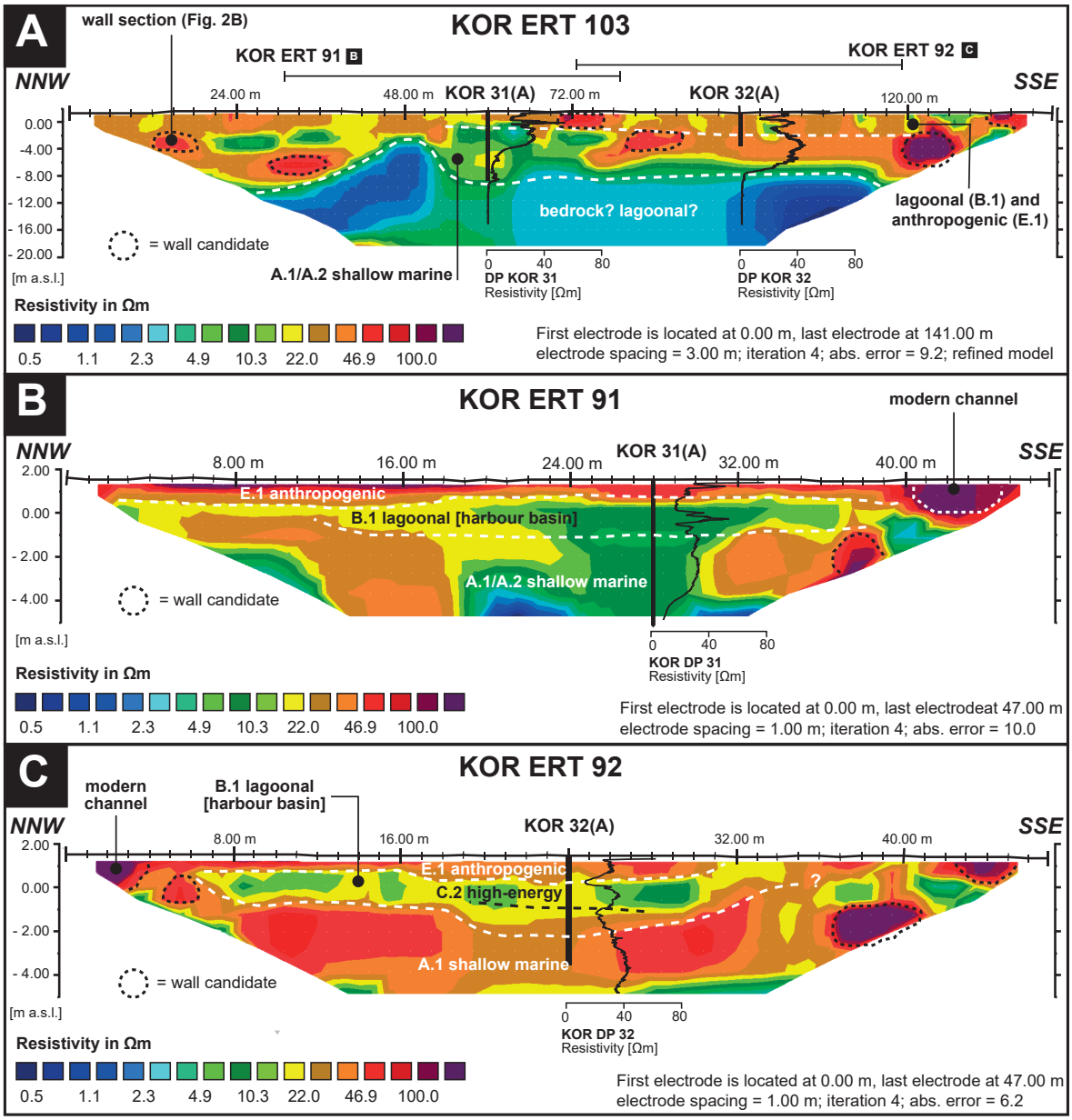

Figure 4.6: Depth sections of Electrical Resistivity Tomography (ERT) transects KOR ERT 103 (A), KOR ERT 91 (B) and KOR ERT 92 (C) carried out at the Desylla site. Electrical conductivity measurements by DP EC logging at sites KOR DP 31 and KOR DP 31 were transformed into resistivity logs and integrated into the profiles. Both, resistivity logs and ERT depth sections, clearly show a fine-grained harbour basin, thinning out towards drilling site KOR 31A. Furthermore, several distinctly delimited structures of high resistivity indicate wall structures in the subsurface, most likely related to man-made subdivisions.

showing increasing thickness towards the beginning of the ERT transect. Both near-surface layers include several delimited structures with resistivity values > 50 Ωm that are situated on two different elevation levels, in particular at *c.* 8 m b.s.l. and *c.* 2 m b.s.l. (areas marked with dotted lines).

ERT transect KOR ERT 91 (Figure 4.6 B) represents an enlargement of the northern part of transect KOR ERT 103. Due to smaller electrode spacing and thus better resolution, a consistent layer of high resistivity material is visible near the surface. It overlays a sequence characterised by varying resistivity values, reaching from < 10 Ωm to > 30 Ωm at the centre and edges of the depth section, respectively. At a distance of *c.* 38 m and 42 m from the zero point of the transect, isolated high-resistivity structures are depicted by red to purple colours. ERT transect KOR ERT 92 (Figure 4.6 C) reveals a more detailed insight into the subsurface of the southern part of transect KOR ERT 103. The depth section can be subdivided into three units: The lower depicts medium to high resisti-

Table 4.1: Simplified local stratigraphic records of vibracores KOR 23, KOR 32A, KOR 35A and KOR 38A.

Vibra-core	Depth [m b.s.]	Grain size	Colour	Characteristics	Unit
KOR 23	0.00–1.51	gravel, silty sand	multi-coloured	contains ceramics and wood fragments	E.1
	1.51–1.70	clayey silt	greyish beige	hydromorphic, contains limestone fragments	D.1
	1.70–2.23	silty fine sand	yellowish grey	sharp basal contact, contains marine molluscs	C.7
	2.23–2.70	clayey silt	yellowish grey	compact, hydromorphic, homogeneous	B.3
	2.70–3.81	mainly fine sand	light grey	sharp basal contact, poorly sorted, silty layers/clasts	C.6
	3.81–4.55	clayey silt	dark grey	very homogeneous	B.3
	4.55-8.06	fine to medium sand	grey	contains high amounts of plant remains, partly peat-like	A.1
	8.06-15.00	clayey silt	grey	very homogeneous	B.3
KOR 32A	0.00–1.23	sandy silt	brownish	contains cultural debris	E.1
	1.23–1.52	clayey silt	brownish	contains ceramics	D.1
	1.52–2.47	fine to finest sand	reddish/yellow	sharp basal contact, marine molluscs	C.2
	2.47–2.58	sandy silt	grey	sharp basal contact, marine molluscs	C.1
	2.58–3.56	clayey silt	grey	higher clay amount to the top	B.1
	3.56–3.62	solid stone	grey	calcareous	E.2
	3.62–4.93	fine to finest sand	grey	well–sorted	A.1
KOR 35A	1.07–1.47	clayey silt	brownish	contains ceramics	D.1
	1.47–2.10	clayey silt	greyish brown	contains many ceramics and charcoal	B.2
	2.10–2.19	medium to coarse sand	reddish grey	sharp basal contact, fining upward tendency	C.4
	2.19–2.83	silty finest sand	grey	yellowish to the top, contains seaweed remains	A.2
	2.83–3.20	medium sand	greyish brown	sharp basal contact, fining upward tendency	C.3
	3.20–3.93	silty fine sand	grey	sediment–filled burrows	A.1
KOR 38A	1.27–1.51	sandy silt	brownish	contains cultural debris	E.1
	1.51–2.34	clayey silt	brownish	weathered, contains ceramics and cultural debris	F
	2.34–2.56	clayey silt	greyish brown	contains ceramics	D
	2.56–3.32	sandy silt	yellowish	contains ceramics and molluscs, sharp basal contact	C.7
	3.32–3.89	clayey silt	dark grey/yellow	compact, hydromorphic, shell debris at base	B.3
	3.89–4.75	medium/coarse sand	yellowish grey	sharp basal contact, marine molluscs, shell debris	C6
	4.75–7.37	fine sand	grey	homogeneous	A.1
	7.37–8.51	gravel, sand	multi-coloured	sharp basal contact, fining upward tendency	C.5
	8.81–9.93	fine sand	grey	homogeneous, well-sorted	A.1

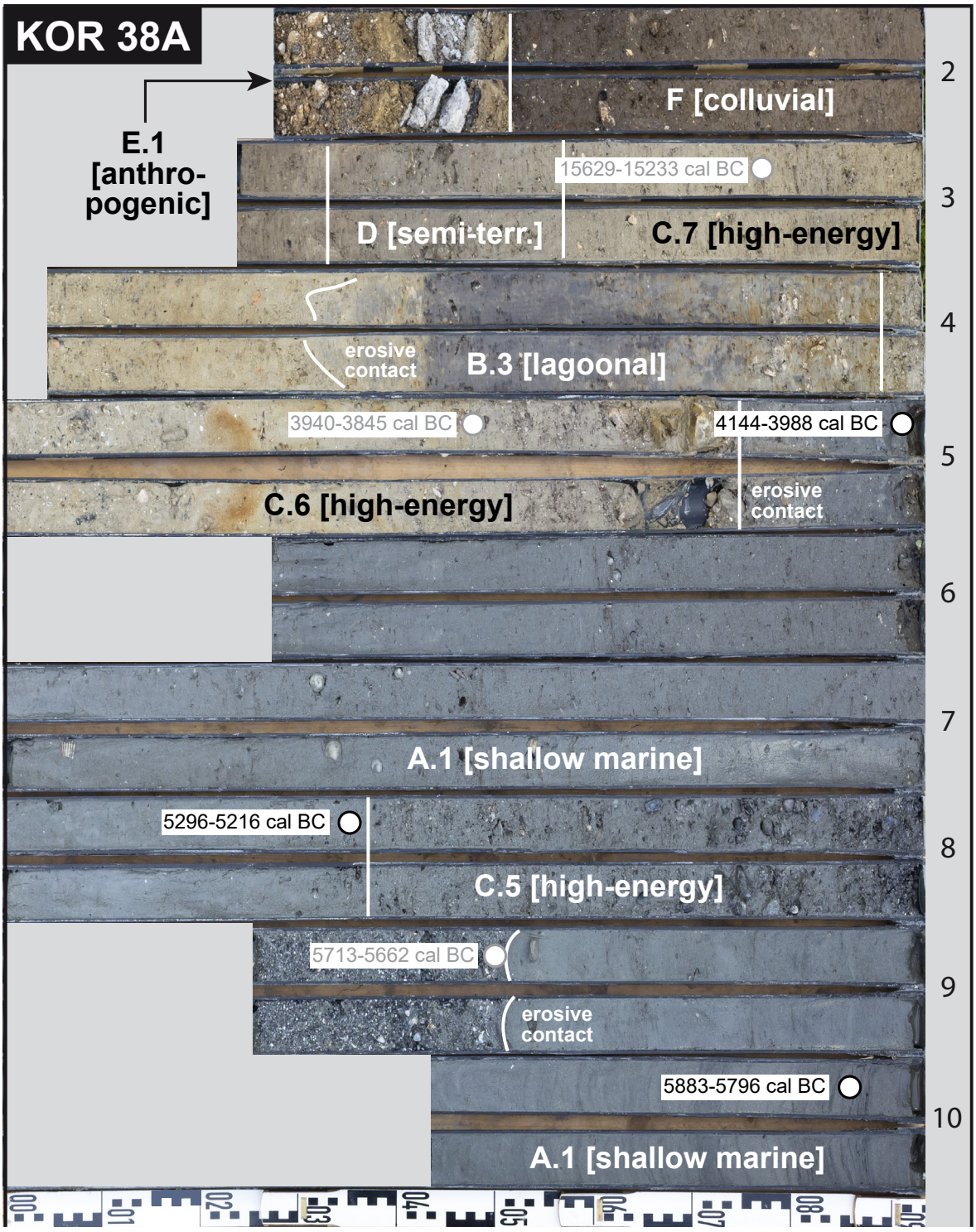

Figure 4.7: Sedimentary record and main stratigraphic units of vibracore KOR 38A, drilled at the western shore of the Analipsis Peninsula. Radiocarbon samples and associated ages (1σ confidential interval) are marked by white dots. Ages not considered for interpretation are depicted in grey (see section 4.5.3 for further explanations). The vibracore is dominated by homogenous shallow marine sands followed by first lagoonal and semi-terrestrial but later colluvial deposits. Following sharp erosional contacts, high-energy sediments were deposited associated with extreme wave impact and extraordinarily high flow velocities mirrored by significant coarse grain size (C.5, C.6) and a mixing of autochthonous lagoonal mud with allochthonous marine sands (C.7).

vity material with values > 30 Ωm (brown to red colours). This unit is overlain by a zone of lower resistivity values represented by green and yellow colours and forming a basin-like structure in the centre of the depth section, where this unit reaches down to 2 m b.s.l. In contrast, it is located higher than 1 m b.s.l. towards the north and south. The uppermost unit is characterised by high values > 50 Ωm. Like in transects KOR ERT 103 and KOR ERT 92, several delimited structures at 2 m, 6 m, 38 m and 44 m show comparatively high resistivity values.

4.4.2 Archaeoseismical and sedimentological results from the eastern shore of the Chalikiopoulou Lagoon

Drilled at the western coast of the Analipsis Peninsula, vibracore KOR 38A was used to decipher the palaeoenvironmental evolution of the peninsula. The stratigraphic record of vibracore KOR 38A (Figure 4.7, Figure 4.8 and Table 4.1) is characterised by a thick basal section of homogeneous grey finest to fine sands, intersected by a unit of poorly sorted coarse-grained sands and gravels at 8.50 to 7.37 m b.s. following an erosional contact. At 4.75 m b.s. a yellowish layer with conside-

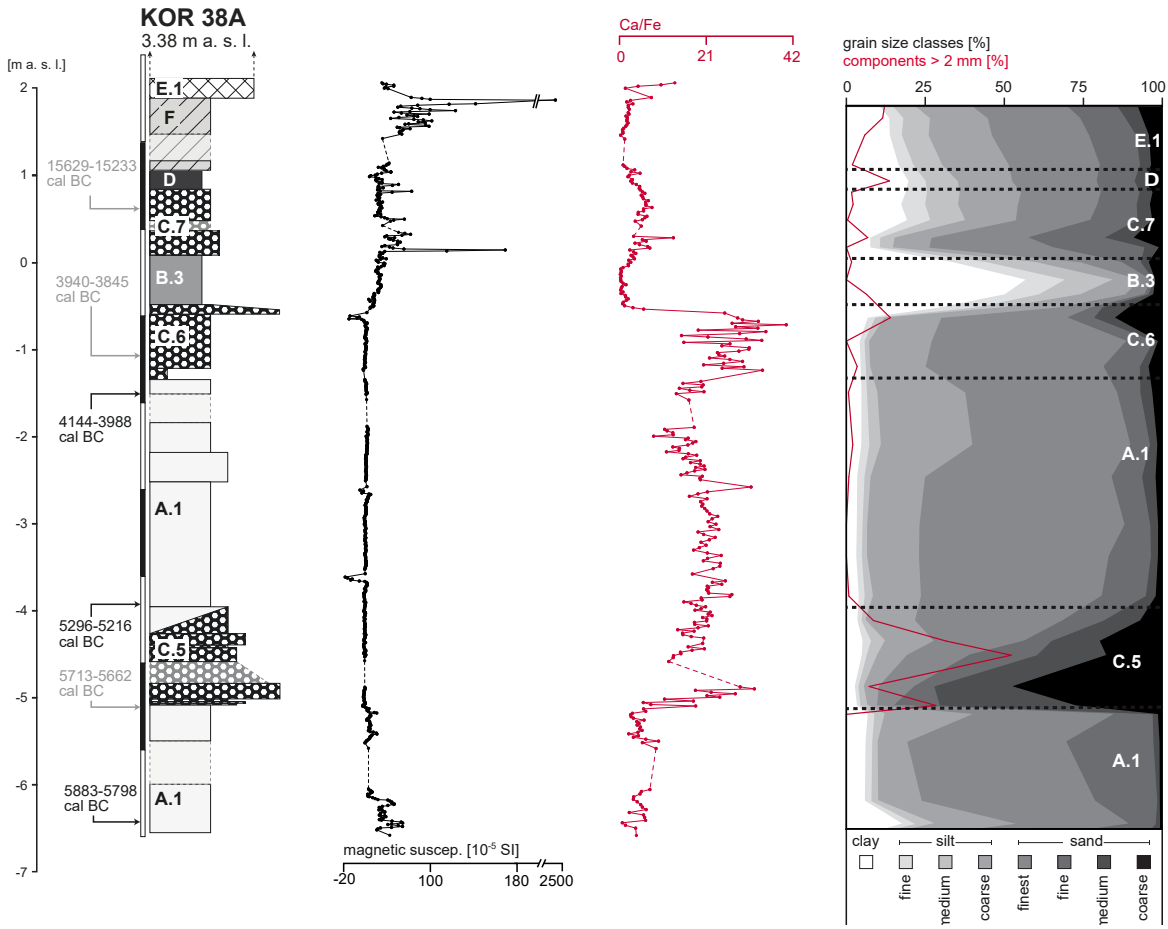

Figure 4.8: Results from multi-proxy analyses of samples from vibracores KOR 38A. Legend according to Figure 4.4. Intersected high-energy layers C.5 to C.7 distinctly differ from under- and overlying shallow marine sands due to the entry of coarse and medium sand as well as increased Ca/Fe values.

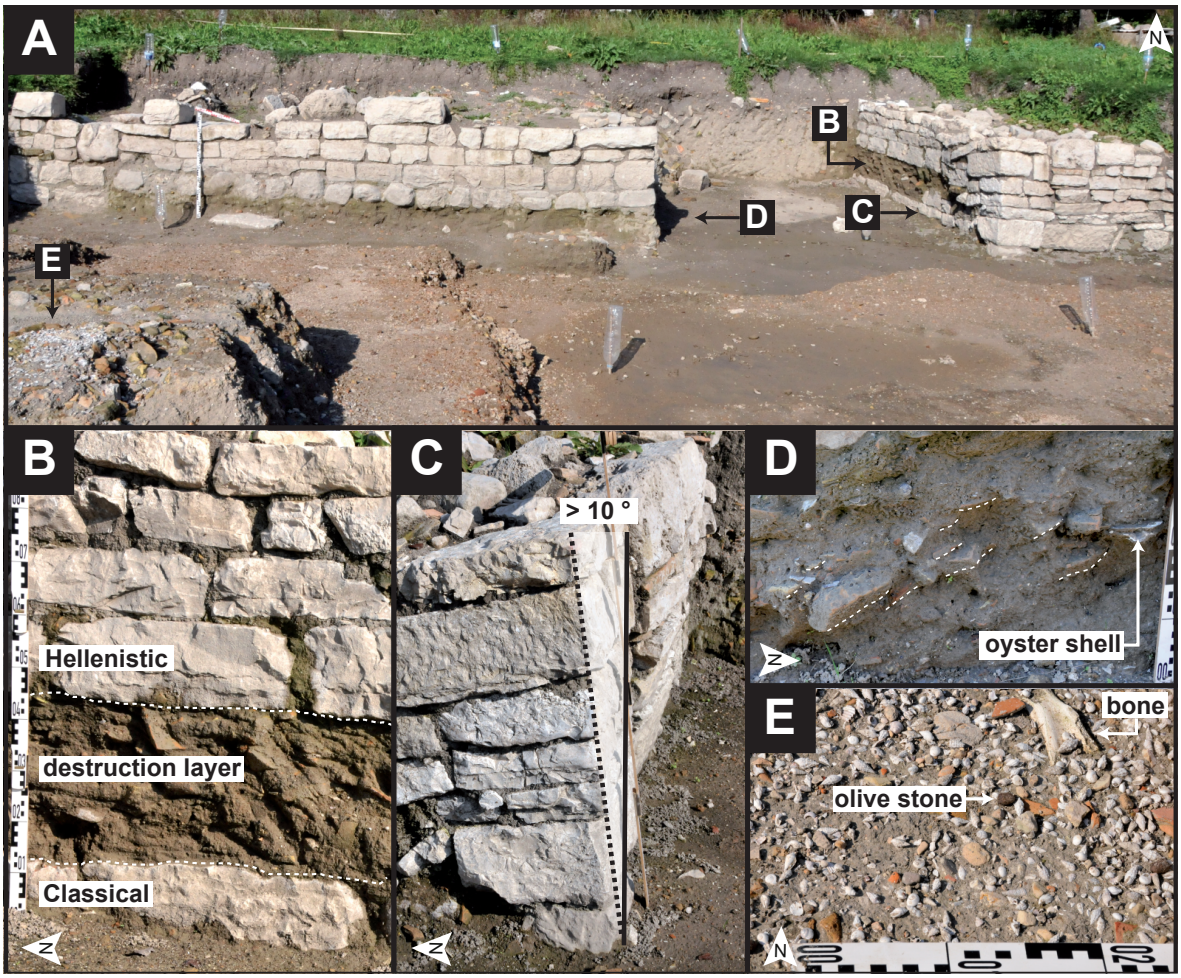

Figure 4.9: Rescue excavation site on the eastern shore of the Chalikiopoulou Lagoon. (A) Archaeoseismical traces of a strong local seismic event at a rescue excavation, situated on the eastern coast of the Chalikiopoulou Lagoon. A destruction layer, made of reworked lagoonal mud with embedded marine specimens and cultural debris (E) was found on top of a Classical foundation. After the event the building was rebuilt in Hellenistic times (B). Furthermore, strong tilted walls (C) and imbrication of ceramic sherds and oyster shells (D) indicated an abrupt seismic impulse and subsequent flooding of the site.

rable amounts of medium to coarse sand appears, covered by a layer of compact clayey silt. The latter is followed by yellowish silty fine sands and brownish silty clays. The uppermost part of the profile is made of brownish silty sediments containing cultural debris.

Approximately 700 to the north, a rescue excavation realised in 2012 brought to light the remains of two ancient buildings, located only few metres away from each other (Tennis site, Figure 4.9 A). The Classical foundations of both buildings are covered by a c. 30 cm thick mixed layer made of brown clayey silt (Figure 4.9 B) containing large amounts of sand, marine molluscs, shell debris, ceramics, bones and cultural remains. Larger items such as oyster shells or ceramics are clearly embedded and show a distinct imbrication (Figure 4.9 D). This poorly sorted layer is covered by in situ ashlars dating to the Hellenistic period (Figure 4.9 B). At the southern edge of the excavated area, Hellenistic ashlars are missing. Here, the mixed layer was found consolidated on top of Classical ashlars (Figure 4.9 E). Moreover, parts of the excavated walls are strongly shifted and tilted such that inclination angles of some walls exceed 10 ° (Figure 4.9 C).

4.4.3 Linking the Desylla and the Chalikiopoulou sites – the stadium site KOR 23

Vibracoring site KOR 23 is located on the isthmus between the Analipsis Peninsula und the modern city of Corfu, facing the bay of Garitsa to the east and the Chalikiopoulou Lagoon to the west. The vibracore was drilled in the modern football arena of Corfu, *c.* 350 m west of the present coastline (Figure 4.2 A).

The base of KOR 23 (Figure 4.10, Figure 4.11, Figure 4.12) is dominated by grey clayey silt, almost 7 m thick, followed by a heterogeneous sequence of fine to medium sand accumulated on top of a sharp contact (Figure 4.10 B). This grey unit contains many plant remains that, in some places, resemble peat. Homogeneous silty clay abruptly re-appears at 4.55 m b.s. From 3.81 m b.s. to 2.70 m b.s. and following an erosional contact, very poorly sorted grey fine to medium sand was found

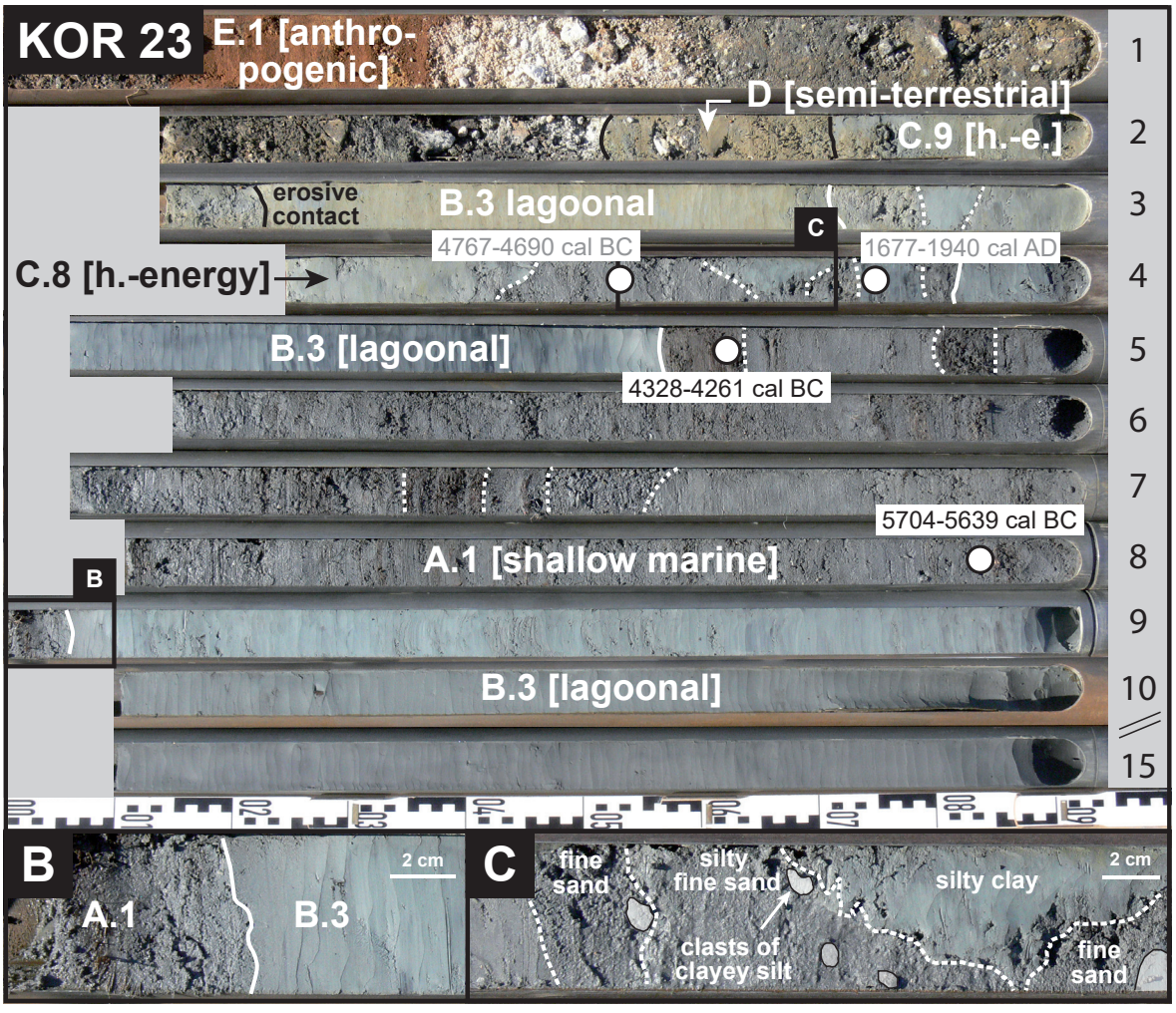

Figure 4.10: Stratigraphical record and simplified facies profile of vibracore KOR 23 retrieved at the narrow isthmus between the modern city of Corfu and the Analipsis Peninsula. Please note that the profile was shortened. The profile meters not depicted do not differ from profile meter ten. Radiocarbon samples and associated ages (1σ confidential interval) are marked by white dots. Unreliable dates (see section 4.5.3 for further explanations) are depicted in grey. Vibracore KOR 23 is primarily dominated by lagoonal deposits which are intersected by a unit of shallow marine sands, more than 3 m thick. According to a sharp contact (B) the transition towards shallow marine conditions happened abruptly. Two high-energy layers were found in the record, the older layer (C) contains several rip-up clasts and silty intersections of irregular shape.

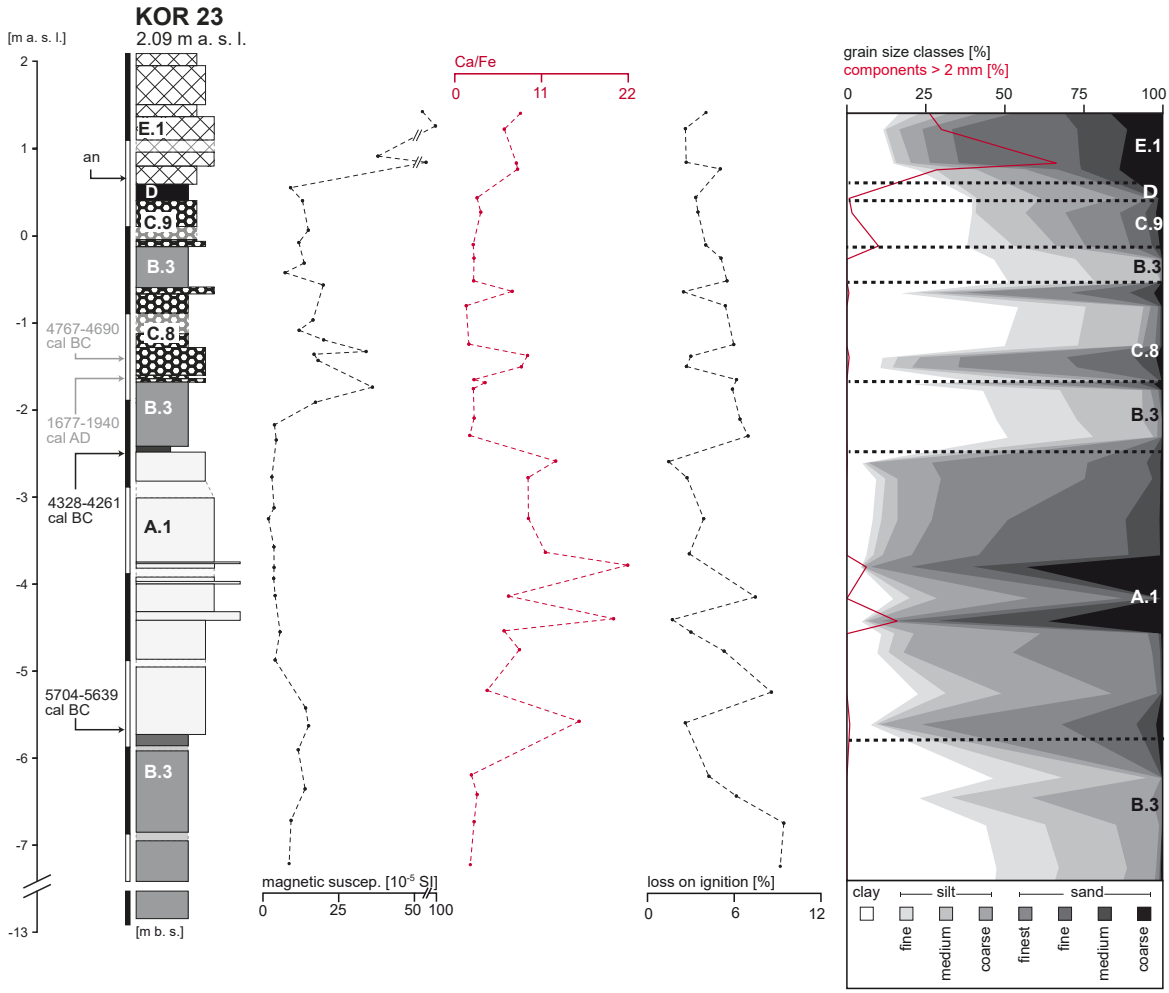

Figure 4.11: Grain size distribution and selected proxies of vibracores KOR 23. Legend according to Figure 4.4. Grain size data clearly depicts coarser-grained marine sands intersected in lagoonal deposits. Moreover, high-energy layer C.6 shows a varying grain size due to the entry of reworked silty components.

containing layers and clasts of silty clay (Figure 4.10 C). This unit is overlain by homogenous clayey silt of yellowish grey colour. Following another erosive contact at 2.23 m b.s., yellowish fine sands including marine molluscs were encountered. The very upper parts of the profile are characterised by hydromorphic clayey silts and multi-coloured gravels in a matrix of silty sand. The latter contain several ceramic sherds and wooden fragments.

4.4.4 Establishing a unified stratigraphy based on stratigraphic, geochemical and microfaunal data

Based on similarities in colour and sedimentary features (Figure 4.3, Figure 4.7, Figure 4.10), grain size and geochemical proxies (Figure 4.4, Figure 4.8, Figure 4.11) and microfaunal content (Figure 4.5, Figure 4.12), a unified stratigraphy (units A to G, Figure 4.13, Figure 4.14) was established to link and compare the local stratigraphies from the Desylla and stadium sites. In some cases (units A to C, unit E), further subunits were classified in order to take into account subtle secondary differences.

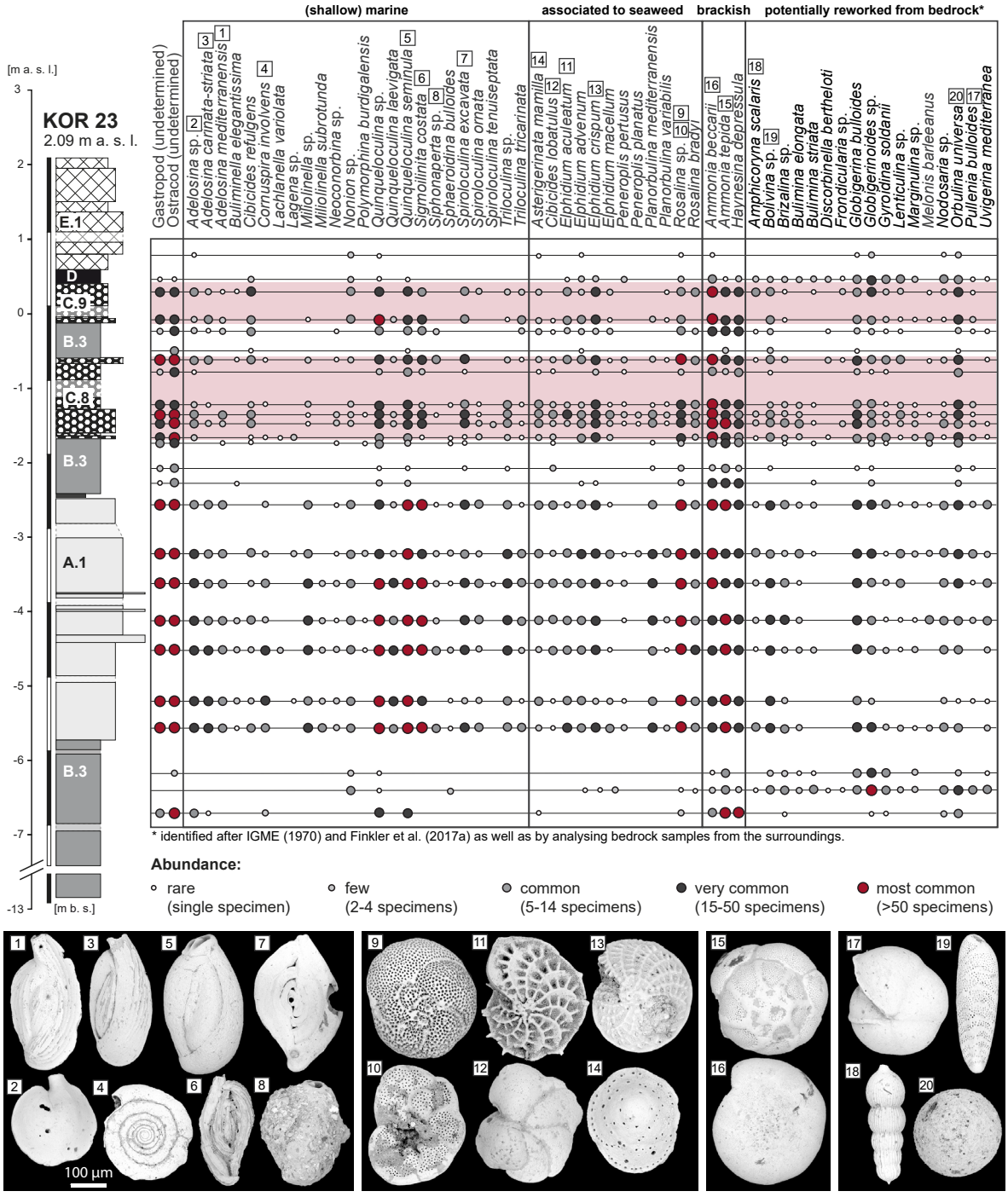

Figure 4.12: Results from microfaunal analysis of vibracore KOR 23 supplemented by SEM photographs of indicative specimens. Species were determined after Loeblich & Tappan (1988) and Cimerman & Langer (1991) and classified according to their ecological preferences after Sen Gupta (1999) and Murray (2006). Potentially reworked species of the local Neogene bedrock identified after IGME (1970) and Finkler et al. (2016) were depicted separately. Foraminiferal studies prove the marine character of intersected A.1 sands. Furthermore the foraminiferal signal of both high-energy layers differs strongly from local lagoonal foraminiferal assemblages.

Unit A sediments are characterized by grey sand ranging from finest to fine sand with varying amounts of medium sand.

Subunit A.1 (4.55–8.06 m b.s. in KOR 23, 3.62–4.93 m b.s. in KOR 32A, 3.20–3.93 in KOR 35A, 4.75–7.37 m b.s. and 8.81–9.93 m b.s. in KOR 38A) shows medium to high Ca/Fe values, while LOI and magnetic susceptibility are on a constantly low level. A.1 sands are void of lead. Regarding their foraminiferal content, unit A.1 sediments reveal a high abundance of well-preserved specimens from different habitats. Apart from Milliolidae, especially *Rosalina bradyi* and *Ammonia* spp. are dominating.

Subunit A.2 (2.19–2.83 in KOR 35A) contains distinctly lower abundances of foraminifera. Marine species are rare while species from lagoonal and seaweed-associated environments are most common. Subunit A.2 exhibits slightly increased silt amounts, concomitant with decreased Ca/Fe values. A.2 deposits show very low Pb concentrations under detection limit of the instrument used.

Unit B represents grey clayey silt. Due to different amounts of fine sand and embedded debris as well as varying Pb concentrations the unit was subdivided into subunits B.1, B.2 and B.3. Subunit B.4 (Figure 4.14) was found in KOR 29 only and is described in detail by Fischer et al. (2016a).

Subunit B.1 (2.58–3.56 m b.s. in KOR 32A) is dominated by clayey silt with considerable amounts of finest and fine sand. Towards the top of the unit, proportions of clay and silt increase, accompanied by rising LOI values. Geochemically, B.1 deposits show low Ca/Fe and medium Pb values. While the lower part shows a very similar foraminiferal fingerprint as subunit A.1, abundance and diversity of foraminifera clearly decrease towards the top of subunit B.1. Here, only few species, e.g. *Elphidium crispum, Ammonia tepida* and *Ammonia beccarii* were found in considerable numbers.

Subunit B.2 (1.47–2.10 m b.s. in KOR 35A) is represented by brown clayey silts containing coarse sand, gravel and ceramic sherds. Like in subunit B.1, Pb concentrations are on a medium level, while Ca/Fe values are low. From a micropalaeontological point of view, this unit differs strongly from subunit B.1 because only few specimens of selected lagoonal and marine species (e.g. *Haynesina* sp. or *Adelosina* sp.) were detected; additionally, potentially reworked specimens were encountered in subunit B.2.

Subunit B.3 (2.23–2.70 m b.s., 3.81–4.55 m b.s., 8.06–15.00 m b.s. in KOR 23 and 3.32–3.89 m b.s. in KOR 38A) is restricted to the record of vibracores KOR 23 and KOR 38A; it is made out of homogeneous silty clays with less than 5 % sand. Values obtained for Ca/Fe and magnetic susceptibility are low, while LOI values are on a high level. Regarding the microfaunal fingerprint of B.3 deposits, we primarily found lagoonal species and species associated to seaweed meadows and marine environments.

Unit C sediments are dominated by sand; they further show basal erosional unconformities and bad sorting. Some subunits are characterised by yellow to brownish colour.

Subunit C.1 (2.47–2.58 m b.s. in KOR 32A) consists of grey finest to fine sand at the base and clayey silt at the top. The deposits include lots of plant remains and marine molluscs, partly broken, and show low Ca/Fe and LOI values. Pb concentrations are on a medium level, similar to subunit B.1. Microfauna strongly resembles unit B.1.

Subunit C.2 (1.52–2.47 m b.s. in KOR 32A) shows yellow to red finest and fine sand. It is void of Pb and features low LOI values. Ca/Fe values are on a medium to high level, decreasing to the top of the subunit. Regarding its foraminiferal content, subunit C.2 resembles subunit A.1 showing high diversity and abundance, although abundance of marine species significantly drops towards the top.

Subunit C.3 (2.83–3.20 m b.s. in KOR 35A) represents greyish brown medium sand containing smaller amounts of finest and fine sand. A general fining upward tendency can be observed in the lower section of the subunit. XRF measurements revealed medium Ca/Fe values while Pb values are below detection limit. The foraminiferal fingerprint is identical with the one observed for subunit A.1.

Subunit C.4 (2.10–2.19 m b.s. in KOR 35A) represents a fining upward sequence of coarse to medium to fine sand with high amounts of skeletal components and clayey silt at the very top. The deposits are characterised by low Ca/Fe and Pb values, the latter below detection limit. Foraminifera content is dominated by potentially reworked species, particularly by planktonic species, associated with species typical of brackish waters and seaweed meadows.

Subunit C.5 (7.37–8.51 m b.s. in KOR 38A) is made of multicoloured gravels embedded in a matrix of grey medium to coarse sand, fining towards the top of the subunit. The deposits overly homogeneous sands of unit A.1 after a sharp erosional contact and show high Ca/Fe values while magnetic susceptibility was found on a very low level.

Subunit C.6 (3.89–4.75 m b.s. in KOR 38A) consists of gravel embedded in a matrix of yellowish sand in the lowermost part but medium to coarse sand of yellowish grey colour in the upper part. The sediments contain significant amounts of shell debris and marine molluscs and are characterised by very high Ca/Fe values.

Subunit C.7 (2.56–3.32 m b.s. in KOR 38A) is following clayey silts of subunit B.3 in vibracore KOR 38A. In contrast to B.3 sediments, yellowish C.7 deposits are characterised by considerable amounts of sands containing reworked silty clasts. Moreover, several ceramic sherds and marine molluscs were found within the subunit which shows low to medium Ca/Fe values.

Subunit C.8 (2.70–3.81 m b.s. in KOR 23, Figure 4.10 C) shows grey fine sand with embedded clasts and layers of silty clay. Subunit C.5 deposits show medium but fluctuating values of magnetic

susceptibility and LOI, while Ca/Fe values are low to medium. The microfaunal content of subunit C.5 is nearly identical to subunit A.1 with slightly decreased numbers of marine foraminifera, e.g. *Quiqueloculina* spp., *Nonion* sp. or *Triloculina* spp.

Subunit C.9 (1.70–2.23 m b.s. in KOR 23A) overlays unit F on top of an erosive contact. Grain size is dominated by grey clayey fine sandy silt. The sediments show low values of magnetic susceptibility, Pb and Ca/Fe. Specimens of *Ammonia beccarii, Quinqueloculina* spp. and *Elphidium* spp. dominate the microfaunal fingerprint, accompanied by common abundances of other species typical of lagoonal, marine and seaweed environments.

Unit D (1.51–1.70 m b.s. in KOR 23, 1.23–1.52 m b.s. in KOR 32A, 1.07–1.47 m b.s. in KOR 35A, 2.34–2.56 m b.s. in KOR 38A) consist of grey to brown clayey silt including medium to high amounts of components > 2 mm as well as plant remains. Ca/Fe, LOI and magnetic susceptibility values are mostly medium and Pb concentrations medium to high. Only few lagoonal species (*Ammonia* spp., *Haynesina* sp.) inhabit this environment. In vibracores KOR 23 and 32A these species are supplemented by seaweed-related species, such as *Elphidium* spp. and *Rosalina bradyi*.

Cultural debris is classified as ***unit E***.

Subunit E.1 (0.00–1.51 in KOR 23, 0.00–1.23 m b.s. in KOR 32A, 1.27–1.51 m b.s. in KOR 38A) comprises cultural debris and gravel embedded in a sandy to silty matrix. Here, Pb concentrations and values of magnetic susceptibility reach maximum values. Microfauna is dominated by few potentially reworked and poorly-preserved specimens.

Subunit E.2 (3.56–3.62 in KOR 32A) is restricted to the Desylla site and overlies A.1 sands. It is mostly made out of fragments of white calcareous stones.

Unit F (1.51–2.34 m b.s. in KOR 38A) is made of brown silty clays, slightly sandy, containing minor amounts of ceramics and cultural debris.

Unit G was found in vibracores KOR 29A and KOR 1A only (Fischer et al. 2016a, Finkler et al. 2017a; see Figure 4.14) and is thus not part of one of the master cores related to this study. Nevertheless, the unit is formed by compact silty clay, characterised by grey colour and including marine molluscs.

4.5 Discussion and interpretation

4.5.1 Facies interpretation

Based on distinct sedimentary, geochemical and microfaunal fingerprints, one can differentiate between the following facies.

Grain size and microfaunal content of unit A indicate a ***shallow marine*** environment. Based on grain size (fine to medium sand) and high Ca/Fe values subunit A.1 suggests stable mid-energy ***littoral to sublittoral*** conditions close to the coast. According to high abundances and high diversity of calcareous Milliolidae and species associated to seaweed, these sediments refer to inner-shelf waters of normal marine to hypersaline salinity with temperate to warm water temperature and shallow water depth of some 10 m (Murray 2006). In contrast, subunit A.2 reflects ***low-energy littoral conditions*** characterised by slightly reduced wave influence (higher amounts of silt) and restricted water exchange (decreased Ca/Fe values). Water depths are slightly shallower in comparison to subunit A.1 and salinity most likely slightly decreased, reflected by missing marine foraminiferal species; instead brackish and seaweed-related species are dominating (Murray 2006).

Unit B is associated to more quiescent conditions, where silty and clayey sediments are deposited in ***inner-shelf lagoonal systems***. Subunit B.1 represents the transition from a marine towards a brackish-lagoonal milieu mirrored by decreased marine indicators. In contrast to subunits A.1 and A.2 that were found void of Pb, subunit B.1 shows considerable Pb pollution. As the natural geogenic background signal of Pb is very low, high Pb concentrations are linked to intense human activities, especially mining and metal-working (Nriagu 1996). Once deposited, Pb is immobile in natural sedimentological archives and represents a reliable proxy to trace human activities during antiquity (Brännvall et al. 2001, Marriner & Morhange 2007). Pb was one of the first metals used by man and its extensive use started already in the 4th/3rd millennium BC and continuously intensified during Bronze and Iron ages (Lessler 1988, Hong et al. 1994). Pb contamination reached its pre-industrial climax during the Greek and Roman periods. In particular, harbour basins were polluted as they provided low-energy environments where waste was accumulated (Marriner & Morhange 2007, Elmaleh et al. 2012). Moreover, Pb was used on a large scale in ancient water distribution systems and shipbuilding (Delile et al. 2014). Recent investigations on ancient harbour deposits have shown that even if maximum concentrations were found in Roman harbour sediments (Le Roux et al. 2005, Stock et al. 2013, Finkler et al. 2017a), considerable Pb contamination in harbours already started during Archaic to Hellenistic times (Le Roux et al. 2003, Véron et al. 2006, Elmaleh et al. 2012, Hadler et al. 2013, 2015, Finkler et al. 2017b). Based on high Pb concentrations and associated silty grain size reflecting deposition within a protected lagoonal system, we identify subunit B.1 as ***harbour sediments***. Subunit B.1 harbour underwent time-related environmental changes. Initially, large numbers of Milliolidae and a high diversity along all habitats suggest that the harbour was only slightly or partly protected, most probably by the construction of breakwaters or comparable infrastructure. This resulted in an unhindered water exchange and in an almost normal marine salinity (Murray 2006). However, changing foraminiferal signals associated

with increasing silt amounts and LOI values indicate that the harbour basin was subject to further protection and separation from the Gulf of Corfu, possibly due to repeated anthropogenic impact or natural sedimentation along the system's barrier. In any case, water exchange was restricted so that fine-grained sediments were accumulated at the bottom of the harbour basin. Subsequently, water depths decreased as shown by primarily seaweed-associated species inhabiting the harbour lagoon. Moreover, rising numbers of lagoonal genera such as *Ammonia* spp. and *Haynesina* sp. document that conditions became more and more brackish, probably caused by the inflow of freshwater into the harbour.

Silt-dominated brown B.2 deposits were only retrieved from the western part of the Desylla site and show a maximum thickness of less than 60 cm. Additional to grain size medium to high Pb concentrations imply harbour conditions. Compared to subunit B.1, subunit B.2 seems to be characterised by more brackish waters as only few, primarily lagoonal, specimens were able to inhabit this environment. High amounts of sand and components > 2 mm (mainly ceramics and gravel) lead to the conclusion that B.2 deposits may be influenced by the input of anthropogenic debris from higher grounds and thus represent ***peripheral harbour basin deposits***. This "granulometric paradox" was observed in many harbours, especially in Roman ones, and underlines that harbours were used as waste dumps for ancient societies (Marriner & Morhange 2007). In the case of the Desylla study site, peripheral B.2 harbour sediments (sites KOR 34A, KOR 35A) were found close to the excavated wall that may have been part of an urban fortification system (Andreadaki-Vlazaki 2012) related with the harbour basin. However, vibracoring site KOR 35A is located west, i.e. outside of the harbour basin (see section 4.2.2).

We interpret subunit B.3 as low-energy ***lagoonal*** facies based on grain size (silt predominant), high LOI values as well as the presence of lagoonal and seaweed-related foraminifera. Sediments of subunit B.3 are void of Pb.

Sand associated to unit C and subunits lies directly on top of a sharp erosional contact representing the onset of ***high-energy*** conditions. By this high-energy influence, autochthonous lagoonal sediments were translocated, reworked and mixed with marine allochthonous deposits. There are considerable differences between subunits C.1 to C.9.

We interpret subunit C.1 as reworked harbour deposits (B.1) because of low Ca/Fe values and medium Pb concentrations, the latter indicating man-made and most probably harbour-related contamination. According to low LOI values and significant amounts of finest to fine sands these deposits originate from the base of B.1 harbour sediments, which was still under the influence of marine waters when deposited; Alternatively they come from another part of the harbour, located close to the harbour entrance, where water exchange with the adjoining (sub)littoral system was possible. Towards the top of subunit C.1, energetic conditions seem to be decreased (fining upward) as reflected by a thin mud cap.

Deposits of subunit C.2 follow C.1 sands after an erosional unconformity. They are made of A.1 sublittoral sands regarding their geochemical and microfaunal fingerprint, showing an overall high abundance and diversity of foraminifera dominated by marine Milliolidae. However, noticeable is a strong difference in colour: C.2 sands are characterised by yellow to red colour, implicating oxidation processes. In contrast, A.1 sands were deposited under water and under anoxic conditions, mirrored by grey colour. We therefore interpret C.2 sands to represent allochthonous A.1 sands which were weathered, oxidised and deposited on top of reworked harbour deposits C.1.

The same sediment source and process can be assumed for sediments of subunit C.3, greyish brown in colour and intersecting grey A.1 and A.2 deposits in vibracore KOR 35A. High-energy conditions are mirrored by medium to coarse sand at the base of the subunit. Based on the general fining-upward tendency of the deposits, energy flux gradually drops towards the top of the subunit.

Fining-upward in grain size was also noticed for sands of subunit C.4, where coarse sand is followed by medium and fine sand and finally by clayey silt. The foraminiferal content suggests that these deposits originate from littoral sands of subunit A.2, characterised by decreased abundances of mainly seaweed-associated and brackish species, most likely caused by low salinity and shallow water depth.

Sediments of subunit C.5 follow a sharp erosional contact and mirror the input of coarse-grained marine sediments due to high Ca/Fe values. However, grain size distinctly differs from shallow marine A.1 and A.2 sands.

In contrast, subunit C.6 strongly resembles A.1 sands according to grain size and Ca/Fe values even if the deposits are of yellowish colour. Intersected layers of shell debris and marine molluscs point to the marine origin of this subunit.

Deposits of high-energy subunit C.7 are following lagoonal deposits of subunit B.3. The overall sandy grain size going ahead with still considerable amounts of silt as well as low to medium Ca/Fe values mirror a mixing of lagoonal and shallow marine deposits, resulting in a poorly sorted layer.

High-energy subunit C.8 covers B.3 lagoonal mud in vibracore KOR 23 and is characterised by fine sand. Based on its foraminiferal fingerprint (high abundances, in particular of Milliolidae, high bio-diversity), the latter reflects reworked A.1 deposits. Moreover, silty layers of irregular shape and several mud clasts are embedded in these fine sands. They indicate reworking and short-term transport of underlying B.3 deposits, which are mixed with allochthonous (sub)littoral sands from local shores.

Subunit C.9 reflects high-energy input into a shallow lagoonal system (subunit B.3) at vibracoring site KOR 23. Similar to the sandy sections of C.8, microfauna indicates the input of littoral sands.

Unit D, consisting of clayey silt and large amounts of organic remains, e.g. plant fragments, was deposited under transitional conditions. In particular, the deposits represent a ***back-beach swamp environment***. Sediments accumulated in such shallow and quiescent wetlands are greyish-brown by initial soil development processes and show a delimited foraminiferal diversity restricted to brackish-lagoonal and partly seaweed-associated species mirroring the transition from marine-brackish towards freshwater conditions. Pollution by Pb and the input of individual pieces of gravel and stones suggest anthropogenic impacts.

Sediments of unit E embody human intervention. Man-made influence in E.1 sediments is attested by considerable contamination by Pb associated with high values of magnetic susceptibility related to weathering and reworking processes of man-made metals. Large amounts of debris and gravel, especially ceramic sherds, identify this unit as ***cultural infill***. Subunit E.2 is characterised by man-made ashlars associated to ***human infrastructure***. As E.2 marks the border between A.1 littoral sands and B.1 lagoonal mud, it is probably part of a large-scale harbour-related construction, e.g. a dredged harbour basin.

The brown colour of unit F, dominating the uppermost part of vibracore KOR 38A points to considerable weathering by iron oxidation and subsequent soil formation. These deposits represent terrestrial conditions, where ***colluvial*** material is deposited due to erosion and translocation from the adjoining Analipsis hillslopes.

Sediments of unit G are identified as Neogene marl, forming the ***bedrock*** in the area of ancient Corcyra and cropping out at the Analipsis Ridge (IGME 1970, Fischer et al. 2016a, Finkler et al. 2017a, 2017b). Faunal remains from the Neogene bedrock may contaminate younger Holocene deposits due to erosion processes and subsequent translocation (see unit F above). This is problematic as many species are described for both periods, the Neogene and the Holocene (Loeblich & Tappan 1988). Reworked Neogene faunal remains might be well-preserved, in particular in marine carbonate-rich environments like those analysed in the presented study, which is why a good conservation status of individual specimens cannot function as reliable indicator for Holocene age. Thus, all species found in the Neogene marls of Corfu (e.g. IGME 1970, Finkler et al. 2017a) are regarded as potentially reworked as they might represent possibly relocated fossil species.

4.5.2 High-energy impacts on the study sites

Sedimentary records at the Desylla site as well as at the drillings sites KOR 23 and KOR 38A include several high-energy layers, classified as unit C deposits. In all vibracores, these units follow a sharp erosional contact. The sediments overlie and/or intersect B.1 harbour mud or B.3 lagoonal sediments or were found on top or in between littoral sands of subunits A.1 and A.2.

Event-related impact can be subscribed to different causes such as torrential run-off after extreme precipitation events, flooding due to severe storms and tsunami inundation triggered by seismic events or submarine slides. Even if highly variable regarding the sediment source (section 4.5.1), all high-energy layers observed in the frame of the present study show a brackish or marine foraminiferal signal, implying event-related impact from the seaside. As the foraminiferal signal of Neogene marls on Corcyra (IGME 1970) is not dominated by brackish to marine species contained in high-energy deposits but by mainly cold-marine species (Murray 2006; see potentially reworked species in Figure 4.5, Figure 4.9 and Figure 4.12), torrential run-off from higher grounds of the Analipsis Peninsula towards the coastal lowlands of the Bay of Garitsa and the Chalikiopoulou Lagoon can be excluded as major trigger for unit C deposits.

Regarding seaward sources of high-energy inundation, both storms or tsunamis must be considered on the base of sedimentary signatures, geochemical proxies and microfaunal fingerprints. Geochemical and microfaunal signals are strongly linked to the sources of the sediment that is translocated in the course of an event (Goff et al. 2001, Kortekaas & Dawson 2007, Chagué-Goff et al. 2017, Judd et al. 2017). We identify four different sediment sources for the study sites, namely sediments from slightly protected B.1 harbour basins (C.1), shallow marine sublittoral sands of unit A.1 (C.2, C.3, C.6, C.9), partly mixed with lagoonal B.3 mud (C.7, C8), littoral sands of unit A.2 (C.4) as well as coarse-grained marine gravels (C.5). Tsunami deposits are basically originating from the near-shore zone reaching from the local subtidal to the beach and a narrow fringe of the adjacent land (Gelfenbaum & Jaffe 2003, Morton et al. 2007, Jagodziński et al. 2012, Szczucińskia et al. 2012). However, the same is true for most tempestites, especially those deposited by tropical cyclones, even if storms usually recruit sediments from a comparatively smaller nearshore erosional zone (Kortekaas 2002, Allison et al. 2005). Nevertheless, in our study, two criteria strongly support tsunami landfall against storm-related flooding: First, high-energy deposits also include terrestrial components and artefacts which indicates backflow currents directed seaward (e.g. Nanayama et al. 2000) and, second, event-related sediments were deposited on elevated, protected and far-inland positions (e.g. Kortekaas & Dawson 2007, Morton et al. 2007).

Regarding sedimentary signatures, numerous studies presented sedimentary features related with modern tsunami events, for example the Indian Ocean Tsunami 2004 (c.f. Bahlburg & Weiss 2007, Hawkes et al. 2007, Sakuma et al. 2012, Veerasingam et al. 2014, Sakuna-Schwartz et al. 2015) and the Tōhoku Tsunami 2011 in Japan (e.g Goto et al. 2012, Nakamura 2012, Pilarczyk et al. 2012). Based on these findings and by reviewing signatures of modern and palaeoevents worldwide, compilations of typical and diagnostic criteria of tsunamites were published, for example, by Goff et al. (2001), Kortekaas & Dawson (2007), Dominey-Howes et al. (2006), Morton et al. (2007), Sugawara et al. (2008), Switzer & Jones (2008) and Chagué-Goff et al. (2011). Several of these criteria were also detected in high-energy deposits of subunits C.1 to C.7, namely

i. fining upward sequences or general fining upward tendencies in grain size (C.1, C.3, C.4, C.5, C.6) due to decreased hydraulic energy in the course of an event,

ii. internal mud layers made of silt, clay or peat (C.1, C.4, C.7, C.8), for example in the form of thin mud caps on top of sand-dominated high-energy units, mirroring stagnation of flow velocities between run-up and backflow,

iii. poor sorting (C.3, C.4, C.5, C.6, C.8, C.9), associated by bimodal grain size distribution,

iv. breaks in the general depositional patterns, represented by abrupt changes in colour, geochemistry or foraminiferal content (C.2, C.3, C.5, C.6, C.7, C.8, C.9) and

v. rip-up clasts consisting of reworked material of the underlying unit (C.5, C.8), mostly lagoonal mud or bedrock marl.

However, outside the Mediterranean most of these depositional structures have also been found in storm-related sediments as well, so that – on a theoretical base – there seems to be no univocal criteria to classify tsunami deposits solely based on sedimentary evidence (Lario et al. 2010). Sedimentary features as described above, however, prove high-energy impact from the seaside associated with massive inundation of coastal areas and therefore document extreme wave impact in general (Kortekaas 2002, Switzer & Jones 2008). We underline that it is not on the base of a single sedimentary feature or a set of sedimentary features to decide whether a sediment unit was laid down by storm or tsunami but rather the synthesis of geomorphological, sedimentological, geochemical and (geo-)archaeological findings have to be considered against the background of the (palaeo-)geographical setting.

A pro-tsunami argument is provided by geoarchaeological and archaeoseismological traces recovered in the frame of a rescue excavation at the western shore of the Analipsis Peninsula (Figure 4.2 A, Figure 4.9) in 2012. Here, a layer of cultural debris embedded in brown sandy mud separates two construction phases of a building, namely the Classical foundation from a Hellenistic rebuilding phase (section 4.4.2). We interpret this layer as tsunami-related deposit based on the following arguments:

i. The sediment is poorly sorted and contains clastic components from both marine (molluscs) and terrestrial sources, as well as human waste (bones, olive stones) and ceramic sherds (Figure 4.9 E);

ii. the strong tilting of nearby walls (Figure 4.9 C) indicates an abrupt and short-time seismic impulse, probably associated with co-seismic movements;

iii. imbrication of oyster shells and ceramic sherds (Figure 4.9 D) prove landward-orientated flow from the sea side (e.g. Bahlburg & Spiske 2002, Hadler et al. 2013).

We conclude, that considerable parts of a Classical building were destroyed and tilted by an earthquake. Shortly after, a tsunami wave arrived leading to massive reworking of local lagoonal sediments – e.g. reported by Donato et al. (2008) for Oman – and artefacts. These sediments were accumulated on top of the Classical foundation and subsequently integrated in the reconstruction of the building during Hellenistic times. Traces of this local seismic event were also found on top of the Analipsis Ridge at the Hera temple and in the Pierri harbour (Figure 4.1A, Finkler et al. 2017b).

Finally, the local geographic and hydrodynamic background helps to exclude storm-related event impact on ancient Corcyra. Corfu, as the most northern island of the Ionian archipelago, is situated in the northern Ionian Sea, characterised by a steadily low to medium annual wave climate (Cavaleri 2005, Lionelli et al. 2012, Karathanasi et al. 2015). However, the area is affected by frequently occurring storms, usually related to Sirocco winds, and by the rare meteorological phenomena of Mediterranean tropical-like cyclones, so called Medicanes that might lead to flooding of coastal areas (Davolio et al. 2009, Tous & Romero 2013, Cavicchia et al. 2014). Maximum wave heights do not exceed 6-7 m in the northwestern Ionian Sea near Sicily according to studies of Scicchitano et al. (2007). Ghionis et al. (2015) observed wave heights of around 5 m offshore Lefkada Island during an extreme storm in 2007. However, such extreme high-energy events occur very rarely and are restricted to the deeper parts of the Ionian Ssea (HCMR 2015).

For the ancient city of Corcyra, such rare extreme events have a minor influence and can be even excluded due to the geographical setting. The city is located on the eastern shore of the island exposed to the low-energy Gulf of Corfu, maximum 25 km wide and described by Partsch (1887) as being similar to a lake. Both the northern and southern entrances to the Gulf of Corfu are comparatively narrow, namely 2 km and 8 km, respectively (Finkler et al. 2017b). Fetch conditions and water depths of less than 70 m (GEBCO 2014) are not sufficient to produce fully arisen sea (FAS) conditions (Figure 4.1). The gulf is well-protected from storm wave impact as it is protected from the open Ionian Sea by the C-shaped island of Corfu. As a consequence, storm waters do not intrude into the Gulf of Corfu. Mazarakis et al. (2012) analysed observed and modelled wave heights caused by severe cyclone-linked storms in November 2007 and February 2011 that caused considerable damage at several coastal areas in Greece. Their results prove wave heights of less than 1 m in the Gulf of Corfu while wave heights of 5 m occurred off Corfu in the Ionian Sea. Englebretson et al. (1992) already described the negligible effects of extreme weather phenomena on the modern harbour of Corfu which is located only 100 m north of the ancient Alkinoos Harbour.

In a summary view, the Gulf of Corfu provides one of the best protected natural harbour-environments of the Mediterranean, where the influence of storm-induced extreme waves can be *a priori* excluded. Unsurprisingly, not a single storm surge is recorded by historical sources for the eastern coasts of the entire Ionian Islands, whereas entries in tsunami and earthquake catalogues report of repeated seismic-related marine inundations (Partsch 1887, Soloviev et al. 2000, Ambraseys & Synolakis 2010, Hadler et al. 2012). Hence, extreme wave events detected in the geoarchives of ancient Corcyra are interpreted as being related to tsunami influence and strongly linked to local and supra-regional seismic events.

4.5.3 Dating Approach

Altogether 29 samples out of organic material and biogenic carbonate were dated by means of ^{14}C AMS analysis and calibrated using the software Calib 7.1 (Stuiver & Reimer 1993; Reimer et al. 2013). Production ages of eight ceramic sherds were determined by archaeological age estimation. Dating results are listed in Table 4.2 and Table 4.3.

Where possible, we preferred non-marine samples for radiocarbon dating (peat, wood and plant remains) to avoid marine reservoir effects (MRE). MRE are related to the fact, that oceans function as long-term reservoirs where carbon is stored with long residence times and mixed with fossil waters void of ^{14}C (Reimer & McCormac 2002). Thus, radiocarbon ages of marine organisms, using dissolved carbonate from sea water to build up their shells, appear much older than their terrestrial counterparts (Wagner 1998, Geyh 2005, Walker 2005). Conventional ages of marine samples are usually calibrated using marine datasets considering MRE-related age deviations. These datasets, however, do not account for local or regional conditions but are based on random samples from very different marine environments more or less close to the regions of interest.

For the Mediterranean, Siani et al. (2000) investigated 26 marine samples and calculated a mean reservoir age of 390 ± 85 years, which is in good accordance to the findings of Reimer & McCormac (2002). Faivré et al. (2015) refer to the east Adriatic Sea, some 100 km north of Corfu, and present reservoir ages of 424 and 378 years. Reservoir ages of 396 and 442 years were found for the Adriatic Sea and the Island of Zante, respectively (Reimer & McCormac 2002). According to these studies, marine ages retrieved on Corfu must be adjusted by a local reservoir correction factor ranging between 390 to 442 years. However, these local estimates for the correction of marine samples are strongly varying in time, such that calibration factors deduced from sub-recent samples may not necessarily represent an appropriate valid reservoir age for the whole Holocene (Wagner 1998, Ascough et al. 2005, Walker 2005). Marine oysters, for example, which represent the water level of the Classical harbour at the Pierri site (Figure 4.2), indicate a Classical MRE of 347 to 426 years on Corfu (Finkler et al. 2017b). Moreover, accurate reservoir ages are restricted to the biological species they are based on, which is why MRE of different species from the same time period may be different (e.g. Faivré et al. 2005). In this paper, we therefore use to a pre-industrial global mean reservoir age of 405 ^{14}C years (Reimer et al. 2013) that provides a good estimation of the MRE, to calibrate conventional radiocarbon ages derived from marine samples.

It is moreover relevant to underline, that – even if local MRE are known or terrestrial sampling was possible– ages based on radiocarbon dating provide mere age approximations but not exact or "absolute" ages, also due to multiple error sources (Wagner 1998, Geyh 2005, Walker 2005). We therefore prefer 1σ confidential intervals of 68.3 % instead of 2σ values to take account for these inaccuracies.

Marine calibration was carried out for nine samples (Table 4.2) which were identified based on their high $\delta^{13}C$ values ranging between -15.1 and 1.2 ppm. Three marine samples were identified as plant remains, mostly seaweed, while six samples refer to biogenic marine carbonate (mainly articulated shells from *Scrobicularia* spp.). Articulated specimens died *in situ* or during, respectively shortly after, their deposition after transported alive (Reimer & McCormac 2002, Donato et al. 2008, Faivré et al. 2005). In contrast to aquatic plants and molluscs, terrestrial samples were calibrated using the intcal13 dataset (Reimer et al. 2013).

Radiocarbon dating resulted in an age spectrum reaching from the late Pleistocene (KOR 38A/PR1) to modern times (KOR 23/15 HR). However, some samples must not be regarded as reliable as they produce age-inversions. The main reason for age inversions can be ascribed to reworking effects. Charcoal samples KOR 35A/HK1, KOR 35A/HK2, KOR 35A/HK3 and KOR 35A/HK4, for example, were found in B.2 peripheral harbour mud between 0.06 m a.s.l. and 0.18 m a.s.l. and date uniformly to the 8th to 5th cent. BC. However, two Hellenistic to Roman ceramic sherds at the base of the same layer, provide younger *termini ad* or *post quos* (maximum ages) for the harbour sediments and prove, that the charcoal samples are reworked. It is likely that the pieces of charcoal were brought in as waste by man (e.g. Marriner & Morhange 2007).

Reworking processes are also a known phenomenon associated to high-energy tsunami inundation where a complex synergy between erosional and depositional processes takes place. During such events, older allochthonous deposits may be reworked and deposited next to autochthonous sediments, for example in the form of rip-up clasts; by erosion high-energy impacts may as well produce considerable hiatuses (Goff et al. 2001). Therefore, samples extracted from high-energy layers (KOR 23/13+ PR, KOR 29/10 HR, KOR 29/11 M2, KOR 29/16 M, KOR 29/19+ M, KOR 29/26 M, KOR 29/32 M, KOR 32A/PR2, KOR 38A/PR1, KOR 38A/PR2 and KOR 38A/PR8) must be considered as potentially reworked and only yield maximum ages (*termini ad* or *post quos*). Sample KOR 38A/PR1 extracted from a high-energy layer at 2.77 m b.s. and yielding an age of 15,845-15,031 cal BC, for example, mirrors reworking processes that affected late Pleistocene deposits. Furthermore, sample KOR 23/15 HR is considered to represent a root due to its modern age of 1677–1940 cal AD.

4.5.4 Palaeogeographical evolution and harbour development at the Desylla site

Based on sedimentary, geochemical and palaeontological results, we were able to decipher the palaeoenvironmental evolution of the Desylla site (Figure 4.13). Initially, shallow marine conditions representing an open marine inner-shelf system with normal marine salinity and temperate to warm water temperatures characterised the site, marked by associated sublittoral sands retrieved at the base of all vibracores except in vibracore KOR 36. These mid-energy conditions turned into a more sheltered littoral system where water exchange and wave influence were distinctly restricted. Radiocarbon sample KOR 35A/PR3, recovered from the base of littoral A.2 sands in vib-

Table 4.2: Radiocarbon dates.

Sample ID	Depth [m b.s.]	Depth [m a.s.l.]	Sample material	Lab. No. [MAMS]	$\delta^{13}C$ [ppm]	^{14}C age [BP]	1σ age [cal BC/AD]	2σ age [cal BC/AD]
KOR 23/13+ PR[d]	3.53	-1.44	unident. plant rem.	19774	-22.1	5848 ± 23	4767; 4690 BC	4789; 4620 BC
KOR 23/15 HR[d]	3.75	-1.66	wood remain (root)	19775	-31.4	151 ± 18	1677; 1940 AD	1669; 1945 AD
KOR 23/19+ HR	4.62	-2.53	wood remain	19776	-38.5	5417 ± 22	4328; 4261 BC	4333-4245 BC
KOR 23/30+ PR	7.84	-5.75	unident. plant rem.	19777	-25.3	6766 ± 25	5704; 5639 BC	5715-5632 BC
KOR 29/10 HR[c, d]	1.60	-1.39	unident. plant rem.	24903	-26.1	2935 ± 21	1207; 1112 BC	1211-1055 BC
KOR 29/11 M2[c, d]	1.68	-1.47	*Scrobicularia* sp.[b]	24904	1.2[a]	3228 ± 21	1131-1037 BC	1187-1001 BC
KOR 29/16 M[c, d]	2.58	-2.37	*Scrobicularia* sp.[b]	24905	-2.4[a]	4652 ± 26	2951-2876 BC	3004-2863 BC
KOR 29/19+ M[c, d]	3.59	-3.38	*Scrobicularia* sp.[b]	24906	0.8[a]	6045 ± 25	4544-4463 BC	4599-4438 BC
KOR 29/26 M[c, d]	6.12	-5.91	*Scrobicularia* sp.[b]	24907	1.0[a]	7017 ± 26	5597-5531 BC	5616-5493 BC
KOR 29/32 M[c, d]	7.73	-7.52	undetermined shell[b]	24908	-1.6[a]	7494 ± 26	6031-5974 BC	6067-5929 BC
KOR 29/37 M[c]	9.2	-8.99	*Scrobicularia* sp.[b]	24909	0.3[a]	7695 ± 27	6252-6160 BC	6310-6098 BC
KOR 32/22 PR	3.44	-1.93	olive stone	24910	-28.7	2230 ± 21	364;213 BC	379;206 BC
KOR 32A/HK4	0.86	0.65	charcoal	26454	-27.4	221 ± 24	1651; 1950 AD	1644; 1950 AD
KOR 32A/PR2[d]	2.45	-0.94	seaweed	26455	-14[a]	4258 ± 29	2467-2369 BC	2523; 2303 BC
KOR 32A/PR3	2.72	-1.21	unident. plant rem.	26456	-27.7	1964 ± 27	7; 69 AD	40 BC-85 AD
KOR 32A/HR	2.78	-1.27	wood remain	26457	-29.8	1936 ± 27	27; 117 AD	7-127 AD
KOR 35A/HK1[d]	1.57	0.18	charcoal	26458	-27	2439 ± 28	730; 430 BC	751; 408 BC
KOR 35A/HK2[d]	1.65	0.10	charcoal	26459	-30	2536 ± 28	793; 591 BC	797; 547 BC
KOR 35A/HK3[d]	1.68	0.07	charcoal	26460	-25.7	2546 ± 28	796; 593 BC	799; 550 BC
KOR 35A/HK4[d]	1.69	0.06	charcoal	26461	-27.9	2553 ± 28	798; 597 BC	801; 554 BC
KOR 35A/PR1	2.52	-0.77	seaweed	26462	-15.1[a]	2752 ± 27	574-430 BC	662-396 BC
KOR 35A/PR2	2.66	-0.91	unident. plant rem.	26463	-29.6	2504 ± 28	768; 554 BC	786; 540 BC
KOR 35A/PR3	2.79	-1.04	unident. plant rem.	26464	-29.6	2479 ± 27	755; 542 BC	771; 489 BC
KOR 38A/PR1	2.77	0.61	unident. plant rem.	24915	-71.9	14280 ±140	15629-15233 BC	15845-15031 BC
KOR 38A/PR2[d]	4.48	-1.10	unident. plant rem.	24920	-7.3[a]	5458 ± 24	3940;3845 BC	3952-3797 BC
KOR 38A/PR4[d]	4.91	-1.53	unident. plant rem.	24916	-27.1	5246 ± 26	4144;3988 BC	4226;3976 BC
KOR 38A/PR7	7.35	-3.97	unident. plant rem.	24917	-33.3	6253 ± 28	5296;5216 BC	5312;5080 BC
KOR 38A/PR8	8.5	-5.12	unident. plant rem.	24918	-30.8	6787 ± 29	5713-5662 BC	5724-5638 BC
KOR 38A/PR9	9.86	-6.48	unident. plant rem.	24919	-25.6	6957 ± 29	5883-5796 BC	5964;5745 BC

Note: All dates are calibrated using Calib 7.1 (Stuiver & Reimer, 1993; Reimer et al., 2013). b.s. – below ground surface. a.s.l. – above sea level. – Klaus-Tschira Laboratory of the Curt-Engelhorn-Centre Archaeometry gGmbH Mannheim, Germany. 1σ/2σ age – calibrated ages related to 1σ confidential interval (68.3 %) or 2σ confidential interval (98.4 %). ";"– several possible age intervals due to multiple intersections with the calibration curve. unident. plant rem. – unidentified plant remains. [a] – marine sample, calibrated by using the marine13 calibration dataset with an average reservoir age of 405 years (Reimer et al. 2013). [b] – all samples of biogene carbonate were extracted from articulated specimens. [c] – for detailed lithostratigraphical information of vibracore KOR 29 please see Fischer et al. (2016a). [d] – ages of marked samples are considered as not reliable due to reworking processes (maximum ages) or intrusion of modern roots (minimum ages). See text for further explanations.

racore KOR 35A, implies that the transition towards a more protected marine system happened at or slightly before 755–542 cal BC (Table 4.2). This age correlates with the age of a strong wall section excavated between vibracoring sites KOR 34A and KOR 35A that was dated by the excavators to Archaic to Hellenistic times (section4.2.2; Andreadaki-Vlazaki 2012). We therefore assume that by the construction of the wall and associated harbour infrastructure (e.g. breakwaters) the former open marine system was extensively shielded and protected from wave influence. Corresponding

Table 4.3: Archaeological age estimates for diagnostic ceramic fragments found in the study area

Sample ID	Depth [m b.s.]	Depth [m a.s.l.]	Sample description	Age estimation
KOR 23/4+ K	1.45	0.64	undetermined	ancient
KOR 31/9+ K	1.39	0.12	undetermined	Roman
KOR 35/9 K	1.98	-0.23	handle of amphora (fragment)	Hellenistic to Roman
KOR 35A/K1	1.76	-0.01	fragment of amphora	Hellenistic to Roman
KOR 35/13 K	2.48	-0.73	fragment of cup	6th to 5th cent. BC
KOR 36/1 K	0.73	0.86	undetermined	Byzantine?
KOR 36/4 K	1.60	0.01	undetermined	Roman, after 2nd cent. AD
KOR 38A/K1	2.68	0.70	fragment of bowl	Hellenistic or Roman

A.2 sediments may therefore be related to an Archaic pre-harbour which was not fully separated from marine influences according to the prevailing sandy grain size.

By the establishment of lagoonal deposits, revealed in vibracores KOR 31A, 32A and 34A, a clear change from slightly protected pre-harbour conditions towards a low-energy harbour milieu is documented. This harbour was in use at least since the 4th to 3rd cent. BC, as sample KOR 32/22 PR provides a *terminus ante quem* of 364–213 cal BC (Table 4.2). During the same time, harbour conditions were also reconstructed for the Pierri site (Finkler et al. 2017b). However, in contrast to the area around Pierri, the harbour area at Desylla was continuously used until at least the 1st cent. AD. This is attested by sample KOR 32A/PR3 yielding a *terminus post quem* for the abandonment of the harbour, namely 7–69 cal AD (Table 4.2).

At vibracoring site KOR 32A the Desylla harbour basin reaches down to approximately 2 m b.s.l., but shows decreased water depths towards the northwest according to ERT results (Figure 4.6). The water level in the 4th to 3rd cent. harbour can be derived from the Pierri site where a bioconstruction band was found adhered on the harbour's quay wall providing a reliable estimate for the Classical/Hellenstic water level of approx. 0.21 to 0.03 m b.s.l. (Finkler et al. 2017b, see dashed line in Figure 4.14). This relative sea level was caused by both, eustatic sea level rise since the Pleistocene and local crustal movements triggerd by tectonic events (Finkler et al. 2017b; see for example Anzidei et al. 2014, Mastronuzzi & Sansò 2014, Sansò et al. 2017). Regarding the Desylla harbour, the Classical/Hellenistic water level indicates a maximum depth of approximate 2 m in its central area for this period of time. This depth was most likely obtained by dredging activities.

Regarding the extent of the Desylla harbour, corresponding harbour sediments could not be found in vibracore KOR 35A; here, B.2 harbour mud dates to the Roman period or later. While harbour sediments were deposited further to the southeast, slightly marine conditions were prevalent at site KOR 35A. This indicates that the long, thick wall section encountered to the east of the coring site (section 4.2.2) may represent the western delimitation of the Classical/Hellenistic harbour basin. This is supported by the stratigraphical record at vibracoring site KOR 34A where B.2 harbour sediments mirror a peripherical zone of the harbour with strongly decreased depths

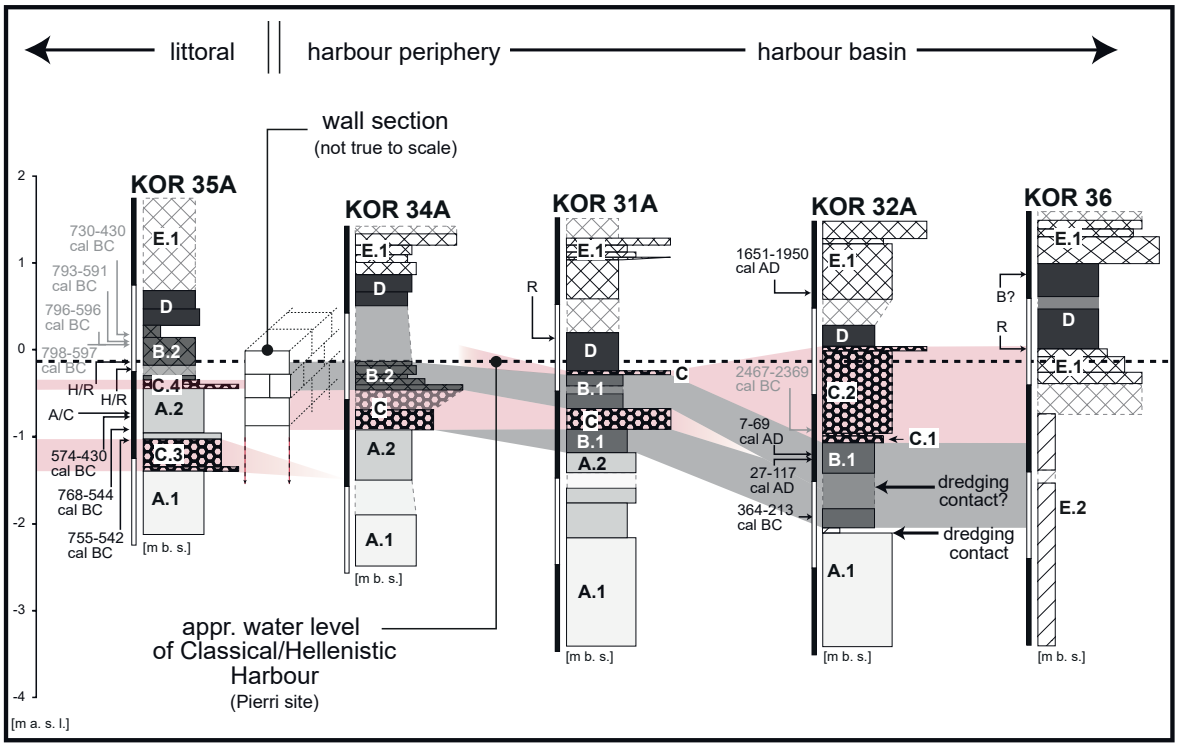

Figure 4.13: Cross-section of vibracores drilled at the Desylla site with simplified facies pattern and radiocarbon ages. Ages not considered for interpretation are depicted in grey (see section 4.5.3 for further explanations). Legend according to Figure 4.4. Sea level reconstruction for Pierri Harbour based on radiocarbon dating of sea level indicators (see section 5.3 and Finkler et al. 2017b). A thick wall excavated between vibracoring sites KOR 34A and KOR 35A marks the western delimitation of the harbour basin which was found c. 2 m deep at site KOR 32A. Shallow marine conditions prevailed at site KOR 35A beyond the wall. Event layers of Pre-Archaic, Classical/Hellenistic and Roman age are included in the Desylla record.

and considerable input of waste and cultural debris. Further towards the southeast, the sedimentary record at site KOR 36 may comprise another wall structure in the form of E.2 stones and gravel, stratigraphically consistent with harbour deposits in vibracores KOR 32A and KOR 31A. Given the fact that the upper surface of this wall correlates with the approximate water level of the 4th to 3rd BC harbour, one may speculate that this wall may be part of a harbour-intern wall system, subdividing the harbour basin into different sections. At least for the central part of the basin such subdivisions are indicated by ERT depth sections (Figure 4.6) showing solid blocks in between harbour deposits found at vibracoring sites KOR 31A and KOR 32A. However, archaeological research is needed to check this hypothesis.

The harbour at the Desylla site was finally subject to considerable silting processes, as documented by semi-terrestrial deposits found on top of harbour mud. According to ceramic sherds KOR 36/4 K and KOR 31A/9+ K (Table 4.3) silting happened to or shortly after Roman times. By this time, the potential delimitating walls were no longer in function but buried under younger deposits. At vibracoring site KOR 35A, a shallow lagoon of few decimetres depth developed where shallow marine conditions existed before. Later, these lagoonal sediments are followed by semi-terrestrial conditions. Ceramic samples KOR 35/9K and KOR 35A/K1 (Table 4.3) show that the lagoon still existed during Hellenistic/Roman times; a charcoal sample suggesting an Archaic age represents

reworking. Finally, the site was covered by anthropogenic sediments, most likely during or after the Byzantine period as indicated by sample KOR 36/K1 yielding a possibly Byzantine age (Table 4.3).

The Desylla transect comprises at least three generations of tsunami layers that were trapped in the harbour geoarchives (Figure 4.13). A first possible event happened before 755–542 cal BC (KOR 35A/PR3, Table 4.2) and is mirrored by subunit C.3 found in vibracore KOR 35A. However, the event layer marks the contact between fully marine A.1 sands and protected A.2 sands; it cannot be excluded that the layer is related to anthropogenic displacement of material during construction works associated with the excavated wall. Yet, sedimentary features such as a sharp basal contact and a fining upward in grain size rather suggest the impact of an extreme wave event. Additionally, a combination of both processes is possible as well. However, as no further chronological and sedimentological data are available for this event, its origin and exact time frame cannot be completely clarified.

In contrast, substantial conclusions can be made for a later event that hit the Desylla site as evidenced by high-energy layers found below and in between harbour deposits in vibracores KOR 31A, KOR 34A and KOR 35A. The event can be dated to younger than 574–430 cal BC and older than Hellenistic/Roman times based on samples KOR 35A/PR1 and KOR 35/9 K, respectively (Table 4.2 , Table 4.3). It is most likely that this impact is identical with the local earthquake and subsequent tsunami traces of which were at the rescue excavation at the eastern shore of the Chalikiopoulou Lagoon as well as in the harbour record at the Pierri site which could be dated to the 4th to 3th cent. BC (see Figure 4.1 and Figure 4.9; section 4.5.2).

Another tsunami hit the harbour after the 1st cent. AD, namely after 7–69 cal AD (KOR 32A/PR3) and 27–117 cal AD (KOR 32A/HR; Table 4.2). Due to this impact, a thick sequence of reworked harbour mud (layer C.1) and reworked sublittoral sands (layer C.2) filled the harbour basin at site KOR 32A. As both tsunami-related subunits C.1 and C.2 represent discrete sequences, each showing a basal erosional contact, they might represent two subsequent tsunami waves. Similar traces were detected in the sequence of vibracore KOR 31A as well. Furthermore, radiocarbon age of sample KOR 32A/HK4 functions as *terminus ante quem* for the tsunami impact, so that the event can be dated to the time before 1651–1950 cal AD. After tsunami impact and considerable infill of the harbour basin, the site was not used as a harbour anymore and, consequently, silted up gradually. Diagnostic ceramics fragments dated to Roman times (KOR 31/9+ K and KOR 36/4 K) collected in associated semi-terrestrial sediments as well as a possibly Byzantine ceramic sherd (KOR 36/1 K) found right below overlying anthropogenic deposits, support the idea, that the event happened already during Roman times.

4.5.5 Reconstructing the overall development of Corcyra's northern harbour zone

Sedimentary records from the presented study sites allow to draw conclusions on the general palaeoenvironmental development in the environs of the Analipsis Peninsula and the ancient harbours of Corcyra (Figure 4.14). We compared our results with data already published, namely with vibracore KOR 29 drilled at the northern fringe of the Chalikiopoulou Lagoon (Fischer et al. 2016a), vibracore KOR 1A drilled in the Roman Alkinoos Harbour (Finkler et al. 2017a) and vibracore KOR 37A drilled right in front of the Pierri quay wall that belonged to a Classical/Hellenistic harbour (Finkler et al. 2017b; for location of vibracoring sites see Figure 4.2 A).

Considerable palaeoenvironmental changes in the surroundings of the Analipsis Ridge happened already during the 6th mill. BC. At vibracoring site KOR 23, lagoonal conditions turned into mid-energy shallow marine conditions around 5704–5639 cal BC (sample KOR 23/30+ PR, Table 4.2). Hence, at this time, the Analipsis Peninsula was separated from the rest of the island by a shallow marine embayment (Figure 4.14 A). However, low-energy lagoonal conditions were still existing at vibracoring site KOR 29. We therefore suggest that a small beach barrier system existed between vibracoring sites KOR 23 and KOR 29 and separated a shallow marine environment in the east from the predecessor of the Chalikiopoulou Lagoon in the west. Regarding the trigger for changing palaeogeographies during the 6th mill. BC, we point to high-energy deposits encountered at site KOR 29. We interpret them as evidence of tsunami impact and hypothesize that tsunami waves breached and destroyed the former coastal barrier that, so far, had protected the stadium area around vibracoring site KOR 23 from littoral processes. This event (event I, Figure 4.14 B) is also documented in vibracore KOR 29 as high-energy layer at approximately 6 m b.s.l. An articulated specimen of Scrobicularia sp. (KOR 29/26 M, Table 4.2) collected from the event layer provides a maximum age of 5597–5531 cal BC. Additionally, plant remains retrieved from vibracore KOR 38A (samples KOR 38A/PR8 and KOR 38A/PR7, Figure 4.14) provided a *terminus ad* or *post quem* of 5713–5662 cal BC and a t*erminus ante quem* of 5296–5216 cal BC for the event. Thus, the event must have happened at or after 5600 BC (maximum age, KOR 29) and 5200 cal BC. Due to its position in a narrow between the Analipsis Peninsula and Corfu's mainland no impact-related sediments were accumulated at vibracoring site KOR 23 as maximum flow velocities during tsunami landfall cause erosion and reworking at this site instead. The latter is indicated, for example, by radiocarbon sample KOR 23/30+ PR which we retrieved from the base of the shallow marine sands in KOR 23 and which provided an age slightly too old. Tsunami traces of the same age were found in various geoarchives in adjacent regions of Corfu Island, for example in the Sound of Lefkada (Vött et al. 2009b), the Bay of Aghios Nikolaos (Vött et al. 2009a, 2009b), the Lixouri coastal plain on Cefalonia Island (Willershäuser et al. 2013) and the harbour site of ancient Olympia, Pheia (Vött et al. 2011b).

It seems as if in the 4th mill. BC, the barrier system was abruptly shifted further to the east forming a wider isthmus between the Chalikiopoulou Lagoon and the Bay of Garitsa. We assume that this rapid shift was associated with another tsunami event (event II, Figure 4.14) documented by a thick event layer of first reworked lagoonal sediments followed by allochthonous sands in

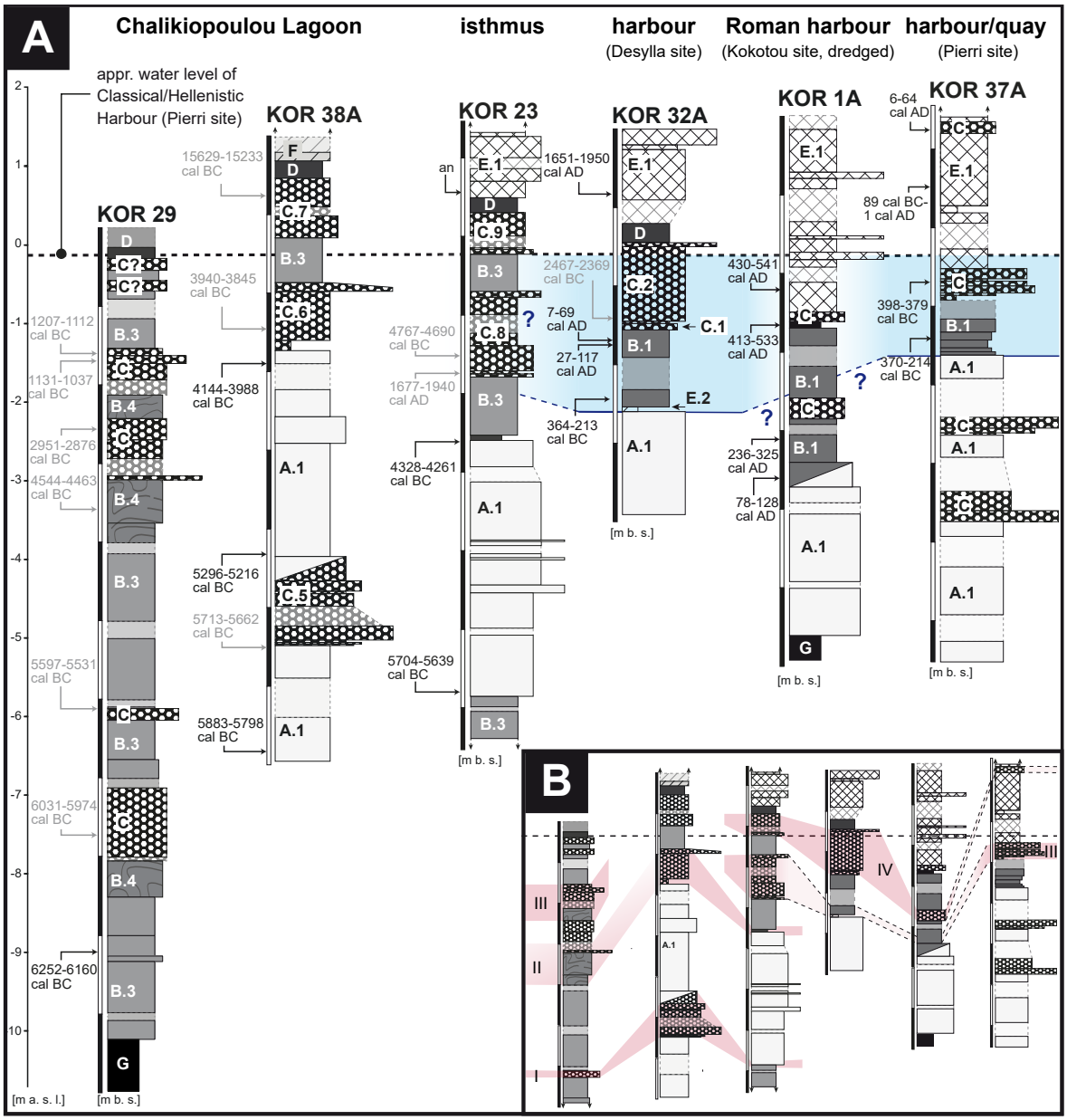

Figure 4.14: (A) Cross-section of selected vibracores from the surroundings of ancient Corcyra. Vibracores KOR 23, 32A and KOR 38A are complemented by vibracores from the Roman Alkinoos Harbour (Finkler et al. 2017a), the Pierri quay wall site (Finkler et al. 2017b) and the northern fringe of the Chalikiopoulou Lagoon (Fischer et al. 2016a). Radiocarbon ages not considered for interpretation are depicted in grey (see section 4.5.3 for further explanations). Harbour sediments dating to Classical and younger times (shaded in blue) can be traced from the Pierri quay wall in the east to the Desylla site in the west. Dredging contacts (solid blue lines) document the efforts to keep the harbour navigable. (B) Impact of a pre-historical teletsunamis, a locally triggered Classical-Hellenistic tsunami and the 365 AD teletsunami can be traced all over the area. Consistent stratigraphic layers are shaded in pink colour.

vibracore KOR 29 (Figure 4.14 A). The enormous thickness of this layer indicates formation by repeated event impact which is mirrored by radiocarbon ages ranging from the 4th to 1st mill. BC (Figure 4.14, Table 4.2). However, an articulated bivalve was collected from the very bottom of the reworked lagoonal mud yielding an age of 4544–4463 cal BC (KOR 29/19+ M, Table 4.2) and thus indicating a maximum age for tsunami event II of *c.* 4500 BC. Another age approximation is given by vibracore KOR 38A (Figure 4.7), where shallow marine sands are followed by a layer of reworked marine sands, which were dated to the time after 4144–3988 cal BC (KOR 38A/PR4,

Table 4.2). A reworked remain of an unidentified plant (KOR 38A/PR2, Table 4.2) further yields a *terminus ad* or *post quem* of 3940–3845 cal BC for this tsunami event. Similar to event I, we suggest that event II caused major palaeoenvironmental changes at vibracoring site KOR 23. Here, the open shallow marine system was cut-off and transformed into a protected lagoonal system at some point in time after 4328–4261 cal BC (KOR 23/19+ HR, Table 4.2). This might be related to the accumulation of event deposits at the seaward side of vibracoring site KOR 23 shielding the area behind from further wave influence, or to co-seismic uplift. Willershäuser et al. (2013) found traces of earthquake related uplift of *c.* 1 m in the Gulf of Argostoli on Cefalonia that occurred around 3950–3750 BC. Event II of the present study, dating to a point in time at or after 3900 BC, correlates well with this age.

Subsequently, a low-energy lagoon established at vibracoring site KOR 23, well-protected from wave-influence of the Bay of Garitsa. This lagoon is documented by thick homogenous lagoonal mud in vibracore KOR 23, while open-marine conditions are still mirrored by associated sands in vibracores KOR 1A, 32A and 37A, located to the seaward side of this barrier system.

Sedimentary records from the Pierri (KOR 37A; Finkler et al. 2017a) and the Desylla sites show that the Alkinoos Harbour was developed out of this shallow marine environment at least during Classical times, most probably by the construction of protective infrastructure such as breakwaters (Figure 4.15 A). The Classical harbour basin covered the area between the Desylla site and the Kokotou shipsheds. Furthermore, the Pierri quay wall and associated harbour infrastructure were in use at least since the 4th to 3rd cent. BC; however, it still has to be clarified whether or not these sites were connected to one large harbour zone associated to the harbour sequences and infrastructures revealed at the Desylla and Pierri sites. For the northern part of the Chalikiopoulou Lagoon, vibracore KOR 29 documents lagoonal conditions in a back-beach position. Lagoonal mud in a similar elevation was also found in core KOR 23 at the stadium site.

Our results show that Corfu's harbour infrastructure became subject to tsunami wave impact during Classical times (event III, Figure 4.14 B, Figure 4.15 B). Associated layers found in vibracores recovered from the Desylla site (Figure 4.13) imply that the event happened after 574–430 cal BC and before the Hellenistic/Roman Period based on samples KOR 35A/PR1 and KOR 35/9 K, respectively (Table 4.2, Table 4.3). These age estimates correlate well with archaeoseismological findings from the rescue excavation (Tennis site) on the eastern shore of the Chalikiopoulou Lagoon (Figure 4.9) where event impact could be dated to the time between the Classical and Hellenistic periods, and with findings by Pirazzoli et al. (1994) and Mastronuzzi et al. (2014) who found strong co-seismic movements for this period on the western coasts of Corfu. For the Pierri site, Finkler et al. (2017b) found evidence for strong co-seismic uplift and subsequent tsunami inundation dated to the Classical to Hellenistic Period, most likely to the time between the 4th and 3rd cent. BC (Finkler et al. 2017b). According to our findings, first co-seismic uplift took place, causing considerable decreasing water depths in the ancient harbours and adjacent lagoons. Shortly after, tsunami waves arrived at the Bay of Garitsa, from where they proceeded to the south. We assume that tsunami waves also inundated the Chalikiopoulou Lagoon from its southern entrance in SE-NW

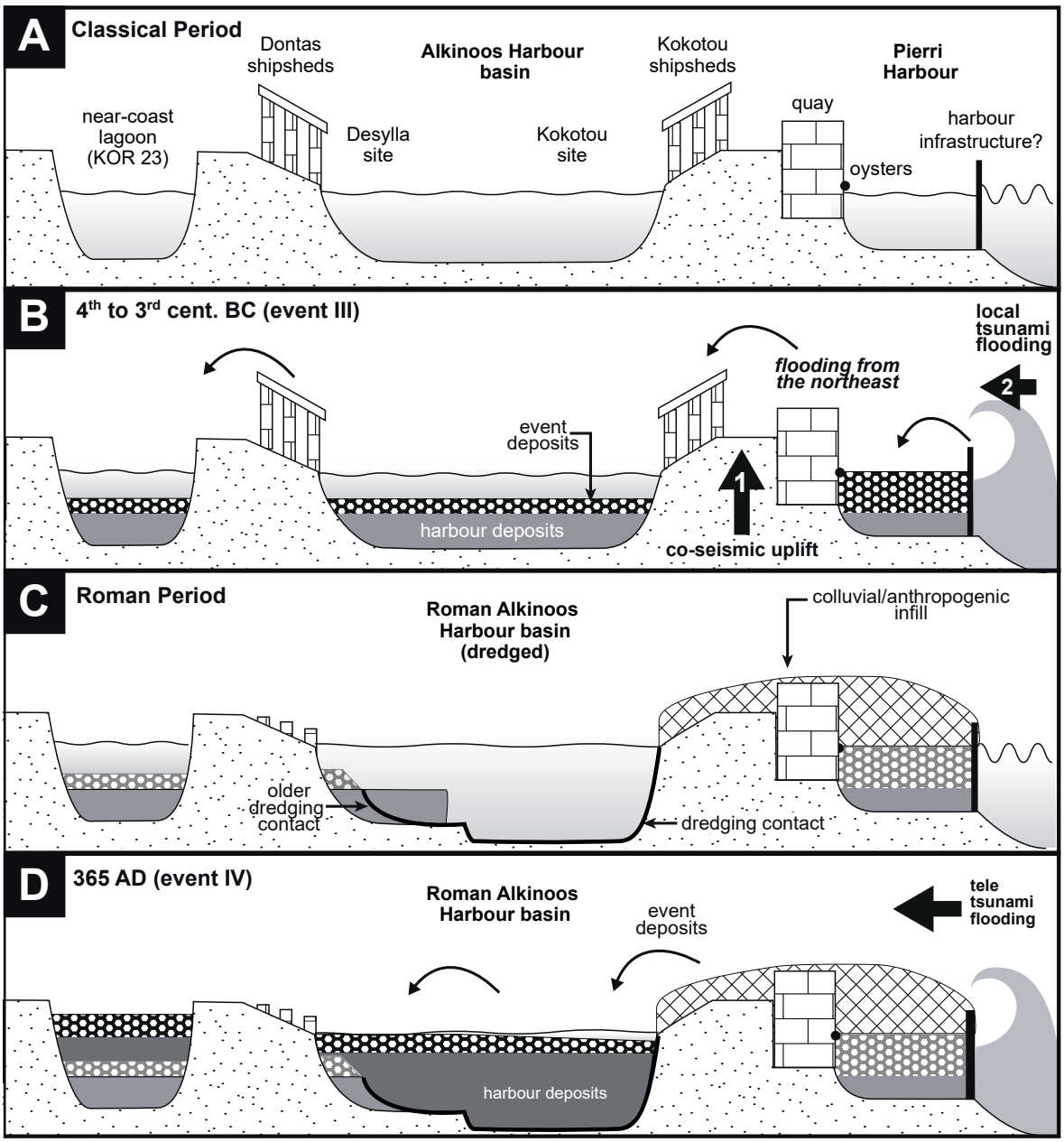

Figure 4.15: Schematic palaeoenvironmental development of ancient Corcyra and its harbours. (A) During the Classical period the Alkinoos Harbour extended from the Desylla site in the northwest towards the Kokotou shipsheds in the southeast and the Pierri quay towards the present coastline. (B) Triggered by a local earthquake, co-seismic uplift occurred between the 4th and 3rd cent. BC (event III) leading to decreased water depth within the harbour basins and natural lagoons. A subsequent tsunami hit the Bay of Garitsa filling the harbour basins with event deposits and breaching the barrier system at vibracoring site KOR 23. (C) During Roman times, a part of the former Alkinoos Harbour was dredged and re-used, while the Pierri site was buried under colluvial and anthropogenic infill. (D) Between the 3rd and early 6th cent. AD, most probably in 365 AD, a supraregional teletsunami hit Corcyra (event IV), leaving thick event deposits in the Roman harbours and lagoons (Finkler et al. 2016a).

direction leading to the deposition of contemporaneous allochthonous littoral sands at vibracoring site KOR 29 (Fischer et al. 2016a).

After event III, the harbours were abandoned (Pierri site) or subject to progressive silting and decreased water depths (Desylla and Kokotou sites). During the Roman period, the Pierri quay wall was buried under anthropogenic and colluvial material. At the same time, extensive dredging activities were undertaken at the Kokotou site and most likely at the Desylla site to reuse the inner part of the Alkinoos Harbour and to regain its full navigability (Figure 4.15 C). As documented by vibracore KOR 1A, Classical harbour sediments were entirely removed at the Kokotou site by dredging in order to obtain a harbour basin with at least 2 m water depth (Figure 4.14; see also Finkler et al. 2017a).

Another tsunami event hit Corfu during the Roman period (event IV, Figure 4.15 D). According to results retrieved from the Desylla site, this event occurred after the 1st cent. AD, namely after 7–69 cal AD (KOR 32A/PR3) and 27–117 cal AD (KOR 32A/HR; Table 4.2), but before modern times (1651–1950 cal AD; KOR 32A/HK4). At the Kokotou site (KOR 1A), radiocarbon dating of a stratigraphically consistent layer provides a time window between the late 3rd and the early 6th cent. AD for the event (Figure 4.14; for further explanations see Finkler et al. 2017a). This correlates well with the earthquake in 365 AD on Crete that triggered a teletsunami affecting wide parts of the Mediterranean and reaching remote parts as far away as the Adriatic Sea (Shaw et al. 2008). In a supraregional context, the event had major effects on the coasts of the Ionian Sea (Vött et al. 2006, 2009a, May et al. 2012a) and Sicily (Smedile et al. 2011, De Martini et al. 2012). After event IV, only the Kokotou site was further used as a harbour but was soon abandoned due to reduced water depth and ongoing silting processes (Finkler et al. 2017a).

4.6 Conclusions

The main objective of this study was to reconstruct the palaeoenvironmental evolution and the comprehensive harbour development in the environs of the Analipsis Peninsula, where the ancient city of Corcyra developed since Archaic times. A multi-methdological approach comprising sedimentological, geochemical and microfaunal methods was applied based on vibracores drilled in the area of the former Desylla factory and two further vibracores located at geomorphological key sites. These results were supplemented by data from geophysical prospection and archaeoseismical studies. The following main conclusion can be made:

i. It was possible, for the first time, to locate and assess the extent and perimeter of the Classical Alkinoos Harbour based on sedimentary evidence. It extended from the Desylla site in the northwest to the Kokotou site in the southeast. If the Pierri site harbour infrastructure was also part of a larger Alkinoos Harbour basin during the 4th to 3rd cent. BC is uncertain and needs to be clarified by further geoarchaeological research and fieldwork. The topographical relationship between the Kokotou and Pierri harbour sites remain conjectural as well. In the Roman period, however, only a part of the 4th to 3rd cent. harbour basin was dredged and re-used as a harbour while the Pierri Harbour infrastructure had already been abandoned.

ii. The Desylla harbour developed out of an open marine system by the construction of a strong wall section at or slightly before 755–542 cal BC giving rise to an Archaic pre-harbour that was only slightly protected. During the 4th to 3rd cent. BC at the latest, according to the existing radiocarbon data set, this pre-harbour was transformed into the protected Alkinoos harbour.

iii. Apart from human impact, the overall evolution of the Gulf of Corfu is strongly linked to the repeated influence of extreme wave events. Considering oceanographic characteristics of the northern Ionian Sea and the geographical as well bathymetric settings of the Gulf of Corfu itself, storms can be excluded as triggers. Instead, sedimentary, geochemical and micropalaeontological evidence of high-energy inundation are ascribed to tsunami impact. Strong earthquakes and tsunamis repeatedly hit the island of Corfu as reported by historical accounts while, for the Gulf of Corfu, historical information on destructions by extreme storms is not existing.

iv. Event-geochronostratigraphical data document four different palaeotsunami events for the study area. Event I took place between 5600 and 5200 cal BC, event II at or after 3900 BC, event III in the 4th to 3rd cent. BC and event IV between the 3rd and early 6th cent. AD.

v. Tsunami event I led to major environmental changes by partly breaching and translocating the narrow isthmus that existed between the Analipsis Ridge and the rest of Corfu Island by this time. Event II triggered the relocation of the isthmus to the east. From a geochronological point of view, both events correlate well with known seismic events and tsunami traces found along the shores of the Ionian Sea suggesting a remote origin for tsunami events I and II.

vi. Event III strongly affected the ancient harbours of Corfu and could be associated to a local earthquake. Co-seismic uplift and subsequent tsunami inundation, hit the Bay of Garitsa and the Alkinoos Harbour. After event III the Pierri quay wall was out of function due to uplift and siltation. The Desylla and Kokotou harbour basins were dredged and re-used.

vii. Based on geochronostratigraphical data tsunami event IV can be related to the earthquake and tsunami that hit Crete on 12 July 365 AD and which is known to have affected large parts of the eastern Mediterranean. Tsunami impact on the shores of the Gulf of Corfu is thus associated to teletsunami dynamics hitting the ancient city and leaving distinct traces in the records of the Chalikiopoulou Lagoon and the Alkinoos Harbour. The latter progressively silted after the event and finally lost its functionality.

5 Synthesis and conclusion

The present study aimed to decipher the harbour geoarchives of ancient Corcyra, once a powerful thalassocracy in the Mediterranean Sea in Archaic to Hellenistic times. Geoarchaeological research was carried out at three study sites were archaeological remains indicate a nearby harbour basin or associated infrastructure. In particular, the broader area around excavated Classical shipsheds (Kokotou site, chapter 2), the sedimentary record around the Pierri quay wall (chapter 3) and the former Desylla factory ground (chapter 4) were investigated by geoscientific, micropalaeontological and geophysical methods. These sites were complemented by geoarchaeological studies on ancient building structures located on the eastern shore of the Chalikiopoulou Lagoon as well as three geomorphological key sites, essential for the understanding of the palaeoenvironmental evolution of ancient Corcyra (chapter 4).

In the following, the results of these study sites will be compiled and linked to each other to present a synoptic view on the late Holocene palaeoenvironmental history of Corcyra in terms of its ancient harbours and their development through space and time (chapter 5.1) as well as the impact of extreme events (chapter 5.2).

5.1 The harbours of ancient Corcyra – a synoptic view

5.1.1 The sedimentary record of Corcyra's ancient harbours in the Mediterranean context

By means of a geoarchaeological approach containing sedimentological, geomorphological, geochemical, geophysical and micropalaeontological methods the harbour geoarchives of ancient Corcyra were investigated in the frame of this study. Harbour deposits were identified by their silt-dominated grain size, high contents of organic material and specific geochemical signals, including reduced Ca values but increased Pb concentrations. These characteristics were found for many ancient Mediterranean harbours (e.g. Le Roux et al. 2005, Hadler et al. 2015, Stock et al. 2016) which show, apart from some minor variations, similar sedimentary and chronological features.

Based on previous geoarchaeological studies all over the Mediterranean (chapter 1.2) Marriner & Morhange (2006b) found sedimentary similarities between different harbour records and established the Ancient Harbour Parasequence (AHP, Figure 5.1 A). In general terms, the AHP marks the transition from natural mid-energy conditions towards anthropogenically modified environments influenced by modest sea-level fluctuations, sediment supply from the hinterland and event impact (Marriner et al. 2010, Anthony et al. 2014). Even if this typical harbour sequence might slightly vary in thickness and appearance, Marriner & Morhange (2006b, 2007) emphasise key facies belts and sedimentary features that they identified in harbour sequences (Figure 5.1 A): The lower boundary of the AHP is formed by the Maximum Flooding Surface reflecting the most landward position of the shoreline due to maximum marine incursion around 4000 BC. Following this

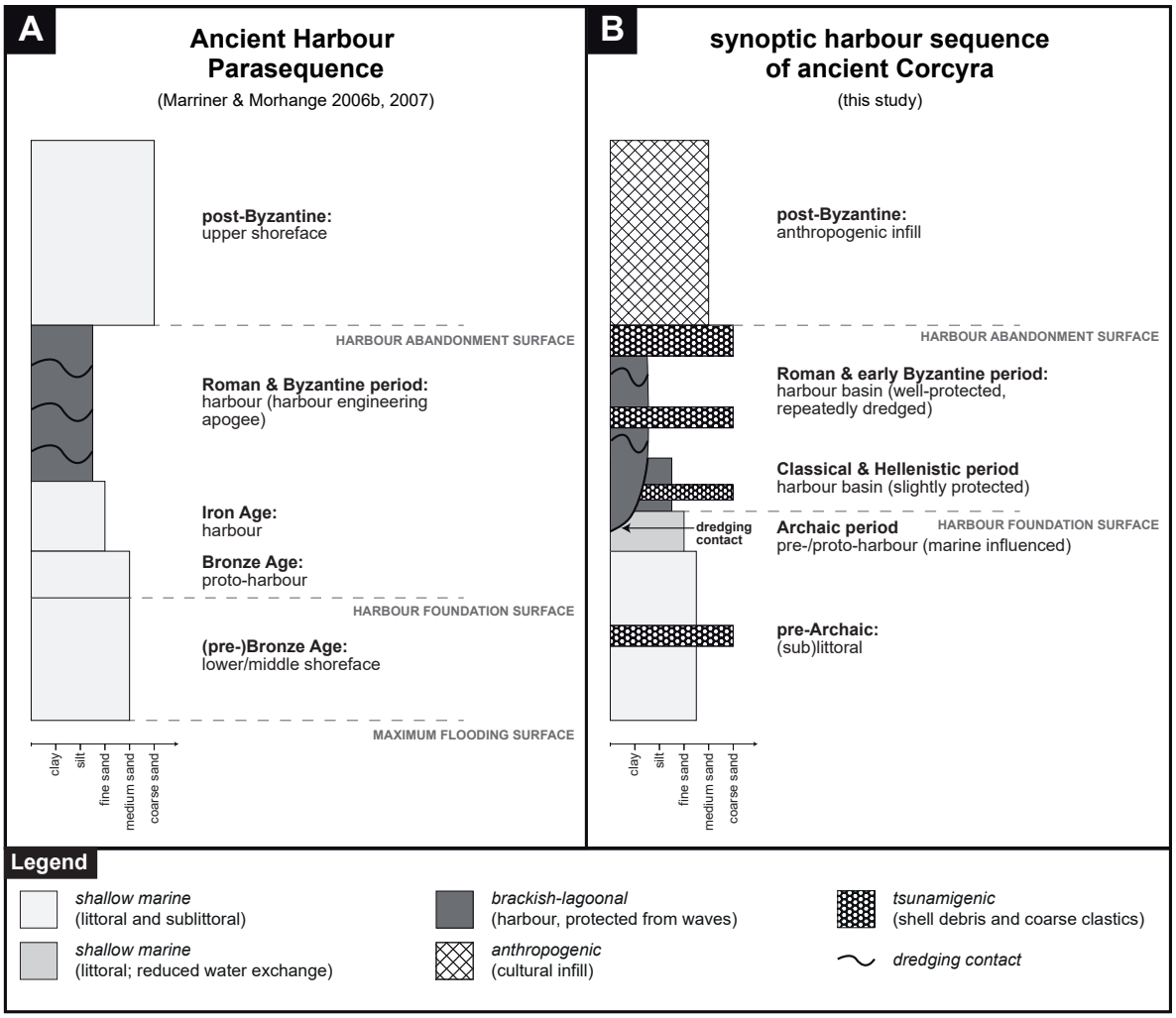

Figure 5.1: The harbour sequence of Corcyra in the Mediterranean context. (A) Lithostratigraphical features of the Ancient Harbour Parasequence deduced from general observed stratigraphic patterns in ancient Mediterranean harbours by Marriner & Morhange (2006b, 2007). (B) Synoptic and summarised harbour sequence of the ancient harbours of Corcyra based on the findings presented in this study.

surface, naturally aggrading sands of a lower to middle clastic shoreface occur that established during the Bronze Age or slightly earlier. Out of this mid-energy environment, Bronze Age proto-harbours were developed, following "*one of the most important stratigraphic surfaces in ancient harbour geology*", the Harbour Foundation Surface (Marriner & Morhange 2007). This sedimentary boundary marks initial human modifications of the natural environment, e.g. by the construction of artificial barriers in order to protect the beach from wave influence. Subsequently, grain size gradually changed towards smaller size. In particular, the fine sandy harbour deposits of the Iron age bear witness of ongoing human efforts to establish well-protected and quiescent harbour basins. The apogee of harbour engineering, however, can be dated to the Roman to Byzantine periods, where the use of concrete in a marine context was a true revolution in terms of harbour protection (Oleson & Hohlfelder 2011, see chapter 1.1). By this time, the transition from natural to artificial harbour basins was fully implemented mirrored by plastic harbour clays. Yet, large scaled protective infrastructure accompanied with naturally and anthropogenically forced sediment supply led to the silting of the harbour basins, a phenomenon which caused extensive Roman

dredging activities to keep the harbour navigable (Figure 5.1 A, chapter 1.2.3). Finally, the Harbour Abandonment Surface marks the semi or complete abandonment of the harbour basin due to siltation, coastal progradation, co-seismic movements or other catastrophic events. Thus, in post-Byzantine times the former harbour site was covered by sands of an exposed beach facies. The latter is related to the degradation of harbour infrastructure that formerly shielded the harbour basins from littoral dynamics (Marriner & Morhange 2006b, 2007).

Findings retrieved in the frame of the present study regarding the ancient harbours of Corcyra are in general accordance with these typical sedimentary patterns (Figure 5.1 B). Similar to the AHP, all harbour sequences found in the Corcyra records show sublittoral to littoral sands at their base mirroring a shallow marine environment since at least ~ 4000 BC. In some case (e.g. vibracores KOR 23, 38A or 25), these shallow marine sands were found on top of thick lagoonal sections mirroring that the littoral sands represent the most landward coastline (Maximum Flooding Surface; Marriner & Morhange 2006b). However, when taking a more detailed look on the synoptic harbour sequence of Corcyra some considerable differences have to be discussed.

A characteristic feature of the harbour sequence of Corcyra are coarse-grained clastic layers intersecting the basal (sub-)littoral deposits. These high-energy layers were found across all study sites of this work and are interpreted as multiple tsunami impact during Pre-Archaic times (see e.g. chapter 4.5.5).

Concerning the establishment of harbours out of the natural littoral system by the construction of artificial barriers such as breakwaters, first attempts of the Corcyreans may be reflected by littoral sands showing a reduced marine signal and representing thus a pre- or proto-harbour, slightly protected from marine dynamics (Figure 5.1 B). Yet, the associated sediments at the Desylla site are of Archaic age and do not date back to the Bronze Age like concurrent sediments found e.g. in harbour archives at the Levantine coasts (Marriner et al. 2014, Noureddine 2015, Knapp & Demesticha 2017). For the sites investigated on Corcyra, no pre-Archaic interventions of human societies in the natural coastal settings is documented in the sedimentary record, which is why it is most likely that ships were hosted on the beaches until the Archaic period – generally a widespread practice until at least Classical times (Oleson & Hohlfelder 2011).

Considering the overall sandy grain size, the pre-harbour of Corcyra cannot be classified as fully protected harbour basin but represent the initial and gradual transition from natural littoral systems towards the protected harbours of the Classical period. However, whether the harbour foundation surface is situated below or on top of these proto-harbour deposits is worthy to discuss. Of course, the establishment of harbours requires the construction of first rudimentary infrastructure – a pro-argument for placing the harbour foundation surface on the base of the proto-harbour sediments. Nevertheless, these sediments strongly resemble the underlying fully marine sands such that a differentiation solely based on sedimentary aspects is not possible. Following this, the harbour foundation surface must be located on top of the Archaic sands, where a clear boundary to the finer grained Classical harbour sediments is visible to the unaided eye. The fol-

lowing Classical harbours are dominated by considerable amounts of silt and components typical of closed harbour basins (ancient waste, organic material, ceramics). Due to still high amounts of (fine) sand, the associated sediments clearly show that the harbour basins were not fully enclosed but protected by advanced seaward barriers.

Related to the seismically exposed location of Corfu Island and the fact that Corcyra's ancient harbours were located in areas well protected from major storm influence, tsunami impact was found for the Classical and the Roman harbour basins as well (see e.g. the Pierri site record, chapter 3.5.5). Regarding the Roman time, the well-protected and enclosed basins functioned as efficient sediment traps for repeated tsunami impact. Similar to the AHP, dredging activities due to reinforced silting processes caused by seaward infrastructure and increased landward sediment supply are a main characteristic of the Roman harbour section of Corcyra. In particular, considerable parts of the pre-Roman harbour record were removed by extensive Roman dredging and deepening (e.g. at the Kokotou site, see chapter 2.6.1), such that the period between Archaic and Roman times remains without sedimentary record in some places on Corfu.

Finally, the Harbour Abandonment Surface at Corcyra is marked by the boundary to colluvial to anthropogenic deposits overlying the Roman harbour muds. In contrast to the compilation of Marriner & Morhange (2006b, 2007), the abandonment of the ancient harbours on Corfu is strongly linked to seismogenic events: At Pierri co-seismic uplift between Classical and Hellenistic times led to decreased water depths and the subsequent unnavigability of the harbour basin (chapter 3.5.5) whereas the Kokotou harbour site was buried under tsunami event deposits in Roman times (chapter 2.6.2).

In conclusion, the comparison of the synoptic local harbour sequence of Corcyra to the Ancient Harbour Parasequence by Marriner & Morhange (2006b) is problematic. The latter represents a strongly generalised abstraction deduced from a set of geoarchaeological in-depth studies; the Corcyra sequence is based on three geoarchives, representing a small-scaled area resulting in distinct differences in terms of protection level, chronology and harbour infrastructure. Considering the significant differences in temporal harbour development between the eastern and western Mediterranean basin (chapter1.1) as well as the fact, that many Mediterranean harbours have not yet been investigated as they were destroyed, buried or submerged (Lehmann-Hartleben 1923, Blackman 1982a, Oleson & Hohlfelder 2011), the AHP must be seen as simplified model, providing a broad idea of how harbours might be stratigraphically structured, rather than as a fixed sequence that is applicable to all Mediterranean harbours. The investigation of the ancient harbours of Corcyra has shown that particularly local to regional conditions have major influence on the sedimentary record of ancient harbours. For Corcyra, tsunami-related impact and co-seismic uplift were identified as main triggers for the development, progression and decline of Corcyra's ancient harbours.

5.1.2 Changing palaeogeographies and harbour settings of Corcyra through space and time

We investigated three different harbour-related sites in the environs of ancient Corcyra which were subject to a distinctly different development in terms of extent and time of harbour use on a very small scale (Figure 5.2 A, B).

Slightly protected pre-harbour deposits bearing witness of first rudimentary artificial barriers were only retrieved at the Desylla site, dating to the time period at or slightly after 755-542 cal BC (Figure 5.2 A). The associated infrastructure might temporally coincide with the foundation of Corcyra as Corinthian colony, stated for the late 8th cent. BC, or was constructed some decades later, probably in the context of Corcyra's efforts to prevail against its *metropolis* Corinth. At the nearby Kokotou and Pierri sites contemporaneous sublittoral to littoral sands characterised by fully marine palaeontological and geochemical fingerprints reveal that only a very restricted area was shielded, the latter most likely by the construction of a wall section dated to the Archaic period.

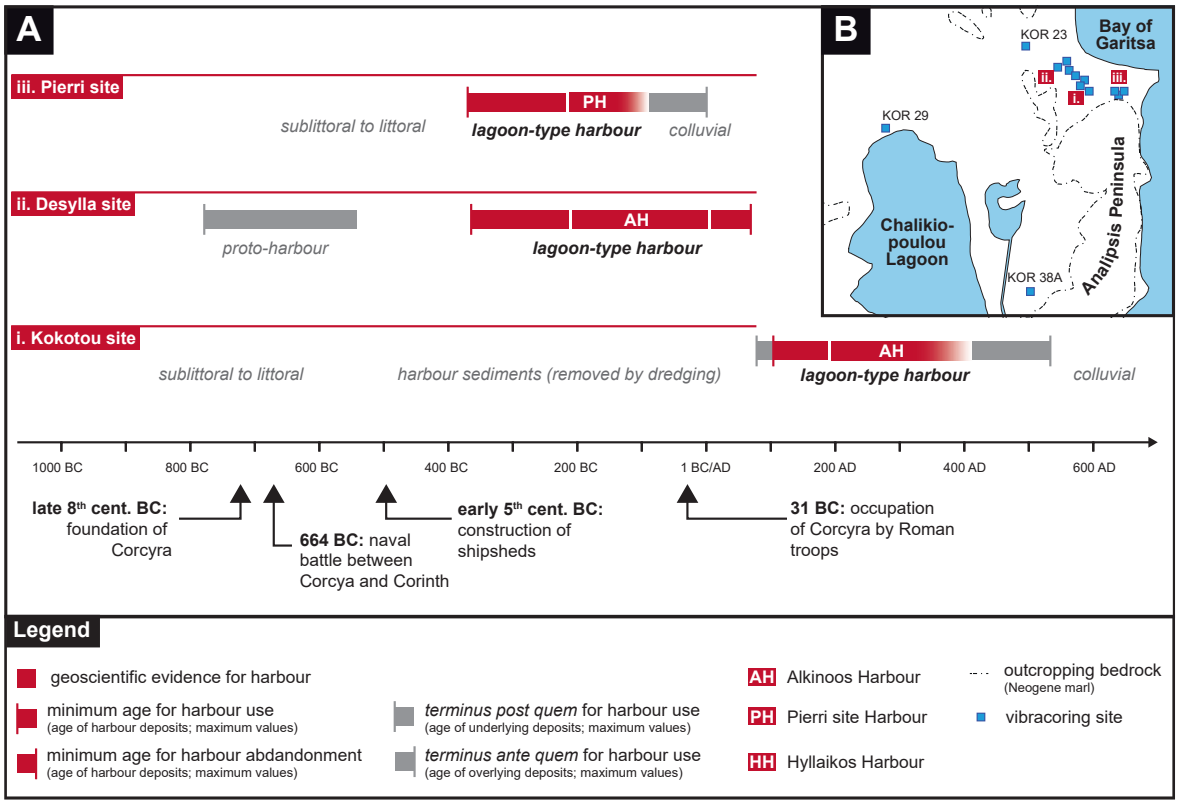

Figure 5.2: The harbours of ancient Corcyra through space and time. (A) Schematic timeline with main historical events and major geoarchaeological findings concerning the harbours of ancient Corcyra classified according to the three main study sites Kokotou (i), Pierri (ii) and Desylla (iii). Harbour sediments are marked by red rectangles and temporally framed by ages of under- and overlying deposits (grey, see legend). In the 8th to 6th cent. BC or slightly earlier an Archaic proto-harbour developed at the Desylla site out of which a lagoonal harbour was constructed in the 4th cent. BC. Simultaneously the Pierri harbour and associated quay wall came to function. which was abandoned in the 4th to 3rd cent. BC. In contrast, the Desylla harbour basin lasted until Roman times. At the Kokotou site only Roman harbour (1st to 5th cent. AD) mud was found as the earlier Classical harbour record was removed by dredging. (B) Overview on the main harbours sites (i-iii) of Corcyra in the context of vibracoring locations presented in the study. Dashed lines mark outcropping bedrock in the form of Neogene marl (after IGME 1970)

Concerning the overall geographical setting of Corcyra in Archaic times, the northern fringe of the Chalikiopoulou Lagoon was already protected by a natural beach barrier as deduced from lagoonal deposits found at vibracoring site KOR 29 (see Figure 4.14). Lagoonal conditions might have extended to the east towards vibracoring site KOR 23. However, lagoonal sediments at site KOR 23 might also document a second lagoon facing the Bay of Garitsa which was separated from the Chalikiopoulou Lagoon by natural sedimentation processes along the ridges of Neogene marl.

Earliest harbour-type sediments date to at least the 4th to 3rd cent. BC and were found at the northern shores of the Analipsis Peninsula, facing the Bay of Garitsa. Here, silty harbour sediments were retrieved in front of the Pierri quay wall as well as on the Desylla factory ground, dating consistently to the time before 364–213 cal BC and 370–214 cal BC, respectively. As already stated in chapter 5.1.1, both harbour sites were not fully protected from littoral dynamics as documented by still considerable amounts of sand found in the associated deposits. Instead, artificial barriers such as breakwaters or moles were most likely established in the natural shallow marine system to protect the coastline and harbours from littoral dynamics and winter storms. Contemporaneous harbour sediments were not found at the Kokotou site although the remains of a Classical shipsheds provide archaeological evidence for a harbour basin linked to this infrastructure. The results presented in chapter 2 show that by Roman dredging activities, the Classical harbour record at Kokotou was completely removed. Even if the overall setup of Corcyra's northern harbour zone remains unclear, it is assumed that the Desylla and Kokotou harbour sites belonged to the same Alkinoos Harbour and were both established during the Classical period as they are located in close proximity to each other. The harbour basin in front of the Pierri quay wall, however, must not have necessarily been part of the Alkinoos harbour but could represent a second harbour basin facing the Bay of Garitsa.

Distinct traces of co-seismic uplift in the 4th to 3rd cent. BC as well as associated tsunami deposits (see chapters 3.5.5 and 4.5.5) document that extreme events impacted the Classical harbour sites of Corcyra, leading to the abandonment of the Pierri site quay wall. Thus, by the transition from Hellenistic to Roman times only the western part of the Alkinoos harbour was still in function, covering the Desylla and Kokotou harbour sites, even if the water depth of both sites must have been considerably decreased. Meanwhile, colluvial sedimentation prevailed at the western flank of the Analipsis Ridge at site KOR 38A, while the Pierri quay wall and its harbour basin in front had been covered by anthropogenic infill. Initialised by co-seismic uplift, coastlines along the shores of the Chalikiopoulou Lagoon probably further regressed to a seaward direction, such that the large lagoonal system covering the northern part of today's Chalikiopoulou Lagoon further extended to the south.

After the occupation of Corcyra by the Romans in 31 BC, parts of the ancient harbour sites were reactivated and extensively dredged as documented by stratigraphical gaps and dredging contacts (Kokotou site, chapter 2) as well as Roman harbour sediments located on a lower elevation level than older Classical harbour deposits (chapter 4). Consequently, deep harbour basins were

present at the Kokotou and Desylla sites. The Roman harbours required continuous and intensive maintenance by dredging to prevent siltation. Related to tsunami impact most likely in the 4th cent. AD, the Roman harbour was filled by event deposits such that the shallower western part nearby the Desylla factory was not navigable anymore. After this event, only a small part of the former harbour basin was still in function but was abandoned before 430-541 cal AD.

In a summary view, the palaeoenvironmental reconstruction of Corcyra's harbours based on the sedimentary records of three different study sites, shows that the transition from natural littoral conditions towards protected harbour basins was not a uniform and constant process. Instead, different harbour environments showing distinct similarities but also considerable differences in terms of sedimentology, micropalaeontological content and protection level, were developed at various locations and during different time periods.

5.2 The influence of extreme events on Corfu

On-shore geological record of tsunamis is strongly depending on site-specific conditions because both erosional and accumulative processes occur by the impact of tsunami waves (Dawson & Stewart 2007). In order to trace episodic tsunami-related deposits accumulated within a very short time, suitable geoarchives are needed. Favourable scenarios are based on homogenuous background signals, e.g. bound to backbeach lagoonal environments, so that tsunami-related high-energy sediments can be discriminated from autochthonous deposits (Bourgeois 2009). Fulfilling these requirements, near coastal lagoons, lakes and backbeach swamps represent excellent potential archives for tsunami-related impact due to two main reasons: First, these archives are mostly bound to basin-like structures which is why they function as efficient sediment traps for sediment input from the sea side. Second, such geomorphological environments are dominated by low-energy conditions which inhibit post-depositional reworking processes but benefit good preservation of tsunamigenic sediments (Goff et al. 2000, Dawson & Stewart 2007, Andrade et al. 2014).

Unlike backbeach swamps or coastal lakes, harbour lagoons bear a further advantage in terms of palaeoevent reconstruction: Harbours and their associated infrastructure mirror the interactions between societies and the environment, so that also the human response to extreme events might be preserved. Extensive dredging activities, for example, might indicate that the harbour basin was filled by event-related deposits so that it was not navigable anymore, a scenario suggested for Lechaion, the ancient Harbour of Corinth (Hadler et al. 2013). Similarly, the adjustment of harbour infrastructure might document co-seismic movements as shown by Stiros & Blackman (2014) for a ship ramp structure on Rhodes.

The present study showed that the harbours of ancient Corcyra not only functioned as efficient geoarchives to trap tsunami-related deposits but also to document co-seismic uplift. These

events caused major environmental changes in the ancient harbour basins during Classical/Hellenistic and Roman times but were also documented to have occurred much earlier, as also event deposits dating back to the Mid-Holocene were archived in the Corcyra record. In the following, an overall event chronology for Corfu will be presented (chapter 5.2.1) in order to compare it to other Mediterranean geoarchives (chapter 5.2.2).

5.2.1 Seismic events trapped in the ancient harbours of Corcyra

The composition and nature of tsunami deposits is strongly depending on the source from which sediments are eroded and translocated by tsunami waters (Kortekaas & Dawson 2007, Chagué-Goff et al. 2017). Tsunami deposits on Corfu cannot be described as uniform sediment layers showing the same uniformly occurring sedimentological characteristics. However, several features diagnostic of high-energy impact from the sea side have been found across all geoarchives of Corcyra, including

i. coarse-grained layers made of allochthonous translocated sediments from the local shorelines,

ii. basal erosional contacts to the underlying sediments,

iii. fining upward sequences,

iv. bi-modal distribution of grain size,

v. poor sorting,

vi. thin mud caps and rip-up clasts and

vii. specific breaks in geochemical and microfaunal fingerprints

(for a detailed explanation see chapters 3.5.2 and 4.5.2 as well as compilations of Goff et al. 2001, Kortekaas & Dawson 2007, Dominey-Howes et al. 2006, Morton et al. 2007, Sugawara et al. 2008, Switzer & Jones 2008 and Chagué-Goff et al. 2011). As the imprint of storms can be excluded *a priori* at the well protected archives on the eastern coasts of Corfu (see e.g. chapter 3.5.2) these high-energy impacts are interpreted to represent tsunami landfall (see also Marriner et al. 2017).

At least five tsunami impacts were reconstructed based on the geological record of the Alkinoos Harbour, the Pierri site and the shores of the Chalikiopoulou Lagoon (Figure 4.14 B; Figure 5.3 A).

The oldest record (tsunami event I) dates back to the 6th mill. BC and was documented in the Alkinoos Harbour and on the eastern shores of the Chalikiopoulou Lagoon. The event can be temporally framed to have happened between 5713 cal BC and 5216 cal BC. Yet, this 6th mill. BC event was not retrieved in the Pierri site record. This might have the following reasons: The associated event deposit might be included in the geological record at Pierri but was not retrieved in the vibracores drilled in the context of this study due to insufficient drilling depth. This is supported by the fact, that the oldest radiocarbon age at Pierri dates to the mid-3rd mill. BC. Yet, vibracore KOR 3 shows Miocene bedrock at its base, so that this cannot be the only reason for missing event deposits from the 6th mill. Another factor might be the close proximity of the Pierri site to the ridge of outcropping bedrock (Figure 5.2 B) having major effects on sedimentation. The latter hypothesis is supported by missing event layers in those vibracores drilled at the Kokotou site that show bedrock at their base (see e.g. Figure 2.2).

Tsunami event II was dated to the time at or after 3940–3845 cal BC and was revealed solely in the Chalikiopoulou Lagoon and at vibracoring location KOR 23. However, a distinct tsunami layer in the stratigraphical record of vibracore KOR 28A, found in consistent stratigraphical position and dating to the time before 2483–2400 cal BC might represent the same event II at the Pierri site. Further research is needed to clarify this relation.

Layers of tsunami event III were identified in all three harbour geoarchives dated to the time between 370 cal BC and 1 AD according to radiocarbon ages retrieved from vibracores at the Pierri site. At the western coasts of the Analipsis Hill event III is framed by underlying Classical and overlying Hellenistic walls of a building. Based on sedimentological and archaeoseismological results (chapters 3.5.5 and 4.5.5) event III was triggered by a local earthquake causing asymmetrical crustal uplift on Corfu and leading to the abonnement of the Pierri quay wall and harbour basin.

Events IV and V occurred during Roman times. Their identification is difficult at the Pierri site and at the eastern shores of the Chalikiopoulou Lagoon because both sites were already solid land during that period of time and influenced by colluvial and anthropogenic sedimentation. Event IV and V are however documented in the Alkinoos Harbour geoarchives where associated layers were deposited at the well-protected Roman harbour basins at the Kokotou and Desylla sites. Tsunami event IV can be dated to the time between 236-325 cal AD and 413-533 cal AD, while event V hit Corcyra between 413-533 cal AD and 430-541 cal AD.

5.2.2 The event history of Corcyra in a supra-regional context

Traces of five different tsunami impacts were found preserved in the geoarchives of ancient Corcyra covering an overall time span of about 4500 years (Figure 5.3). Yet, to establish a reliable and continuous local palaeotsunami chronology and to differentiate major events that were of supra-regional nature from smaller, local events, the results have to be compared with other geoarchives in the Mediterranean context. Episodes of local co-seismic crust uplifts known from geomorphological research by Pirazzoli et al. (1994) and Evelpidou et al. (2014) were added to the local tsunami chronology deduced from this study (reference 6, Figure 5.3). Regarding local crustal movements, a period of strong co-seismic uplift of Corfu was dated to at or shortly after 790-490 cal BC by Pirazzoli et al. (1994) and Evelpidou et al. (2014). These findings are based on geomorphological investigations of tidal notches, benches and holes found on the western shores of Corfu Island.

The same generation of uplifted geomorphological features (including raised notches, wave cut platforms, coralligenous-like bioherms and beachrock) was dated by Mastronuzzi et al. (2014) to around 500/400 BC as they established an age-elevation model based on recalibrated radiocarbon dates of Pirazzoli et al. (1994) and four new radiocarbon ages. Comparing these ages to the time frame of event III (at or slightly after 335-183 cal BC), it seems like crustal uplift at the western coasts of Corfu and in the ancient harbours at the eastern shores were triggered by the same event. Event III is considered as local event due to contemporaneous earthquake induced damages at the Hera temple as well as at the western shore of the Analipsis Ridge (see chapter 4.5.5;

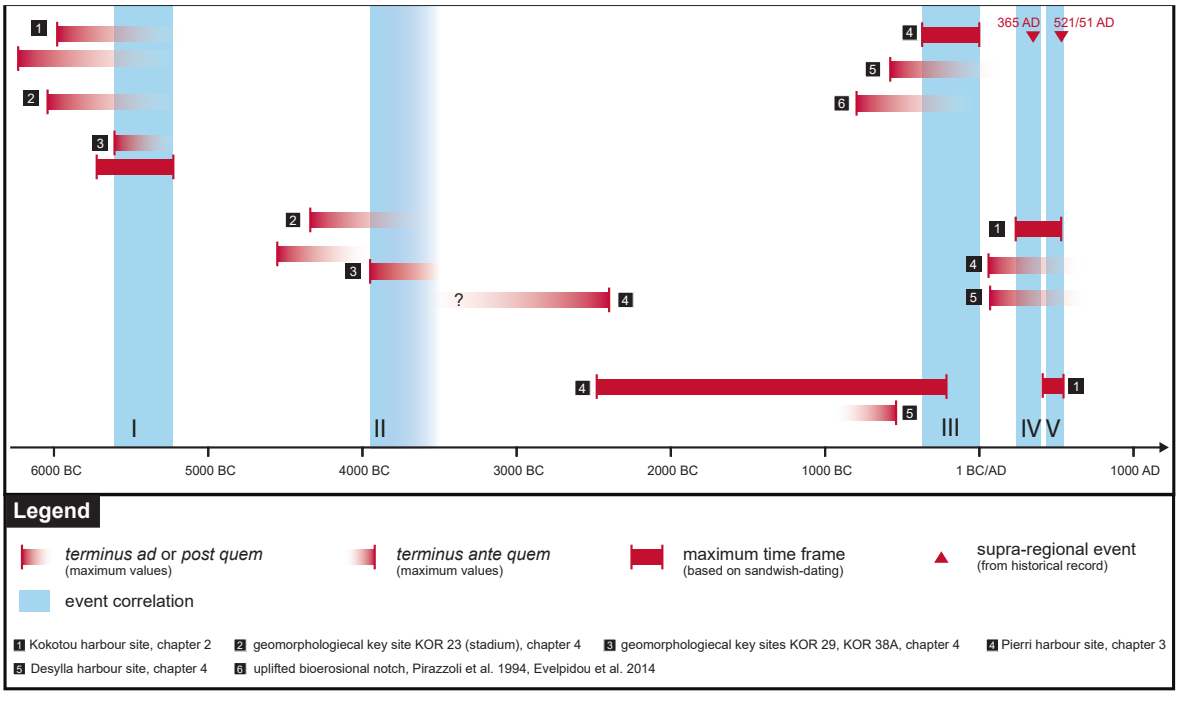

Figure 5.3: Seismic events trapped in the local geoarchives of ancient Corcyra.

Figure 3.11 and Figure 4.9). The event was triggered at or around Corfu and caused not only the uplift of bio-erosive features by about 0.8 m but also the abandonment of at least one harbour site of ancient Corcyra (Pierri site). Further correlations of event III with tsunami impacts in Italy and Greece seem likely: On Siclily, De Martini et al. (2010) and Smedile et al. (2011) found evidence for repeated tsunami impact in the record of the Augusta Bay, less than 500 km away from Corfu. Their findings revealed strong tsunami landfall at *c.* 600–400 BC as well as 350-130 BC, both impacts being potential candidates for event III. On Lefkada Island tsunami layers investigated by Vött et al. (2009b) date to 395–247 cal BC, providing a further correlating candidate. Similar ages between Classical and maximum Roman times were obtained for tsunami imprints in the Lake Voulkaria, located in northwestern Greece (Vött et al. 2009a).

Apart from the 8th to 5th cent. BC notch on Corfu, a younger uplifted notch was documented by Pirazzoli et al. (1994) but remained undated such that a correlation with events IV and V is highly speculative. However, studies carried out on Pag Island in Croatia by Marriner et al. (2014b) revealed the presence of a thick so-called "collapse layer" made of coarse-grained marine material detected in a quiescent salt-march environment. The marine layer was dated to around 1000 to 1200 cal AD and implies an abrupt and temporary marine transgression. As it correlates well with the elevation of a regional-wide tidal notch the authors assume that both, collapse deposits as well as submerged notch, were caused by one and the same seismic event, triggering rapid land-level change along the Adriatic coasts of Croatia. Considering the overall tectonic situation in the northern Ionian and Adriatic Sea, where a small-scaled and complex puzzle of extensional and compressional structures is prevailing (e.g. Kokkalas et al. 2006), the same Roman earthquake might have provoked raised shorelines on Corfu but flooding of coastal landscapes in Croatia. However, this correlation is highly speculative as far as no further dating is presented for the younger coastal notch on Corfu.

Nevertheless, two tsunami events during Roman times were documented by geoarchaeological evidence in the frame of the study at hand: Event IV occurred between 236-533 cal AD and represents a good candidate for the 365 AD earthquake and tsunami generated off Crete. Event V was dated to 413-541 cal AD; a series of strong earthquakes were registered in the 6th cent. AD in the Gulf of Corinth (e.g. Soloviev et al. 2000, Ambraseys & Synolakis 2010) and might be somehow related to event V and other tsunamites described from, for example, the Levantine coast (Goodman-Tchernov et al. 2009) and the ancient harbour of Pheia, western Peloponnese (Vött et al. 2011a).

Comparing the ages of these events with those retrieved for tsunami inundation phases on Sicily (De Martini et al. 2010, Smedile et al. 2011) distinct similarities can be found. At least three events were revealed in the record of Augusta Bay for Roman to Byzantine times, namely dating to the time between 90-370 AD and 430-660 AD (Smedile et al. 2011) and before 650–770 AD (De Martini et al. 2010). While the two younger ages temporally match event V, the older age significantly correlate with event IV of the present study. As both, event IV deposits on Corfu and tsunami traces between the 1st and 4th cent. AD detected on Sicily were assumed to have been triggered by the famous 365 AD Crete tsunami, the existence of associated event deposits on a large Mediterra-

nean scale seems possible. Contemporaneous tsunami imprints were also published by May et al. (2012b) referring to the Gyra washover fan on Lefkada Island at or after 349–533 AD and by Vött et al. (2009a) who detected thick tsunamigenic layers dating to the time between between 261-407 cal AD and 403-533 cal AD in the Lake Voulkaria in Akarnania, Greece.

In terms of older, pre-ancient events, event I may correlate with event impacts described for Lefkada Island (Vött et al. 2009b), Pheia and Epitalio in western Greece (Vött et al. 2011a, 2015b) as well as Akarnania in northwestern Greece (Vött et al. 2009a) dating to be younger than 5286–5071 cal BC, 5843–5747 cal BC, to between 5300 – 5200 cal BC and to be younger than 5984–5895 cal BC, respectively. A tsunami impact hitting the Gulf of Argostoli on Cefalonia was dated by Willershäuser et al. (2013) to the time before 5834–5710 cal BC which is barely outside the time window of event I on Corfu.

Event II was dated to the period at or after 3940–3845 cal BC. However, this maximum age retrieved from vibracore KOR 38A is a single finding while two further radiocarbon ages from vibracores KOR 23 and KOR 29 indicate older maximum ages of *c.* 4300 and 4500 cal BC, respectively. The latter ages correlate noticeably to ages of tsunami traces found on Cefalonia and on the Greek mainland, which were dated to after 4210–4084 cal BC in suitable geoarchives on Cefalonia (Hadler et al. 2011, Vött et al. 2015a) and to or slightly after 4350 – 4250 cal BC near Epitalio (Vött et al. 2015b). No imprint of event II was documented on Sicily or Lefkada by contrast.

However, apart from these well-correlating tsunami imprints, also single evidence for tsunami impacts dating to the wide time span between events II and III was documented in the archives of Corcyra. At the Desylla site, a potential tsunami layer traces back to the period before 755–542 cal BC, while at the Pierri site, tsunami sediments accumulated between 2483–2400 cal BC and 370–214 cal BC. These deposits might originate from one and the same tsunami landfall but might also represent two distinct periods of event impact. Data deduced from an age-depth-model of raised geomorphological features published by Mastronuzzi et al. (2014) point to three further periods of seismic-induced uplift on Corfu, namely around 1500 BC, 1250 BC and 1000 BC, matching the time frame of single tsunami evidences revealed by this study. Similar ages of tsunami deposits were detected in geoarchives at the Greek, Italian and Albian coasts. On Siclily, De Martini et al. (2010) and Smedile et al. (2011) found evidence for strong tsunami impact between 975–800 BC and 1720–1200 cal BC. In the geoarchive of Lake Butrint in Albania, Morrellón et al. (2015) retrieved a section of homogeneous layers deposited shortly after *c.* 1515 cal BC by severe mass-movements – most likely triggered by a major earthquake. These ages are in accordance with results from Cefalonia and Lefkada, were a major flooding event is suggested for the 2nd mill. BC by Willershäuser et al. (2013) and Vött et al. (2009b). Similarly, tsunami impact is documented on the northwestern Greek mainland around 1000 BC, in particular between 1739–1635 cal BC and 909–826 cal BC (Vött et al. 2009a).

By conclusion, there might be correlations between the five tsunami events found on Corfu and events documented in other geoarchives across the Mediterranean. The supra-regional distribution of event deposits highlights their major impact and gives a rough estimation of the magnitude of the associated seismic events. Event III by contrast, has to be considered as local seismic event with its epicentre located close to Corfu, were local seismic activity triggered major crustal movements and severe damage (e.g. at the eastern shores of the Chalikiopoulou Lagoon or at the Hera temple, see chapter3.5.5).

5.3 Perspectives and conclusions

By this study, the palaeoenvironmental history of Corfu was reconstructed spanning a total time of 8000 years, reaching from the 6th mill. BC to modern times. Apart from different palaeogeographies for different time slices, especially comprehensive information on the ancient harbours of Corfu were retrieved: First attempts to modify the natural coastal environments can be traced back to Archaic times where the natural littoral system was protected against wave influence by most likely rudimentary barriers forming an Archaic pre-harbour. A protected Classical harbour basin was traced at two different sites, belonging to the Alkinoos Harbour, known from historical records (Thucydides 3.72.3 after Crawley 1910). However, the results show how small-scaled and in how many ways harbour development took place in ancient Corcyra. Classical Harbours were facing the seaside at its northern fringe, shielded of littoral dynamics by breakwaters or other protective infrastructure while the Roman harbour basin was well-protected. Moreover, by the impact of seismogenic events, some harbour sites were abandoned to the benefit of other harbour basins, which were subject to considerable maintenance and dredging operations to keep them navigable. The latter happened especially during the Roman period, when only the northern harbour zone was re-activated, forming an enclosed and well-protected quiescent harbour basin.

In summary, the ancient harbours of Corcyra turned out to be appropriate geoarchives to reconstruct the overall palaeogeographical development of Corfu. Yet, the comparison with the generalized harbour concept of other Mediterranean harbours, summarised by Marriner & Morhange (2006b, 2007) in the Ancient Harbour Parasequence, had shown, that harbour evolution is strongly linked to local geographies and conditions as well as site-specific factors. Regarding the main triggers for environmental changes in the harbours of Corcyra, both natural extreme events and human interventions in terms of geochemical pollution as well as deepening and dredging activities are important. Multiple tsunami impact led to massive destruction of the urban and harbour-related infrastructure and the burial of particular harbour sites under event deposits. Additionally, rapid co-seismic uplift caused by severe local earthquakes was found to be a crucial factor for the coastal development of Corcyra. A major event occurred in the 4th to 3rd cent. BC in the course of which considerable harbour infrastructure was significantly uplifted so that is was not usable anymore.

Five tsunami events were identified for Corcyra. These events seem to correlate with event records from other Mediterranean geoarchives. Major events occurred with a return rate of *c.* 1300 years. Yet, when considering further single tsunami evidence as well as supra-regional data, this value may be too high and might score up to values of 800 or even less years (Figure 5.3).

The fact that not a single historical record of pre-medieval tsunami impact is available for the Ionian Sea clearly depicts the relevance of geoscientific studies along the Ionian coasts in order to identify, trace and analyse palaeotsunamis and associated seismic events. The knowledge of the overall nature, magnitude and distribution of palaeoevents might help to gain a reliable and helpful risk mitigation in the future. The severe earthquake in 1953 that led to massive destruction and coastal uplift of several decimetres on Cefalonia (e.g. Stiros et al. 1994), proved that co-seismic crustal movements are not restricted to ancient times but are also a threat for modern Mediterranean societies. Recent studies by Papageorgiou et al. (2015) document that the public awareness of the tsunami risk is very low in Greece, so that tourists are usually better-informed concerning the susceptibility towards seismic events than local inhabitants. A comprehensive dataset on the palaeotsunamis history of geoarchives all along the Mediterranean coasts might help to change this circumstance in order to prevent potential catastrophes in the future.

References

Ad hoc-Arbeitsgruppe Boden (2005): Bodenkundliche Kartieranleitung. – E. Schweizerbart'sche Verlagsbuchhandlung, Stuttgart.

Abulafia, D. (2011): The Great Sea: A Human History of the Mediterranean. – Oxford University Press, Oxford.

Albini, P. (2004): A survey of the past earthquakes in the Eastern Adriatic (14th to early 19th century). – Annals of Geophysics **47**: 675–703.

Algan, O., Yalçin, M.N., Özdoğan, M., Yilmaz, İ., Sari, E., Kirci-Elmas, E., Ongan, D., Bulkan-Yeşiladali, Ö., Yilmaz, Y. & Karamut, İ. (2009): A short note on the geo-archeological significance of the ancient Theodosius harbour (İstanbul, Turkey). – Quaternary Research **72**: 457–461.

Algan, O., Yalçin, N. M., Özdoğan, M., Yilmaz, Y., Sari, E., Kirci-Elmas, E., Yilmaz, İ., Bulkan, Ö., Ongan, D., Gazioğlu, C., Nazik, A., Polat, M. A. & Meriç, E. (2011): Holocene coastal change in the ancient harbour of Yenikapı–İstanbul and its impact on cultural history. – Quaternary Research **76**: 30–45.

Allevato, E., Saracino, A., Fici, S. & Di Pasquale, G. (2016): The contribution of archaeological plant remains in tracing the cultural history of Mediterranean trees: The example of the Roman harbour of Neapolis. – The Holocene **26** (4): 603–613.

Allison, M.A., Sheremet, A., Goñi, M.A. & Stone, G.W. (2005): Storm layer deposition on the Mississippi–Atchafalaya subaqueous delta generated by Hurricane Lili in 2002. – Continental Shelf Research **25**: 2213–2232.

Ambraseys, N. & Synolakis, C. (2010): Tsunami Catalogs for the Eastern Mediterranean, Revisited. – Journal of Earthquake Engineering **14**: 309–330.

Andrade, V., Rajendran, K. & Rajendran, C.P. (2014): Sheltered coastal environments as archives of paleo-tsunami deposits: Observations from the 2004 Indian Ocean tsunami. – Journal of Asian Earth Sciences **95**: 331–341.

Andreadaki-Vlazaki, M. (2012): 2000-2010. Από το ανασκαφικό έργο των Εφορειών Αρχαιοτήτων (2000-2010. From the excavations of the Archaeological Committees). – Ministry of Culture and Sports, Athens.

Anthony, E.J., Marriner, N. & Morhange, C. (2014): Human influence and the changing geomorphology of Mediterranean deltas and coasts over the last 6000 years: From progradation to destruction phase? – Earth-Science Reviews **139**: 336–361.

Anzidei, M, Lambeck, K., Antonioli, F., Furlani, S., Mastronuzzi, G., Serpelloni, E. & Vannucci, G. (2014): Coastal structure, sea-level changes and vertical motion of the land in the Mediterranean. – Geological Society of London, Special Publications 388 (1): 453–479.

Argyraki, A., Ramsey, M.H. & Potts, P.J. (1997): Evaluation of Portable X-ray Fluorescence Instrumentation for in situ Measurements of Lead on Contaminated Land. – The Analyst **122**: 743–749.

Ascough, P., Cook, G. & Dugmore, A. (2005): Methodological approaches to determining the marine radiocarbon reservoir effect. – Progress in Physical Geography **29** (4): 532–547

Auriemma, R. & Solinas, E. (2009): Archaeological remains as sea level change markers: A review. – Quaternary International **206**: 134–146.

Babbucci, D., Tamburelli, C., Viti, M., Mantovani, E., Albarello, D., D'Onza, F., Cenni, N. & Mugnaioli, E. (2004): Relative motion of the Adriatic with respect to the confining plates: seismological and geodetic constraints. – Geophysical Journal International **159**: 765–775.

Bahlburg, H., & Spiske, M. (2002): Sedimentology of tsunami inflow and backflow deposits: key differences revealed in a modern example. – Sedimentology **59**: 1063–1086.

Bahlburg, H. & Weiss, R. (2007): Sedimentology of the December 26, 2004, Sumatra tsunami deposits in eastern India (Tamil Nadu) and Kenya. – International Journal of Earth Sciences **96**: 1195–1209.

Baika, K. (2003): ΝΕΩΣΟΙΚΟΙ. Installations navales en Méditerranée. Les neoria de Corcyre. – Unpublished doctoral thesis. Université de Paris I (Panthéon-Sorbonne), Paris.

Baika, K. (2013a): Corcyra (Corfu). In: Blackman, D., Rankov, B., Baika, K., Gerding, H. & Pakkanen J. (Eds.): Shipsheds of the Ancient Mediterranean. – Cambridge University Press, Cambridge: 319–334.

Baika, K. (2013b): The topography of shipshed complexes and naval dockyards. In: Blackman, D., Rankov, B., Baika, K., Gerding, H. & Pakkanen, J. (Eds.): Shipsheds of the Ancient Mediterranean. – Cambridge University Press, Cambridge: 185–209.

Baika, K. (2013c): The fortification of shipsheds and naval arsenals. In: Blackman, D., Rankov, B., Baika, K., Gerding, H. & Pakkanen, J. (Eds.): Shipsheds of the Ancient Mediterranean. – Cambridge University Press, Cambridge: 210–230.

Baika, K. (2015). Ancient harbour cities - New methodological perspectives and recent research in Greece. In: Ladstatter, S. Pirson, F. & Schmidts, T. (Eds.): Harbours and Harbour Cities in the Eastern Mediterranean from Antiquity to the Byzantine Period. Recent Discoveries & New Approaches. – BYZAS 19 (= Österreichisches Archäologisches Institut Sonderband 52), Vol. II, Ege Yayinlari, Istanbul: 445–491.

Barbano, M. S., Pirrotta, C. & Gerardi, F. (2010): Large boulders along the south-eastern Ionian coast of Sicily: Storm or tsunami deposits? – Marine Geology **275**:140–154.

Battaglia, M., Murray, M. H., Serpelloni, E. & Bürgmann, R. (2004): The Adriatic region: An independent microplate within the Africa-Eurasia collision zone. – Geophysical Research Letters **31** (9): L09605.

Bernasconi, M.P., Melis, R. & Stanley, J.-D. (2006): Benthic biofacies to interpret Holocene environmental changes and human impact in Alexandria's Eastern Harbour, Egypt. – The Holocene **16** (8):1163–1176.

Berger, J.-F., Metallinou, G. & Guilaine, J. (2014): Reconsidering the Mesolithic-Neolithic transition at the site of Sidari (Corfu, Greece). New geoarchaeological and radiocarbon data, evaluation of the post-depositional processes. In: Manen, C., Perrin, T. & Guilaine, J. (Eds.): La transition néolithique en Méditerranée. Actes du colloque Transitions en Méditerranée, ou comment des chasseurs devinrent agriculteurs, Muséum de Toulouse, 14-15 avril 2011. – Errance, Arles: 213–232.

Billi, A., Gambini, R., Nicolai, C. & Storti, F. (2007): Neogene-Quaternary intraforeland transpression along a Mesozoic platform-basin margin: The Gargano fault system, Adria, Italy. – Geosphere **3** (1): 1–15.

Bini, M., Chelli, A., Durante, A. M., Gervasini, L. & Pappalardo, M. (2009): Geoarchaeological sea-level proxies from a silted up harbour: A case study of the Roman colony of Luni (northern Tyrrhenian Sea, Italy). – Quaternary International **206**: 147–157.

Blackman, D.J. (1982a): Ancient harbours in the Mediterranean. Part 1. – The International Journal of Nautical Archaeology and Underwater Exploration **11** (1): 79–104.

Blackman, D.J. (1982b): Ancient harbours in the Mediterranean. Part 2. – The International Journal of Nautical Archaeology and Underwater Exploration **11** (2): 185–211.

Blackman, D., Baker, J. & Hardwick, N. (1998): Archaeology in Greece 1997-1998. – Archaeological Reports **44**: 1–136.

Blackman, D.J. (2013a): Ramps and substructures. In: Blackman, D., Rankov, B., Baika, K., Gerding, H. & Pakkanen J. (Eds.): Shipsheds of the Ancient Mediterranean. – Cambridge University Press, Cambridge: 124–140.

Blackman, D.J. (2013b): Classical and Hellenistic Sheds. In: Blackman, D., Rankov, B., Baika, K., Gerding, H. & Pakkanen J. (Eds.): Shipsheds of the Ancient Mediterranean. – Cambridge University Press, Cambridge: 16–29.

Blume, H.-P., Stahr, K. & Leinweber, P. (2011): Bodenkundliches Praktikum. – Spektrum, Heidelberg.

Bony, G., Marriner, N., Morhange, C., Kaniewski, D. & Perinçek, D. (2012): A high-energy deposit in the Byzantine harbour of Yenikapı, Istanbul (Turkey). – Quaternary International **266**: 117–130.

Bourgeois, J. (2009): Geologic effects and records of tsunamis. In: Robinson, A.R. & Bernard, E.N. (Eds.); The Sea, Volume 15: Tsunamis. – Harvard University Press, Cambridge: 53–91.

Brännvall, M.-L., Bindler, R., Emteryd, O. & Renberg, I. (2001): Four thousand years of atmospheric lead pollution in northern Europe: a summary from Swedish lake sediments. – Journal of Paleolimnology **25**: 421–435.

Briggs, R. W., Engelhart, S. E., Nelson, A. R., Dura, T., Kemp, A. C., Haeussler, P. J., Corbett, D. R., Angster, S. J. & Bradley, L.-A. (2014): Uplift and subsidence reveal a nonpersistent megathrust rupture boundary (Sitkinak Island, Alaska). – Geophysical Research Letters **41** (7): 2289–2296.

Broadley, L., Platzman, E., Platt, J., Papanikolaou, M. & Matthews, S. (2006): Paleomagnetism and the tectonic evolution of the Ionian zone, northwestern Greece. – Geological Society of America Special Paper **409**: 137–155.

Brückner, H., Kelterbaum, D., Marunchak, O., Porotov, A. & Vött, A. (2010): The Holocene sea level story since 7500 BP – Lessons from the Eastern Mediterranean, the Black and the Azov Seas. – Quarternary International **225** (2): 160–179.

Bryant, E. (2008): Tsunami. The Underrated Hazard – Springer, Berlin & Heidelberg.

Campins, J., Genovés, A., Picornell, M. A. & Jansà, A. (2011): Climatology of Mediterranean cyclones using the ERA-40 dataset. – International Journal of Climatology **31**: 1596–1614.

Carsana, V., Febbraro, S., Giampaola, D., Guastaferro, C., Irollo, G. & Ruello, M.R. (2009): Evoluzione del paesaggio costiero tra Parthenope e Neapolis. – Méditerranée **112**: 14–22.

Cavaleri, L. (2005): The wind and wave atlas of the Mediterranean Sea – the calibration phase. – Advances in Geoscience **2**: 255–257.

Cavicchia, L., von Storch, H. & Gualdi, S. (2014): A long-term climatology of medicanes. – Climate Dynamics **43**: 1183–1195.

Chagué-Goff, C., Schneider, J.-L., Goff, J.R, Dominey-Howes, D. & Strotz, L. (2011): Expanding the proxy toolkit to help identify past events — Lessons from the 2004 Indian Ocean Tsunami and the 2009 South Pacific Tsunami. – Earth-Science Reviews **107**: 107–122.

Chagué-Goff, C., Goff, J., Wong, H.K.Y. & Cisternas, M. (2015): Insights from geochemistry and diatoms to characterise a tsunami's deposit and maximum inundation limit. – Marine Geology **359**: 22–34.

Chagué-Goff, C., Szczuciński, W. & Shinozaki, T. (2017): Applications of geochemistry in tsunami research: A review. – Earth-Science Reviews **165**: 203–244.

Chalari, A., Papatheodorou, Geraga, M, Christodoulou & Ferentinos, G. (2009): A Marine Geophysical Survey illustrates Alexandria's Hellenistic Past. – Zeitschrift für Geomorphologie N.F. Supplementary Issue **53** (1): 191–212.

Cimermann, F. & Langer, M.R. (1991): Mediterranean Formaminifera. – Slovenska Akademija Znanosti in Umetnosti, Ljubljana.

D'Agostini, N., Avallone, A., Cheloni, D., D'Anastasio, E. & Mantenuto, S. (2008): Active tectonics of the Adriatic region from GPS and earthquake slip vectors. – Journal of Geophysical Research: Solid Earth **113**: B12413.

Daux, G. (1966): Chronique des fouilles et découvertes archéologiques en Grèce en 1965. – Bulletin de correspondence hellénique **90** (2): 715-1019.

Davolio, S., Miglietta, M. M., Moscatello, A., Pacifico, F., Buzzi, A. & Rotunno, R. (2009): Numerical forecast and analysis of a tropical-like cyclone in the Ionian Sea. – Natural Hazards and Earth System Science **9**: 551–562.

Darawcheh, R., Sbeinati, M.R., Margottini, C. & Paolini, S. (2000): The 9 July 551 AD Beirut Earthquake, Eastern Mediterranean Region. – Journal of Earthquake Engineering **4** (4): 403–141.

Dawson, A.G. & Stewart, I. (2007): Tsunami deposits in the geological record. – Sedimentary Geology **200**: 166–183.

Delile, H., Blichert-Toft, J., Goiran, J.-P., Keay, S. & Albarède, F. (2014a): Lead in ancient Rome's city waters. – Proceedings of the National Academy of Sciences **111**: 6594–6599.

Delile, H., Mazzini, I., Blichert-Toft, J., Goiran, J.P., Arnaud-Godet, F., Salomon, F. & Albarède, F. (2014b): Geochemical investigation of a sediment core from the Trajan basin at Portus, the harbor of ancient Rome. – Quaternary Science Review **87**: 34–45.

Delile, H., Abichou, A., Gadhoum, A., Goiran, J.-P., Pleuger, E., Monchambert, J.-Y., Wilson, A., Fentress, E., Quinn, J., Ben Jerbania, I. & Ghozzi, F. (2015a): The Geoarchaeology of Utica, Tunisia: The Paleogeography of the Mejerda Delta and Hypotheses Concerning the Location of the Ancient Harbour. – Geoarchaeology **30**: 291–306.

Delile, H., Mazzini, I., Blichert-Toft, J., Goiran, J.P., Stock, F., Arnaud-Godet, F., Bravard, J.-P., Brückner, H. & Albarède, F. (2015b): Demise of a harbor: a geochemical chronicle from Ephesus. – Journal of Archaeological Science **53**: 202–213.

Delile, H., Goiran, J.-P., Blichert-Toft, J., Arnaud-Godet, F., Romano, P. & Bravard, J.-P. (2016): A geochemical and sedimentological perspective of the life cycle of Neapolis harbor (Naples, southern Italy). – Quaternary Science Reviews **150**: 84–97.

De Martini, P.M., Burrato, P., Pantosti, D., Maramai, A., Graziani, L. & Abramson, H. (2003): Identification of tsunami deposits and liquefaction features in the Gargano area (Italy): paleoseismological implication. – Annals of Geophysics **46** (5): 883–902.

De Martini, P.M., Barbano, M.S., Smedile, A., Gerardi, F., Pantosti, D., Del Carlo, P. & Pirrotta, C. (2010): A unique 4000 year long geological record of multiple tsunami inundations in the Augusta Bay (eastern Sicily, Italy). – Marine Geology **276**: 42–57.

De Martini, P. M., Barbano, M. S., Pantosti, D., Smedile, A., Pirrotta, C., Del Carlo, P. & Pinzi, S. (2012): Geological evidence for palaeotsunamis along eastern Sicily (Italy): an overview. – Natural Hazards and Earth System Science **12**: 2569–2580.

Di Bella, L., Bellotti, P., Frezza, V., Bergamin, L. & Carboni, M.G. (2011): Benthic foraminiferal assemblages of the imperial harbor of Claudius (Rome): Further paleoenvironmental and geoarcheological evidences. – The Holocene **21**(8): 1245–1259.

Di Bella, L., Bellotti, P., Frezza, V., Bergamin, L. & Carboni, M. G. (2011): Benthic foraminiferal assemblages of the imperial harbour of Claudius (Rome): Further palaeoenvironmental and geoarcheological evidences. – The Holocene **21**: 1245–1259.

Di Bucci, D. & Angeloni, P. (2013): Adria seismicity and seismotectonics: Review and critical discussion. – Marine and Petroleum Geology **42**: 182–190.

Dierichs, A. (2004): Korfu-Kerkyra: die grüne Insel im Ionischen Meer von Nausikaa bis Kaiser Wilhelm II. – Philipp von Zabern Verlag, Mainz.

DIN ISO 11277 (2002): Bodenbeschaffenheit - Bestimmung der Partikelgrößenverteilung in Mineralböden – Verfahren mittels Siebung und Sedimentation. ISO 11277:1998 and ISO 11277, Corrigendum 1. – Beuth Verlag, Berlin.

Dominey-Howes; D., Dawson, A. & Smith, D. (1998): Late Holocene coastal tectonics at Falasarna western Crete: a sedimentary study. – In: Stewart, I. S. & C. Vita-Finzi (Eds.): Coastal Tectonics. – Geological Society London **146**: 343–552.

Dominey-Howes, D., Cundy, A. & Croudace, I. (2000): High energy marine flood deposits on Astypalaea Island, Greece: possible evidence for the A.D. 1956 southern Aegean tsunami. – Marine Geology **163**: 303–315.

Dominey-Howes, D. T. M., Humphreys, G. S. & Hesse, P. P. (2006): Tsunami and palaeotsunami depositional signatures and their potential values in understanding the late-Holocene tsunami record. – The Holocene **16**: 1095–1107.

Donato, S.V., Reinhardt, E.G., Boyce, J.I., Rothaus, R. & Vosmer, T. (2008): Identifying tsunami deposits using bivalve shell taphonomy. – Geology **36** (3): 199–202.

Dontas, G. (1965): Τοπογραφικά θέματα της πολιορκίας της Κέρκυρας του έτους 373 π. Χ. (*Topographical issues of the siege of Corcyra in 373 B.C.*). – Archaiologiki Ephimeris **1965:** 139–144.

Dontas, G. (1966): Ανασκαφαί Κέρκυρας (*Excavations at Corcyra*). – Praktika Archaeologikis Etaireias **1966**: 85–94.

Doutsos, T. & Kokkalas, S. (2001): Stress and deformation patterns in the Aegean region. – Journal of Structural Geology **23**: 455–472.

Elmaleh, A., Galy, A., Allard, T., Dairon, R., Day, J. A., Michel, F., Marriner, N., Morhange, C. & Couffignal, F. (2012): Anthropogenic accumulation of metals and metalloids in carbonate-rich sediments: Insights from the ancient harbour setting of Tyre (Lebanon). – Geochimica et Cosmochimica Acta **82**: 23–38.

Englebretson, R.E., Gilmore, R.D. & Perryman, D.C. (1992): Severe Weather Guide – Mediterranean Ports – 47. Kerkira (Corfu). – NOARL Technical Note 239. Naval Oceanographic and atmospheric Research Laboratory, Monterey.

EPA – U.S. Environmental Protection Agency (2007): Method 6200: Field portable x-ray fluorescence spectrometry for the determination of elemental concentrations in soil and sediment. – URL: http://www.epa.gov/hw-sw846/sw-846-test-method-6200-field-portable-x-ray-fluorescence-spectrometry-determination (2017-03-20).

Erol, O. & Pirazzoli, P.A. (1992): Seleucia Pieria – An Ancient Harbor submitted to 2 successive Uplifts. – International Journal of Nautical Archaeology **21** (4): 317–327.

Evelpidou, N., Karkani, A. & Pirazzoli, P. A. (2014): Fossil shorelines at Corfu and surrounding islands deduced from erosional notches. – The Holocene **24**: 1565–1572.

Fabre, D. (2004): Seafaring in ancient Egypt. – Periplus, London.

Fairbanks, R. G. (1989): A 17,000-year glacio-eustatic sea level record: influence of glacial melting rates on the Younger Dryas event and deep-ocean circulation. – Nature **324**: 637–641.

Faivre, S., Fouache, E., Ghilardi, M., Antonioli, F., Furlani, S. & Kovačić, V. (2011): Relative sea level change in western Istria (Croatia) during the last millennium. – Quaternary International **232**: 132–143.

Faivré, S., Bakran-Petricioli, T., Barešić & Horvatinčić, N. (2015): New Data on Marine Radiocarbon Reservoir Effect in the Eastern Adriatic Based on Pre-Bomb Marine Organisms from the Intertidal Zone and Shallow Sea. – Radiocarbon **57** (4): 527–538.

Fauber, C.M. (2002): Archaic Kerkyra: an historiographical examination of the formation and formulation of an ancient Greek polis. – PhD thesis, University of Chicago, Chicago.

Ferentinos, G., Gkioni, M., Geraga, M. & Papatheodorou, G. (2012): Early seafaring activity in the southern Ionian Islands, Mediterranean Sea. – Journal of Archaeological Science **39**: 2167–2176.

Finkler, C., Fischer, P., Baika, K., Rigakou, D., Metallinou, G., Hadler, H. & Vött, A. (2017a): Tracing the Alkinoos Harbour of ancient Kerkyra, Greece, and reconstructing its palaeotsunami history. – Geoarchaeology 2017: 1–19 (DOI: 10.1002/gea.21609).

Finkler, C., Baika, K., Rigakou, D., Metallinou, G., Fischer, P, Hadler, H. & Vött, A. (2017b): Geoarchaeological investigations of a prominent quay wall in ancient Corcyra – implications for harbour development, palaeoenvironmental changes and tectonic geomorphology of Corfu Island (Ionian Islands, Greece) – Quaternary International (DOI: 10.1016/j.quaint.2017.05.013).

Finkler, C., Baika, K., Rigakou, D., Metallinou, G., Fischer, P, Hadler, H. & Vött, A. (2018): The sedimentary record of the Alkinoos Harbour of ancient Corcyra (Corfu Island, Greece) – geoarchaeological evidence for rapid coastal changes induced by co-seismic uplift, tsunami inundation and human interventions – Zeitschrift für Geomorphologie (accepted).

Fischer, P., Finkler, C., Röbke, B.R., Baika, K., Hadler, H., Willershäuser, T., Rigakou, D., Metallinou, G. & Vött, A. (2016a): Impact of Holocene tsunamis detected in lagoonal environments on Corfu (Ionian Islands, Greece) – geomorphological, sedimentary and microfaunal evidence. – Quaternary International **401**: 4–16.

Fischer, P., Wunderlich, T., Rabbel, W., Vött, A., Willershäuser, T., Baika, K., Rigakou, D. & Metallinou, G. (2016b): Combined electrical resistivity tomography (ERT), direct-push electrical conductivity logging (DP-EC) and vibracoring – a new methodological approach in geoarchaeological research. – Archaeological Prospection **23** (3): 213–228.

Fontana, A., Vinci, G., Tasca, G., Mozzi, P., Vacchi, M., Bivi, G., Salvador, S., Rossato, S., Antonioli, F., Asioli, A., Bresolin, M., Di Mario, F. & Hajdas, I. (2017): Lagoonal settlements and relative sea level during Bronze Age in Northern Adriatic: Geoarchaeological evidence and paleogeographic constraints. – Quaternary International 2017: 1–20 (DOI: 10.1016/j.quaint.2016.12.038).

Fouache, E., Dalongeville, R., Kunesch, S., Suc, J.-P., Subally, D., Prieur, A. & Lozouet, P. (2005): The Environmental Setting of the Harbour of the Classical Site of Oeniades on the Acheloos Delta, Greece. – Geoarchaeology **20**: 285–302.

Franco, L. (1996): Ancient Mediterranean harbours: a heritage to preserve. – Ocean & Coastal Management **30** (2-3): 115–151.

Fregonese, L., Fassi, F., Achille, C. & Adami, A. (2016): 3D survey technologies: investigations on accuracy and usability in archaeology. The case study of the new "Municipio" underground station in Naples. – ACTA IMEKO **5** (2): 55–63.

Fujiwara, O., Masudab, F., Sakaib, T., Irizukic T. & Fused, K. (2000): Tsunami deposits in Holocene bay mud in southern Kanto region, Pacific coast of central Japan. – Sedimentary Geology **135**: 219–230.

GEBCO – General Bathymetric Chart of the Oceans (2014): The GEBCO_2014 Grid. – URL: http://www.gebco.net (2015-04-28).

Gehrke, H.-J. & Wirbelauer, E. (2004): Korkyra. In: Hansen, M. H. & Nielsen, T. H. (Eds.): An Inventory of Archaic and Classical Poleis. – Oxford University Press, Oxford: 361–363.

Gelfenbaum, G. & Jaffe, B. (2003): Erosion and sedimentation from the 17 July, 1998 Papua New Guinea tsunami. – Pure and Applied Geophysics **160**: 1969–1999.

Gerardi, F., Smedile, A., Pirrottal, C., Barbano, M.S., De Martini, P.M., Pinzi, S., Gueli, M., Ristuccia, G.M., Stella, G. & Troja, S.O. (2012): Geological record of tsunami inundations in Pantano Morghella (south-eastern Sicily) both from near and far-field sources. – Natural Hazards and Earth System Sciences **12**: 1185–1200.

Gerding, H. (2013): Oiniadai. – In: Blackman, D., Rankov, B., Baika, K., Gerding, H. & Pakkanen, J. (Eds.): Shipsheds of the Ancient Mediterranean. – Cambridge University Press, Cambridge: 410–419.

Geyh, M.A. (2005): Handbuch der physikalischen und chemischen Alterbestimmung. – Wissenschaftliche Buchgesellschaft, Darmstadt.

Ghionis, G., Poulos, S.E., Verykiou, E., Karditsa, A., Alexandrakis, G. & Andris, P. (2015): The Impact of an Extreme Storm Event on the Barrier Beach of the Lefkada Lagoon, NE Ionian Sea (Greece). – Mediterranean Marine Science **16** (3): 562–572.

Gianfreda, F., Mastronuszzi, G. & Sansó, P. (2001): Impact of historical tsunamis on a sandy coastal barrier:an example from the northern Gargano coast, southern Italy. – Natural Hazards and Earth System Science **1**: 213–219.

Goff, J. R. & Chagué-Goff, C. (1999): A late Holocene record of environmental changes from coastal wetlands: Abel Tasman National Park, New Zealand. – Quaternary International **56**: 39–51.

Goff, J. R., Rouse, H. L., Jones, S. L., Hayward, B. W., Cochran, U., McLea, W., Dickinson, W. W. & Morley, M. S. (2000): Evidence for an earthquake and tsunami about 3100±3400 yr ago, and other catastrophic saltwater inundations recorded in a coastal lagoon, New Zealand. – Marine Geology **170**: 213–249.

Goff, J., Chagué-Goff, C. & Nichol, S. (2001): Palaeotsunami deposits: a New Zealand perspective. – Sedimentary Geology **143**: 1–6.

Goiran, J.-P., Tronchére, H., Salomon, F., Carbonel, P-. Djerbi, H. & Ognard, C. (2010): Palaeoenvironmental reconstruction of the ancient harbors of Rome: Claudius and Trajan's marine harbors on the Tiber delta. – Quaternary International **216**: 3–13.

Goiran, J.-P., Salomon, F., Mazzini, I., Bravard, J.-P., Pleuger, E., Vittori, C., Boetto, G., Christiansen, J., Arnaud, P., Pellegrino, A., Pepe, C. & Sadori, L. (2014): Geoarchaeology confirms location of the ancient harbour basin of Ostia (Italy). – Journal of Archaeological Science **41**: 389–398.

Goodman, B. N., Reinhardt, E. G., Dey, H. W., Boyce, J. I., Schwarcz, H. P., Sahoğlu, V., Erkanal, H. & Artzy, M. (2009): Multi-proxy geoarchaeological study redefines understanding of the palaeocoastlines and ancient harbours of Liman Tepe (Iskele, Turkey). – Terra Nova **21**: 97–104.

Goodman-Tchernov, B.N., Hendrik, W.D., Reinhardt, E.G., McCoy, F. & Mart, Y. (2009): Tsunami waves generated by the Santorini eruption reached Eastern Mediterranean shores. – Geological Society of America 37: 943–946.

Goodman-Tchernov, B.N. & Austin, J.A. (2015): Deterioration of Israel's Caesarea Maritima's ancient harbor linked to repeated tsunami events identified in geophysical mapping of offshore stratigraphy. – Journal of Archaeological Science **3**: 444–454.

Goodman-Tchernov, B. N., Dey, H. W., Reinhardt, E. G., McCoy, F. & Mart, Y. (2009): Tsunami waves generated by the Santorini eruption reached Eastern Mediterranean shores. – Geology **37**: 943–946.

Goto, K., Chagué-Goff, C., Goff, J & Jaffe, B. (2012): The future of tsunami research following the 2011 Tohoku-oki event. – Sedimentary Geology **282**: 1–13.

Hadler, H., Vött, A., Brückner, H., Bareth, G., Ntageretzis, K., Warnecke, H. & Willershäuser, T. (2011): The harbour of ancient Krane, Kutavos Bay (Cefalonia, Greece) – an excellent geo-archive for palaeo-tsunami research. In: Karius, V., Hadler, H., Deicke, M., Van Eynatter, H., Brückner, H. & Vött, A. (Eds): Dynamische Küsten – Grundlagen, Zusammenhänge und Auswirkungen im Spiegel angewandter Küstenforschung. – Coastline Reports **17**: 111–122.

Hadler, H., Willershäuser, T., Ntageretzis, K., Henning, P. & Vött, A. (2012): Catalogue entries and non-entries of earthquake and tsunami events in the Ionian Sea and the Gulf of Corinth (eastern Mediterranean, Greece) and their interpretation with regard to palaeotsunami research. In: Vött, A. & Venzke, J.-F. (Eds.): Beiträge der 29. Jahrestagung des Arbeitskreises „Geographie der Meere und Küsten", 28. bis 30. April 2011 in Bremen. – Bremer Beiträge zur Geographie und Raumplanung **44**: 1–15.

Hadler, H., Vött, A., Koster, B., Mathes-Schmidt, M., Mattern, T., Ntageretzis, K., Reicherter, K. & Willershäuser, T. (2013): Multiple late-Holocene tsunami landfall in the eastern Gulf of Corinth recorded in the palaeotsunami geo-archive at Lechaion, harbour of ancient Corinth (Peloponnese, Greece). – Zeitschrift für Geomorphologie N.F. Supplementary Issue **57** (4): 139–180.

Hadler, H., Baika, K., Pakkanen, J., Evangelistis, D., Emde, K., Fischer, P., Ntageretzis, K., Röbke, B., Willershäuser, T. & Vött, A. (2015a): Palaeotsunami impact on the ancient harbour site Kyllini (western Peloponnese, Greece) based on a geomorphological multi-proxy approach. – Zeitschrift für Geomorphologie N.F. Supplementary Issue **59** (4): 7–41.

Hadler, H., Vött, A., Fischer, P., Ludwig, S., Heinzelmann, M. & Rohn, C. (2015b): Temple-complex postdates tsunami deposits found in the ancient harbour basin of Ostia (Rome, Italy). – Journal of Archaeological Science **61** (2015) 78–89.

Harrington, G. A. & Hendry, M. J. (2006): Using Direct-Push EC Logging to Delineate Heterogeneity in a Clay-Rich Aquitard. – Ground Water Monitoring & Remediation **26** (1): 92–100.

Hawkes, A. D., Bird, M., Cowie, S., Grundy-Warr, C., Horton, B. P., Hwai, A. T. S., Law, L., Macgregor, C., Nott, J., Ong, J. E., Rigg, J., Robinson, R., Tab-Mullins, M., Tiong Sa, T., Yasin, Z. & Aik, L. W. (2007): Sediments deposited by the 2004 Indian Ocean Tsunami along the Malaysia–Thailand Peninsula. – Marine Geology **242**: 169–190.

HCMR – Hellenic Center for Marine Research (2015): Poseidon Data Base (unpublished data). – URL: http://poseidon.hcmr.gr/listview.php?id=136 (2016-03-01).

Hesnard, A. (1994): Une nouvelle fouille du port de Marseille, place Jules-Verne. – Comptes rendus des séances de l'Académie des Inscriptions et Belles-Lettres **138** (1): 195–217.

Higgins, M.D. & Higgins, R. (1996): A Geological companion to Greece and the Aegean. – Duckworth, London.

Hollenstein, C., Müller, M., Geiger, A. & Kahle, H.G. (2008): Crustal motion and deformation in Greece from a decade of GPS measurements, 1993 – 2003. – Tectonophysics **449**: 17–40.

Homer after Murray, A.T. (1924): The Iliad with an English Translation. – Harvard University Press, London.

Hong, S., Candelone, J.-P., Patterson, C. C. & Boutron, C. F. (1994): Greenland Ice Evidence of Hemispheric Lead Pollution Two Millennia Ago by Greek and Roman Civilizations. – Science **265**: 1841–1843.

IGME - Institute of Geology and Mineral Exploration (1970): Geological Map of Greece – Sheet North and South Corfu. Scale 1:50.000. – IGME, Athens.

Inman, D.L. (1974): Ancient and modern Harbors: A repeating Phylogeny – ASCE **3**: 2049–2967.

Jacobshagen, V. (1986): Geologie von Griechenland - Beiträge zur regionalen Geologie der Erde. – Gebrüder Bornträger, Berlin & Stuttgart.

Jagodziński, R., Sternal, B., Szczuciński, W., Chagué-Goff, C. & Sugawara, D. (2012): Heavy minerals in the 2011 Tohoku-oki tsunami deposits—insights into sediment sources and hydrodynamics. – Sedimentary Geology **282**: 57–64.

Jolivet, L., Faccenna, C. & Piromallo, C. (2009): From mantle to crust: Stretching the Mediterranean. – Earth and Planetary Science Letters **285**: 198–209.

Judd, K., Chagué-Goff, C., Goff, J., Gadd, P., Zawadzki, A. & Fierri, D. (2017): Multi-proxy evidence for small historical tsunamis leaving little or no sedimentary record. – Marine Geology **385**: 204–215.

Kanta-Kitsou, A. (2001): Ένας νεώσοικος, τμήμα των νεωρίων του Υλλαϊκού λιμανιού της Αρχαίας Κέρκυρας (*A shipshed, section of the neorion of the Hyllaikos Harbour of ancient Corcyra*). In: Tzalas, H. (Ed.): Tropis VI. 6th International Symposium on Ship Construction in Antiquity, Lamia 1996. – Hellenic Institute for the Preservation of Nautical Tradition, Athens: 273–299.

Karathanasi, F., Soukissian, T. & Sifnioti, D. (2015): Offshore wave potential of the Mediterranean Sea. – Renewable Energy and Power Quality Journal **13** (online journal).

Keary, P., Brooks, M. & Hill, I. (2002): An introduction to Geophysical Exploration. – Blackwell Science, Malden, Oxford & Carlton.

Kiechle, F.K. (1979): Korkyra und der Handelsweg durch das Adriatische Meer im 5. Jh. v. Chr. – Historia: Zeitschrift für Alte Geschichte **28**: 173–191.

Knapp, A.B. & Demesticha, S. (2017): Mediterranean Connections: Maritime Transport Containers and Seaborne Trade in the Bronze and Early Iron Ages (3D Photorealistic Rendering). – Routledge, New York.

Köhn, M. (1929): Korngrößenbestimmung vermittels Pipettanalyse. – Tonindustrie-Zeitung **55**: 729–731.

Kolaiti, E., Papadopoulos, G.A., Morhange, C., Vacchi, M., Triantafyllou, I. & Mourtzas, N. (2017): Palaeoenvironmental evolution of the ancient harbor of Lechaion (Corith Gulf, Greece): Were changes driven by human impacts and gradual coastal processes or catastrophic tsunamis? – Marine Geology **392**: 105–121.

Kokkalas, S., Xypolias, P., Koukouvelas, I. & Doutsos, T. (2006): Postcollisional contractional and extensional deformation in the Aegean region. In: Dilek, Y. & Pavlides, S. (Eds.): Postcollisional tectonics and magmatism in the Mediterranean region and Asia. – Geological Society of America Special Paper **409**: 97–123.

Kortekaas, S. (2002): Tsunamis, storms and earthquakes: Distinguishing coastal flooding events. – PhD-Thesis, Coventry University, Coventry.

Kortekaas, S. & Dawson, A.G. (2007): Distinguishing tsunami and storm deposits: An example from Martinhal, SW Portugal. – Sedimentary Geology **200** (3–4): 208–221.

Kourtessi-Philippakis, G. (1999): The Lower and Middle Palaeolithic in the Ionian islands: new finds. – In: Bailey, G.N. (Ed.): The Palaeolithic Archaeology of Greece and adjacent areas: Proceedings of the ICOPAG Conference, Ioannina, September 1994. – British School at Athens Studies **3**: 282–287.

Kraft, J.C., Kayan, I. & Erol, O. (1980): Geomorphic Reconstructions in the Environs of Ancient Troy. – Science **209**: 776–782.

Kraft, J. C., Rapp, G., Kayan, I. & Luce, J. V. (2003): Harbour areas at ancient Troy: Sedimentology and geomorphology complement Homer's Iliad. – Geology **31**: 163–166.

Lario, J., Luque, L., Zazo, C,m Goy, J.L., Spencer, C., Cabero, A., Bardají, T., Borja, F., Dabrio, C.J., Civis, J., González-Delgado, J.A., Borja, C. & Alonso-Azcárate, J. (2010): Tsunami vs. Storm surge deposits: a review of the sedimentological and geomoprhological records of extreme wave events (EWE) during the Holocene in the Gulf of Cadiz, Spain. – Zeitschrift für Geomorphologie N.F. Supplementary Issue **54** (3): 301–316.

Lehmann-Hartleben, K. (1923): Die antiken Hafenanlagen des Mittelmeeres. Beiträge zur Geschichte des Städtebaus im Altertum. Klio: Beiträge zur alten Geschichte, Beiheft XIV. – Dietrich'sche Verlagsbuchhandlung, Leipzig. Le Roux, G., Véron, A. & Morhange, C. (2003): Geochemical evidences of early anthropogenic activity in harbour sediments from Sidon. – Archaeology and History in Lebanon **18**: 115–118.

Le Roux, G., Véron & Morhange, C. (2003): Geochemical evidences of early anthropogenic activity in harbour sediments from Sidon. – Archaeology and History in Lebanon **18**: 115–118.

Le Roux, G., Véron, A. & Morhange, C. (2005): Lead pollution in the ancient harbours of Marseille. – Méditerranée **1**: 31–35.

Lessler, M. A. (1988): Lead and Lead Poisoning from Antiquity to Modern Times. – The Ohio Journal of Science **88** (3): 78–84.

Lionello, P., Abrantes, F., Congedi, L., Dulac, M. G., Gomis, D., Goodess, C., Hoff, H., Kutiel, H., Luterbacher, J., Planton, S., Reale, M., Schröder. K., Struglia, M. V., Toreti, A., Tsimplis, M., Ulbrich, U. & Xoplaki, E. (2012): Introduction: Mediterranean Climate – Background Information. In: Lionello, P. (Ed.): The Climate of the Mediterranean Region. From the Past to the Future. – Elsevier, London: xxxv–xc.

Llasat, M.C. (2009): High magnitude storms and floods. In: Woodward, J.C. (Ed.): The Physical Geography of the Mediterranean. – Oxford University Press, Oxford: 513–540.

Loeblich, A.R. & Tappan, H.N. (1988): Foraminiferal genera and their classification. – Springer, New York.

Loke, M.H. & Dahlin, T. (2002): A comparison of the Gauss–Newton and quasi-Newton methods in resistivity imaging inversion. – Journal of Applied Geophysics **49**: 149–162.

Loke, M.H., Acworth, I. & Dahlin, T. (2003): A comparison of smooth and blocky inversion methods in 2D electrical imaging surveys. – Exploration Geophysics **34**: 182–187.

Malkin, I. (2011): A Small Greek World. Networks in the Ancient Mediterranean. – Oxford University Press.

Mamo, B., Strotz, L. & Dominey-Howes, D. (2009). Tsunami sediments and their foraminiferal assemblages. – Earth-Science Reviews **96**: 263–278.

Maramai, A., Graziani, L. & Tinti, S. (2007): Investigation on tsunami effects in the central Adriatic Sea during the last century – a contribution. – Natural Hazards and Earth System Science **7**: 15–19.

Marinos, G. & Sakellariou-Mane, E. (1964): Über das Alter der letzten Senkungen des Ionischen Meeres. Entdecken prehistorischen Schicht der Steinzeit in NW Korfu. – Bulletin of the Geological Society of Greece **6**: 14–24.

Marriner, N. & Morhange, C. (2005): Under the city centre, the ancient harbour. Tyre and Sidon: heritage to preserve. – Journal of Cultural Heritage **6**: 183–189.

Marriner, N. & Morhange, C. (2006a): Geoarchaeological evidence for dredging in Tyre's ancient harbour, Levant. – Quaternary Research **65**: 164–171.

Marriner, N. & Morhange, C. (2006b): The 'Ancient Harbour Parasequence': Anthropogenic forcing of the stratigraphic highstand record. – Sedimetary Geology **186**: 13–17.

Marriner, N. & Morhange, C. (2007): Geoscience of ancient Mediterranean harbours. – Earth-Science Reviews **80**: 137–194.

Marriner, N., Morhange, C., Boudagher-Fadel, M., Bourcier & Carbonel, P. (2005): Geoarchaeology of Tyre's ancient northern harbour, Phoenicia. - Journal of Archaeological Science **32**:1302–1327.

Marriner, N., Morhange, C. & Doumet-Serhal, C. (2006): Geoarchaeology of Sidon's ancient harbours, Phoenicia – Journal of Archaeological Science **33**: 1514–1535.

Marriner, N., Morhange, C. & Carayon, N. (2008a): Ancient Tyre and its harbours: 5000 years of human-environment interactions. – Journal of Archaeological Science **35**: 1281–1310.

Marriner, N., Morhange, C. & Saghieh-Beydoun, M. (2008b): Geoarchaeology of Beirut's ancient harbour, Phoenicia. – Journal of Archaeological Science **35**: 2495–2516.

Marriner, N., Morhange, C. & Goiran, J.P. (2010): Coastal and ancient harbour geoarchaeology. –Geology Today **26** (1): 21–27.

Marriner, N., Morhange, C., Kaniewski, D. & Carayon, N. (2014a): Ancient harbour infrastructure in the Levant: tracking the birth and rise of new forms of anthropogenic pressure. – Science Reports 4 (5554): 1–11.

Marriner, N., Morhange, C., Faivre, S., Flaux, C., Vacchi, M., Miko, S., Dumas, V., Boetto, G., Radic Rossi, I. (2014b): Post-Roman sea-level change on Pag Island (Adriatic Sea): dating Croatia's "enigmatic" coastal notch? – Geomorphology **221**: 83–94.

Marriner, N., Kaniewski, D., Morhange, C., Flaux, C., Giaime, M., Vacchi, M. & Goff, J. (2017): Tsunamis in the geological record: Making waves with a cautionary tale from the Mediterranean. – Science Advances **3** (10): e1700485.

Mastronuzzi, G. & Sansó, P. (2004): Large boulder accumulations by extreme waves along the Adriatic coast of southern Apulia (Italy). – Quaternary International **120**: 173–184.

Mastronuzzi, G., Pignatelli, C., Sansó, P. & Selleri, G. (2007): Boulder accumulations produced by the 20th February 1743 tsunami along the coast of southeastern Salento. – Marine Geology **242**: 191–205.

Mastronuzzi, G. (2010): Tsunami in the Mediterranean Sea. – The Egyptian Journal of Environmental Change **2** (1): 1–17.

Mastronuzzi, G., Calcagnile, L., Pignatelli, C., Quarta, G., Stamatopoulos, L. & Venisti, N. (2014): Late Holocene tsunamigenic uplift in Kerkira Island, Greece. – Quaternary International **332**: 48–60.

Mastronuzzi, G. & Sansò, P. (2014): Coastal towers and historical sea level change along the Salento coast (southern Apulia, Italy). – Quaternary International **332**: 61–72

Mather, A. (2009): Tectonic Setting and Landscape Development – In: Woodward, J. (Ed.): The Physical Geography of the Mediterranean. – Oxford University Press, Oxford: 5–32.

Mathes-Schmidt, M., Schwarzbauer, J., Papanikolaou, I., Syberberg, F., Thiele, A., Wittkopp, F. & Reicherter, K. (2013): Geochemical and micropalaeontological investigations of tsunamigenic layers along the Thracian Coast (Northern Aegean Sea, Greece). – Zeitschrift für Geomorphologie N.F. Supplementary Issue **57** (4): 5–27.

May, S. M., Vött, A., Brückner, H., Grapmayer, R., Handl, M. & Wennrich, V. (2012a): The Lefkada barrier and beachrock system (NW Greece) — Controls on coastal evolution and the significance of extreme wave events. – Geomorphology **139-140**: 330–347.

May, S.M., Vött, A., Brückner, H. & Smedile, A. (2012b): The Gyra washover fan in the Lefkada Lagoon, NW Greece—possible evidence of the 365 AD Crete earthquake and tsunami. – Earth, Planets and Space **64**: 859–874.

Mazarakis, N., Kotroni, V., Lagouvardos, K. & Bertotti, L. (2012): High-resolution wave model validation over the Greek maritime areas. – Natural Hazards and Earth System Science **12**: 3433–3440.

Mazzini, I., Faranda, C., Giardini, M., Giraudi, C. & Sadori, L. (2011): Late Holocene palaeoenvironmental evolution of the Roman harbour of Portus, Italy. – Journal of Paleolimnology **46**: 243–256.

McKenzie, J. (2003): Glimpsing Alexandria from archaeological evidence. – Journal of Roman Archaeology **16**: 35–63.

Melis, R., Bernasconi, M.P., Colizza, E., Di Rita, F., Equini Schneider, E., Forte, E., Montenegro, M.E., Pugliese, N. & Ricci, M. (2015): Late Holocene palaeoenvironmental evolution of the northern harbour at the Elaiussa Sebaste archaeological site (south-eastern Turkey): evidence from core ELA6. – Turkish Journal of Earth Sciences **24**: 566–584.

Metallinou, G. (2007): Η προιστορική έρευνα στην Κέρκυρα και η συμβολή του Αύγουστου Σορδίνα Θεωρητιές προσεγγίσεις –προοπτικές (*The prehistoric research on Corfu and the contribution of Augustus Sordinas. Theoretical Approaches-Prospects*). – In: Metallinou, G. (Ed.): Η Προιστορική Κέρκυρα και ο ευρύτερος περίγυρός της. Προβλήματα–Προοπτικές (*Prehistoric Corfu and its adjacent areas. Problems–Perspectives*). Proceedings of the conference dedicated to Augustus Sordinas, Corfu, December the 17th 2004. – Ministry of Culture, Corfu: 35–47.

Miglietta, M.M., Mastrangelo, D. & Conte, D. (2015): Influence of physics parameterization schemes on the simulation of a tropical-like cyclone in the Mediterranean Sea. – Atmospheric Research **153**: 360–375.

Millet, B., Tronchère, H. & Goiran, J.-P. (2014): Hydrodynamic Modeling of the Roman Harbour of Portus in the Tiber Delta: The Impact of the North-Eastern Channel on Current and Sediment Dynamics. – Geoarchaeology **29**: 357–370.

Monaco, C. & Tortorici, L. (2000): Active faulting in the Calabrian arc and eastern Sicily. – Journal of Geodynamics **29**: 407–424.

Morellón, M., Anselmetti, F., Ariztegui, D., Brushulli, B., Sinopoli, G., Wagner, B., Sadori, L., Gilli, A. & Pambuku, A. (2016): Human-climate interactions in the central Mediterranean region during the last millennia: The laminated record of Lake Butrint (Albania). – Quaternary Science Reviews **136**: 134–152.

Morgan, C. (2010): Ionian Islands, excluding Kythera. – Archaeological Reports **56**: 67–72.

Morgan, C. (2012): Corfu (Desylla Factory) (Archaeology in Greece Online Report 2607). – URL: http://chronique.efa.gr/index.php/fiches/voir/2607/ (05.10.2017).

Morhange, C. & Marriner, N. (2010): Mind the (stratigraphic) gap: Roman dredging in ancient Mediterranean harbours. – Bollettino di Archeologia on line **B7** (4): 23–32.

Morhange, C. & Marriner, N. (2011): Paleo-Hazards in the Coastal Mediterranean: A Geoarchaeological Approach. In: Martini, I.P. & Chesworth, W. (Eds.): Landscapes and Societies – Springer, Heidelberg & New York: 223–234.

Morhange, C., Laborel, J., Hesnard, A., & Prone, A. (1996): Variation of Relative Mean Sea Level during the Last 4000 Years on the Northern Shores of Lacydon, the Ancient Harbour of Marseilles (Chantier J. Verne). – Journal of Coastal Research **12** (4): 841–849.

Morhange, C., Laborel, J. & Hesnard, A. (2001): Changes of relative sea level during the past 5000 years in the ancient harbor of Marseilles, Southern France. – Palaeogeography, Palaeoclimatology, Palaeoecology **166**: 319–329.

Morhange, C., Blanc, F., Schmitt-Mercury, S., Bourcier, M., Carbonel, P., Oberlin, C., Prone, A., Vivent, D. & Hesnard, A. (2003): Stratigraphy of late-Holocene deposits of the ancient harbour of Marseilles, southern France. – The Holocene **13** (4): 593–604.

Morhange, C., Pirazzoli, P.A., Evelpidou, N., & Marriner, N. (2012): Late Holocene Tectonic Uplift and the Silting Up of Lechaion, the Western Harbor of Ancient Corinth, Greece. – Geoarchaeology **27** (3): 278–283.

Morhange, C., Marriner, N. & Carayon, N. (2014): The geoarchaeology of ancient Mediterranean harbours. In: Carcaud, N. & Arnaud-Fassetta, G. (Eds.): La géoarchéologie française au XXIe siècle. – CNRS Edition, Paris: 245–254.

Morhange, C., Marriner, N. & Carayon, N. (2016): The eco-history of ancient Mediterranean harbours. In: Bekker-Nielsen, T. & Gertwagen, R. (Eds.): The Inland Seas. – Towards an Ecohistory of the Mediterranean and the Black Sea. – Geographica Historica **35**: 85–106.

Morton, R. A., Gelfenbaum, G. & Jaffe, B. E. (2007): Physical criteria for distinguishing sandy tsunami and storm deposits using modern examples. – Sedimentary Geology **200**: 184–207.

Mourtzas, N.D., Kissas, C. & Kolaiti, E. (2014): Archaeological and geomorphological indicators of the historical sea level changes and the related palaeogeographical reconstruction of the ancient foreharbour of Lechaion, East Corinth Gulf (Greece). – Quaternary International **332**: 151–171.

Murray, J.W. (1991): Ecology and paleoecology of Benthic Foraminifera. – Longman Scientific & Technical, Essex.

Murray, J.W. (2006): Ecology and Applications of Benthic Foraminifera. – Cambridge University Press, Cambridge.

Nakamura, Y., Nishimura, Y., & Putra, P.S. (2012): Local variation of inundation, sedimentary characteristics, and mineral assemblages of the 2011 Tohoku-oki tsunami on the Misawa coast, Aomori, Japan. – Sedimentary Geology **282**: 216–227.

Nanayama, F Shigeno, K., Satake, K., Shimokawa, K., Koitabashi, S., Miyasaka, S. & Ishii, M. (2000): Sedimentary differences between the 1993 Hokkaido-nansei-oki tsunami and the 1959 Miyakojima typhoon at Taisei, southwestern Hokkaido, northern Japan. – Sedimentary Geology **135**: 255–264.

NCMA S.A. – National Cadastre and Mapping Agency S.A. (2014): Orthophotos for Greece 2007-2009 (WMS-Service). – URL: http://gis.ktimanet.gr/wms/ktbasemap/default.aspx (2016-02-02).

Noureddine, I. (2015): Late Quaternary sea-level changes and archaeology. – Doctoral thesis. University of Granada, Granada.

Nriagu, J.O. (1996): A History of Global Metal Pollution. – Science **272**: 223–224.

Oleson, J.P. & Hohlfelder, R.L. (2011): Ancient Harbors in the mediterranean. In: Catsambis, A., Ford, B. & D.L. Hamilton (Eds.): The Oxford Handbook of Maritime Archaeology. – Oxford University Press, New York: 809–833.

Papadopoulos, G.A. & Papageorgiou, A. (2012): Large earthquakes and tsunamis in the Mediterranean region and its connected seas. In: Ismail-Zadeh, A., Fucugauchi, J.U., Kijko, A., Tekeuchi, K. & Zaliapin, I. (Eds.): Extreme Natural Hazards, Disaster Risks and Social Implications. – Cambridge University Press, Cambridge: 252–266.

Papadopoulos, G.A. (2015): Tsunamis in the European Mediterranean Region. Form Historical Record to Risk Mitigation. – Elsevier, Amsterdam.

Papageorgiou, S., Arnold, M., Laborel, J. & Stiros, S. (1993): Seismic Uplift of the Harbour of Ancient Aigeira, Central Greece. – The International Journal of Nautical Archaeology **22** (3): 275–281.

Papageorgiou, A., Tsimi, C., Organogiannaki, K., Papadopoulos, G., Sachpazi, M., Lavigne, F. & Grancher, D. (2015): Tsunami Questionnaire Survey in Heraklion Test Site, Crete Island, Greece. In: Lavigne, F. (Ed): Assessment, STrategy And Risk Reduction forTsunamis in Europe (ASTARTE) Deliverable 9.7. Report on preparedness skills, resources and attitudes within the communities. – URL: http://www.astarte-project.eu/files/astarte/documents/deliverables/d9-7/ASTARTE%20deliverable%20D9.7%20-%2028.10.14.pdf (2017-10-03).

Papazachos, B. & Dimitriu, P.P. (1991): Tsunamis in and near Greece and their relation to the earthquake focal mechanisms. – Natural Hazards **4**: 161–170.

Partsch, J. (1887): Die Insel Korfu. Eine geographische Monographie. Petermanns Mitteilungen, Ergänzungsheft 88. – Justus Perthes, Gotha.

Pepe, C., Giardini, M., Giraudi, C., Masi, A., Mazzini, I., Sadori, L. (2013): Plant landscape and environmental changes recorded in marginal marine environments: The ancient Roman harbour of Portus (Rome, Italy). – Quaternary International **303**: 73–81.

Perissoratis, C. & Conispoliatis, N. (2003): The impacts of sea-level changes during latest Pleistocene and Holocene times on the morphology of the Ionian and Aegean seas (SE Alpine Europe). – Marine Geology **196**: 145–156.

Pilarczyk, J.E., Horton, B.P., Witter, R.C., Vane, C.H., Chagué-Goff, C. & Goff, J. (2012): Sedimentary and foraminiferal evidence of the 2011 Tōhoku-oki tsunami on the Sendai coastal plain, Japan. – Sedimentary Geology **282**: 78–89.

Pilarczyk, J.E., Dura, T., Horton, B.P., Engelhart, S.E., Kemp, A.C. & Sawai, Y. (2014): Microfossils from coastal environments as indicators of palaeo-earthquakes, tsunamis and storms. – Palaeogeography, Palaeoclimatology, Palaeoecology **413**: 144–157.

Pint, A., Seeliger, M., Frenzel, P., Feuser, S., Erkul, E., Berndt, C., Klein, C., Pirson, F. & Brückner, H. (2015): The environs of Elaia's ancient open harbour – a reconstruction based on microfaunal evidence. – Journal of Archaeological Science **54**: 340–355.

Pirazzoli, P.A., Laborel, J., Saliége, J.F., Erol, O., Kayen, I & Person, A. (1991): Holocene raised shorelines on the Hatay coasts (Turkey): Palaeoecological and tectonic implications. – Marine Geology **96** (3–4): 295–311.

Pirazzoli, P.A., Ausseil-Badie, J., Giresse, P., Hadjidaki, E. & Arnold, M. (1992): Historical Environmental Changes at Phalassarna Harbor, West Crete. – Geoarchaeology: An International Journey **7** (4): 371–392.

Pirazzoli, P.A., Stiros, S.C., Laborel, J., Laborel-Deguen, F., Arnold, M., Papageorgiou, S. & Morhange, C. (1994): Late-Holocene shoreline changes related to palaeoseismic events in the Ionian Islands, Greece. – The Holocene **4** (4): 397–405.

Pomey, P. (1995): Les épaves grecques et romaines de la place Jules-Verne à Marseille. – Comptes rendus des séances de l'Académie des Inscriptions et Belles-Lettres **2**: 459-484.

Pomey, P. (2011): Defining a Ship: Architecture, Function, and Human Space. In: Catsambis, A., Ford, B. & Hamilton, D.L. (Eds.): The Oxford Handbook of Maritime Archaeology. – Oxford University Press, New York: 25–46.

Poulos, S. E., Lykousis, V., Collins, M. B., Rohling, E. J. & Pattiaratchi, C. B. (1999): Sedimentation processes in a tectonically active environment: the Kerkyra-Kefalonia submarine valley system (NE Ionian Sea). – Marine Geology **160**: 25–44.

Preka-Alexandri, K. (1986): Κέρκυρα, Παλαιόπολη (*Corcyra, Palaiopoli*). – Archaiologikon Deltion **41** (B): 125–9.

Raban, A. & Galili, E. (1985): Recent maritime archaeological research in Israel – A preliminary report. – The International Journal of Nautical Archaeology and Underwater Exploration **14** (4): 321–356.

Rajendran, N. (2006): History of Tsunami. In: Ramasamy S.M., Kumanan, C.J., Sivakumar, R. & Singh, B. (Eds.): Geomatics in Tsunamis – New India Publishing Agency, New Delhi: 1–9.

Reimer, P. J. & McCormac, F. G. (2002): Marine radiocarbon reservoir corrections for the Mediterranean and Aegean Seas. – Radiocarbon **44**: 159–166.

Reimer, P. J., Bard, E., Bayliss, A., Becks, J. W., Blackwell, P. G., Bronk Ramsey, C., Buck, C. E., Cheng, H., Edwards, R. L., Friedrich, M., Grootes, P. M., Guilderson, T. P., Haflidason, H., Hajdas, I., Harré, C., Heaton, T. J., Hoffmann, D. L., Hogg, A. G., Hughen, K. A., Kaiser, K. F., Kromer, B., Manning, S. W., Niu, M., Reimer, R. W., Richards, D. A., Scott, E. M., Southon, J. R., Staff, R. A., Turney, C. S. M. & Van der Pflicht, J. (2013): INTCAL13 and MARINE13 radiocarbon age calibration curves 0-50,000 years cal BP. – Radiocarbon **55**: 1869–1887.

Reinhardt, E.G., Patterson, R.T. & Schroeder-Adams, C.J. (1994): Geoarchaeology of the ancient harbor site of Caesarea Maritima, Israel; evidence from sedimentology and paleoecology of benthic foraminifera. – Journal of Foraminiferal Research **24** (1): 37–48.

Reinhardt, E. G., Goodman, B. N., Boyce, J. I., Lopez, G., Van Hengstum, P., Rink, W. J., Mart, Y., Raban, A. (2006): The tsunami of 13 December A.D. 115 and the destruction of Herod the Great's harbour at Caesarea Maritima, Israel. – Geology **34**: 1061–1064.

Riginos, G., Karamanou, A., Kanta, K., Metallinou G. & Zernioti, D. (2000): Η Αρχαία Κέρκυρα - Πόλη και Ύπαιθρος- Μέσα από τα πορίσματα των πρόσφατων ερευνών (*Ancient Kerkyra – City and rural areas – from the results of the recent investigations*). Στ΄ Διεθνές Πανιόνιο Συνέδριο, (*6th International Panionian Conference*), Center of Ionian Studies, Thessaloniki: 25–38.

Röbke, B.R. & Vött, A. (2017): The tsunami phenomenon. – Progress in Oceanography (DOI: 10.1016/j.pocean.2017.09.003).

Runnels, C. (1995): Review of Aegean Prehistory IV: The Stone Age of Greece from the Palaeolithic to the Advent of the Neolithic. – American Journal of Archaeology **99** (4): 699–728.

Sachpazi, M., Hirn, A., Clément, C., Haslinger, F., Laigle, M., Kissling, E., Charvis, P., Hello, Y., Lépine, J.-C., Sapin, M. & Ansorge, J. (2000): Western Hellenic subduction and Cephalonia Transform: local earthquakes and plate transport and strain. – Tectonophysics **319**: 301–319.

Sadori, L., Giardini, M., Giraudi, C., Mazzini, I. (2010): The plant landscape of the imperial harbour of Rome. – Journal of Archaeological Science **37**: 3294–3305.

Sakuna, D., Szczuciński, W., Feldens, P., Schwarzer, K. & Khokiattiwong, S. (2012): Sedimentary deposits left by the 2004 Indian Ocean tsunami on the inner continental shelf offshore of Khao Lak, Andaman Sea (Thailand). – Earth, Planets and Space **64**: 931–943.

Sakuna-Schwartz, D., Feldens, P., Schwarzer, K., Khokiattiwong, S. & Stattegger, K. (2015): Internal structure of event layers preserved on the Andaman Sea continental shelf, Thailand: tsunami vs. storm and flash-flood deposits. – Natural Hazards and Earth System Science **15:** 1181–1199.

Salomon F., Keay S., Carayon N., Goiran J.P. (2017): The Development and Characteristics of Ancient Harbours—Applying the PADM Chart to the Case Studies of Ostia and Portus. PLOS One **12** (1): e0170140.

Sansò, P., Gianfreda, F., Leucci, G. & Mastronuzzi, G. (2017): Cliff evolution and late Holocene relative sea level change along the Otranto coast (Salento peninsula, southern Apulia, Italy). – GeoResJ **9**–12: 42-53.

Sapirstein, P. (2012): The Monumental Archaic Roof of the Temple of Hera at Mon Repos, Corfu. – The Journal of the American School of Classical Studies at Athens **81** (1): 31–61.

Schliemann, H. (1875): Troy and its remains. A narrative of researches and discoveries made on the site of Ilium, and the Trojan Plain. – Murray, London.

Schrott, L. (2015): Gelände-Arbeitsmethoden in der Geomorphologie. In: Ahnert, F. (Ed.). Einführung in die Geomorphologie. – Verlag Eugen Ulmer KG, Stuttgart: 396–413.

Schulmeister, M. K., Butler, J. J., Healey, J. M., Zheng, L., Wysocki, D. A. & McCall, G. W. (2003): Direct-Push Electrical Conductivity Logging for High-Resolution Hydrostratigraphic Characterization. – Ground Water Monitoring & Remediation **23** (3): 52–62.

Scicchitano, G., Monaco, C. & Tortorici, L. (2007): Large boulder deposits by tsunami waves along the Ionian coast of south-eastern Sicily (Italy). – Marine Geology **238**: 75–91.

Schmidt, B. (1890): Korkyräische Studien: Beiträge zur Topographie Korkyras und zur Erklärung des Thukydides, Xenophon und Diodoros. Teubner, Leipzig.

Seeliger, M., Bartz, M., Erkul, E., Feuser, S., Kelterbaum, D., Klein, C., Pirson, F., Vött, A. & Brückner, H. (2013): Taken from the sea, reclaimed by the sea: The fate of the closed harbour of Elaia, the maritime satellite city of Pergamum (Turkey). – Quaternary International **312**: 70–83.

Seeliger, M., Brill, D., Feuser, S., Bartz, M., Erkul, E., Kelterbaum, D., Vött, A., Klein, C., Pirson, F. & Brückner, H. (2014): The Purpose and Age of Underwater Walls in the Bay of Elaia of Western Turkey: A Multidisciplinary Approach. – Geoarchaeology **29**: 138–155.

Sen Gupta, B.K.S. (1999): Modern foraminifera. – Kluwer Academic Publisher, Dordrecht.

Shaw, B. (2012): Active Tectonics of the Hellenic Subduction Zone. – Springer, Berlin and Heidelberg.

Shaw, B., Ambraseys, N.N., England, P.C., Floyd, M.A., Gorman, G.J., Higham, T.F.G., Jackson, J.A., Nocquet, J.M., Pain, C.C. & Piggott, M.D. (2008): Eastern Mediterranean tectonics and tsunami hazard inferred from the A.D. 365 earthquake. – Nature Geoscience **1** (4): 268–276.

Shaw, B. & Jackson, J. (2010): Earthquake mechanisms and active tectonics of the Hellenic subduction zone. – Geophysical Journal International **181**: 966–984. Shefsky, S. (1997): Comparing Field Portable X-Ray Fluorescence (XRF) To Laboratory Analysis Of Heavy Metals In Soil. International Symposium of Field Screening Methods for Hazardous Wastes and Toxic Chemicals, Las Vegas, Nevada, USA. – URL: https://clu-in.org/download/char/dataquality/sshefsky02.pdf (2016-10-16).

Shennan, I., Long, A. J., Rutherford, M. M., Green, F. M., Innes, J. B., Lloyd, J. M., Zong, Y. & Walker, J. (1996): Tidal marsh stratigraphy, sea-level change and large earthquakes, I: a 5000 year record in Washington, U.S.A. – Quaternary Science Reviews **15** (10): 1023–1059.

Shi, S., Dawson, A. & Smith, D. (1995): Coastal Sedimentation Associated with the December 12th, 1992 Tsunami in Flores, Indonesia. – Pure and Applied Geophysics **144** (3/4): 525–536.

Siani, G., Paterne, M., Arnold, M., Bard E., Métivier, B., Tisnerat, N., & Bassinot, F. (2000): Radiocarbon reservoir ages in the Mediterranean Sea and Black Sea. – Radiocarbon **42**: 271–280.

Smedile, A., De Martini, P. M., Pantosti, D., Bellucci, L., Del Carlo, P., Gasperini, L., Pirrotta, C., Polonia, A. & Boschi, E. (2011): Possible tsunami signatures from an integrated study in the Augusta Bay offshore (Eastern Sicily – Italy). – Marine Geology **281**: 1–13.

Soloviev, S.L., Solovieva, O.N., Go, C.N., Kim, K.S. & Shchetnikov, N.A. (2000): Tsunamis in the Mediterranean Sea 2000 B.C.-2000 A.D. – Kluwer Academic Publishers, Dordrecht.

Sordinas, A. (2003): The‚Sidarian': maritime Mesolithic non-geometric microliths in western Greece. – In: Galanidou, N. & Perlès, C. (Eds.): The Greek Mesolithic: Problems and perspectives. – British School at Athens Studies **10**: 89–97.

Soter, S. & Katsonopoulou, D. (2011): Submergence and Uplift of Settlements in the Area of Helike, Greece, from the Early Bronze Age to Late Antiquity. – Geoarchaeology **27** (4): 584–610.

Spetsieri-Choremi, A. (1996): Das Antike Kerkyra. – Archaeological Receipts Fund, Ministry of Culture, Athens.

Stanley, J.-D & Bernhardt, C.E. (2010): Alexandria's Eastern Harbor, Egypt: Pollen, Microscopic Charcoal, and the Transition from Natural to Human-Modified Basin. – Journal of Coastal Research **26** (1): 67–79.

Stanley, J.-D. & Bernasconi, M.P. (2006): Holocene Depositional Patterns and Evolution in Alexandria's Eastern Harbor, Egypt. – Journal of Coastal Research **22** (2): 283–297.

Stiros, S.C., Pirazzoli, P.A., Laborel, J. & Laborel-Deguen, F. (1994): The 1953 earthquake in Cephalonia (Western Hellenic Arc): coastal uplift and halotectonic faulting. – Geophysical Journal International **117**: 834–849.

Stiros, S., Pirazzoli, P., Rothaus, R., Papageorgiou, S., Laborel, J. & Arnold, M. (1996): On the Date of Construction of Lechaion, Western Harbor of Ancient Corinth, Greece. - Geoarchaeology: An International Journey **11** (3): 152–263.

Stiros, S. C., Pirazzoli, P. A., Laborel, J. & Laborel-Deguen, F. (1994): The 1953 earthquake in Cephalonia (Western Hellenic Arc): coastal uplift and halotectonic faulting. – Geophysical Journal International **117**: 834–49.

Stiros, S.C. & Blackman, D.J. (2014): Seismic coastal uplift and subsidence in Rhodes Island, Aegean Arc: Evidence from an uplifted ancient harbour. – Tectonphysics **611**: 114–120.

Stock, F., Pint, A., Horejs, B., Ladstätter, S. & Brückner, H. (2013): In search of the harbours: New evidence of Late Roman and Byzantine harbours of Ephesus. – Quaternary International **312**: 57–69.

Stock, F., Kerschner, M., Kraft, J.C., Pint, A., Frenzel, P. & Brückner, H. (2014): The palaeogeographies of Ephesos (Turkey), its harbours, and the Artemision – a geoarchaeological reconstruction for the timespan 1500–300 BC. – Zeitschrift für Geomorphologie **58** (2): 33–66.

Stock, F., Knipping, M., Pint, A., Ladstätter, S., Delile, H., Heiss, A.G., Laermanns, H., Mitchell, P.D., Ployer, R., Steskal, M., Thanheiser, U., Urz, R., Wennrich, V. & Brückner, H. (2016): Human impact on Holocene sediment dynamics in the Eastern Mediterranean – the example of the Roman harbour of Ephesus. – Earth Surface Processes and Landforms Volume **41** (7): 980–996.

Strabo after Jones, H.L. (1924): The Geography of Strabo. – Harvard University Press, London.

Strasser, T.F., Runnels, C., Wegmann, K., Panagopoulou, E., McCoy, F., Digregorio, C., Karkanas, P. & Thompson, N. (2011): Dating Palaeolithic sites in southwestern Crete, Greece. – Journal of Quaternary Science **26** (5): 553–560.

Stucchi, M., Rovida, A., Gomez Capera, A. A., Alexandre , P., Camelbeeck, T., Demircioglu, M. B., Gasperini, P., Kouskouna, V., Musson, R. M. W., Radulian, M., Sesetyan, K., Vilanova, S., Baumont, D., Bungum, H., Fäh, D., Lenhardt, W., Makropoulos, K., Martinze Solares, Scotti, J., Živčić, M., Albini, P., Batllo, J., Papaioannou, C. , Tatevossian, R., Locati, M., Meletti, C., Viganò, D. & Giardini, D. (2013): The SHARE European Earthquake Catalogue (SHEEC) 1000–1899. – Journal of Seismology **17**: 523–544.

Stuiver, M. & Reimer, P.J. (1993): Extended 14C data base and revised Calib 3.0 14C age calibration program. – Radiocarbon **35**: 215–230.

Sugawara, D., Minoura, K & Imamura, F. (2008): Tsunamis and Tsunami Sedimentology. – In: Shiki, T., Tsuji, Y., Yamazaki, T., & Minoura, K. (Eds.): Tsunamiites – Features and Implications. Elsevier, Amsterdam: 9–49.

Suric, M., Korbar, T., & Juračić, M. (2014): Tectonic constraints on the late Pleistocene-Holocene relative sea-level change along the north-eastern Adriatic coast (Croatia). – Geomorphology **220**: 93–103.

Switzer, A. D. & Jones, B. G. (2008): Large-scale washover sedimentation in a freshwater lagoon from the southeast Australian coast: sea-level change, tsunami or exceptionally large storm? – The Holocene 18 (5): 787–803.

Szczuciński, W., Kokociński, M., Rzeszewski, M., Chagué-Goff, C., Cachão, M., Goto, K. & Sugawara, D. (2012): Sediment sources and sedimentation processes of 2011 Tohoku-oki tsunami deposits on the Sendai Plain, Japan – Insights from diatoms, nannoliths and grain size distribution. – Sedimentary Geology **282**: 40–56.

Tacitus after Church, J.A., Brodribb, W.J. & Bryant, S. (1942): Annals – Complete Works of Tacitus. – Perseus, New York.

Thucydides after Crawley, R. (1910): The Peloponnesian War. Translated by Richard Crawley. – E.P. Dutton, New York.

Tous, M. & Romero, R. (2013): Meteorological environments associated with medicane development. – International Journal of Climatology **33**: 1-14.

Vacchi, M., Marriner, N., Morhange, C., Spada, G., Fontana, A. & Rovere, A. (2016): Multiproxy assessment of Holocene relative sea-level changes in the western Mediterranean: Sea-level variability and improvements in the definition of the isostatic signal. – Earth-Science Reviews **155**: 172–197.

van Andel, T.H. (1989): Late Quaternary sea-level changes and archaeology. – Antiquity Volume **63** (241): 733–745.

van Hinsbergen, D. J. J., van der Meer, D. G., Zachariasse, W. J. & Meulenkamp, J. E. (2006): Deformation of western Greece during Neogene clockwise rotation and collision with Apulia. – International Journal of Earth Science **95**: 463–490.

van Rijn, P. (1995): The Roman Harbour of Velsen. – Terra et Aqua **61**: 25–28.

Vannucci, G., Pondrelli, S., Argnani, A., Morelli, A., Gasperini, P. & Boschi, E. (2004): An atlas of Mediterranean seismicity. – Annals of Geophysics **47** (1): 247–306.

Veerasingam, S., Venkatachalapathy, R., Basavaiah, N., Ramkumar, T., Venkatramanan, S. & Deenadayalan, K. (2014): Identification and characterization of tsunami deposits off southeast coast of India from the 2004 Indian Ocean tsunami: Rock magnetic and geochemical approach. – Journal of Earth System Science **123**: 905–921.

Véron, A., Goiran, J. P., Morhange, C., Marriner, N. & Empereur, J. Y. (2006): Pollutant lead reveals the pre-Hellenistic occupation and ancient growth of Alexandria, Egypt. – Geophysical Research Letters **33**: L06409.

Vött, A. & Brückner, H. (2006): Versunkene Häfen im Mittelmeerraum. – Geographische Rundschau **58** (4): 12–21.

Vött, A., May, M., Brückner, H. & Brockmüller, S. (2006): Sedimentary Evidence of Late Holocene Tsunami Events near Lefkada Island (NW Greece). – Zeitschrift für Geomorphologie N.F. Supplementary Issue **146**: 139–172.

Vött, A. (2007a): Silting up Oiniadai's harbours (Acheloos River delta, NW Greece). Geoarchaeological implications of late Holocene landscape changes. – Géomorphologie: relief, processus, environnement **1**: 19–36.

Vött, A. (2007b): Relative sea level changes and regional tectonic evolution of seven coastal areas in NW Greece since the mid-Holocene. – Quarternay Science Reviews **26** (7-8): 894–919.

Vött, A., Schriever, A., Handl, M. & Brückner, H. (2007): Holocene palaeogeographies of the central Acheloos River delta (NW Greece) in the vicinity of the ancient seaport Oiniadai. – Geodinamica Acta **20**: 241–256.

Vött, A., Brückner, H., May, S. M., Sakellariou, D., Nelle, O., Lang, F., Kapsimalis, V., Jahns, S., Herd, R., Handl, M. & Fountoulis, I. (2009a): The Lake Voulkaria (Akarnania, NW Greece) palaeoenvironmental archive – a sediment trap for multiple tsunami impact since the mid- Holocene. – Zeitschrift für Geomorphologie N.F. Supplementary Issue **53** (1): 1–37.

Vött, A., Brückner, H., Brockmüller, S., Handl, M., May, S.M., Gaki-Papanastassiou, K., Herd, R., Lang, F., Maroukian, H., Nelle, O. & Papanastassiou, D. (2009b): Traces of Holocene tsunamis across the Sound of Lefkada, NW Greece. – Global and Planetary Change **66** (1-2): 112–128.

Vött, A., Brückner, H., Brockmüller, S., Handl, M., May, S.M., Gaki- Papanastassiou, K., Herd, R., Lang, F., Maroukian, H., Nelle, O. & Papanastassiou, D. (2009b): Traces of Holocene tsunamis across the Sound of Lefkada, NW Greece. – Global and Planetary Change **66**: 112–128.

Vött, A., Bareth, G., Brückner, H., Curdt, C., Fountoulis, I., Grapmayer, R., Hadler, H., Hoffmeister, D., Klasen, N., Lang, F., Masberg, P., May, S. M., Ntageretzis, K., Sakellariou, D. & Willershäuser, T. (2010): Beachrock-type calcarenitic tsunamites along the shores of the eastern Ionian Sea (western Greece) – case studies from Akarnania, the Ionian Islands and the western Peloponnese. – Zeitschrift für Geomorphologie N.F. Supplementary Issue **54** (3): 1–50.

Vött, A., Bareth, G., Brückner, H., Lang, F., Sakellariou, D., Hadler, H., Ntageretzis, K. & Willershäuser, T. (2011a): Olympia's Harbour Site Pheia (Elis, Western Peloponnese, Greece). Destroyed by Tsunami Impact. – Die Erde **142**: 259–288.

Vött, A., Lang, F., Brückner, H., Gaki-Papanastassiou, K., Maroukian, H., Papanastassiou, D., Giannikos, A., Hadler, H., Handl, M., Ntageretzis, K., Willershäuser, T. & Zander, A. (2011b): Sedimentological and geoarchaeological evidence of multiple tsunamigenic imprint on the Bay of Palairos-Pogonia (Akarnania, NW Greece). – Quaternary International **242**: 213–239.

Vött, A., Hadler, H., Willershäuser, T., Ntageretzis, K., Brückner, H., Warnecke, H., Grootes, P.M., Lang, F., Nelle, O. & Sakellariou, D. (2015a): Ancient harbours used as tsunami sediment traps – the case study of Krane (Cefalonia Island, Greece). – In: Ladstaater, S., Pirson, F. & Schmidts, T. (Eds.): Harbours and Harbour Cities in the Eastern Mediterranean from Antiquity to the Byzantine Period. Recent Discoveries & New Approaches. – BYZAS 19 (= Österreichisches Archäologisches Institut Sonderband 52), Vol. II, Ege Yayinlari, Istanbul: 743–772.

Vött, A., Fischer, P., Röbke, B.R., Werner, V., Emde, K., Finkler, C., Hadler, H., Handl, M., Ntageretzis, K. & Willershäuser, T. (2015b): Holocene fan alluviation and terrace formation by repeated tsunami passage at Epitalio near Olympia (Alpheios River valley, Greece). – Zeitschrift für Geomorphologie N.F. Supplementary Issue **59** (4): 81–123.

Wagner, G.A. (1998): Age Determination of Young Rocks and Artifacts. Physical and Chemical Clocks in Quaternary Geology and Archaeology. – Springer, Berlin & Heidelberg.

Walker, M. (2005): Quaternary Dating Methods. Wiley, Chichester.

Walsh, K. (2004): Caring about Sediments: The Role of Cultural Geoarchaeology in Mediterranean Landscapes. – Journal of Mediterranean Archaeology **17** (2): 223–245.

Warnecke, H. (2002): Zur Phänomenologie und zum Verlauf antiker Überseewege. – In: Olshausen, E. & Sonnabend, H. (Eds.): Zu Wasser und zu Land. Verkehrswege in der antiken Welt. – Steiner Verlag, Stuttgart: 93–104.

Werner, V., Baika, K., Fischer, P., Hadler, H., Obrocki, L., Willershäuser, T., Tzigoun, A., Tsigkou, A., Reicherter, K., Papanikolaou, I., Emde, K. & Vött, A. (2017): The sedimentary and geomorphological imprint of the AD 365 tsunami on the coasts of southwestern Crete (Greece) – Examples from Sougia and Palaiochora. – Quaternary International (DOI: 10.1016/j.quaint.2017.07.016).

Willershäuser, T., Vött, A., Brückner, H., Bareth, G., Nelle, O., Nadeau, M.-J., Hadler, H. & Ntageretzis, K. (2013): Holocene tsunami landfalls along the shores of the inner Gulf of Argostoli (Cefalonia Island, Greece). – Zeitschrift für Geomorphologie N.F. Supplementary Issue **57** (4): 105–138.

Wilson, A. (2011): Developments in Mediterranean shipping and maritime trade from the Hellenistic period to AD 1000. In: Robinson, D. & Wilson, A. (Eds.): Maritime Archaeology and Ancient Trade in the Mediterranean. – Oxford Centre for Maritime Archaeology Monographs, Oxford: 33–59.

Woodward, J. (2009): Editorial Information. – In: Woodward, J. (Ed.): The Physical Geography of the Mediterranean. Oxford University Press, Oxford: 3–4.

Yu, K.-F., Zhao, J.-X., Shi, Q. & Meng, Q.-S. (2009): Reconstruction of storm/tsunami records over the last 4000 years using transported coral blocks and lagoon sediments in the southern South China Sea. – Quaternary International **195**: 128–137.

Zacharioudaki, A., Korres, G. & Perivoliotis, L. (2015): Wave climate of the Hellenic Seas obtained from a wavehindcast for the period 1960–2001. – Ocean Dynamics **65**: 795–816.